EFFECT OF FOOD EXTRACTS AND BIOACTIVE FOOD COMPOUNDS ON THE MECHANISM OF ATHEROSCLEROSIS AND NUTRITIONAL BIOMARKERS

Úrsula Catalán Santos

Dipòsit Legal: T. 1058-2012

EFFECT OF FOOD EXTRACTS AND BIOACTIVE FOOD COMPOUNDS ON THE MECHANISM OF ATHEROSCLEROSIS AND NUTRITIONAL BIOMARKERS
Úrsula Catalán Santos
Dipòsit Legal: T. 1058-2012

UNIVERSITAT ROVIRA I VIRGILI

campus of international excellence southern catalonia

Effect of Food Extracts and Bioactive Food Compounds on the Mechanism of Atherosclerosis and Nutritional Biomarkers – Catalán Ú

European Thesis

UNIVERSITAT ROVIRA I VIRGILI

FACULTAT DE MEDICINA I CIÈNCIES DE LA SALUT

Department of Medicine and Surgery

Unit of Lipids and Atherosclerosis Research

Effect of Food Extracts and Bioactive Food Compounds on the Mechanism of Atherosclerosis and Nutritional Biomarkers

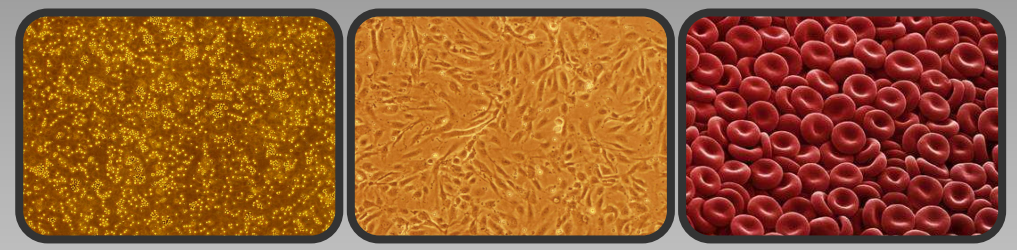

Úrsula Catalán Santos

European Thesis 2012

EFFECT OF FOOD EXTRACTS AND BIOACTIVE FOOD COMPOUNDS ON THE MECHANISM OF ATHEROSCLEROSIS AND NUTRITIONAL BIOMARKERS

Úrsula Catalán Santos

Dipòsit Legal: T. 1058-2012

EFFECT OF FOOD EXTRACTS AND BIOACTIVE FOOD COMPOUNDS ON THE MECHANISM OF ATHEROSCLEROSIS AND NUTRITIONAL BIOMARKERS

Úrsula Catalán Santos

Dipòsit Legal: T. 1058-2012

Úrsula Catalán Santos

Effect of Food Extracts and Bioactive Food Compounds on the Mechanism of Atherosclerosis and Nutritional Biomarkers

EUROPEAN THESIS

supervised by Dr. Rosa Solà i Alberich

PhD in Nutrition and Metabolism

Universitat Rovira i Virgili

Department of Medicine and Surgery

Unit of Lipids and Atherosclerosis Research

Reus, Tarragona, Spain 2012

EFFECT OF FOOD EXTRACTS AND BIOACTIVE FOOD COMPOUNDS ON THE MECHANISM OF ATHEROSCLEROSIS AND NUTRITIONAL BIOMARKERS

Úrsula Catalán Santos

Dipòsit Legal: T. 1058-2012

EFFECT OF FOOD EXTRACTS AND BIOACTIVE FOOD COMPOUNDS ON THE MECHANISM OF ATHEROSCLEROSIS AND NUTRITIONAL BIOMARKERS
Úrsula Catalán Santos
Dipòsit Legal: T. 1058-2012

"A person who never made a mistake, never tried anything new"

Albert Einstein

EFFECT OF FOOD EXTRACTS AND BIOACTIVE FOOD COMPOUNDS ON THE MECHANISM OF ATHEROSCLEROSIS AND NUTRITIONAL BIOMARKERS

Úrsula Catalán Santos

Dipòsit Legal: T. 1058-2012

UNIVERSITAT ROVIRA I VIRGILI

FACULTAT DE MEDICINA I CIÈNCIES DE LA SALUT
DEPARTAMENT DE MEDICINA I CIRURGIA

Carrer Sant Llorenç, 21
43201 Reus
Tel. 977 759 306
Fax. 977 759 352

FAIG CONSTAR:

Que aquest treball, titulat "*Effect of Food Extracts and Bioactive Food Compounds on the Mechanism of Atherosclerosis and Nutritional Biomarkers*", que presenta **Úrsula Catalán Santos**, ha estat realitzat sota la meva direcció al Departament de Medicina I Cirurgia i que acompleix els requeriments per a poder optar al títol de Doctor.

Reus, 02 de maig de 2012

El director de la Tesi doctoral

Dra. Rosa SOLÀ I ALBERICH

EFFECT OF FOOD EXTRACTS AND BIOACTIVE FOOD COMPOUNDS ON THE MECHANISM OF ATHEROSCLEROSIS AND NUTRITIONAL BIOMARKERS

Úrsula Catalán Santos

Dipòsit Legal: T. 1058-2012

UNIVERSITAT ROVIRA I VIRGILI

Autorització del director/a o codirector/s/a/es de la tesi doctoral

DADES IDENTIFICATIVES DE LA TESI DOCTORAL	
Títol de la tesi doctoral **Effect of Food Extracts and Bioactive Food Compounds on the Mechanism of Atherosclerosis and Nutritional Biomarkers**	
Doctorand/a **Úrsula CATALÁN SANTOS**	
Programa de Doctorat / Programa Oficial de Postgrau Nutrició i Metabolisme	
Departament Medicina i Cirurgia	Grup de recerca Unitat de Recerca en Lípids i Arteriosclerosi
Director/a Rosa SOLÀ ALBERICH	Correu electrònic del Directora rosa.sola@urv.cat.
Codirector/a	Correu electrònic del Codirector/a
Tutor/a (si s'escau)	Correu electrònic del Tutor/a

INFORME DEL DIRECTOR DE TESI

El/s (co)director/s sotasignats emeten l'informe de la tesi doctoral presentada a tràmit de dipòsit, en base a la revisió dels següents elements de qualitat:

	SI	NO
La tesi consisteix en un treball original de recerca	X	
El títol reflecteix acuradament el contingut de la tesi	X	
Les hipòtesis i/o els objectius de la tesi estan clarament formulats	X	
La metodologia està descrita	X	
Hi consta el procediment	X	
Hi consten els resultats i la discussió dels mateixos	X	
Les conclusions de la tesi corresponen a les hipòtesis i/o objectius formulats	X	
La bibliografia està ben reflectida	X	

D'aquesta tesi es deriven les següents aportacions científiques:

- Catalán Ú, Fernández-Castillejo S, Pons L, Heras M, Aragonés G, Anglès N, Morello JR and Solà R. Alpha-tocopherol and BAY 11-7082 Reduce Vascular Cell Adhesion Molecule in Human Aortic Endothelial Cells. (accepted for publication in the Journal of Vascular Research 2012)
- Catalán Ú, Rodríguez MA, Ras MR, Macià A, Mallol R, Vinaixa M, et al. Biomarkers of Food intake and Metabolite Differences between Plasma and Red Blood Cell Matrices; a Human Metabolomic profile approach. (editor submitted).
- Catalán Ú, Fernández-Castillejo S, Anglès N, Morello JR, Yebras M and Sola R. Inhibition of the transcription factor c-Jun by the MAPK family, and not the NF-κB pathway, suggests that peanut extract has anti-inflammatory properties. (editor submitted).

Varis articles científics en fase d'elaboració, comunicacions científiques a congresos.

Altres comentaris sobre la qualitat de la tesi:

I en conclusió, s'emet l'informe FAVORABLE pel tràmit de dipòsit de la tesi doctoral i posterior defensa pública.

Reus, 3 de Maig de 2012
Nom i cognoms. Rosa SOLÀ ALBERICH.
Directora de la tesi

EFFECT OF FOOD EXTRACTS AND BIOACTIVE FOOD COMPOUNDS ON THE MECHANISM OF ATHEROSCLEROSIS AND NUTRITIONAL BIOMARKERS

Úrsula Catalán Santos

Dipòsit Legal: T. 1058-2012

EFFECT OF FOOD EXTRACTS AND BIOACTIVE FOOD COMPOUNDS ON THE MECHANISM OF ATHEROSCLEROSIS AND NUTRITIONAL BIOMARKERS
Úrsula Catalán Santos
Dipòsit Legal: T. 1058-2012

To my family, Óscar and Nemesio

EFFECT OF FOOD EXTRACTS AND BIOACTIVE FOOD COMPOUNDS ON THE MECHANISM OF ATHEROSCLEROSIS AND NUTRITIONAL BIOMARKERS

Úrsula Catalán Santos

Dipòsit Legal: T. 1058-2012

EFFECT OF FOOD EXTRACTS AND BIOACTIVE FOOD COMPOUNDS ON THE MECHANISM OF ATHEROSCLEROSIS AND NUTRITIONAL BIOMARKERS
Úrsula Catalán Santos
Dipòsit Legal: T. 1058-2012

SUMMARY

EFFECT OF FOOD EXTRACTS AND BIOACTIVE FOOD COMPOUNDS ON THE MECHANISM OF ATHEROSCLEROSIS AND NUTRITIONAL BIOMARKERS

Úrsula Catalán Santos

Dipòsit Legal: T. 1058-2012

INTRODUCTION

Atherosclerosis is considered the underlying cause of cardiovascular disease (CVD). Involved in the pathogenesis of atherosclerosis are inflammation, endothelial dysfunction, thrombosis and oxidative stress, as well as the intrinsic characteristics of the arterial wall.

Some natural compounds or extracts from certain foods have been reported to reverse endothelial dysfunction or have anti-inflammatory properties. Cellular models can be used to detect such biological activity.

The nutrient profiles of plasma, urine, whole blood, erythrocytes and platelets may be used to identify specific nutritional biomarkers of dietary components. Determining which type of sample is most appropriate for the detection of nutritional biomarkers is necessary in order to link specific metabolites to food consumption. Specifically, differences in the metabolomic profile of matrices such as plasma and/or red blood cells (RBC) may provide interesting sources of information that have not been fully explored, to date. “Omics” technologies offer a promising route towards obtaining scientific evidence from these metabolomic profiles.

HYPOTHESIS AND OBJECTIVES:

We hypothesize that atherosclerosis-specific biological cell approach, such as THP-1 monocytes and human aortic endothelial cells (HAEC), could be used successfully to study the mechanism-of-action of food extracts and/or bioactive compounds while assessing their effects on inflammation and endothelial dysfunction. Further, we hypothesize that two different biological samples, RBC and plasma from the same blood extraction, can provide complementary metabolomic profile information.

Objectives:

1. To standardize experimental methodology for testing the mechanism-of-action of food extracts (such as polyphenol-rich peanut extract) and bioactive compounds (such as alpha-tocopherol; AT) while assessing their

effect on inflammation and endothelial dysfunction. The procedures used are:

a) THP-1 monocyte system; a lipopolysaccharide (LPS)-inflammation model exposed to peanut extract. Measurements include the tumour necrosis factor-alpha (TNF-α) cascade: nuclear factor-κB (NF-κB) and mitogen-activated protein kinase (MAPK) family, TNF-α mRNA expression, TNF-α mRNA stability, TNF-α converting enzyme (TACE) activity and total TNF-α protein including intra- and extracellular protein (**Study 1**).

b) TNF-α-stimulated HAEC; an endothelial dysfunction model to study the effect of the AT molecule on different cellular adhesion molecules (CAMs) such as: intercellular cell adhesion molecule-1 (ICAM-1), vascular cell adhesion molecule-1 (VCAM-1) and E-selectin. Measurements were conducted at the mRNA and soluble protein level to explore their individual involvements in leukocyte adhesion to endothelium (**Study 2**).

2. To apply and standardize high-throughput metabolomic analytical techniques such as nuclear magnetic resonance (NMR) spectroscopy, gas chromatography-mass spectrometry (GC-MS) and ultra performance liquid chromatography coupled to tandem mass spectrometry (UPLC-MS/MS) to characterize the metabolomic profile of human RBC and human plasma (**Study 3**).

MATERIALS AND METHODS:

Testing food extracts, or bioactive compound, in *in vitro* model

- Anti-inflammatory properties (**Study 1**):

THP-1 monocytes were incubated with peanut extract (5, 25, 50 and 100 µg/mL) consisting of 39% flavonols, 37% flavanols and 24% phenolic acid (or BAY 11-7082 (5µM) as experiment control) for 1h and then stimulated with LPS (500 ng/mL) for 4h. Cytotoxicity was measured as lactate dehydrogenase (LDH) activity release. NF-κB and MAPK family were

determined by TransAm kit while TNF-α mRNA levels and its mRNA stability by RT-PCR. Intra- and extra-cellular TNF-α protein was measured by ELISA, and TACE activity by a fluorimetric assay.

- Endothelial function improvement (**Study 2**)

The effects of AT (10-150 µM) and BAY 11-7082 (BAY; 0.1 or 1 µM) on CAMs mRNA expression as well as their protein soluble form release (sCAMs) were tested in HAEC activated by TNF-α (1 or 10 ng/mL). Also, the extent of lymphocyte adhesion to activated HAEC was determined.

Nutritional biomarkers profile derived from plasma and RBC (**Study 3)**

Fasting blood was drawn from 10 ostensibly healthy individuals, using sodium citrate and lithium heparin as anticoagulants. Both plasma and RBCs were separated into aqueous and lipid fractions to be analyzed using 1D and 2D ^{1}H NMR spectroscopy. Fatty acids were analyzed using GC-MS. Polyphenols were extracted from plasma and RBC by micro-elution solid-phase extraction and analyzed by UPLC-MS/MS.

RESULTS

Study 1

Peanut extract inhibited the maximal LPS-induced extra-cellular TNF-α protein secretion by 18%, 29% and 47% at 25, 50 and 100 µg/mL, respectively ($P<0.05$). LPS stimulation showed that 85% of TNF-α was released into the extracellular medium while 15% remained intracellular. Peanut extract did not modify NF-κB but, instead, caused a reduction in c-Jun transcription factor activity ($P<0.05$), and decreased TNF-α mRNA (albeit non-significantly), while having no effect on mRNA stability and TACE activity.

Study 2

Addition of BAY to HAEC stimulated by TNF-α caused a reduction of VCAM-1, E-selectin and ICAM-1 mRNA expression by 30%, 30% and 10%, respectively. Further, a reduction in the protein quantity of sVCAM-1 by

70%, of sE-selectin by 51% and of sICAM-1 by 25% was observed compared to HAEC stimulated by TNF-α (P<0.05).
AT (50, 75 and 150 µM) decreased VCAM-1 mRNA expression by 30% and sVCAM-1 protein by 33% compared to HAEC stimulated by TNF-α (P<0.05).

TNF-α-activated HAEC adhesion to human Jurkat-T-lymphocytes was higher compared to non-activated HAEC (P<0.05). BAY (2 and 5 µM) reduced this lymphocyte adhesion (P<0.05).

Study 3

^{1}H NMR demonstrated higher aqueous metabolites such as glucose in plasma compared to RBC, while RBC contained higher levels of ADP-ATP, creatine and acetone than plasma. Lipoproteins and their subclasses were higher in plasma than in RBC.
The percentages of saturated fatty acids (SFA) 16:0, 17:0, 20:0, 24:0 and polyunsaturated fatty acids (PUFA) 22:6 n-3 (docosahexaenoic acid) and 20:4 n-6 (arachidonic acid) were higher in RBC than in plasma (p<0.05) while SFA 14:0, monounsaturated fatty acids (MUFA) 14:1 n-5, 16:1 n-7, 17:1 n-7 and 18:1 n-9 and PUFA 18:3 n-3, 18:2 n-6, 18:3 n-6 and 20:3 n-6 were higher in plasma than in RBC (P<0.05). Polyphenols differed in plasma from those of RBC. Biomarker concentrations were lower in sodium citrate compared to lithium heparin plasma.

CONCLUSIONS

1. The models, of inflammation using THP-1 monocytes and of endothelial dysfunction using HAEC, are effective as biological-cell approaches in the investigation of atherosclerosis. The methods are repeatable and reproducible in testing the potential beneficial effects of natural and manufactured extracts, and/or compounds.

2. A pre-incubation with polyphenol-rich peanut extract and AT, in the cellular models studied, is necessary in order to observe protective effects against inflammation and endothelial dysfunction stimuli.

3. Polyphenol-rich peanut extract exerts an anti-inflammatory effect by reducing extracellular TNF-α protein. This peanut extract mechanism-of-action is via the inhibition of c-Jun transcription factor activity. AT improves endothelial function specifically by inhibiting VCAM-1 at the mRNA and the protein levels.

4. BAY is confirmed as an effective control molecule for the cell models under study. BAY can reduce TNF-α protein (total, extra- and intracellular) and TNF-α mRNA levels by inhibiting c-Jun, MEF2 and NF-κB transcription factor activity and TACE activity in THP-1 cells. BAY can also reduce sVCAM-1, sE-selectin and sICAM-1 protein as well as their mRNA levels and, in the endothelial dysfunction model, the adhesion between activated HAECs and Jurkat-T-cells.

5. The combination of NMR spectroscopy, GC-MS and UPLC-MS/MS techniques are efficient in generating metabolomic profiles of several specific biomarkers of food intake and metabolites (FA, polyphenol, aqueous metabolites and lipoprotein content) in plasma and RBC of human subjects.

6. Plasma and RBC are two matrices that add complementary information when assessing biomarkers (metabolites) of food intake.

Financial support: This work was funded by *CENIT* 2006-2009 MET-DEV-FUN project with the leadership of *La Morella Nuts S.A.* Support was also obtained within the AGL2009-13517-C03-03 project and the mobility PhD fellowship TME2009-00409 of EDU/2933/2009 (both from the Spanish Ministry of Education and Science, Spain). Additional support was from the Centre Tecnològic de Nutrició i Salut (CTNS).

EFFECT OF FOOD EXTRACTS AND BIOACTIVE FOOD COMPOUNDS ON THE MECHANISM OF ATHEROSCLEROSIS AND NUTRITIONAL BIOMARKERS
Úrsula Catalán Santos
Dipòsit Legal: T. 1058-2012

RESUMEN

EFFECT OF FOOD EXTRACTS AND BIOACTIVE FOOD COMPOUNDS ON THE MECHANISM OF ATHEROSCLEROSIS AND NUTRITIONAL BIOMARKERS

Úrsula Catalán Santos

Dipòsit Legal: T. 1058-2012

INTRODUCCIÓN

La arteriosclerosis se considera la causa subyacente de la enfermedad cardiovascular (ECV). Involucrado en la patogénesis de la arteriosclerosis son la inflamación, la disfunción endotelial, la trombosis y el estrés oxidativo, así como, las características intrínsecas de la pared arterial.

Algunos compuestos naturales o extractos de ciertos alimentos se han descrito como revertir la disfunción endotelial o tener propiedades anti-inflamatorias. Los modelos celulares se pueden utilizar para detectar dicha actividad biológica.

Los perfiles nutricionales de plasma, orina, sangre, glóbulos rojos (RBC), plaquetas, etc. se pueden utilizar para realizar la búsqueda de biomarcadores nutricionales específicos de componentes de la dieta. Determinar qué tipo de muestra es la más apropiada para la detección de biomarcadores nutricionales es necesario para poder relacionar metabolitos específicos con el consumo de ciertos alimentos. Específicamente, diferencias en el perfil metabolómico de matrices como plasma y RBC pueden ofrecer una interesante fuente de información no ampliamente explorado hasta la fecha. Las tecnologías ómicas ofrecen una manera prometedora de contribuir a obtener la evidencia científica de estos perfiles metabolómicos.

HIPÓTESIS Y OBJETIVOS:

Se postula que en la arteriosclerosis, mediante una aproximación celular biológica, tales como monocitos humanos THP-1 y células endoteliales de aorta humana (HAEC), podrían ser utilizados para estudiar el mecanismo de acción de los extractos de alimentos y / o compuestos bioactivos sobre su efecto en la inflamación y disfunción endotelial. Por otra parte, se postula que dos matrices biológicas (RBC y el plasma) son capaces de proporcionar información complementaria sobre su perfil metabolómico.

Objetivos:

1. Normalizar la metodología experimental para testar el mecanismo de acción de extractos de alimentos (extracto de cacahuete rico en polifenoles) y compuestos bioactivos (alfa-tocoferol; AT) y evaluar su efecto sobre la inflamación y disfunción endotelial. Para llevar a cabo dicho objetivo realizamos:

a) sistema de monocitos THP-1, como un modelo de inflamación estimulado con lipopolisacárido (LPS), después de la incubación del extracto de cacahuete, para estudiar la cascada del *tumor necrosis factor-alpha* (TNF-α): *nuclear factor-κB* (NF-κB) y la familia *mitogen-activated protein kinase* (MAPK), la expresión de mRNA del TNF-α, la estabilidad del mRNA del TNF-α, la actividad de la enzima convertidora del TNF-α (TACE) y la proteína total del TNF-α incluyendo la proteína intra- y extracelular (**Estudio 1**) del TNF-α.

b) HAEC estimuladas con TNF-α, como un modelo de disfunción endotelial, para estudiar el efecto de la molécula AT en diferentes moléculas de adhesión celular (CAMs), tales como la *intercellular cell adhesion molecule-1* (ICAM-1), *vascular cell adhesion molecule-1* (VCAM-1) y E-selectina, a nivel de mRNA y proteína y su implicación en la adhesión de los leucocitos al endotelio (**Estudio 2**).

2. Aplicar y estandarizar técnicas de alto rendimiento de análisis metabolómico como espectroscopía de resonáncia magnética nuclear (NMR), cromatografía de gases acoplada a un espectrómetro de masas (GC-MS) y cromatografía líquida ultra sensible acoplada a un tándem de espectrómetro de masas (UPLC-MS/MS), con el fin de caracterizar el perfil metabolómico de los RBC y el plasma humano (**Estudio 3**).

MATERIAL Y MÉTODOS:

Evaluación de los extractos de alimentos o compuestos bioactivos en modelos *in vitro*:

- Propiedades anti-inflamatorias (**Estudio 1**):

Los monocitos THP-1 se incubaron con el extracto de cacahuete (5, 25, 50 y 100 µg / mL) o BAY 11-7082 (BAY; 5µM) como control experimento, durante 1 h y luego fueron estimulados con LPS (500 ng / mL) durante 4 h. La actividad de la liberación de la lactato deshidrogenasa (LDH) fue utilizada como indicador de la citotoxicidad. NF-kB y la familia MAPK fueron determinados por TransAm kit, los niveles del mRNA del TNF-α y la estabilidad del mRNA del TNF-α por RT-PCR, la proteína intra- y extracelular del TNF-α por ELISA y la actividad de la TACE mediante un ensayo fluorimétrico.

- Mejora de la función endotelial (**Estudio 2**):

Se evaluó el efecto del AT (10-150 µM) y BAY (0.1 o 1 µM) sobre la expresión de mRNA de las CAMs, así como su liberación en forma de proteína soluble (sCAMs) en HAECs estimuladas por TNF-α (1 o 10 ng / mL). Además, se determinó el grado de adhesión de linfocitos-T-Jurkat a las HAECs estimuladas.

Diferencias entre el perfil metabolómico del plasma y los RBC (**Estudio 3**):

Se obtuvo sangre en ayunas a partir de 10 individuos aparentemente sanos, en tubos con citrato de sodio y heparina de litio como anticoagulantes. Tanto el plasma y los RBC se separaron en fracciones acuosas y lipídicas y fueron analizados mediante 1D y 2D ^{1}H NMR. Los ácidos grasos se analizaron mediante GC-MS. Los polifenoles fueron extraídos de plasma y glóbulos rojos mediante micro-elución por extracción de fase sólida y se analizaron mediante UPLC-MS/MS.

RESULTADOS

Estudio 1

El extracto de cacahuete inhibió la proteína del TNF-α extracelular inducido por LPS en un 18%, 29% y 47% a 25, 50 y 100 µg / mL, respectivamente ($P<0.05$). La estimulación con LPS reveló que el 85% de TNF-α fue liberado extracelularmente, mientras que el 15% permaneció intracelular. El extracto de cacahuete no redujo la actividad de NF-κB, pero sí del factor

de transcripción c-Jun (P<0.05), disminuyó el mRNA del TNF-α (aunque no significativamente) y no tuvo efecto sobre la estabilidad del mRNA ni sobre la actividad de TACE.

Estudio 2

BAY redujo la expresión de mRNA de VCAM-1, de E-selectina y de ICAM-1 en un 30%, 30% y 10% respectivamente. Además, se observó una reducción de la proteína de sVCAM-1 en un 70%, sE-selectina en un 51% y sICAM 1-en un 25% comparado con HAECs estimuladas solamente con TNF-α (P<0.05).

AT (50, 75 y 150 μM) disminuyó la expresión del mRNA de VCAM-1 en un 30% y de su proteína sVCAM-1 en un 33% en comparación con HAECs estimuladas solamente con TNF-α (P<0.05).

El TNF-α activó, de forma significativa, la adhesión de linfocitos-T-Jurkat a HAEC en comparación con HAEC no activadas (P<0.05). BAY (2 y 5 μM) redujo esta adhesión de linfocitos a HAECs (P<0.05).

Estudio 3

^{1}H NMR demostró mayores metabolitos acuosos tales como la glucosa en plasma en comparación con RBC, mientras que RBC contenían niveles más altos de ADP-ATP, creatina y acetona que el plasma. Los niveles de lipoproteínas y sus subclases fueron más altos en plasma que en RBC.

Los porcentajes de ácidos grasos saturados (SFA) 16:0, 17:0, 20:0, 24:0 y ácidos grasos poliinsaturados (PUFA) 22:6 n-3 (ácido docosahexaenoico) y 20:4 n-6 (ácido araquidónico ácido) fueron mayores en los RBC que en el plasma (P<0.05), mientras que SFA 14:0, ácidos grasos monoinsaturados (MUFA) 14:01 n-5, 16:1 n-7, 17:1 n-7 y 18:1 n-9 y PUFA 18:3 n-3, 18:2 n-6, 18:3 n-6 y 20:3 n-6 eran superiores en el plasma que en RBC (P<0.05). Los polifenoles encontrados en plasma difieren de los encontrados en RBC. Los biomarcadores encontrados en plasma estaban más diluidos en las muestras de citrato de sodio comparadas con las de heparina de litio.

CONCLUSIONES

1. Los modelos de inflamación en células monocíticas THP-1 y de disfunción endotelial en células HAEC utilizados como enfoque biológico celular específico de arteriosclerosis son métodos repetibles y reproducibles para probar los posibles efectos beneficiosos de los extractos naturales y sintéticos y / o compuestos.

2. La pre-incubación con extracto de cacahuete rico en polifenoles y AT, en los modelos celulares estudiados, es necesario para poder observar efectos protectores contra estímulos como la inflamación y disfunción endotelial.

3. El extracto de cacahuete rico en polifenoles ejerce un efecto anti-inflamatorio, reduciendo el la proteína del TNF-α extracelular. Este mecanismo de acción del extracto de cacahuete es a través de la inhibición de la actividad del factor de transcripción c-Jun. AT mejora la función endotelial específicamente inhibiendo VCAM-1 a nivel de mRNA y proteína.

4. Se confirma que BAY es una molécula efectiva como control de los modelos celulares estudiados. BAY reduce la proteína del TNF-α (total, extra- e intracelular) y el mRNA del TNF-α mediante la inhibición de la actividad de los factores de transcripción c-Jun, MEF2 y NF-κB y de la actividad de TACE en el modelo de la inflamación. Además, BAY reduce las proteína sVCAM-1, sE-selectina y sICAM-1 y su expresión de mRNA, así como la adhesión de limfocitos a las células endoteliales en el modelo de disfunción endotelial.

5. La combinación de las técnicas espectrometría de NMR, GC-MS y UPLC-MS/MS son eficientes para generar perfiles metabolómicos de varios biomarcadores específicos de la ingesta de alimentos y sus

metabolitos (FA, polifenoles, metabolitos acuosos y el contenido de lipoproteínas) en plasma y RBC humanos.

6. Plasma y RBC son dos matrices que añaden información complementaria en la evaluación de biomarcadores (metabolitos) de la ingesta de alimentos y sus metabolitos.

Fuente de financiación: Este trabajo ha sido realizado dentro de las actividades del proyecto CENIT 2006-2009 MET-DEV-FUN liderado por La Morella Nuts S.A. También ha sido respaldado por el proyecto AGL2009-13517-C03-03 y por la beca de movilidad para esdudiantes de doctorado TME2009-00409 de EDU/2933/2009 (ambos del Ministerio de Ciencia y Educación, España). Por último, ha obtenido la colaboración del Centre Tecnològic de Nutrició i Salut (CTNS).

INDEX

EFFECT OF FOOD EXTRACTS AND BIOACTIVE FOOD COMPOUNDS ON THE MECHANISM OF ATHEROSCLEROSIS AND NUTRITIONAL BIOMARKERS

Úrsula Catalán Santos

Dipòsit Legal: T. 1058-2012

ABBREVIATIONS

EFFECT OF FOOD EXTRACTS AND BIOACTIVE FOOD COMPOUNDS ON THE MECHANISM OF ATHEROSCLEROSIS AND NUTRITIONAL BIOMARKERS

Úrsula Catalán Santos

Dipòsit Legal: T. 1058-2012

ADAM-17 - a disintegrin and metalloprotease (TACE)

ADP – adenosine diphosphate

ANOVA – analysis of variance

AT – alpha-tocopherol

ATP – adenosine triphosphate

BAY – BAY 11-7082

CAMs – cell adhesion molecules

cDNA – complementary deoxyribonucleic acid

CE – capillary electrophoresis

CHD – coronary heart disease

CM – culture medium

CV – coefficient of variation

CVD – cardiovascular disease

D_2O – deuterated water

DHA – docosahexaenoic acid

DMSO – dimethyl sulfoxide

DNA – deoxyribonucleic acid

DSTE – double-stimulated echo

EDTA – ethylenediaminetetraacetic acid

ELISA – enzyme immunosorbent assay

EPA – eicosapentaenoic acid

ERK – extracellular signal-regulated kinase

ESI – electronspray ionization

EtOH – ethanol

FA – fatty acids

FAME – fatty acid methyl ester

FBS – fetal bovine serum

FFQ – food frequency questionnaire

FID – free induction decay

FT-IR – Fourier transform infrared

GAPDH – glyceraldehyde 3-phosphate dehydrogenase

GC-MS – gas chromatography-mass spectrometry

Abbreviations

HAEC – human aortic endothelial cells

HDL – high-density lipoprotein

HPLC – high-performance liquid chromatography

HRMAS – high resolution magic angle spinning

HUVEC – human umbilical vein endothelial cells

Hz – hertz

ICAM-1 – intercellular cell adhesion molecule-1

ICR-FT MS – ion-cyclotron resonance Fourier transform mass spectrometry

IL-6 – interleukin 6

IL-8 – interleukin 8

IS – internal standard

JNK – c-Jun N-terminal kinase

LBP – LPS bearing protein

LC-MS – liquid chromatography-mass spectrometry

LDH – lactate dehydrogenase

LDL – low-density lipoprotein

LED – longitudinal eddy-current delay

LFA-1 – leukocyte function antigen-1

LPS – lipopolysaccharide

LSGS – low serum growth supplement

MALDI – matrix-assisted laser desorption/ionisation

MAPK – mitogen-activated protein kinase

MCP-1 – monocyte chemoattractant protein-1

mg – milligrams

min – minutes

mL - mililiters

MMP – matrix metalloproteinase

mPa – milliPascals

mRNA – messenger ribonucleic acid

MUFA – monounsaturated fatty acids

NF-κB – nuclear factor-kappa B

ng – nanograms

NMR – nuclear magnetic resonance spectroscopy

NOESY – nuclear overhauser effect spectroscopy

ºC – degree Celsius

OPLS-DA – orthogonal partial least squares-discriminant analysis

PBS – phosphate buffered saline

PC – principal component

PCA – principal component analysis

PCR – polymerase chain reaction

PLS-DA – partial least squares-discriminant analysis

PMA – phorbol 12-myristate 13-acetate

ppm – parts per million

PSGL-1 – P-selectin glycoprotein ligand-1

PTM – post-translational modifications

PUFA – polyunsaturated fatty acids

RBC – red blood cells

RF – radiofrequency

RFU – relative fluorescence units

RIPA – radio-immunoprecipitation assay

RNA – ribonucleic acid

ROS – reactive oxygen species

RSD – relative standard deviation

rt RT-PCR – real time reverse transcription polymerase chain reaction

RT-PCR – reverse transcription polymerase chain reaction

sCAMs – soluble cell adhesion molecules

SD – standard deviation

sec – seconds

SEM – standard error of the mean

sE-selectin – soluble E-selectin

SFA – saturated fatty acids

sICAM-1 – soluble intercellular cell adhesion molecule-1

SMC – smooth muscle cells

SPSS – statistical package for the social sciences

SRM – selected reaction monitoring mode

sVCAM-1 – soluble vascular cell adhesion molecule1

TACE – TNF-α converting enzyme

TF – tissue factor

THP-1 – monocytic cells

TLR4 – toll-like receptor-4

TMS – trimethylsilyl

TNF-α – tumour necrosis factor-alpha

TSP – trimethylsilyl propionate

UPLC-MS/MS – ultra performance liquid chromatography coupled to tandem mass spectrometry

VCAM-1 – vascular cell adhesion molecule-1

VLA-4 – very late antigen-4

VSMC – vascular smooth muscle cells

WHO – world health organization

µL – microliters

µ-SPE – micro solid-phase extraction

INTRODUCTION

EFFECT OF FOOD EXTRACTS AND BIOACTIVE FOOD COMPOUNDS ON THE MECHANISM OF ATHEROSCLEROSIS AND NUTRITIONAL BIOMARKERS

Úrsula Catalán Santos

Dipòsit Legal: T. 1058-2012

Chapter 1. Atherosclerosis

Atherosclerosis is considered the underlying cause of cardiovascular disease (CVD) (Hansson GK, 2005). It is a progressive, chronic, inflammatory disease characterized by the accumulation of lipids and fibrous elements within the artery wall. It constitutes the single most important contributor to the growing burden of CVD (Libby P *et al.*, 2002). Atherosclerosis is characterized by the formation of lesions in the large and medium sized arteries, often at sites of disturbed blood flow. The World Health Organization (WHO) has published a serial of key facts related to the importance of CVD facts in the world (Organization WWHFWS, 2011):

1. CVD is the number one cause of death globally: more people die annually from CVD than from any other cause.
2. An estimated 17.3 million of people died from CVD in 2008, representing 30% of all global deaths. An estimated 7.3 million, out of these deaths, were due to coronary heart disease and 6.2 million of them were due to stroke.
3. Low- and middle-income countries are disproportionately affected: over 80% of CVD deaths take place in low- and middle-income countries and occur almost equally in men and women.
4. By 2030, it is calculated that almost 23.6 million of people will die from CVD, mainly from heart disease and stroke. These causes remain as the leading causes of death in the world.

1.1 Pathogenesis of atherosclerosis

The first stage in the development of atherosclerotic plaques is the recruitment of monocytes at arterial lumen. The recruitment of circulating monocytes occurs via a tightly regulated multi-stage process mediated by combination of cell surface adhesion molecules (Libby P *et al.*, 2011) (**Figure 1**).

Activated endothelial cells, at sites of incipient atherosclerosis, initially, express E- and P-selectin (Rader DJ and Daugherty A, 2008). They

mediate the tethering and rolling of circulating monocytes, which, at the same time, express L-selectin. P-selectin binds to P-selectin glycoprotein ligand-1 (PSGL-1) and other glycosylated ligands on monocytes (Elstad MR *et al.*, 1995; Weyrich AS *et al.*, 1995). There is data suggesting that E-selectin is inducible expressed at sites of atherosclerosis. However, functional data, in relevant models that would directly support a role for this molecule, are lacking. Under normal blood flow, selectin-mediated interactions are not sufficient to arrest rolling leukocytes (Burnier L *et al.*, 2009). Selectins (P, E and L) not only allow the capturing and rolling of leukocytes on the endothelium, but they also signal through PSGL-1 to activate integrins and induce monocyte activation (Weyrich AS *et al.*, 1995). Integrins are heterodimeric cell surface receptors and support both

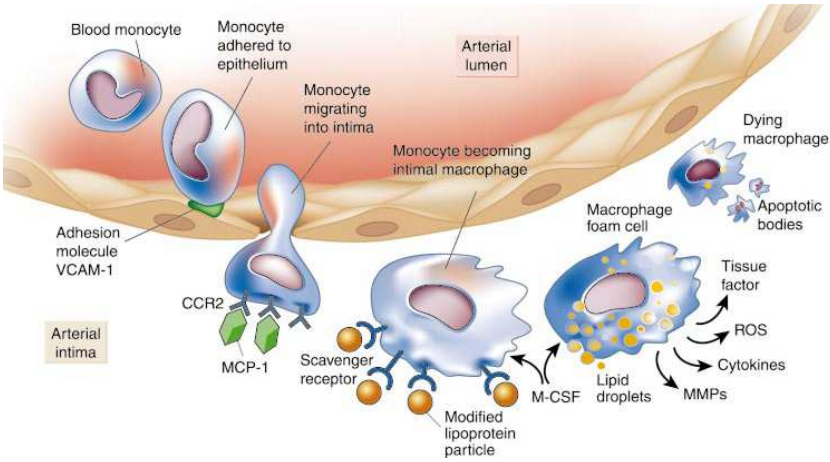

Figure 1. Early stages of atherosclerotis. Endothelial cell activation can be initiated by inflammation, which leads to an increase in the expression of leukocyte adhesion molecules (e.g., E-selectin, VCAM-1 and ICAM-1). Migration of monocytes to the vessel wall is largely controlled by VCAM-1. Adherent monocytes pass between intact endothelial cells to penetrate into the intima, the innermost layer of the arterial wall. Within the intima, monocytes transform into macrophages, which, throuth scavenger receptors, bind oxidized LDL, thereby leading to the formation of foam cells. The progressive accumulation of lipids and foam cells leads to the formation of fatty streaks. Foam cells produce ROS and proinflammatory cytokines. Foam cells produce ROS and proinflammatory cytokines (TNF-α, IL-1β, IL-6) that, in turn, activate the expression of adhesion molecules, facilitating further recruitment of T cells and macrophages. The activated mononuclear phagocyte has a key role in the thrombotic complications of atherosclerosis of atherosclerosis by producing MMPs, which can degrade extracellular matrix that lends strength to the fibrous cap of the plaque. Source: (Libby P *et al.*, 2002)

rolling and adhesion of leukocytes. Upon activation, integrins undergo a series of conformational changes that result in increased binding affinity for their respective ligands, such as vascular cell adhesion molecule-1 (VCAM-1). That binding affinity creates a firm adhesion state to endothelium. VCAM-1 is a member of the immunoglobulin-like superfamily of adhesion molecules and, although not routinely expressed under physiological conditions, is induced on the cytokine-stimulated endothelium by tumour necrosis factor-alpha (TNF-α), a cytokine present in the initiation and progression of atherosclerosis (Kleemann R *et al.*, 2008).

Once adhered and contacted with the activated endothelial layer, monocytes migrate into the tunica intima. In this process, various chemokines participate and interact, for example monocyte chemoattractant protein-1 (MCP-1) (Mestas J and Ley K, 2008).

Once resident in the intima, monocytes acquire characteristics of the tissue macrophage. The macrophage expresses scavenger receptors that bind internalized lipoprotein particles, previously modified by oxidation or glycation. These processes give rise to arterial foam cells, a hallmark of the arterial lesion. This lesion is the result of accumulation of lipid droplets within the cytoplasm (Libby P *et al.*, 2009). Foam cells secrete pro-inflammatory cytokines, which amplify the local inflammatory response in the lesion, and reactive oxygen species (ROS). The activated macrophage foam cells (**Figure 1**) have a key role in the thrombotic complications of atherosclerosis because they produce matrix metalloproteinases (MMPs) (Rajavashisth TB *et al.*, 1999). MMPs degrade extracellular matrix leading to the accumulation of dead cells that strengthen plaque's fibrous cap. If the plaque ruptures, the blood flow contacts the potent pro-coagulant protein tissue factor (TF). This is another macrophage product, which could lead to thrombosis. (Blankenberg S *et al.*, 2003). Macrophages congregate in a central core in the typical atherosclerotic plaque. Macrophages can die in this location (e.g. by apoptosis) hence producing the so-called 'lipid or necrotic core' of the atherosclerotic lesion (Ross R, 1999b; Libby P *et al.*, 2002; Libby P *et al.*, 2011).

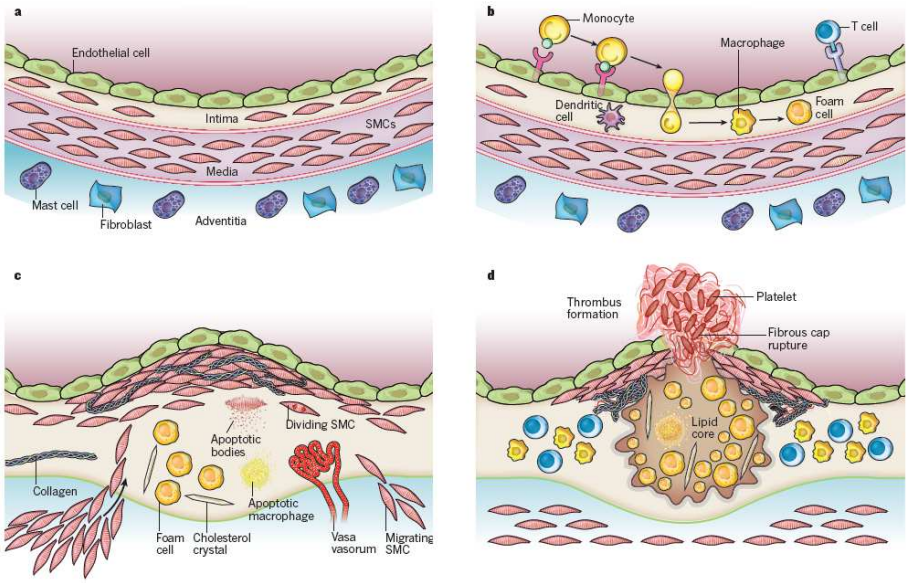

Figure 2. Atherosclerotic lesion development. Atherosclerosis occurs at sites in the arterial tree where laminar flow is disrupted. (**a**) The normal artery contains three layers. The inner layer, the tunica intima, is lined by a monolayer of endothelial cells that is in contact with blood overlying a basement membrane. In contrast to many animal species used for atherosclerosis experiments, the human intima contains resident smooth muscle cells (SMCs). (**b**) The initial steps of atherosclerosis include adhesion of blood leukocytes to the activated endothelial monolayer, directed migration of the bound leukocytes into the intima, maturation of monocytes (the most numerous of the leukocytes recruited) into macrophages, and their uptake of lipid, yielding foam cells. (**c**) Lesion progression involves the migration of SMCs from the media to the intima. Plaque macrophages and SMCs can die in advancing lesions, some by apoptosis. Extracellular lipid derived from dead and dying cells can accumulate in the central region of a plaque, often denoted the lipid or necrotic core. Advancing plaques also contain cholesterol crystals and microvessels. (**d**) Thrombosis, the ultimate complication of atherosclerosis, often complicates a physical disruption of the atherosclerotic plaque. Shown is a fracture of the plaque's fibrous cap, which has enabled blood coagulation components to come into contact with tissue factors in the plaque's interior, triggering the thrombus that extends into the vessel lumen, where it can impede blood flow. Source: (Libby P *et al.*, 2011)

This advanced obstructive lesion leads to the final stages of atherosclerosis, which includes calcification and probably plaque rupture (**Figure 2**). This physical disruption not always results in plaque rupture. Physical disruption of plaques may trigger thrombosis and thus promote sudden expansion of atheromatous lesions (Stary HC *et al.*, 1995; Davis PA *et al.*, 2006).

Three types of physical disruption may occur (Virmani R *et al.*, 2002a; Virmani R *et al.*, 2002b):

1. **Superficial erosion** or microscopic areas of desquamation of endothelial cells that form the monolayer covering the intima. Although common and most often asymptomatic, such superficial erosion may account for approximately 25% of fatal coronary thromboses.
2. **Disruption of the microvessels.** Atheromatous lesions develop microvascular channels because of neo-angiogenesis. Intra-plaque deposition of fibrin, fibrin-split products, and haemosiderin provide evidence of intra-plaque haemorrhage. In this way, a silent microvascular haemorrhage, within the atherosclerotic intima, could give rise to a growth spurt in the evolution of the plaque.
3. **Plaque rupture.** The plaque fibrous cap encompasses inflammation events and usually serves to attract the thrombogenic lipid-rich core of the atheroma from the bloodstream, which contains circulating coagulation proteins. Rupture of the fibrous cap allows the coagulation factors to contact with TF, the main pro-thrombotic stimulus found in the lesion's lipid core. The ruptured fibrous cap causes approximately 75% of acute myocardial infarctions.

These examples illustrate the inextricable links between thrombosis and lesion progression. Usually, below the clinical threshold, evolution of the lesion occurs silently, leading to transition from the fatty to the fibrous atherosclerotic plaque (Libby P *et al.*, 2002).

1.2 Mechanisms involved in atherosclerosis

Endothelial dysfunction and inflammation, often induced by hypercholesterolemia or other cardiovascular risk factors, are the initial stages of atherosclerosis and play a key role on its development. In the

present work, we focus on these early stages of atherosclerosis; inflammation and endothelial dysfunction.

1.2.1 Inflammation

Up to date, the relationship between inflammation and atherogenesis has been studied mainly by focusing on prognostic influence of inflammatory biomarkers, with respect to conventional risk factors, and less by assessing the possible pathogenic effect of atherosclerotic plaque progression.

The interactions between monocytes and endothelial cells play a key role in the development of vascular lesion, inflammation, and atherosclerosis. Inflammatory and innate immune mechanisms, both employing monocytes, innate receptors, innate cytokines, and chemokines are suggested to be involved in atherogenesis (Loppnow H *et al.*, 2008). Among the inflammatory mechanisms, the cytokines are central players (**Figure 3**).

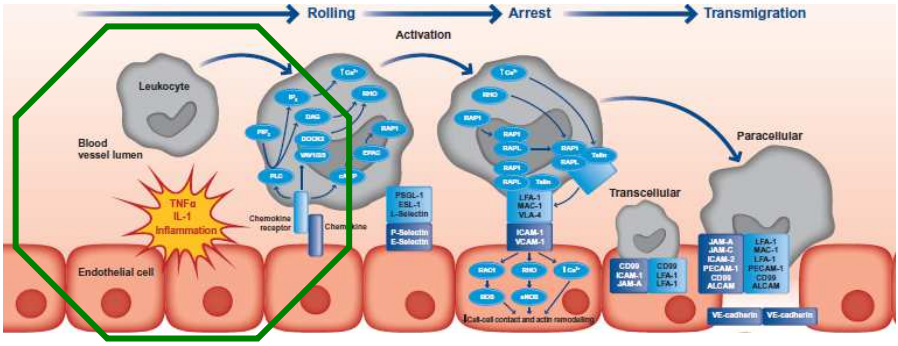

Figure 3. Leukocyte recruitment in atherosclerosis inflammation. Non-specific pro-inflammatory factors (TNF-alpha, interleukin-1, -6 and -18) and endothelial activation factors (soluble VCAM-1, ICAM-1 and CD40L) are some of the inflammatory markers correlated with the activation of the atherosclerotic cascade process. Source: Beat Imhof from Abcam ®

Innate cytokines, such as IL-1 or TNF-α, may activate the cells. Cytokines potentially activate multiple mechanisms relevant to maintenance or impairment of homeostasis within the vessel wall. Vascular cells, but not least smooth muscle cells, can actively contribute to the inflammatory cytokine-dependent network in the blood vessel wall (Balanescu S *et al.*, 2010).

1.2.2 Endothelial dysfunction

When inflammation process has initiated, endothelial dysfunction develops rapidly. The first changes preceding the formation of atherosclerotic lesions take place in the endothelium. These changes include the up-regulation of leukocyte adhesion molecules, by L-selectin, integrins, and platelet–endothelial-cell adhesion molecule-1, and the up-regulation of endothelial adhesion molecules, which include E-selectin, P-selectin, intercellular adhesion molecule-1 (ICAM-1), and VCAM-1. Endothelial permeability to lipoproteins and other plasma constituents increases. This permeability is mediated by nitric oxide, prostacyclin, platelet-derived growth factor, angiotensin II, and endothelin. Thanks to this permeability, leukocytes can migrate to the artery wall. The migration is mediated by oxidized low-density lipoprotein, monocyte chemotactic protein-1, interleukin-8, platelet-derived growth factor, macrophage colony-stimulating factor, and osteopontin (Ross R, 1999a) (**Figure 4**).

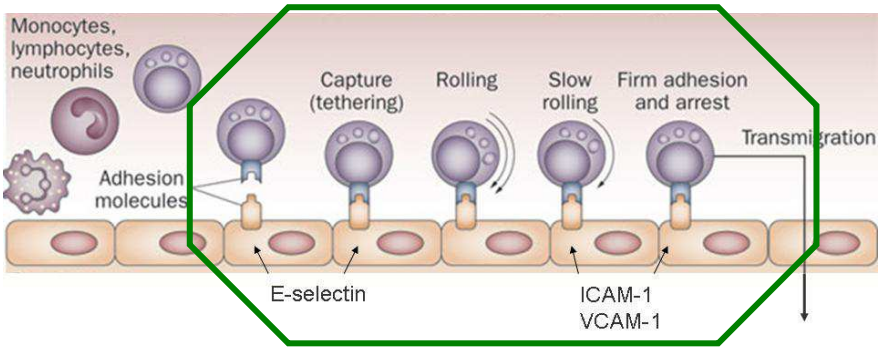

Figure 4. Endothelial dysfunction. E-selectin-mediated slow rolling, and indirectly by signals transmitted through adjacent receptors. Leukocyte arrest is mediated by firm binding to adhesion molecules, including E-selectin, ICAM-1 and VCAM-1. Adapted figure from: (Navarro-Gonzalez JF *et al.*, 2011)

1.3 Atherosclerosis risk factors

The human advanced age predisposes to endothelial dysfunction and subsequent development of atherosclerosis. However, the presence of

several risk factors, for example elevated blood cholesterol, does not always accompanies the development of atherosclerosis. In the contrary, suffering from endothelial dysfunction always does (Catapano AL *et al.*, 2011).

The exact cause of atherosclerosis remains unknown and certain traits, conditions, exposures or habits may raise an individual's probability of developing it. These conditions are known as risk factors and a person's likehood of developing atherosclerosis increases with the number of risk factors he or she accumulates. Most of these risk factors can be modifiable and thus controlled such as diet, physical activity, alcohol and tobacco consumption. Others, called non-modifiable, cannot be controlled like age, sex and genetic predisposition (family history of premature coronary heart disease (CHD)/genotype) (Ordovas JM, 2006).

Atherosclerosis risk factors can also be intermediate. These include a) high levels of total blood cholesterol, b) high levels of blood low-density lipoprotein cholesterol (LDL), c) low levels of blood high-density lipoprotein cholesterol (HDL), d) hypertension (high blood pressure), e) diabetes mellitus/glucose intolerance and f) obesity/overweight. Moreover, exist atherosclerosis emerging risk factors such as lipoptrotein (a), homocysteine, prothrombotic factors, proinflammatory factors and impaired fasting glucose levels (Longo DL, 2011). The combination of the above risk factors can lead to the development of CHD, stroke peripheral vascular disease and CVD in general (Catapano AL *et al.*, 2011).

Multiple biochemical risk factors for atherosclerosis and CVD include disordered lipid profiles, autoimmunity, infection, high levels of homocysteine, asymmetrical dimethylarginine, C-reactive protein, genetic predisposition and various metabolic diseases (Dominiczak MH, 2001; Grant PJ, 2003; Maas R and Boger RH, 2003). Many risk factors act in a coordinated or synergistic way participating in one or more inflammatory pathways. Markers of these risk factors can be detected on three cell types where they coordinate their action to influence cardiovascular dynamics, function, and structure (Osiecki H, 2004).

These cell types are:

- **Immune cells**: monocytes / macrophages and T lymphocytes, situated in the circulating blood, which defend the endothelium and smooth muscle cells (SMC) from chemical and biological insult.
- **Endothelial cells:** situated between circulating blood in the lumen and the rest of the vessel wall. They control the intra- and trans-cellular flow of nutrients, hormones, and immune cells, and regulate vascular tone and blood flow.
- **SMC or vascular smooth muscle cells (VSMC):** found at the vessel wall, maintain vascular tone and structure.

Activation of the molecular mechanisms, involved in the recruitment of monocytes by endothelial cells, leads to the development of early atherosclerosis stages.

Screening for early stages of atherosclerosis, at which intervention is most effective, proves to be better than just following disease evolution and aid in the titration of therapy, by detecting the presence of vulnerable plaque that requires aggressive intervention (Cai JM *et al.*, 2002). Screening molecular biomarkers should be specific for each atherosclerosis early stage because its management may vary at different stages of the disease. Thus, detection of biomarkers can be useful for the screening of patients with cardiac risk factors. Biochemical risk biomarkers, in particular, play a crucial role in all stages of atherosclerosis process, and entail a great relevance in risk stratification and early prevention (Montagnana M *et al.*, 2008).

Chapter 2. Biomarkers

A biomarker or biological marker is a characteristic that is objectively measured and evaluated as an indicator of normal biological processes, pathogenic processes, or pharmacologic responses to a therapeutic (Vasan RS, 2006) or nutritional (Puiggros F *et al.*, 2011) intervention.

2.1 Classification of biomarkers

Biomarkers reflect the entire spectrum of a disease from the earliest manifestations to the terminal stages. The current literature contains numerous reports on the relationship between various biomarkers of atherosclerosis early stages and prospective cardiovascular risk, in apparently healthy individuals (van Kimmenade RR and Januzzi JL, Jr., 2012).

As mentioned before, a risk factor is associated with a disease when it belongs to the causal pathway leading to the disease. Related to that, a risk biomarker is associated with the disease (statistically) but not always causally linked to it. Risk biomarker may be a measure of the disease process itself (Vasan RS, 2006).

To evaluate the exceptional value of a new biomarker, investigators must demonstrate the elevated risk of a disease outcome associated with higher levels of the new biomarker after adjustment for other established risk factors (Kattan MW, 2003). Very strong associations between biomarkers and a certain disease are required for a given biomarker to have good discrimination properties (Pepe MS *et al.*, 2004; Revkin JH *et al.*, 2007).

Biomarkers are directly or indirectly linked to the stages of the causal pathway of a disease and thus strongly related to it (Mayeux R, 2004). Level or type of exposure to an external factor, response to exposures genetic susceptibility, symptoms of subclinical or clinical disease, and indicators of therapy response are some of the characteristics that a biomarker should also have. An easy way to think of biomarker is as indicators of a disease trait, disease state, or disease advanced stages (Vasan RS, 2006).

As we can see in **Figure 5**, Mayeux R has classified biomarkers as:

1. **Antecedent biomarkers**, those which are able to predict the developing of a disease.
2. **Screening biomarkers**, those which can detect the subclinical stages of a disease.
3. **Diagnostic biomarkers**, those which are representative of a specific disease.
4. **Staging biomarkers**, those which determine the degree of a disease.
5. **Prognostic biomarkers**, those which give some information about the disease evolution or the intervention therapeutic efficacy.

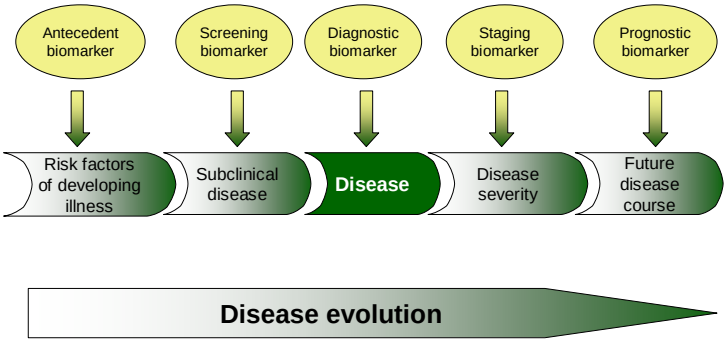

Figure 5. Disease pathway and impact of biomarkers. Biomarkers can act at different levels of disease stages and according to that they can be classified as: **antecedent biomarkers**, identifying the risk of developing an illness; **screening biomarkers**, screening for subclinical disease; **diagnostic biomarkers**, recognizing the disease *per se*; **staging biomarkers**, categorizing disease severity; or **prognostic biomarkers**, predicting future disease course, including recurrence and response to therapy, and monitoring efficacy of therapy. Adapted figure from (Mayeux R, 2004)

The clinical use of a biomarker for a disease risk prediction and/or prevention depends on its feasibility, ease, cost, and reproducibility of the measurement, and the ability to add value to the predictability of existing biomarkers (Libby P *et al.*, 2009).

It is very difficult to identify biomarkers of exposures to any agent (drug, environmental factor, food, etc.) that are stable over long periods, as

required in biomarker prospective studies. Timing, persistence, dose, and storage site must all be evaluated for the evaluation of a biomarker. Numerous studies, addressing single food components or nutrients biomarkers, have been conducted *in vitro* but few, if any, have been translated *in vivo* into free-living population studies (Puiggros F *et al.*, 2011).

2.2 Nutritional biomarkers

Another type of increasingly interesting class of biomarkers is the biomarkers of dietary intake. These are called nutritional biomarkers and they play a major underlying role in the causation of the global burden of chronic diseases (Heinzmann SS *et al.*, 2010); for example, a healthy diet rich in fruit and vegetables is associated with lower rates of some diseases such as CVDs, and its related risk factors (Roodenburg AJ *et al.*, 2000).

Diet questionnaires, such as 24-h recalls (24 hR), weighted food diaries and food frequency questionnaires (FFQs), offer an historical account of the exposure (diet), but direct measurement of food consumption can provide more accurate information regarding the kind of ingestion (Puiggros F *et al.*, 2011).

Moreover, foods, like fruit, vegetables, red wine and coffee, are usually complex mixtures of a large amount of molecules, nutrients and non-nutrients, present either naturally or accidentally. All of them affect the tissues of the organisms producing chemical changes on the anabolism and catabolism known as metabolic effects.

The metabolome includes not only the above-mentioned molecules but also hundreds of thousands of food compounds that do not have metabolic effects but they are rather used to convert a food into a gastronomic delight (Heinzmann SS *et al.*, 2010). Thus, it is of great importance the use of a specific biomarker able to provide valuable and accurate information of particular foods consumption.

Nutrient profiles derived from biologic samples such as plasma, urine, blood, erythrocytes, platelets and hair samples may be used to search for

biomarkers of specific dietary components consumption (de Roos B *et al.*, 2008). The challenge is to choose the appropriate sample-substrate for the detection of a specific nutrient compound. Information reflecting recent or sustained consumption depends on the tested biological sample. Hence, a nutritional biomarker can reflect either a recent intake (testing the compliance of short-term studies e.g. postprandial) or the consumption over a longer period (e.g. epidemiological studies or long-term interventions).

2.2.1 Promising applications of nutritional biomarkers

In order to identify nutritional biomarkers and establish their relationship to food consumption, it is useful to create a strategy that combines metabolome-wide association. This strategy includes evaluating untargeted metabolic profiles in nutritional intervention studies. The validation of these profiles in free-living populations helps to identify nutritional biomarkers of food intake. The use of a nutrimetabolomics (Savage AK *et al.*, 2009) approach to identify and verify a new nutritional biomarker may facilitate the evaluation of a disease risk factor. Moreover, nutrimetabolomics could facilitate individual diets effect aiming at a healthier eating, lifestyle and longevity. The development of robust nutritional biomarkers may reduce disease risk by better characterizing the metabolic phenotype, at the individual level, after the adherence to a specific diet (Heinzmann SS *et al.*, 2010).

The growth of molecular biology techniques has been largely and rapidly expanded during the last decades. The use of those advanced methods will lead to the detection of new biomarkers (Puiggros F *et al.*, 2011). Nutritional and risk biomarkers will provide a dynamic and powerful approach for the understanding of CVD. Moreover, they will have significant applications in analytic epidemiology, clinical trials and prevention, diagnosis, and management of the disease.

At this point, it is important to introduce the relative new concept of "**foodomics**". Foodomics is defined as the discipline that studies the Food

and Nutrition areas through the application of “omics” technologies to characterise and demonstrate the beneficial effects of food ingredients on human health (Cifuentes A, 2009). Today, foodomics analysis is considered a well-established systems approach to characterise the global metabolic profile of low molecular mass compounds (<1,500 Da) in biofluids (e.g., plasma, serum, urine). These complex biochemical fingerprints of hundreds, or even thousands, of metabolites reflect the overall metabolic status of an individual (Puiggros F *et al.*, 2011; Herrero M *et al.*, 2012).

Advanced analytical methodologies, ‘‘omics’’ approaches and bioinformatics tools—together with *in vitro*, *in vivo*, and/or clinical assays—are applied to investigate topics in food science and nutrition field that few years ago were considered unfeasible (Herrero M *et al.*, 2012).

Nuclear magnetic resonance (NMR) spectroscopy or mass spectrometry (MS) are used as high-resolution spectral analyses tools to determine metabolic signatures from biological samples (Nicholson JK *et al.*, 1999). These techniques help us obtain complex profiles of a wide range of metabolite classes (Lindon JC and Nicholson JK, 2008). The metabolic signatures fully characterize the metabolism and contribute to our understanding of cell biology, physiology and medicine (Heinzmann SS *et al.*, 2010; Patti GJ *et al.*, 2012).

Chapter 3. Metabolomics

3.1 Overview

On of the most important tasks in the field of molecular biology is to understand the complex molecular interactions of biological systems. This task is becoming one of the most rapidly growing areas over the last decade. 'Omics' technologies, like functional genomics tools, enable us to bridge the gap between genotype and phenotype at system level. Transcriptomics and proteomics allow a comprehensive analysis of the expression changes of genes and proteins, respectively, in a biological system. The metabolome represents the collection of all metabolites in a biological cell, tissue, organ or organism, which are the end products of cellular processes (Schmidt CW, 2004).

In the first place, metabonomics was defined as the quantitative measurement of the dynamic multiparametric metabolic response of living systems to pathophysiological stimuli or genetic modification (Nicholson JK *et al.*, 1999). Nowadays, metabolomics is defined as the systematic study of metabolite profiles of small molecules-unique chemical fingerprints resulting after specific cellular processes (Schmidt CW, 2004).

Metabolomics, a relatively new discipline, completes the 'omic' hierarchy by quantifying and identifying all the metabolites existing in or produced by an organism (**Figure 6**) (Tweeddale H *et al.*, 1998; Ellis DI *et al.*, 2007).

Up to now, metabolomics itself lacks a direct connection to the genome, as happens with transcriptomics and proteomics. Metabolomics is the final stage in the analysis of the genetic information flow, which reflects more closely the phenotypic changes in a cell, tissue or organism upon a genetic modification or physiological perturbation. The present estimate of the human metabolome is over 7,900 metabolites (Wishart DS *et al.*, 2009).

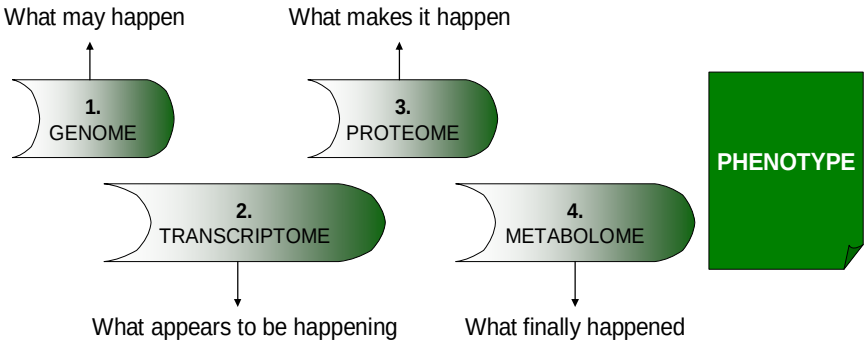

Figure 6. The "omics" cascade.

Although the size of metabolome is considerably smaller than the size of genome, challenges remain in detecting and identifying all the metabolites within the body. A metabolite is defined as a molecule with less than 1 kDa size (Samuelsson LM and Larsson DG, 2008). However, there are exceptions depending on the sample and detection method. For example, macromolecules such as lipoproteins and albumin are reliably detected in NMR-based metabolomics studies of blood plasma and could also serve as metabolites (Nicholson JK *et al.*, 1995). These small molecules vary significantly in terms of their molecular weights, concentrations, polarity, solubility and volatility. Unlike genes, mRNAs and proteins, which are all species-specific, metabolites are universal and metabolic pathways are highly conserved among species. This enable us to safely transfer our metabolic changes knowledge from model systems of human pathology to the human organism (Oliver S, 2000).

In a specific biological system, metabolites may rapidly suffer various modifications, in response to environmental stimuli. Studies show that even minor changes of enzymatic activity may result in great changes in metabolite concentrations despite the little changes in metabolic flux (van der Greef J *et al.*, 2004). This characteristic enables metabolomics to function as a more sensitive tool to discover novel biomarkers and to gain a better understanding of the disease process. Raamsdonk LM et al. demonstrated that metabolomics can be used as a valuable tool to identify

silent mutations in yeast, which shows no obvious phenotype despite the deletion of genes (Raamsdonk LM *et al.*, 2001). An array of different analytical platforms is employed in metabolomics studies to maximize the coverage of metabolites that can be detected within a sample. Metabolomics can offer further advances in nutritional biomarker discovery and pathway identification due to their cheaper per sample basis, when compared with transcriptomics and proteomics approaches (Griffin JL, 2006; Rhee EP and Gerszten RE, 2012). An important part in the study of nutritional biomarkers is the developments of analytic techniques that allow us to determine specific components or molecules after food consumption. These techniques should be robust, reproducible, rapid and low cost.

3.2 Application of metabolomics in atherosclerosis research

CVD provides an exciting area that could be explored by metabolomics. Apart from the individual genetic predisposition of the disease, the majority of the CVD cases are closely associated to environmental factors. Diabetes, obesity and a sedentary lifestyle greatly contribute to the development of CVD by disturbing the homeostasis (balance of internal environment) of system metabolism in the human body. Thus, the importance of measuring metabolic changes at multiple levels, in the study of atherosclerosis, has become increasingly necessary to better understand the phenotype of the disease (**Figure 7**) (Jones GL *et al.*, 2005). For example, Chen X et al. has recently applied gas chromatography-mass spectrometry (GC-MS)-based metabolomics analysis to reveal novel atherosclerosis biomarkers (Chen X *et al.*, 2010). Analysis of plasma samples from study patients showed that atherosclerosis alters fatty acid metabolism, especially that of palmitate, suggesting that the development of atherosclerosis can induce overproduction of palmitate (Chen X *et al.*, 2010).

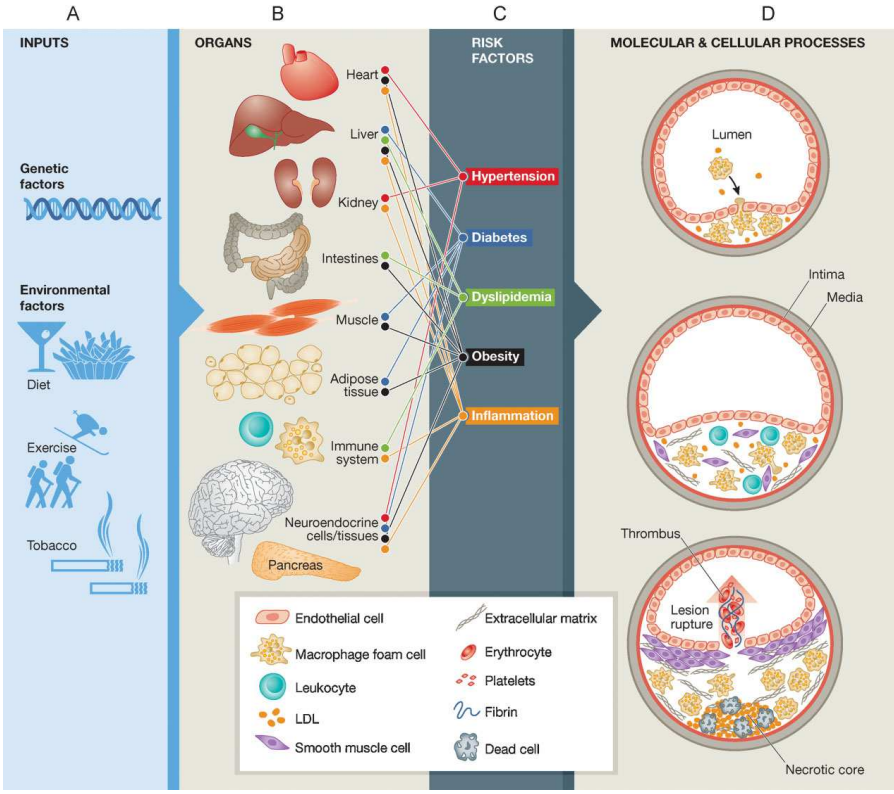

Figure 7. The pathophysiology of atherosclerosis involves interacting systems at multiple levels. **A**) Genetic and environmental factors; **B**) Multiple organs and organ systems are involved in the disease process; **C**) Risk factors that are influenced by genetic and environmental inputs and that involve multiple organ systems contribute to the development and progression of atherosclerosis; **D**) Atherosclerosis progresses through several stages, each of which involves the interaction of multiple cell types and molecular processes. Source: (Ramsey SA *et al.*, 2010)

Thus, palmitate metabolic profile changes could be used as a potential biomarker to assist the clinical diagnosis of such disease.

The nature of collecting plasma or urine samples from patients facilitates the success of CVD biomarker discovery. However, plasma and urine metabolic profiling may not be the best reporter of CVD. These profiles only represent the sum of all the metabolic changes occurring in the human body, and also suffer from inter-individual variability produced by diet and drug effects. Thus, a lot of the cardiovascular studies focus on cellular and

animal models of the disease, and study the tissues of interest to gain a more detailed picture of the disease process (Doring Y *et al.*, 2012).

3.3 Analytical laboratory techniques

From an analytical point of view, metabolomic methodologies are a highly valuable tool that provides an adequate evaluation of the low molecular weight food metabolites present in biological samples (Rull A *et al.*, 2009; Vinaixa M *et al.*, 2010). The methodologies used in metabolomics experiments may use different type of biological samples. Fluids secreted or excreted from a living organism (biofluids) reflect a concrete biochemical status because their composition is a direct consequence of a cell function, an organ dysfunction or a disease. Dietary, diurnal, and hormonal variations may also influence biofluid compositions. Thus, it is important to distinguish these effects in order to conclude accurate biochemical information from biofluid analysis (Lindon JC *et al.*, 2000).

Some of the most common biofluids used in metabolomic analysis include but not limited to urine, blood plasma, blood serum, whole blood, bile, gastric juice, seminal fluid, etc. A specific analytical approach is required to analyse a biofluid, a tissue extract or an intact tissue.

Metabolomics methodologies are divided into two distinct groups: a) untargeted metabolomics, a detailed comprehensive analysis of all the measurable analytes in a sample; and b) targeted metabolomics, the measurement of previously known biochemically annotated metabolites (Roberts LD *et al.*, 2012). Buscher JM has classified metabolomic technologies into two methods:

- **Separation methods:** gas chromatography (GC), high-performance liquid chromatography (HPLC) and capillary electrophoresis (CE).
- **Detection methods:** mass spectrometry (MS) and NMR spectroscopy.

To identify and to quantify metabolites it is necessary to combine separation methods (GC, HPLC and CE) with a MS detection method.

NMR spectroscopy is the only detection method which does not based on separation of the analytes, thus the sample can be recovered for further analyses (Buscher JM *et al.*, 2009).

The major technologies that are used in metabolomics include: a) ^{1}H NMR spectroscopy, b) gas chromatography–mass spectrometry (GC–MS) and c) liquid chromatography–mass spectrometry (LC–MS). Other techniques are also used and include Fourier transform infrared (FT-IR) spectroscopy, HPLC or CE in conjunction with diode or Coulometric arrays and ion-cyclotron resonance Fourier transform (ICR-FT)-MS (Griffin JL and Shockcor JP, 2004; Puiggros F *et al.*, 2011). In this present work, we use NMR, GC-MS and LC-MS techniques to study the biological samples of interest.

3.3.1 Nuclear magnetic resonance spectroscopy

NMR spectroscopy is a non-invasive analytical chemistry technique based on the magnetic property of a molecules-atom's nucleus (Weber H and Brecker L, 2000). NMR spectroscopy has been widely used in metabolomics. It is a robust, high-throughput and non-destructive approach and its advantage is the requirement of minimal sample preparations (Lindon JC *et al.*, 2003).

NMR relies on the study of a magnetic nucleus by aligning it with a very powerful external magnetic field and disturbing the alignment using an electromagnetic field (**Figure 8**). NMR studies the nucleus response to the field after this disturbance. Different atoms, within a molecule, resonate at different frequencies at a given field strength. The observation of a molecule's frequencies allows us to discover its structural information.

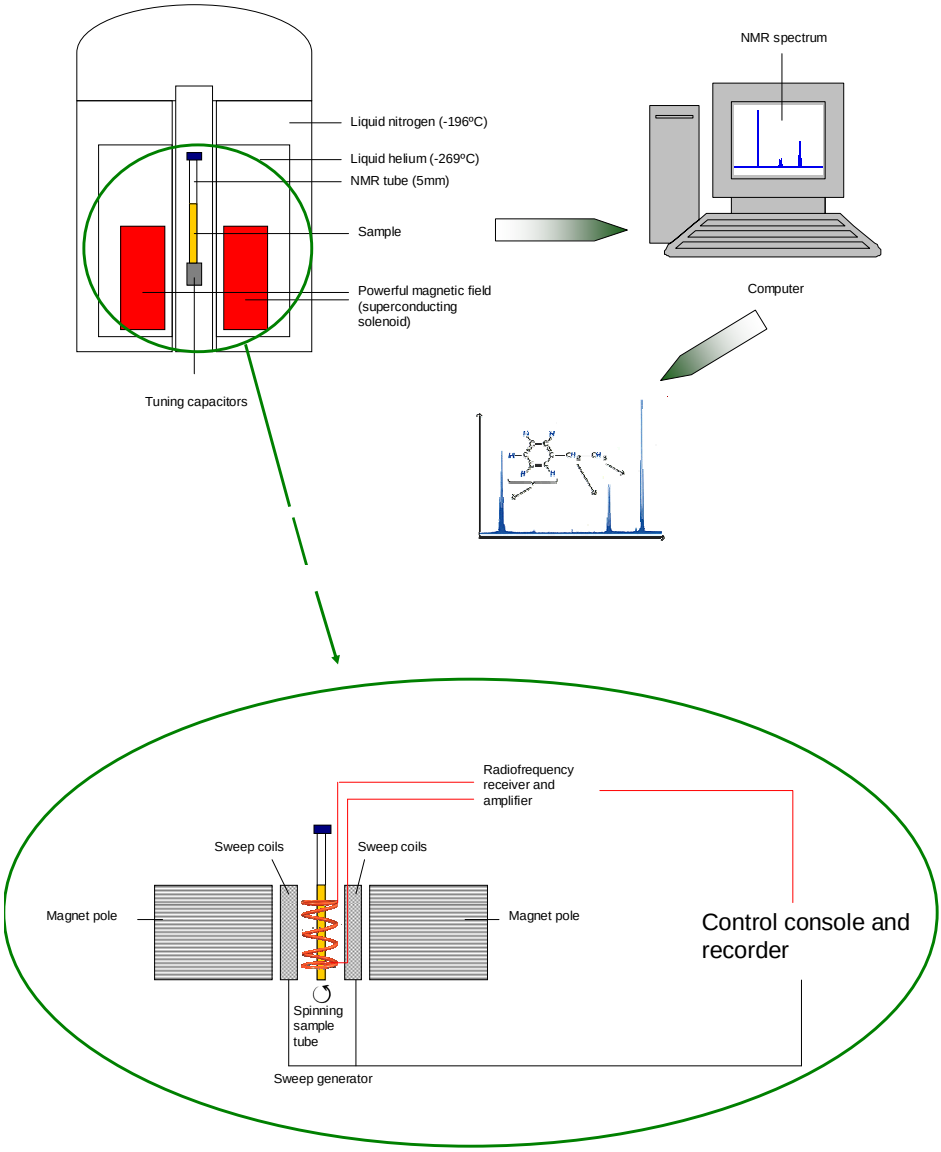

Figure 8. The basic arrangement of an NMR spectrometer. The sample is positioned in a very strong magnetic field. The super conducting magnet is cooled by liquid nitrogen and helium. Pulses of radio waves are sent into the sample which emits a radio wave response. This response is analyzed in a computer, resulting an NMR spectrum. The pulse is repeated as many times as necessary to allow the signals to be identified from the background noise. Each group of signals corresponds to protons in different part of the molecules.

The usually applied isotopes in NMR are hydrogen-1 (^{1}H) and carbon-13 (^{13}C). These isotopes are non-radioactive. Certain isotopes of many other nuclei elements may also be used. Subatomic particles (electrons, protons and neutrons) can be simulated as spinning on their axes. In some atoms (such as ^{1}H and ^{13}C) the nucleus possesses an overall spin. This overall spin is important. Quantum theories suggest that nucleus with spin has different orientations. These orientations are actually nuclear energy levels called 'spin states' where 'spin' refers to the fact that the magnetism of a given nucleus may be considered to arise from the spinning motion of its electrical charge (Bothwell JH and Griffin JL, 2011). In the absence of an external magnetic field, these orientations are of equal energy, but when a magnetic field is applied, the energy levels split (**Figure 9**).

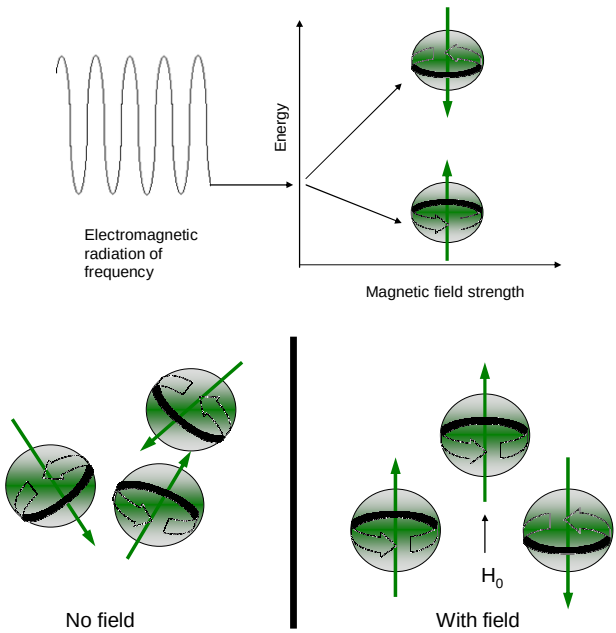

Figure 9. Energy levels for a nucleus with spin. In the absence of a magnetic field, these are randomly oriented but when a field is applied they line up parallel to the applied field, either spin aligned or spin opposed.

In the case of NMR, the nucleus is in a magnetic field and the initial populations of the energy levels are determined by thermodynamics, as described by the Boltzmann distribution. This means that lower energy levels will contain slightly more nuclei than higher levels. It is possible to excite these nuclei into higher levels, by electromagnetic radiation, which is observable by NMR signal. This signal is called free induction decay (FID). FID is a non-equilibrium nuclear spin magnetisation precessing about the magnetic field. Precessing is the motion of the axis of a spinning body, such as the wobble of a spinning top, when external force exists and acts on the axis. The FIDs may be simplified into the frequency domain, using a transformation technique called Fourier transformation (**Figure 10**). Fourier transformation is usually present in the form of a one-dimensional (1D) or two-dimensional (2D) spectrum.

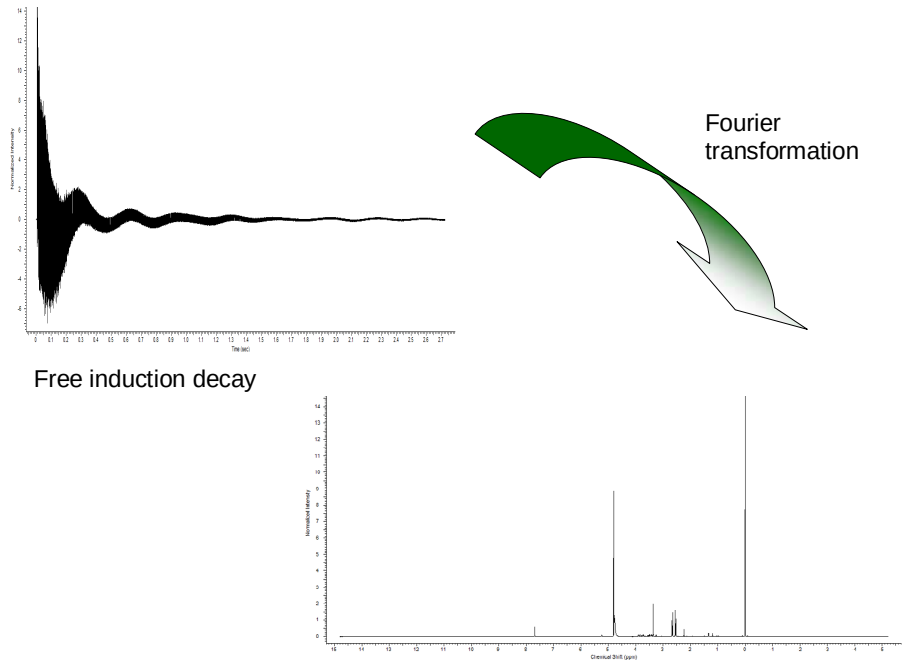

Figure 10. Free induction decay (FID) and its Fourier tranformation. The FIDs may be simplified into the frequency domain, using a transformation technique called Fourier transformation.

The energy difference between spin states depends on nuclear environment. Excited nuclei from one element, but in different nuclear environments, will emit slightly different radiofrequency (RF) wavelengths of electromagnetic radiation. In NMR, the energy of the emitted electromagnetic radiation is expressed as chemical shift, defined as the position of a peak on the spectrum. The exact value of chemical shift (usually given in parts per million; ppm) gives a reasonable indication of the molecule's identity. In order to set the scale of the spectrum, an internal standard (IS) is needed. This IS is often trimethylsilyl (TMS) or trimethylsilyl propionate (TSP). TMS or TSP are used because are the most shielded molecules and all their protons are equivalent. Therefore, it should show up as one peak which can be used to set the 0 ppm mark on the spectrum (Bothwell JH and Griffin JL, 2011).

Before the determination of which peaks correspond to specific nuclei, the scale for the chemical shifts of the spectrum must be set. Each molecule has a characteristic number and pattern of these peaks and sub-peaks. That is why a simple comparison of unidentified peaks with standard reference spectra will often allow identification of the metabolites in a sample. A number of NMR spectral databases have been set up for helping this metabolite assignation. One of the most known databases is the Human Metabolome Database (Wishart DS *et al.*, 2007).

Today, NMR spectroscopy has become one of the most powerful and flexible analytical techniques, being one of the few methods to give analytical information from the internal environment of living tissues. NMR can quantitatively analyze mixtures containing known compounds. In the case of unknown compounds, NMR can be used either to match against spectral libraries, such as previously mentioned, or to directly determine molecules basic structure. Once the basic structure is known, NMR can be used to determine molecular conformation in solution as well as studying physical properties at the molecular level like conformational exchange, phase changes, solubility, and diffusion (Bothwell JH and Griffin JL, 2011).

A NMR spectrum of a biofluid or tissue is extremely complex, consisting of thousands of well-resolved signals. Their intensities are related to the concentration of the metabolites in the sample. Moreover, NMR is applied not only to biofluids and tissues extracts, but also to intact tissue (cell cultures and/or red blood cells (RBC) suspensions), named high resolution magic angle spinning (HRMAS) ^{1}H NMR spectroscopy (Griffin JL *et al.*, 2000). The physical properties of whole blood have serious limitations when tested by NMR. RBC yield more useful information on cell biochemistry. The NMR spectra of blood serum and plasma can provide an excess of useful biochemical information on both low molecular weight metabolites and macromolecular structure and organization.

NMR-based metabolomics has the disadvantage of low metabolome coverage since it can only detect metabolites with high concentrations. Nevertheless, promising improvements have been made to resolve NMR spectroscopy sensitivity (Lenz EM and Wilson ID, 2007).

3.3.2 Mass spectrometry

MS is another analytical technique largely used in metabolomics. It becomes a very powerful tool for metabolic profiling when it is combined with a chromatographic technique and provides much better sensitivity in terms of the size of metabolome detected (Pan S *et al.*, 2009).

The chromatographic techniques commonly used and coupled to MS are GC and LC. Such techniques use a column that varies in length, diameter and chemical properties (stationary phases). A mixture of metabolites is separated as they travel through the column, depending on their different chemical properties. Metabolites elute at different time and then are subjected to MS analysis. MS mainly consists of 3 different components: ion source, mass analyzer and ion detector (**Figure 11**).

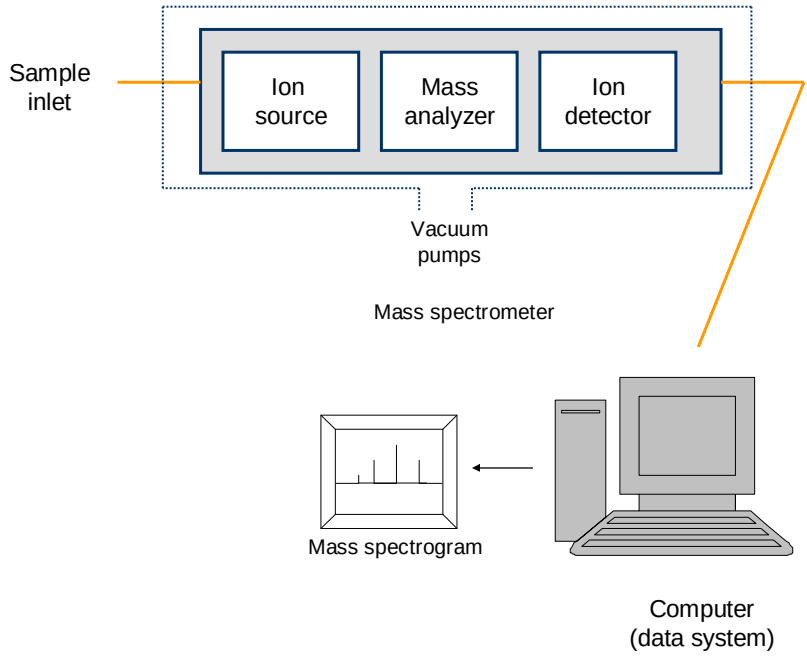

Figure 11. Mass spectrometer.

Metabolites are ionised by ion source, and then transported to mass analyzer by magnetic or electric fields. A number of ionisation techniques are available, and include electron spray ionisation (ESI) and matrix-assisted laser desorption/ionisation (MALDI). Different ionisation techniques are used depending on the nature of the samples under analysis (gas, liquid or solid). Molecular ions are further separated by mass analyzer according to their mass-to-charge ratio (m/z). Different configurations of ion source and mass analyzer are frequently used in the research. They differ in design and performance, and each one has its own strengths and limitations. These MS analysers can be stand alone or, in some cases, put together in tandem mass spectrometry (MS/MS) (Aebersold R and Mann M, 2003). A molecular ion with a specific mass is selected in the first mass analyzer, passes through a collision cell to

generate ions fragments and get separated in the second mass analyzer (Dettmer K *et al.*, 2007).

3.3.2.1 Gas chromatography-mass spectrometry

GC-MS has been widely used to analyze volatile and thermally stable metabolites and acquire high separation efficiency (**Figure 12**).

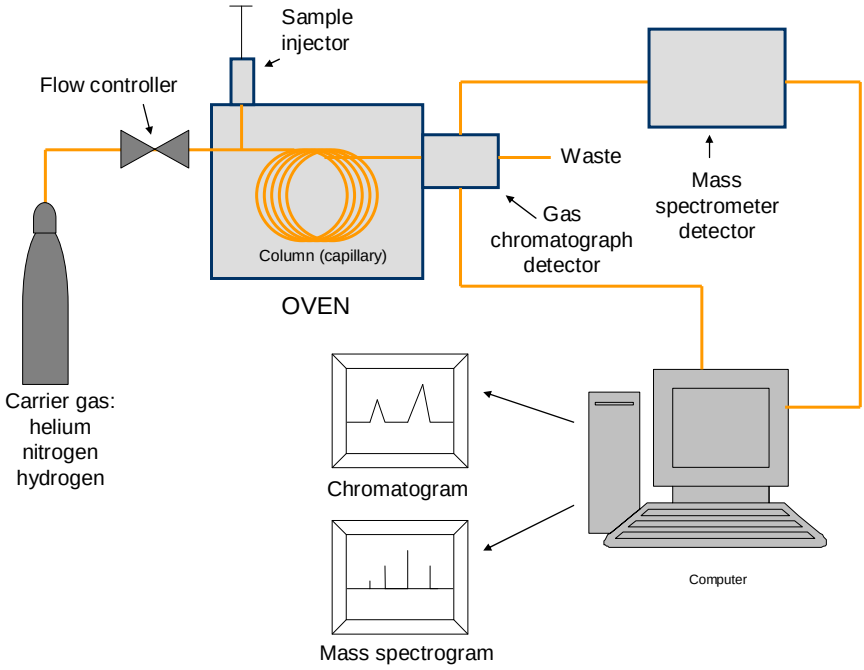

Figure 12. Gas chromatography-mass spectrometry.

Many metabolites might contain polar functional groups and might be thermally labile at temperatures required for their separation or might not be volatile at all. Therefore, derivatization prior to GC analysis is necessary to extend the application range of GC based methods. The majority of GC methods rely on derivatization with an oximation reagent followed by silylation, or solely silylation. The additional derivatisation step may introduce variability and contamination into the samples. However, GC-MS

is an overall sensitive analytical approach and metabolites are separated and detected with high resolution (Koek MM *et al.*, 2011).

3.3.2.2 Liquid chromatography-mass spectrometry

LC-MS does not require volatilized samples, thus it is not limited to particular classes of metabolites. LC-MS is the most sensitive metabolic profiling tool, and can operate in both positive electronspray ionization (ESI) and negative ESI to ensure the maximum coverage of metabolites detected (Lu W *et al.*, 2008).

Metabolite extraction from each biofluid sample is required before the injection into the LC column. The flow liquid carries compounds through the column. The column retains metabolites based on physical properties, and the different metabolites reach the mass spectrometer at different times. Ion abundances for each individual mass are measured relatively to the time each extract is injected to the chromatography column and the time of elution of that extract (retention time). Calculation of the area under the chromatographic peak for a particular mass and retention time provides a measurement of the quantity of the eluted metabolite at that time.

LC-MS suffers from a matrix effect known as ion suppression. Ion suppression causes errors in the quantification of metabolites of interest. Less volatile compounds are capable of altering the efficiency of droplet formation or evaporation, consequently changing the amount of charged ions that reaches the detector (Annesley TM, 2003).

3.3.2.2.1 Ultra performance liquid chromatography coupled to tandem mass spectrometry

Ultra performance liquid chromatography (UPLC), which employs sub-2-μm porus particle columns, gives superior sensitivity and resolution compared to the conventional LC (Want EJ *et al.*, 2010). The sub-2-μm stationary phases operate at high linear mobile-phase velocity and the sensitivity is increased when combined with MS. This allows the detection and

identification of more impurities in comparison to traditional HPLC methodology (Jones MD and Plumb RS, 2006).

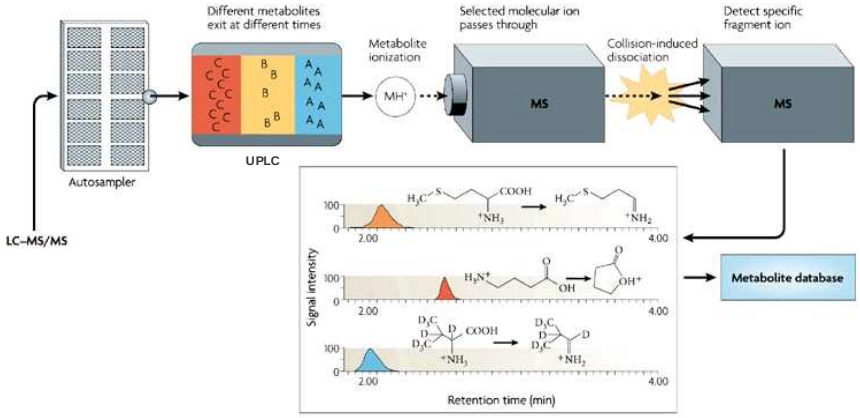

Figure 13. Ultra performance liquid chromatography coupled to tandem mass spectrometry. UPLC-MS/MS provides physical separation of metabolites, introducing different compounds into the mass spectrometer at different times. Chromatography decreases analysis speed but offers two main benefits: metabolites with identical masses but different retention times can be distinguished, and the separation of metabolites from interfering substances allows for improved quantitative accuracy. Adapted figure from: (Last RL *et al.*, 2007)

Nowadays, there are some exciting approaches based on platform developments and incipient trends pointing towards a convergence of the "untargeted-discovery" and "targeted-verification" dichotomy. The technological developments in progress, such as faster separations, more-effective ion sources, higher MS resolution, and detectors with higher dynamic ranges, will increasingly allow broad untargeted measurements that retain the benefits of targeted measurements (Smith RD, 2012). For example, for targeted metabolic profiling analyses, two steps of mass spectrometry (MS/MS) filter out interfering signals, after molecular ions are broken into fragments, between the mass-analysis steps. Reductions in background interference by the MS/MS technique allow for more rapid and accurate metabolite analyses, which are necessary in large-scale

metabolite-profiling studies (**Figure 13**). The coupling of UPLC technique to MS/MS further enhances specificity and provides an improved signal-to-noise ratio compared with single-stage MS (Alnouti Y *et al.*, 2008).

Chapter 4. Research Studies

In the present work, we are particularly interested to study:

1. The effect of natural products, with unknown anti-inflammatory (peanut extract) and endothelial function properties (alpha-tocopherol; AT) on the modulation of risk factors for inflammation and endothelial dysfunction, after their incubation in cellular models.

2. The characterization of two matrices of biofluids, such as RBC and plasma, by means of metabolomics techniques and their application into the novel nutritional biomarkers investigation.

For this reason, it is of utmost importance to introduce specific background knowledge of the field. These concepts are organized based on the three studies performed during the present work.

4.1 Inhibition of the Transcription factor c-Jun by the MAPK family, and not the NF-κB Pathway, Suggests that Peanut Extract has Anti-inflammatory Properties (Study 1)

4.1.1 Lipopolysaccharide such as pro-inflammatory inductor of atherosclerosis

Atherosclerosis is a complex inflammatory process involved in CVD, the principal cause of morbidity and mortality in industrialized countries (Gerszten RE *et al.*, 2011). Inflammation is characterized by the presence of monocytes/macrophages and T lymphocytes in the atheroma plaque (Ross R, 1999a). Monocytes promote atherosclerosis via production of various key mediators such as TNF-α. TNF-α is commonly found in

atherosclerotic lesions contributing to the inflammatory process (Katsume A *et al.*, 2011). Concentrations of TNF-α are increased in patients with increased risk of atherosclerosis (Devaraj S *et al.*, 2002).

The mechanisms underlying the first part of the pro-inflammatory lipopolysaccharide (LPS)-induced TNF-α signaling pathway have been well described (Gee K *et al.*, 2002). The exposure of cells to LPS, which is a major component of the outer membrane of Gram-negative bacteria, triggers the binding of LPS to the LPS bearing protein (LBP) and is transferred to the CD14 at the cell surface. LPS then interacts with the signaling toll-like receptor 4 (TLR4) and the accessory protein MD-2. LPS stimulates the activation of various mitogen-activated protein kinase (MAPK) family pathways, including the extracellular signal-regulated kinase (ERK) 1 and 2, c-Jun N-terminal kinase (JNK), and p38 pathways. These pathways directly or indirectly phosphorylate and activate various transcription factors including Elk-1, c-Jun, c-Fos, ATF-1, ATF-2, SRF, and CREB. In addition, LPS activates the IKK pathway which in turn phosphorylates IkBs. Subsequent degradation of

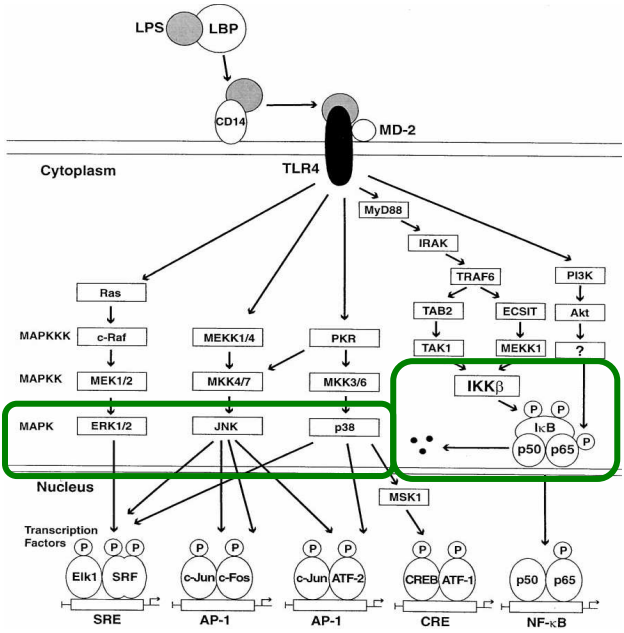

Figure 14. LPS stimulation of monocytes activates signaling pathways and transcription factors. LPS stimulates the activation of various MAPK pathways, including the ERK, JNK, and p38 pathways. These pathways directly or indirectly phosphorylate and activate various transcription factors. In addition, LPS activates the IKK pathway which in turn phosphorylates IκBs. Subsequent degradation of IκBs permits nuclear translocation of NFκB/Rel complexes, such as p50/p65. Source: (Guha M and Mackman N, 2001)

IkBs permits nuclear translocation of nuclear factor-κB (NF-κB) complexes such as p50/p65 (Guha M and Mackman N, 2001). The PI3K-Akt pathway phosphorylates and activates p65 via an unknown kinase. In the nucleus, activated transcription factors bind to recognition elements in the promoter regions of inflammatory and immune genes (**Figure 14**). These include pro-inflammatory cytokines, chemokines, inflammatory enzymes and adhesion molecules such as TNF-α (Barnes PJ and Karin M, 1997).

4.1.2 TNF-α production by LPS stimulated monocytes

TNF-α is assembled intracellularly to form a trans-membrane protein which contains a cytoplasmic domain, a trans-membrane segment and an extracellular region (**Figure 15**). There are two forms of TNF-α: the full-length type II membrane-bound form, and the soluble form resulting from a proteolytic cleavage that releases the active C-terminal portion from the cell surface to the extracellular medium (Black RA, 2002). This proteolysis converts membrane bound "pro" form (pro-TNF-α) into its biologically active

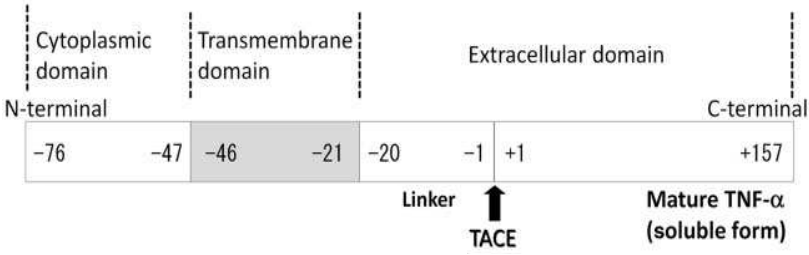

Figure 15. Structure of TNF-α. Transmembrane TNF-α is composed of an extracellular domain, a transmembrane domain and an intracellular domain. Mature TNF-α (soluble TNF-α) is cleaved from transmembrane TNF-α by TACE (black arrow). The transmembrane domain of transmembrane TNF-α is shaded as well and, the intracellular domain is translocated into the nucleus to possibly modulate gene expression of the TNF-α-bearing cells. Adapted figure from: (Horiuchi T *et al.*, 2010)

soluble form (**Figure 16**); sTNF-α (Ishisaka R *et al.*, 1999; Horiuchi T *et al.*, 2010). This proteolysis is supervised by a protease. TNF-α converting enzyme (TACE) also called ADAM17 (a disintegrin and metalloprotease) family of proteins possess α-secretase activity

(Katakowski M *et al.*, 2007; Zheng X *et al.*, 2007). TNF-α can be cleaved by TACE to release a soluble, mature subunit (sTNF-α; 17 kDa) that becomes biologically active (Tang P *et al.*, 1996; Black RA *et al.*, 1997; Ramana KV, 2010; Chou YC *et al.*, 2011).

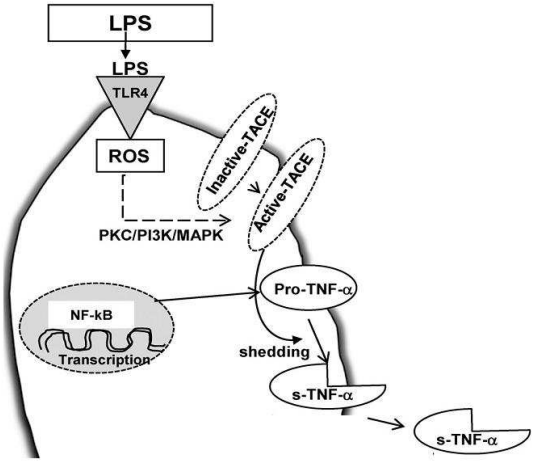

Figure 16. TACE mediated ectodomain shedding of TNF-α. LPS-induced TNF-α processing by TACE. Adapted figure from: (Ramana KV, 2010)

TACE is a multi domain type 1 transmembrane protein (**Figure 17**). TACE requires cleavage of its pro domain to become a "mature" and fully active protease. TACE can be activated by nitrosation, alkylation and oxidation, resulting in the dissociation of cysteine thiol-zinc linkage and thereby release of the pro domain inhibitory function.

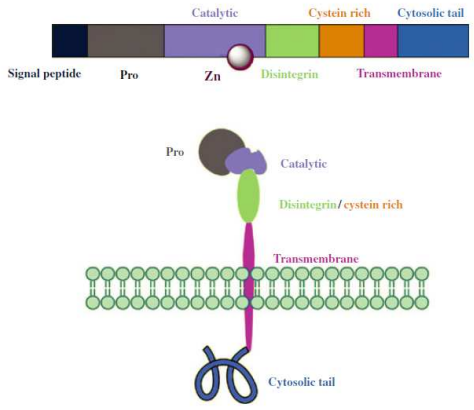

Figure 17. TACE. Domain structures from TACE. A single transmembrane domain defines the topology of TACE as a class-I membrane protein with Pro, Catalytic and Cys domains. Source: (Bahia MS and Silakari O, 2010)

Pro domain removal mainly occurs by autocatalysis and action of furin of related pro-hormone convertases in Golgi compartment. The role of disintegrin domain in TACE is not known but it may have an adhesion function as this domain has been shown to interact with integrins in some other ADAMs.

The function of cytoplasmatic tail is not definite but it seems to be involved in the control of TACE's intracellular trafficking. Most important, the catalytic domain of Zn metalloproteases possesses a conserved zinc ligating sequence. TACE is a promising target for treatment of many inflammatory diseases (Ramana KV, 2010).

Although the mechanism of the LPS-induced TNF-α signaling pathway via MAPK and NF-κB activation has been well described in monocytes (Beutler B, 2000; Witkamp R and Monshouwer M, 2000; Dayer JM *et al.*, 2005), there is a gap in the knowledge of which molecules are involved, starting from the TNF-α mRNA expression and extending to the extracellular protein secretion of TNF-α. The first route of diversification of proteins is at the transcriptional level (by mRNA splicing and including tissue-specific alternate splicing, editing and stability (Cheneval D *et al.*, 2010; Subramaniam D *et al.*, 2011)). The second route to proteome expansion is the post-translational modification (PTM) of proteins at one or more sites (Walsh CT *et al.*, 2005). Therefore, NF-κB and MAPK family needs to be

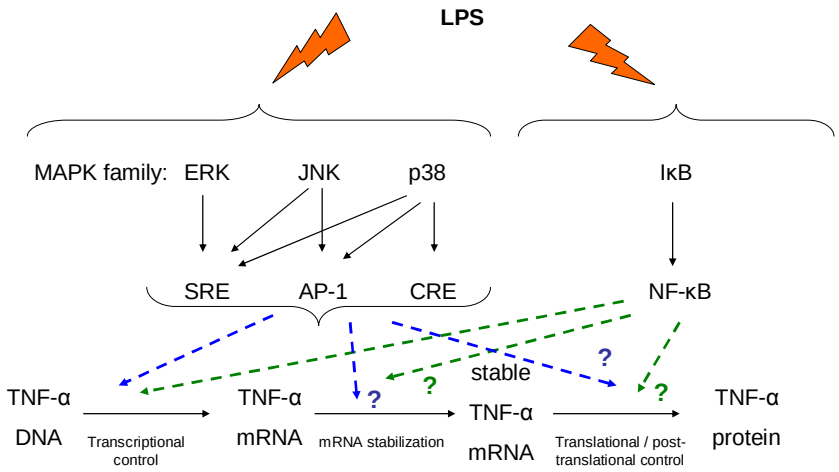

Figure 18. Possible relationships to transcriptional and post-transcriptional regulation of TNF-α expression.

evaluated more thoroughly so that the inflammatory route that follows TNF-α in atherogenic inflammation may be better understood. Targeting the proximal triggers such as TNF-α would be the more promising strategy for interrupting inflammation in atherogenesis (Ishisaka R *et al.*, 1999). Possible relationships to transcriptional and post-transcriptional regulation of TNF-α expression mediated by NF-κB or MAPK family transcription factors is shown in **Figure 18**.

Further, BAY 11-7082 ((E)3-[(4-methylphenyl)sulfonyl]-2-propenenitrile; BAY) is a synthetic molecule that has demonstrated anti-inflammatory activity by inhibiting the NF-κB and MAPK pathway that can be used as control product in comparing the anti-inflammatory effects of test molecules (Barnes PJ and Karin M, 1997; Guha M and Mackman N, 2001; Black RA, 2002). However, the effect of BAY on TACE activity on monocyte THP-1 cells has not been evaluated, to date.

4.1.3 Natural extracts or compounds such as anti-inflammatory substratum

Some natural extracts (or compounds) of certain foods have anti-inflammatory properties and *in vitro* cellular models can be used to screen for biological activity (Singh U *et al.*, 2005). When a natural extract or compound shows anti-inflammatory effects, the different mechanism of action ought to be explored systematically in the same cell model so as to improve the methodological reliability (Essafi-Benkhadir K *et al.*, 2012). Dried fruits, for example, are rich in polyphenols and exert beneficial effects on inflammation and, as a result, decrease CVD progression (Kris-Etherton PM *et al.*, 2002; Calixto JB *et al.*, 2003; Ortega RM, 2006).

The polyphenol-rich peanut extract

There have been many studies published on the harmful effects of peanuts (**Figure 19**), such as the allergy promoted by this natural extract (Chen X *et al.*, 2011; Moverare R *et al.*, 2011; Schulz VJ *et al.*, 2011). However,

Figure 19. Peanuts.

there is a paucity of studies addressing its potential beneficial effect on atherosclerosis resulting from its anti-inflammatory activity.

4.2 Alpha-Tocopherol and BAY 11-7082 Reduce Vascular Cell Adhesion Molecule In Human Aortic Endothelial Cells (Study 2)

4.2.1 TNF-α such as inductor of endothelial dysfunction in atherosclerosis

Atherosclerosis can be considered the clinical endpoint of an inflammatory process and endothelial dysfunction. The binding of monocytes to the vascular endothelium is mediated by cross-linkage of cell adhesion molecules (CAMs) such as VCAM-1, E-selectin and/or ICAM-1. The cell surface expression of these molecules is greatly increased in atherosclerotic lesions as a result of stimulation by pro-inflammatory cytokines such as TNF-α. This cytokine has been selected as a stressor molecule in assessing the underlying mechanisms because it induces release and surface expression of CAMs, all of which contribute to the inflammatory process and endothelial dysfunction (Amberger A *et al.*, 1997; Wu D *et al.*, 1999; Zhou Z *et al.*, 2005; Davis PA *et al.*, 2006; Lee G *et al.*, 2006). Further, there is *in vivo* evidence of increased VCAM-1 production in animal models of inflammation (Lee G *et al.*, 2006).

4.2.2 The role of cellular adhesion molecules

Endothelial CAMs are known to be up-regulated in atherosclerotic endothelium in an environment of circulating blood. They participate in leukocyte recruitment and, subsequently, in atherosclerosis progression and/or tissue damage (Dagia NM *et al.*, 2004).

E-selectin is an inducible endothelial cell surface glycoprotein of the selectin family of adhesion molecules. It mediates the binding of

neutrophils, eosinophils, monocytes and T lymphocytes to the endothelium (Vannini N *et al.*, 2008).

VCAM-1 and ICAM-1 are members of the immunoglobulin superfamily of CAMs. They mediate lymphocyte adhesion to major elements of the aortic wall such as endothelial cells and vascular smooth muscle cells (Lawson C and Wolf S, 2009).

Induction of these three CAMs (VCAM, ICAM and E-selectin) by TNF-α is regulated at the level of gene transcription, and requires the transcription NF-κB. Located in the cytoplasm of cells in an inactive form in close association with the inhibitor IκB-α, NF-κB binds to regulatory regions within promoter regions of the VCAM-1 gene (Pierce JW *et al.*, 1997; Dieguez-Acuna FJ *et al.*, 2004) via a process involving the phosphorylation and degradation of IκB-α (Pierce JW *et al.*, 1997; Spiecker M *et al.*, 1997; Izban KF *et al.*, 2000).

In vitro studies indicate that VCAM-1, E-selectin and ICAM-1 are involved in adhesion of eosinophils, monocytes and T lymphocytes via their cell surface (Martin KR *et al.*, 2000). Proteolytic cleavage of membrane-bound CAMs result in the release of their soluble forms: soluble CAMs (sCAMs) i.e. sVCAM-1, sE-selectin and sICAM-1 (Leeuwenberg JF *et al.*, 1992; Just N *et al.*, 2003; Dagia NM *et al.*, 2004; Constans J and Conri C, 2006).

BAY is an anti-inflammatory and antioxidant molecule that selectively and non-reversibly inhibits the inducible phosphorylation of IkB-α in human pancreatic MIA PaCa-2 cancer cells (Kamthong PJ and Wu M, 2001) and endothelial cells (Kopp E and Ghosh S, 1994). As such, IkB-α avoids being degraded, resulting in a high level of cytosolic NF-κB sequestered by IkB, together with decreased transcription and surface expression of the adhesion molecules (Kamthong PJ and Wu M, 2001).

However, the effect of BAY (**Figure 20**) on VCAM-1 mRNA expression and its soluble protein (sVCAM-1) on endothelial dysfunction induced by TNF-α in human aortic endothelial cells (HAEC) has not, as yet, been evaluated in detail.

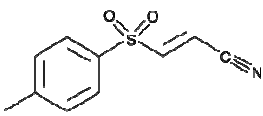

Figure 20. Molecular structure of BAY 11-7082.

4.2.3 Natural extracts or compounds may improve endothelial dysfunction

Some natural compounds or extracts of certain foods have been described as reversing endothelial dysfunction (Wu D *et al.*, 1999; Martin KR *et al.*, 2000; Chen YH *et al.*, 2001; Chen JW *et al.*, 2003; Davis PA *et al.*, 2006). Prior to evaluating these functions in *in vivo* studies in animals or/and human subjects, *in vitro* cell models are developed to test the effects of these natural extracts (or compounds) based on the expression of cellular adhesion molecules in TNF-α-stimulated cells. As such, *in vitro* models facilitate the study of cells under controlled conditions and can be used as tools to examine the effects of various natural or synthetic pharmacologically active compounds.

Dietary factors play significant roles in the etiology of atherosclerosis by influencing inflammatory and endothelial dysfunction processes associated with the development of this disease.

The AT molecule

Vitamin E, especially AT (**Figure 21**) the main fat-soluble dietary antioxidant (Saremi A and Arora R, 2010), is very effective in reducing the adhesion of monocytes to HAEC *in vivo* and *in vitro* (Liu L *et al.*, 2004).

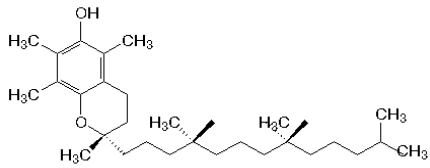

Figure 21. Molecular structure of Vitamin E (alpha-tocopherol).

Several studies have demonstrated that vitamin E decreases cytokine-stimulated HAEC production of chemokines such as sVCAM-1, sICAM-1 (Lee G *et al.*, 2006), interleukine-6 (IL-6), and IL-8 (Liu L *et al.*, 2004) when stimulated with IL-β. Also, VCAM-1 mRNA expression level is consistently elevated when incubated for between 6 and 24h with TNF-α (10 ng/mL) and LPS (10 μg/mL) in human umbilical vein endothelial cells (HUVEC); the levels remaining high under these conditions (Raab M *et al.*, 2002; Tribolo S *et*

al., 2008). However, effects of AT on endothelial dysfunction induced by TNF-α in HAEC are not well documented.

Some of the foods with high AT content, and the bioavailability of this form of vitamin E is highest, are ground hazelnuts, canola-based margarine, wheatgerm oil and other vitamin E-rich foods such as avocado and pumpkin (McGavin JK *et al.*, 2001).

4.3 Biomarkers of Food Intake and Metabolite Differences Between Plasma and Red Blood Cell Matrices; a Human Metabolomic Profile Approach (Study 3)

4.3.1 Blood samples

Whole blood is a biofluid containing RBC. It has active metabolism, mainly the glycolytic or Krebs cycle, catalyzed by a range of enzymes. The whole blood contains about 45-50% of RBC and the abundance of other cell types is around 1%. Serum and plasma represents about 55% of total blood and consist mainly of water with a number of distinct molecules. These include macromolecules such as proteins, lipids, and immunoglobulins.

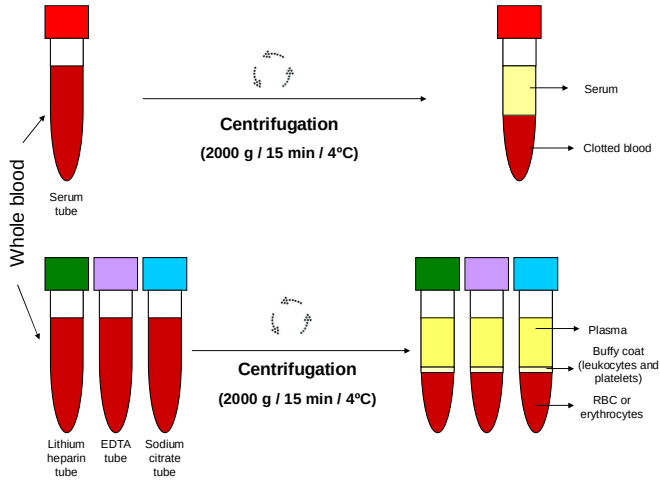

Figure 22. Whole blood separation. Serum or plasma represents 55% of total blood; leukocytes and platelets less than 1% and RBC or erythrocytes about 45-50% of whole blood.

Serum is the yellowish fluid obtained after untreated whole blood centrifugation and separation into its solid and liquid components. Serum tubes may include a gel with intermediate density between blood cells and serum. When the tube is centrifuged, a layer of the gel covers the blood cells sink to the bottom of the tube,, and the serum is left on the top. Serum is depleted in the major clotting protein precursor and is consequently less viscous than plasma (**Figure 22**). Plasma is separated from whole blood after the addition of an anticoagulant to the tube extraction that is normally ethylenediaminetetraacetic acid (EDTA), lithium heparin or sodium citrate. A specific analytical approach is required to analyse a biofluid, a tissue extract or an intact tissue.

4.3.2 Blood sample collection

Intrinsic changes could arise from blood sample collection (sodium citrate *vs.* lithium heparin as anticoagulants) and the subsequent comparison between aqueous *vs.* organic phases of two different matrices such as plasma *vs.* RBC. In the current metabolomics study, analyses of plasma and RBC samples obtained from both anticoagulant tubes will be compared based on a battery of untargeted and several targeted analyses covering different families of compounds with potential interest in the field of nutrition.

Hence, sensitive methods such as, have been used in metabolomics to detect and quantify biomarkers of nutrient intake and/or dietary patterns as well as to assess the relationships between nutrition and the risk of disease (Puiggros F *et al.*, 2011). The combination of various 'omics' technologies (systems biology) will greatly facilitate the discovery of new biomarkers associated with specific nutrients of dietary factors (Zhang X *et al.*, 2008). The identification and optimization, in plasma or in RBC, of biomarkers of dietary consumption can extend the evaluation of nutritional status (Doring Y *et al.*, 2012).

4.3.3 Plasma and RBC matrices

In human studies, the volume of blood that can be accessed from the individual for diagnostic and/or research purposes is limited and, since most analytes are measured in plasma or serum, the erythrocytes or RBC are usually discarded. However, RBC could be an important source of nutritional information not previously accessed (Darghouth D *et al.*, 2010). New dietary biomarkers measured in RBC (Jenab M *et al.*, 2009) may reflect longer-term markers of nutritional intake compared with plasma or urine and, as such, their measurement extends the emerging field of nutritional metabolomics.

Traditionally, serum lipids have been studied in lipoproteins separated by ultracentrifugation. Further analyses have been limited to the distributions of several lipid species such as cholesterol, phospholipids and triglycerides. More recently, metabolomics empowers the study of the full spectrum of lipids and lipoproteins in greater detail (Orešič M, 2009). Quantitative and/or qualitative measurements of dietary fatty acid (FA) are key nutritional factors in CVD evaluation and prevention. The FA profile, as measured in RBC, reflects the medium-term dietary intake (a matter of weeks) (Shearer GC *et al.*, 2009) while plasma FA levels reflect more recent intake (matter of days). As such, under certain circumstances, the RBC profile may provide more valuable information (Hodson L *et al.*, 2008; Assies J *et al.*, 2010; Caspar-Bauguil S *et al.*, 2010). FA composition of cell membranes is dependent on dietary fat intake as well as that from intermediate metabolism (Fuhrman BJ *et al.*, 2006). For example, blood concentrations of eicosapentaenoic acid (EPA), and docosahexaenoic acid (DHA) n-3 are appropriate biomarkers of FA from fish intake (Arab L and Akbar J, 2002; Arab L, 2003; Kuriki K *et al.*, 2006). RBC FA *vs*. plasma FA profiles could provide differential FA biomarkers of not only fish intake but also dairy products. However, this hypothesis has not been explored systematically, to date.

Other molecules such as polyphenols reflect food intake of, mainly, fruits and vegetables. Food rich in polyphenols have protective effects against

chronic diseases such as CVD. Polyphenols are bioactive compounds that display several biological activities, including, anti-oxidant and anti-inflammatory properties (Gonzalez R *et al.*, 2011), and can exert their effects on RBC (Paiva-Martins F *et al.*, 2009; Hapner CD *et al.*, 2010; Koren E *et al.*, 2010; Rizvi SI and Pandey KB, 2010). There have been studies assessing the polyphenols associated with RBC (Fiorani M *et al.*, 2003; Maccaglia A *et al.*, 2003; Koren E *et al.*, 2010) but, to the best of our knowledge, the individual basal types and concentrations of polyphenols of human RBCs have not been evaluated.

Analytical methods are being developed to describe metabolic profiles as indicators of dietary patterns, dietary changes or effectiveness of dietary interventions (Sengupta A and Ghosh M, 2011). Traditional dietary assessment methods are indirect and remain difficult to prove effectiveness of dietary interventions and, often, can obscure disease risk associations (Jenab M *et al.*, 2009).

Challenges associated with the use of metabolomics technology in human nutritional research involve, among others, the standardization of sample collection (Gibney MJ *et al.*, 2005). This becomes mandatory when large-scale human nutritional metabolomics studies are planned. Conversely, serum/plasma or other bio-fluid availability is also an issue in such studies which usually involve larger number of determinations than nutritional metabolomics analysis.

HYPOTHESIS AND OBJECTIVES

EFFECT OF FOOD EXTRACTS AND BIOACTIVE FOOD COMPOUNDS ON THE MECHANISM OF ATHEROSCLEROSIS AND NUTRITIONAL BIOMARKERS

Úrsula Catalán Santos

Dipòsit Legal: T. 1058-2012

Hypothesis

We hypothesize that atherosclerosis-specific biological cell approach, such as THP-1 monocytes and HAEC, could be used successfully to study the mechanism-of-action of food extracts and/or bioactive compounds while assessing their effects on inflammation and endothelial dysfunction. Further, we hypothesize that two different biological samples, RBC and plasma from the same blood extraction, can provide complementary metabolomic profile information.

Objectives:

1. To standardize experimental methodology for testing the mechanism-of-action of food extracts (such as polyphenol-rich peanut extract) and bioactive compounds (such as AT) while assessing their effect on inflammation and endothelial dysfunction. The procedures used are:

- **a)** THP-1 monocyte system; a LPS-inflammation model exposed to peanut extract. Measurements include the TNF-α cascade: NF-κB and MAPK family, TNF-α mRNA expression, TNF-α mRNA stability, TACE activity and total TNF-α protein including intra- and extracellular protein (**Study 1**).
- **b)** TNF-α-stimulated HAEC; an endothelial dysfunction model to study the effect of the AT molecule on different CAMs such as: ICAM-1, VCAM-1 and E-selectin. Measurements were conducted at the mRNA and soluble protein level to explore their individual involvements in leukocyte adhesion to endothelium (**Study 2**).

2. To apply and standardize high-throughput metabolomic analytical techniques such as NMR spectroscopy, GC-MS and UPLC-MS/MS to characterize the metabolomic profile of human RBC and human plasma (**Study 3**).

MATERIAL AND METHODS

EFFECT OF FOOD EXTRACTS AND BIOACTIVE FOOD COMPOUNDS ON THE MECHANISM OF ATHEROSCLEROSIS AND NUTRITIONAL BIOMARKERS

Úrsula Catalán Santos

Dipòsit Legal: T. 1058-2012

1. Inhibition of the Transcription factor c-Jun by the MAPK family, and not the NF-κB Pathway, Suggests that Peanut Extract has Anti-inflammatory Properties (Study 1)

1.1 Reagents

LPS (*Escherichia coli* O55:B5), dimethyl sulfoxide (DMSO) and actinomycin D (Act D) from *Streptomyces sp.* were obtained from Sigma-Aldrich (Madrid, Spain). Ethanol was obtained from Panreac (Barcelona, Spain). Phosphate-buffered saline (PBS) was purchased from Gibco (Barcelona, Spain). Radio-immunoprecipitation assay lysis buffer (RIPA) was generated using the following base ingredients (50mM Tris-HCl, pH 7.52; 150mM NaCl; 0.1% SDS; 1% Nonidet; 0.5% sodium deoxycholic acid) and complete protease inhibitor cocktail (CPIC; Roche Applied Science, Valencia, Spain). To preempt cytotoxicity, ethanol and DMSO concentrations never exceeded 0.1% (v/v) in culture media. Acetone and hexane were purchased from JT Baker (Tarragona, Spain).

1.2 Peanut extract preparation and composition

Peanut extract was kindly supplied by La Morella Nuts (Castellvell del Camp, Tarragona, Spain). The process of extraction was according to the method of Ortega and Monagas (Monagas M *et al.*, 2007; Ortega N *et al.*, 2008). Briefly, the extract was obtained from the skins of roasted peanuts. The peanut skins were ground in a laboratory mill and freeze-dried before extraction with phenol. To achieve maximum extraction efficiency, the raw material was first defatted with hexane (ratio of 1:10; W_{skin}:V_{hexane}) for 15 min in an ultrasound sonicator (Selecta, Tarragona, Spain) containing ice to avoid warming. The defatted skins were then extracted thrice with hexane, and filtered. The organic solvent was removed by rotary evaporation (Büchi R-210, Tarragona, Spain) under partial vacuum. The phenolic extract was obtained by treating the defatted skin with a solution of acetone in MilliQ water (1:1, v/v) in a ratio 1:10 (W_{skin}/V_{sol}). Initially, a soaking process is

needed with manual mixing. The extraction process proceeds in an ultrasound sonicator with ice to avoid warming. The extracting solvent is removed by vacuum filtration and the partially extracted skins are extracted three more times with the same extracting solution. The phenolic extracted fraction is obtained after removing the acetone solvent by rotary evaporation under partial vacuum. Finally, the aqueous extract is freeze-dried in a lyophilizer (Cryodos Telstar, Tarragona, Spain) to obtain the peanut extract to be used in the experiments described.

The bioactive peanut extract phenolic profile is composed by 39% flavonols, 37% flavanols and 24% phenolic acids, dissolved in 3.75% DMSO.

1.3 Cell culture

The THP-1 human monocyte cell line (**Figure 23**), derived from peripheral blood of a 1 year old male with acute monocytic leukemia, was purchased from *Deutsche Sammlung von Mikroorganismen und Zellkulturen GmbH* (DSMZ; Braunschweig, Germany). The THP-1 cell line, rather than human monocytes, was used so as to minimize inter- and intra-experiment variability.

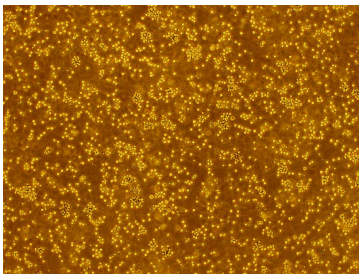

Figure 23. THP-1 monocyte cells.

THP-1 cells were routinely cultured in a humidified incubator containing 5% CO_2 and 95% O_2 at 37 ºC using RPMI medium 1640 + Glutamax-I (Gibco, Spain) supplemented with 20% of heat-inactivated fetal bovine serum (FBS; PAA, Labclinics; Barcelona, Spain) for the two first days followed by 10% FBS + 100 U/mL penicillin and 100 mg/mL streptomycin for further growth and experiments.

Dose-effect and time-response experiments with LPS, BAY and peanut extract were standardized in the course of establishing final experimental conditions. For example, THP-1 cells were plated at a density of $5x10^5$

cells/mL for every experiment conducted, while $1x10^6$ cells/mL was the cell density used for the determination of NF-κB and MAPK family.

Subsequently, THP-1 cells were pre-incubated with peanut extract (5, 25, 50 and 100 µg/mL), BAY (5µM) and/or the vehicle control (3.75% of DMSO) for 1h, depending on the study requirements. After 1h, LPS (500 ng/mL) was added for 4h (for most experiments) or 1h (for NF-κB and MAPK family) or 2h (for TNF-α mRNA stability) to the cell culture medium to induce cell stimulation. Finally, supernatants were isolated and stored at -20 ºC for batched analyses to detect extracellular TNF-α protein, and to measure the activity of lactate dehydrogenase (LDH) release. Cell extracts were lysed in each experiment and stored at -80 ºC for batched measurement of NF-κB, MAPK family, TNF-α mRNA expression and its mRNA stability, intracellular TNF-α protein, and TACE activity.

1.4 Cytotoxicity

A colorimetric assay to measure the activity of LDH release (the LDH Cytotoxicity Detection Kit; Roche Applied Science, Mannheim, Germany) was used to determine cell cytotoxicity. Briefly, LDH is rapidly released into the cell-culture supernatant when the plasma membrane is damaged, and this provides an index of cellular cytotoxicity. LPS treatment was taken as the maximum stress status for the cells, and possible cytotoxicity.

The control culture medium (RPMI-1640 + 10% FBS + LDH released from cells) has high OD at 492nm and is useful as an internal control. Results are expressed as mean optical density (OD) and standard deviation (SD) of the LDH absorbance produced by the cells under each of the treatment conditions.

1.5 NF-κB (p65) and MAPK family transcription factor assay

Activation of NF-κB (p65) and MAPK family from nuclear extracts was measured using the TransAm® NF-κB and MAPK family kit, respectively (Active Motif, Carlsbad, CA). Briefly, this is an enzyme linked immuno-

sorbent assay (ELISA)-based assay during which, when nuclear or whole-cell extract is added, the activated transcription factor-of-interest binds the oligonucleotide at its consensus binding site and is quantified using the linked antibody which is specific for the active form of the transcription factor being studied. The NF-κB and MAPK family detection was according to the manufacture's instructions. Peanut extract at different concentrations (5, 25 and 100 µg/mL) or BAY (5 µM) were incubated with THP-1 for 1h and, then, the cells were stimulated with LPS (500 ng/mL) for a further 1h. Results were expressed as percentage (SD) of NF-κB or OD (SD) of MAPK family activity under each treatment condition.

1.6 Analysis of mRNA expression by RT-PCR

Messenger RNA (mRNA) of TNF-α was measured by reverse transcription-polymerase chain reaction (RT-PCR) after total RNA had been isolated from cells. Cells were lysed with nucleic acid purification lysis solution and total RNA was isolated from cells using the ABI PRISM 6100 Nucleic Acid PrepStation extraction system (Applied Biosystems, Foster City, USA) following the manufacture's protocol. Total RNA was quantified using Quant-it^{TM} RNA Assay Kit. Using 2720 Thermal Cycler (Applied Biosystems, Foster City, USA), 0.5 µg of total RNA was reverse transcribed to cDNA at 42 ºC for 50 min, using Random Hexamers, SuperScript II reverse transcriptase and RNAse Out according to the manufacturer's protocol. To determine the amount of TNF-α mRNA, quantitative real-time PCR was performed using the ABI PRISM® 7900HT Sequence Detection System (Applied Biosystems, Foster City, USA) with the following profile: 95 ºC denaturing (20s), 40 cycles of extension at 95 ºC (1s), and 60 ºC (20s). TNF-α gene expression results were reported as increase/decrease using $2^{-\Delta\Delta Ct}$ mathematical method, using glyceraldehyde 3-phosphate dehydrogenase (GAPDH) as housekeeping gene to normalize the results. The LPS-activated monocytes (500 ng/mL) were defined as the calibrator in these experiments, setting its value at 1 and the other conditions in relation to it. The expression of TNF-α mRNA in cultured THP-1 cells was

determined with and without LPS stimulation. We had previously examined the effects of BAY on the release of TNF-α, which is under NF-κB transcriptional control (Magness ST *et al.*, 2004), together with peanut extract whose synthesis is unknown. Thus, the anti-inflammatory effect of the natural compound tested (peanut extract, in the present study) was the reduction of TNF-α mRNA of the cells incubated with the extract compared to the activation with LPS alone. Results were expressed as mean (SD) of TNF-α mRNA change compared to LPS alone.

1.7 Stability of TNF-α mRNA

Act D is a polypeptide antibiotic isolated from *Streptomyces sp* bacteria. Act D is used as a transcription inhibitor because its intercalation into DNA produces a physical obstruction to RNA polymerase transcription, and inhibits the elongation of RNA chains (Koba M and Konopa J, 2005). Half-life/stability of TNF-α mRNA was measured after all experimental incubations of monocytes, mentioned above. After 2h of incubation with LPS, Act D (5μg/mL) was added to the medium. Incubation times with Act D were 30, 60, 120 and 180 min. At these times, the cells were lysed to obtain total RNA. Results were expressed as mean (SD) of TNF-α mRNA change compared to time 0 min for each experimental condition.

1.8 Determination of total TNF-α protein concentration

Total TNF-α protein concentration (extra- and intracellular) was determined. According to Black et al and Ishisaka et al (Ishisaka R *et al.*, 1999; Black RA, 2002), the total TNF-α protein is the sum of extracellular TNF-α (soluble) plus intracellular TNF-α (cytoplasmic plus trans-membrane) protein.

Extra- and intracellular TNF-α proteins were measured using human TNF-α ELISA kit (R&D Systems, Spain); the reported sensitivity of which was 5.5 pg/mL. Results were expressed as mean (SD) pg/mL/10^6 cells.

1.8.1 Detection and quantification of extracellular TNF-α

Supernatants of the experimental cell cultures were used to measure the extracellular TNF-α protein secretion. To determine the anti-inflammatory effect, the percentage reduction of TNF-α protein release is measured as the extracellular level because the biologically active form of TNF-α is the soluble form i.e. which exerts an effect in the organism. Thus, the anti-inflammatory effect of the natural compound tested (in the present case that of peanut extract) was the difference between the levels of extracellular TNF-α protein secretion of those cells incubated with the extract, compared to the levels from LPS activation alone.

1.8.2 Detection and quantification of intracellular TNF-α

THP-1 cells were washed twice with phosphate buffered saline (PBS) (Jang CH *et al.*, 2006), then ice-cold modified RIPA lysis buffer (50 µL/10^6 cells, as described above) was added to lyse the cells. The insoluble material was removed by centrifugation at 16,000 x *g* at 4 ºC for 10 min (Oda T *et al.*, 2006; Hu JH and Zhu XZ, 2007). The amounts of cytokine in cell lysate were measured as pg/mL produced from 10^6 cells.

1.9 TACE (α-secretase) activity assay

TACE activity from cell lysates (including cytoplasmic and trans-membrane) was determined by the SensoLyte® 520 TACE (α-secretase) Fluorimetric Activity Assay Kit (Anaspec, Fremont, CA, USA) under varying culture conditions. Cells were harvested and lysed using the assay buffer (containing 0.1%, v/v Triton-X 100) provided by the manufacturer. Protein content of cell lysate (cytoplasmic and trans-membrane) was determined using the Bradford protein assay. The kit was used according to the manufacturer's protocol. Fluorescence of the cleavage product was measured in a fluorescence microplate reader using Synergy HT Fluorimeter (BioTek Instruments, Alcobendas, Madrid, Spain), with excitation wavelength set at 490 nm and emission wavelength at 520 nm.

Results were expressed as mean (SD) relative fluorescence units (RFU) produced from TACE activity.

1.10 Statistical analyses

Two independent experiments were performed on different days. Samples were run in triplicate, and the data were pooled for each experiment. A total of six replicates were obtained for each experimental condition. All the results were analyzed with the Statistical Package for the Social Sciences (SPSS) software (version 19.0).

Descriptive statistics (means and standard deviation) and analytical statistics (ANOVA and Bonferroni tests) were used to assess dose-response effects. Statistical significance was set at $P<0.05$.

The measurement of quality was precision repeatability (within-assay) and reproducibility (between-assay) as measured by standard deviation (SD), coefficient of variation (CV) and standard error of the mean (SEM).

Figure 24 represents a graphical description of the design and methodology used in the study 1.

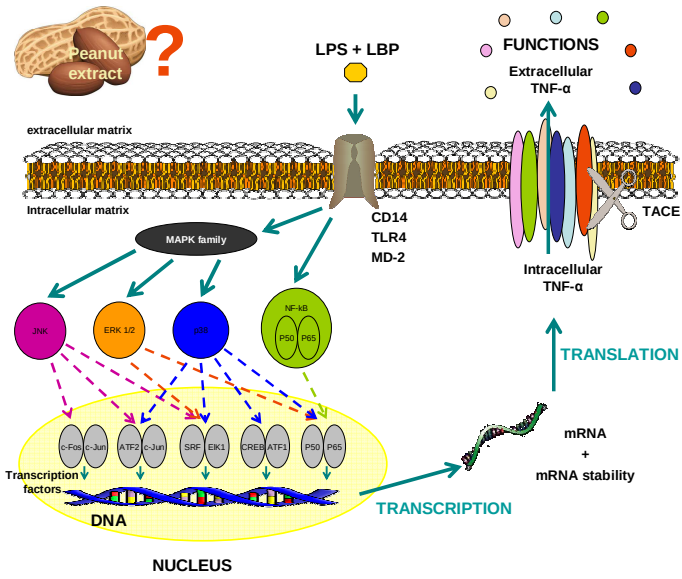

Figure 24. Graphical abstract from study 1. Inhibition of the Transcription factor c-Jun by the MAPK family, and not the NF-κB Pathway, Suggests that Peanut Extract has Anti-inflammatory Properties.

2. Alpha-Tocopherol and BAY 11-7082 Reduce Vascular Cell Adhesion Molecule in Human Aortic Endothelial Cells (Study 2)

2.1 Cell culture

HAEC (Cascade Biologics™, Portland, USA; **Figure 25**) at the 5th passage were seeded on Nunclon™ Δ surface 12-well plates (for the mRNA assays), 24-well plates (for the protein assays) or 96-well plates (for adhesion assays) at density of approximately $12x10^3$ of viable cells/mL. Cells were maintained for the first 24h in complete cell CM composed of M-200 medium supplemented with 2% (v/v) low serum growth supplement (LSGS), 10 mg/mL gentamicin, 0.25 mg/mL amphotericin B (both purchased from Invitrogen; Paisley, UK), 100 U/mL penicillin and 100 mg/mL of streptomycin (both from Labclinics, Barcelona, Spain). The cells were grown to confluence at 37 ºC in a humidified incubator (Heracell 150; Madrid, Spain) with atmosphere containing 5% CO_2. The medium was replenished every two days with fresh CM. Viewed under an Olympus IMT2 microscope (Barcelona, Spain), confluent monolayers displayed, after 5 days in culture, a typical monolayer phenotype of quiescent endothelial cells. All HAEC experiments were conducted at 37 ºC in a humidified atmosphere with 5% CO_2.

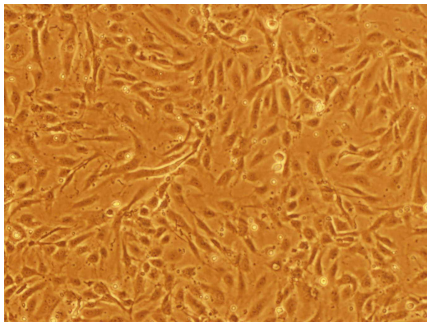

Figure 25. Human aortic endothelial cells (HAEC).

Jurkat T cell lymphocytes were purchased from *Deutsche Sammlung von Mikroorganismen und Zellkulturen GmbH* (DSMZ; Braunschweig, Germany). Jurkat T cells were cultured in RPMI medium 1640 + Glutamax-I (Gibco, Spain) supplemented with 20% heat-inactivated FBS (PAA, Labclinics; Barcelona, Spain) for the two first days followed by 10% FBS +

100 U/mL penicillin and 100 mg/mL streptomycin for growth and the scheduled experiments. The Jurkat T cells were maintained until the cell-cell adhesion assays.

HAEC were pre-incubated with AT (10, 25, 50, 75 and 150 μM; Sigma Chemical Co., St. Louis, Mo, USA), and the respective vehicle control (absolute EtOH; Panreac, Madrid, Spain) for 6h, as recommended in the literature (Martin A *et al.*, 1996; Zhang WJ and Frei B, 2002; Schleser S *et al.*, 2006; Shaw DI *et al.*, 2007; Tribolo S *et al.*, 2008). Then, as and when required, TNF-α (1 or 10 ng/mL; Calbiochem, Darmstadt, Germany) and BAY (0.1 or 1 μM; Merck; Darmstadt, Germany) were added for 24h to the cell CM to induce cell stimulation. Finally, except for cell-cell adhesion assays, supernatants were collected, and stored at -20 ºC for batched measurements of the soluble forms of selected CAMs (sVCAM-1, sE-selectin and sICAM-1), and to measure the activity of LDH released. Cells were lysed and stored at -80 ºC for batched CAMs mRNA expression measurement. Fluorescent intensity was the method used to measure cell-cell adhesion.

2.2 Cell viability and cytotoxicity

Cell viability was assessed by morphology using phase contrast microscopy and by trypan blue exclusion (Merck & Co., Inc; Darmstadt, Germany).

Cell cytotoxicity was assessed with Cytotoxicity Detection Kit LDH (Roche Applied Science, Mannheim, Germany). Briefly, LDH enzyme is rapidly released into the cell-culture supernatant when the plasma membrane is damaged. This results in a colorimetric reaction that can be measured at a wavelength of 492 nm.

For these experiments, TNF-α treatment is considered as the maximum stress condition for the cells.

Activity of LDH released from cells was measured in cell-free supernatants collected at two key points of the experiment: after 6h incubation with AT and after 24h incubation with TNF-α (alone or in the presence of BAY) at

the various concentrations. Results are expressed as mean absorbance and SD (error bars) of LDH produced by the cells under each treatment condition.

2.3 Analysis of CAMs mRNA expression by real-time quantitative reverse transcriptase polymerase chain reaction (RT-PCR) in HAEC stimulated with TNF-α

Dose- and time-course response experiments were performed by stimulating HAEC with TNF-α. Once the appropriate experimental conditions were established (i.e. the capacity to measure minimal decreases in CAMs mRNA expression that may be induced by the compounds under investigation; AT and BAY), we opted for 10 ng/mL (for E-selectin and ICAM-1) or 1 ng/mL (for VCAM-1) of TNF-stimulation over a culture period of 24h, and BAY 1 μM (for E-selectin and ICAM-1) or 0.1 μM (for VCAM-1).

Cells were lysed with nucleic acid purification lysis solution and total RNA was isolated from cells using the ABI PRISM 6100 Nucleic Acid PrepStation extraction system (Applied Biosystems; Foster City, CA, USA) according to the manufacture's protocol. Total RNA was quantified using Quant-it^{TM} RNA Assay Kit and Qubit^{TM} fluorometer (Invitrogen; Paisley, UK). Using the 2720 Thermal Cycler (Applied Biosystems), 0.5 μg of total RNA was reverse transcribed to cDNA at 42 ºC for 50 min using random hexamers, SuperScript II reverse transcriptase and RNAse Out (Invitrogen) according to the manufacturer's protocol. To determine the amount of VCAM-1, E-selectin and ICAM-1 mRNA, semi-quantitative RT-PCR was performed using the ABI PRISM 7900 Detection System (Applied Biosystems) with the following profile: 95 ºC denaturing (20 s) with 40 cycles of extension at 95 ºC (1 s) and 60 ºC (20 s). Each sample was analyzed in triplicate and the cycle-threshold (Ct) was averaged from the values obtained in each reaction. VCAM-1, E-selectin and ICAM-1 mRNA expression results are reported as the increase (x-fold) using $2^{-\Delta\Delta Ct}$ mathematical method. The GAPDH, (obtained from Applied Biosystems)

was used as housekeeping gene to normalize the results. TNF-α-activated endothelial cells were used as calibrator in these experiments; its value was set at 1 and the other conditions were in relation to this reference value. Results are expressed as the mean and SD (error bars) of CAMs mRNA change relative to TNF-α alone.

2.4 Measurement of sCAMs protein secretion by HAEC stimulated with TNF-α

Dose- and time-course response experiments were performed by stimulating HAEC with TNF-α. Once the appropriate experimental conditions were established i.e. the capacity to measure minimal decreases in sCAMs protein secretion that may be induced by the compounds under investigation (in the present case AT and BAY; 1μM), we opted for TNF-α at 10 ng/mL based on the concentrations used in previous reports with HUVEC (Shaw DI *et al.*, 2007; Tribolo S *et al.*, 2008) or with HAEC (Szekanecz Z *et al.*, 1994; Amberger A *et al.*, 1997; Chen YH *et al.*, 2001; Zhang WJ and Frei B, 2002; Chen JW *et al.*, 2003; Schleser S *et al.*, 2006).
At the conclusion of the experiments, cells and supernatants were separated by centrifugation (Multifuge 3L-R; Madrid, Spain) at 1500 x *g* for 10 min at 4 ºC. The cell pellet/debris was discarded and the cell-free supernatants used for sVCAM-1, sE-selectin, sICAM-1 measurements using enzyme-linked immunosorbent assays (ELISA) according to the manufacturer's protocol (for sVCAM-1 ELISA Kit, Diaclone, Besançon, France; for sE-selectin and sICAM-1, Quantikine ELISA kits from R&D Systems, Madrid, Spain).
All experimental data were compared to the outcomes in the TNF-α-alone incubation, since this achieved the maximal secretion of sVCAM-1. A vehicle-alone control (vehicle for AT, absolute EtOH) was run in parallel and used as control in this experiment. Results are expressed as the mean sCAMs protein secretion and SD (error bars).

2.5 Calcein labelling of Jurkat T-cells

Calcein acetoxymethyl ester (Calcein-AM, Molecular Probes, Eugene, OR, USA) was used to fluorescently label Jurkat T-cells. Calcein is a non-fluorescent and lipophilic molecule which is cleaved by endogenous esterases, the resultant product fluorescence can be measured at 485 nm and 530 nm (excitation and emission wavelengths, respectively).

The Jurkat T-cells were fluorescence labeled by incubating cells (25 x 10^6 cells/mL) with a final concentration of 5 μM of calcein-AM for 30 min at 37 °C and 5% CO_2. After calcein-AM loading, the cells were washed twice with RPMI-1640 medium supplemented with 10% of FBS to remove excess dye. Cells were finally re-suspended in CM at a density of 2.5 x 10^6 cells/mL.

2.6 Cell-cell adhesion assay

HAEC were seeded until confluent in black 96-well tissue culture plates. Following the appropriate culture with AT and BAY, calcein-AM-labeled Jurkat T-cells were co-cultured (2.5 x 10^5 cells/well) with the HAEC monolayer for 1h at 37 ºC in a humidified atmosphere with 5% CO_2. The non-adhered Jurkat T-cells were removed from the HAEC monolayer by washing twice with CM. Fluorescence in each well of the culture plate was measured with the Synergy HT Fluorometer (BioTek Instruments; Alcobendas, Madrid, Spain) (Roy S *et al.*, 1998; Sen CK and Bagchi D, 2001). Results are expressed as RFU and SD (error bars).

2.7 Statistical analyses

Data were expressed as the mean and SD (error bars) for sCAMs protein concentration and CAMs mRNA expression. Unless otherwise stated, all experiments were performed at least twice and each incubation condition was set-up in triplicate. Analysis of variance (ANOVA) with Bonferroni's correction was used for multiple comparisons. A value of $P<0.05$ was considered statistically significant.

A requisite for the analytical quality of the model is to control several aspects involved in the cellular process and analytical performance of

measurements. Thus, we evaluated the precision of the model by calculating the SD, the SEM and the coefficients of variation (CV). All the results were analyzed with the SPSS software (version 19.0).

Figure 26 represents a graphical description of the design and methodology used in the study 2.

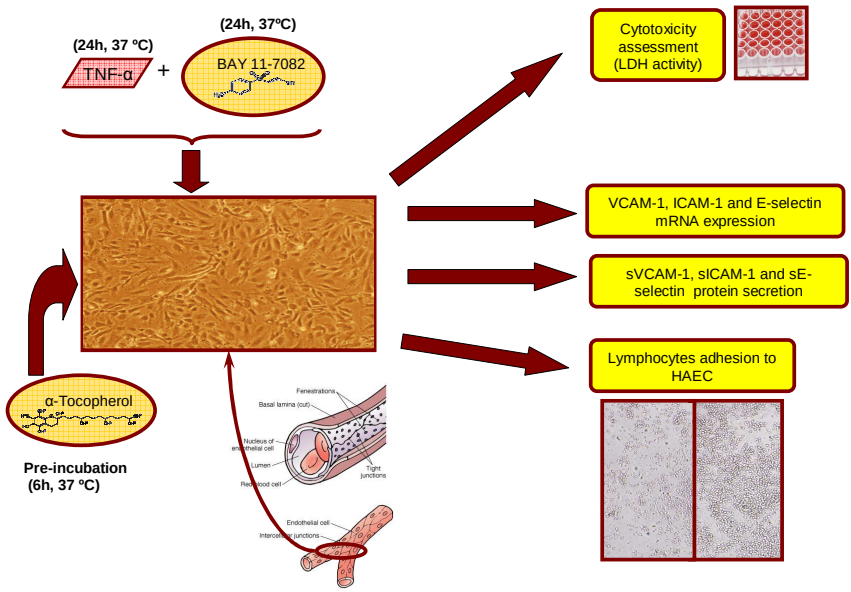

Figure 26. Graphical abstract from study 2. Alpha-Tocopherol and BAY 11-7082 Reduce Vascular Cell Adhesion Molecule in Human Aortic Endothelial Cells.

3. Biomarkers of Food Intake and Metabolite Differences between Plasma and Red Blood Cell Matrices; a Human Metabolomic Profile Approach (Study 3)

3.1 Ethics, subject recruitment and clinic visits

Eligible male volunteers (N=10) between the ages of 20 and 70 were recruited from our volunteer center database. They were non-smokers with no other major CVD risk factors and were not using any medications and/or vitamin supplements.

Participants provided written informed consent prior to enrolment into the study. Eligibility or exclusion was assessed by the attending physician based on a review of the clinical history, as well as physical and biochemical examination. The screening visit was to ensure that the participants were ostensibly healthy without any known illness. The study was approved by the Clinical Research Ethical Committee (Institutional Review Board) of the *Hospital Universitari Sant Joan de Reus* (Reference: 10-04-29/4assN1) where the participants were recruited. The study protocol was in accordance with the Declaration of Helsinki and good clinical practice guidelines.

3.2 Blood sample collection: plasma and RBC

A fasting blood sample from each individual was collected into sodium citrate (~250 µL of 0.129M sodium citrate in 2.7 mL tubes) and lithium heparin (68 I.U.; Anorsa, Hospitalet de Llobregat, Barcelona, Spain) tubes. The samples and techniques used for this study are summarized in **Table 1**. The samples were immediately centrifuged (2,000 x *g*, 15 min, 4 ºC) and then divided into separate aliquots of plasma and RBC. Plasma aliquots were stored at -80 ºC until analysis. RBC were washed three times with PBS (Invitrogen, Barcelona, Spain) and 1 µL of 1 mM butylated hydroxy toluene (BHT; Sigma-Aldrich, Madrid, Spain) / 100 µL of RBC was added to

prevent oxidation contamination, and then stored in aliquots at -80 ºC until analysis.

Table 1. Qualitative and quantitative analysis of plasma and red blood cell (RBC) fractions.

Technique	MATRIX						
	Plasma			RBC			Serum
	Aqueous	Organic	Total	Aqueous	Organic	Total	Total
1D ^{1}H NMR	Metabolite profile	Lipid composition	–	Metabolite profile	Lipid composition	–	–
GC-MS	–	Fatty acid profile	–	–	Fatty acid profile		–
2D diffusion-edited ^{1}H NMR	–	–	Lipoprotein subclasses	–	–	–	–
UPLC-MS/MS	–	–	Polyphenols	–	–	Polyphenols	–
Autoanalyzer	–	–	–	–	–	–	Biochemical parameters

^{1}H NMR: Nuclear magnetic resonance spectroscopy; GC-MS: Gas chromatography - mass spectrometry
UPLC-MS/MS: Ultra performance liquid chromatography coupled to tandem mass spectrometry

With 10 subjects in the study, blood distributed into 2 different sample collection tubes (lithium heparin and sodium citrate), 2 matrices (plasma and RBC) and 2 fractions (organic and aqueous) the total number of samples processed (10 x 2 x 2 x 2) was 80.

3.3 Biochemical parameters

To confirm that the volunteers were ostensibly healthy a fasting blood sample was taken and the serum used for routine biochemical analyses. These included total cholesterol (mmol/L), triglycerides (mmol/L), direct HDL (mmol/L), apolipoprotein A1 (mg/dL), apolipoprotein B100 (mg/dL), glucose (mg/dL), uric acid (mg/dL), bilirubin (mg/dL), creatinine (mg/dL), urea (mg/dL), glutamic oxaloacetic transaminase (U/L), glutamic pyruvic transaminase (U/L), gamma glutamyl transferase (U/L) and alkaline phosphatase (U/L) were determined by routine laboratory methods using a Cobas Mira Plus autoanalyzer (Roche Diagnostic System, Madrid, Spain).

3.4 Plasma viscosity

Plasma samples (250 µL) from sodium citrate and heparin tubes were weighed and the density calculated. Plasma was then placed on an extra-low-charge calibrated viscosimeter (Cannon Instrument Company, State

College, USA) and loaded on a Julabo ME-16G Visco Bath (Julabo Labortechnik GmbH, Seelbach, Germany) previously warmed to 37 ºC. The time taken for the plasma to pass from the top to the bottom of the calibrated viscosimeter was measured (time measured in seconds; mean of triplicate measures). Viscosity (mPa sec) was calculated according to the formula:

$$\eta = \rho\, t\, \kappa$$

Where:

κ is the viscosimeter constant (0.004175), t is the mean of the time measurements (sec), ρ is the density (mg/µL).

3.5 Extraction of aqueous and lipid fractions of plasma and RBC

Methanol-chloroform (Sigma-Aldrich, Alcobendas, Madrid, Spain) mixture (1000 µL) in a ratio of 2:1 (v/v) was added to 200 µL of each matrix sample (plasma and RBC). Homogenates were derived by sonication for 15 min, after which 400 µL solution of chloroform: distilled water (1:1; v/v) was added and mixed thoroughly. The phases were separated (14,000 x *g*, 20 min) in a Multifuge 3L-R centrifuge (Thermo, Madrid, Spain). The upper aqueous phase was removed and flash-frozen at -196 ºC in liquid nitrogen and then lyophilized overnight to remove water and stored at -80 ºC until subsequent NMR experiments. The lower phase (lipid fraction) was allowed to dry in a fume hood overnight and then stored at -80 ºC.

3.6 Preparation of aqueous and lipid fractions for 1D ^{1}H NMR spectroscopy of plasma and RBC

The dried aqueous plasma and RBC extracts were reconstituted in 600 µL of deuterated water (D_2O; Eurisotop , Gif-Sur-Yvette, France) buffered in 40 mM disodium phosphate (Sigma-Aldrich, Steinheim, Germany), 8 mM sodium phosphate (Sigma-Aldrich, Steinheim, Germany) and 0.02% of sodium azide (Sigma-Aldrich, Steinheim, Germany) containing 1 mM of

sodium (3-trimethylsilyl)-2,2,3,3-tetradeuteriopropionate (TSP; Cortecnet, Viosins Le Bretonneux, France) as a chemical shift standard. The mixture was placed into 5 mm NMR tubes (Cortecnet, Viosins Le Bretonneux, France).

The dried organic extracts of plasma and RBC were reconstituted in 700 µL of a 2:1 (v/v) mixture of deuterated chloroform and deuterated methanol ($CDCl_3$: CD_3OD; Eurisotop, Gif-Sur-Yvette, France) containing 0.01% (v/v) of TMS (Cortecnet, Viosins Le Bretonneux, France) as a chemical shift standard, and placed into 5 mm NMR tubes. The NMR tubes were maintained at 4 ºC in the sample changer until the time of analysis.

3.7 1D and 2D ^{1}H NMR spectroscopy of plasma and RBC

All one- and two-dimensional ^{1}H NMR spectra were obtained on a Bruker Avance III 600 spectrometer operating at a proton frequency of 600.20 MHz (14.1 T) equipped with a 10 A GREAT 1/10 gradient amplifier unit using a 5-mm CP-TCI triple resonance (^{1}H, ^{13}C, ^{31}P) pulse field gradient cryoprobe® (Bruker, Cerdanyola del Vallès, Spain).

3.7.1 1D ^{1}H NMR spectroscopy

For the one-dimensional (1D) aqueous extract spectra of plasma or RBC, 1D Nuclear Overhauser Effect Spectroscopy (noesygppr1d Bruker pulse®, RD-90º–τ1–90º–τm–90º ACQ) was measured at 300 K. Solvent pre-saturation with low irradiation power (15 Hz) was applied during recycling delay and mixing time (τm =100 ms) to suppress residual water. The 90° pulse length was calibrated for each sample and ranged from 8.77 ms to 9.22 ms. A total of 256 transients were collected across 12 kHz spectral width (20 ppm) into 64 k data points, and exponential line broadening of 0.3 Hz was applied before Fourier transformation. A recycling delay time of 5 s was applied between scans to ensure correct quantification.

In the case of lipid extracts, a 90º pulse with a pre-saturation sequence (zgpr Bruker pulse) was used. We performed measurements at 287 K, shifting the residual water signal to 4.65 ppm to allow for the quantification

of the characteristic glycerol-backbone signals. In addition, residual water was pre-saturated during recycling delay (RD= 5 s) using a low irradiation power (10 Hz). The 90° pulse length was calibrated for each sample and varied from 7.30 ms to 7.59 ms. A total of 256 free induction decays (FIDs) of 12 kHz of spectral width (20 ppm) were collected into 64 k data points, and exponential line broadening of 0.3 Hz was applied before Fourier transformation.

All the frequency spectra were phased, baseline corrected and then calibrated (TMS or TSP, 0.0 ppm) using TopSpin software (version 2.1, Bruker, Germany). Spectra were segmented into 0.03 ppm chemical shift bins between 0.2 and 9.6 ppm (excluding water and TSP resonances) using a bucket size of 0.03 ppm and the Intelligent Bucketing facility within ACD 1D NMR Manager software (version 12; Berks, England). To account for differences in sample volumes, each integrated region was normalized to the total spectral area for all integral regions in that spectrum, excluding water and TSP resonances. Spectra were assigned by comparison with assignment of Chenomx NMR Suite version 7.0 (Chenomx; Alberta, Canada) for target profiling analysis to determine the metabolites contributing to each bin.

3.7.2 2D ^{1}H NMR spectroscopy

2D diffusion-edited ^{1}H NMR measurements were carried out according to Mallol et al. 2011 (Mallol R *et al.*, 2011). Plasma samples (430 µL) from sodium citrate and lithium heparin tubes were transferred to 5-mm NMR tubes with a double tube system. An internal reference tube (optical density; OD 2 mm, supported by a Teflon adapter) containing 9.9 mmol/L TSP (reference substance) and 0.47 mmol/L $MnSO_4$ in 99.9% D_2O was placed coaxially into the NMR sample tube (OD 5 mm). This double tube system was kept at 4º C in the sample changer until the moment of analysis.

^{1}H NMR spectra of plasma were recorded at 310 K to obtain a full signal from the mobile lipids in the lipoproteins and to avoid plasma degradation during the measurement.

For diffusion measurements of lipoproteins in plasma, the double-stimulated echo (DSTE) pulse program was used, with bipolar gradient pulses and a longitudinal eddy-current delay (LED; dstebpgp3s Bruker pulse sequence). A spectral window of 18028.846 Hz was used, with an acquisition time of 1.82 s. During the experiment, the relaxation delay was 2 s, the FIDs were collected into 64K complex data points, and 32 scans were acquired for each sample. The gradient pulse strength was increased from 5% to 95% of the maximum strength of 53.5 G cm^{-1} (0.535 T m^{-1}) in 32 steps. A diffusion time of 120 ms and bipolar half-sine-shaped gradient pulses of 6 ms were applied. All spectra were Fourier transformed, phase corrected, baseline corrected, and referenced to the glucose signal at 5.233 ppm. Diffusion coefficients were obtained using a surface fitting approach, as described previously (Mallol R *et al.*, 2011).

Once the diffusion coefficients have been estimated, the Stokes–Einstein equation can be applied to derive the radius associated with each function:

$$D = \frac{\kappa T}{6 \pi \eta R}$$

Where:

k (J K^{-1}) is the Boltzmann constant 1.38 10 $^{-23}$, T (K) is the temperature, η (Pa s) is the plasma viscosity (measured on plasma aliquots from sodium citrate and lithium heparin samples) and R (Å) is the hydrodynamic radius.

3.8 FA profile in plasma and RBC by GC-MS

The D_2O lipid aliquots (700 µL) from plasma and RBC samples used for 1D ^1H NMR spectroscopy were evaporated to dryness in the sterile air-flow fume hood overnight and then derivatized. Dried samples were dissolved in 750 µL chloroform/methanol 1:1 (v/v), vortex mixed for 30 s, sonicated for 10 min followed by the addition of 100 µL D_{27}-tetradecanoic acid (200 µM in chloroform; Sigma-Aldrich, Madrid, Spain) as IS. 125 µL of 10% boron trifluoride/methanol (Sigma-Aldrich, Madrid, Spain) was added and the vials were incubated at 80 ºC for 90 min. On cooling, 500 µL of distillated water and 1000 µL hexane (Sigma-Aldrich, Madrid, Spain) were added and vortex mixed for 1 min. Two layers were formed and the aqueous top layer was aspirated and discarded. The lipid layer was evaporated to dryness in the fume hood overnight and 500 µL of hexane was added to the dried samples before GC-MS analysis. Food Industry FAME Mix from Restek (Teknokroma, Barcelona, Spain) was used for the quantification of the fatty acid methyl ester (FAME) from plasma and RBC.

A 6890 gas chromatograph coupled to a 5973 mass spectrometer (Agilent Technologies, Palo Alto, U.S.A.) was used for the FA separation and detection, with a FFAP capillary column with dimensions of 30 m x 0.25 mm x 0.25 µm (Agilent Technologies, Palo Alto, U.S.A.). Helium gas (99.999% pure) was used as the carrier at a constant flow of 1.2 mL/min. A sample volume of 2 µL was injected in split mode, with a split ratio of 10:1. The inlet temperature was of 250 ºC. GC oven temperature program was as follows: 60 ºC held for 2 min, then increased at 6 ºC/min to a final temperature of 240 ºC which was held for 13 min. Total run time per sample was 45 min. Transfer line temperature was of 280 ºC. Source and quadrupole temperatures were set at 230 ºC and 150 ºC, respectively, while the electron impact source was set at a voltage of 70 MeV. The mass spectrometer acquired data in scan mode over a 50 to 650 m/z interval, after 2.1 min solvent delay. The compounds were quantified using a target ion and identified using qualifier ions and retention times. The chromatographic method was calibrated daily by analyzing standard

solutions at a range of concentrations from 3 to 120 mg/L of FAMEs, which were prepared and analyzed under the same conditions as the plasma and RBC samples. The calibration curves obtained by plotting analyte/IS peak abundance ratio and the corresponding analyte/IS concentration ratio showed good linearity; determination coefficients (r^2) being higher than 0.999 for all compounds.

Sensitivity was evaluated by determining the limit of detection (LOD), (S/N=3) and the limit of quantification (LOQ) which was defined as 5 times the LOD. Method detection and quantification limits (MDL and MQL, respectively) were calculated for the analysis of 200 µL of sample, following the procedures described, above. Values showed MDL in a range from 0.02 to 1.6 mg/L, while those for MQL were from 0.08 to 8.7 mg/L. Good method precision was observed for all the compounds, with relative standard deviations (RSD) between 1.2 and 8.3 (n=3).

3.9 Micro-elution solid-phase extraction (µ-SPE) of polyphenols from plasma and RBC

Polyphenols in the defrosted fasting human plasma and RBC (from sodium citrate and lithium heparin samples) were extracted with solid-phase extraction using micro-plates as the device format (µ-SPE). Briefly, 400 µL of plasma and/or RBC were vortex mixed and centrifuged (2,000 x *g*, 7 min, 4 ºC) to sediment cellular debris. From plasma or RBC samples, 350 µL of supernatant were recovered and to which 50 µL of IS (Catechol; Sigma-Aldrich, St. Louis, MO, USA) + 300 µL of 4% phosphoric acid (H_3PO_4; Panreac, Barcelona, Spain) were add to each sample and vortex mixed. Because of the matrix consistency of RBC, 500 µL H_3PO_4 was added and the cells ruptured using an S-150D Digital Sonifier® cell disruptor (Branson, Ultrasonidos, S.A.E., Barcelona, Spain). Then, a 1:7 mixture (RBC : H_3PO_4) was used as a final volume before performing the corresponding polyphenol extraction. Micro-elution plates (Waters, Milford, USA) were packed with 2 mg OASIS HLB sorbent (Waters). The cartridges were initially conditioned using 250 µL methanol and 250 µL of acidified Milli-Q

water at pH 2 in sequence, after which the plasma and RBC samples were loaded.

The plates were "cleaned-up" with sequential 100 µL milliQ water and 100 µL 5% methanol to eliminate any residual interference/contamination in the sample. Finally, polyphenol compounds retained on the column were eluted with 100 µL methanol and injected directly into the UPLC–MS/MS.

3.10 UPLC-MS/MS detection of polyphenols from plasma and RBC

The UPLC system consisted of an AcQuity UPLC™ equipped with a binary pump system (Waters; Milford, MA, USA) using an AcQuity UPLC™ BEH C_{18} column (1.7 µm, 100 mm × 2.1 mm internal diameter). During the analysis, the column was kept at 30 ºC and the flow rate was 0.4 mL/min using 0.2% acetic acid as solvent A and acetonitrile as solvent B. The elution commenced with 5% eluent B for 5 min, then linearly increased to 40% eluent B for 20 min, further increased to 100% eluent B for 0.1 min, and kept isocratic for 1.9 min, then back to initial conditions in 0.1 min, and the re-equilibration for 1.9 min.

The UPLC system was coupled to a PDA detector AcQuity UPLC™ and a TQD™ mass spectrometer (Waters, Milford, MA, USA). The software used was MassLynx 4.1. Ionization was by electrospray (ESI) in negative mode and then in positive mode.

The analyses were conducted in full-scan mode in order to determine molecular weight. This was followed by daughter scan mode and in selected reaction monitoring (SRM) mode to evaluate the fragments generated. Ionization source parameters were capillary voltage of 3.0 kV, source temperature of 150 ºC, and desolvation gas temperature of 400 ºC with a flow rate of 800 L/h. Nitrogen (99% purity, N_2 LCMS nitrogen generator; Claind, Como, Italy) and argon (≥99.99% purity, Aphagaz, Madrid, Spain) were used as the cone and collision gases, respectively.

The SRM transitions and the individual cone voltage and collision energy for each of the standard phenolic compounds were evaluated by infusing

10 mg/L of each compound to obtain the best instrumentation conditions. In the daughter ion scan experiments, tandem mass spectrometry (MS/MS) was used, and the product ions were produced by collision-induced fragmentation of selected precursor ions in the collision cell of the triple quadrupole mass spectrometer (MS). The mass was then analyzed with the instrument's second analyzer.

The standard phenolic compounds 3-hydroxyphenylpropionic acid, *o*-, *m*- and *p*-hydroxyphenylacetic acid, hydroxybenzoic acid phenylacetic acid and hydroxyflavanone were purchased from Sigma-Aldrich (Madrid, Spain). **Table 2** shows the SRM transitions, cone voltage and collision energy for different commercial phenolic compounds. Two transitions were selected for quantification and confirmation purposes.

Table 2. SRM transitions, cone voltage and collision energy for the analysis of phenolic compounds.

Compound	SRM_1 (quantification)	Cone voltage (V)	Collision energy (eV)	SRM_2 (confirmation)	Cone voltage (V)	Collision energy (eV)
3-(4-hydroxy-phenyl) propionic acid	165 > 121	20	10	165 > 149	20	15
o-, *m*- and *p*-hydroxyphenylacetic acid	151 > 107	20	10	-	-	-
p-hydroxybenzoic acid	137 > 93	20	15	-	-	-
Phenylacetic acid	135 > 91	20	5	-	-	-
4-Hydroxyflavone	239 > 119	40	15	239 > 93	40	20

3.11 Statistical analysis

Data were expressed as the mean and SD (error bars). F test was used to determine the normality of variances of the two sample types followed by the two-tailed *t*-test, assuming equal variances. The *t*-test for related samples was used to compare differences between sodium citrate and lithium heparin samples. The data were analyzed with the SPSS software (version 19.0). A value of $P<0.05$ was considered statistically significant.

Since multivariate data analysis plays an essential role in evaluating differences between metabolomes, thus enabling the identification of metabolites relevant to a specific phenotypic characteristic (Koek MM *et al.*, 2011), we applied multivariate analyses using SIMCA-P + 12.0 software (Umetrics AB, Umea, Sweden) with the data having been mean-centered

and Pareto-scaled prior to analysis. Pareto scaling augments the representation of low concentration metabolites in statistical models by dividing each integral region, or variable, by the square root of the standard deviation of the variable, without increasing the contribution of spectral noise to the model. Unit variance (UV) scaling ensures all metabolites identified contribute equally to the multivariate dataset.

Three different multivariate statistical techniques were used within the SIMCA package: principal components analysis (PCA); projection to latent structures by partial least squares discriminant analysis (PLS-DA); and Orthogonal PLS-DA (OPLS-DA). PCA is an unsupervised technique that describes observations (e.g. spectra from plasma or from RBC) in relation to one or more latent variables, termed principal components (PCs) which, in turn, are linear combinations of the original variables (e.g. NMR buckets). PLS-DA and OPLS are supervised techniques separating observations based on class-membership. In OPLS-DA, the objective is to remove the variation in the model that is orthogonal to response. This can more easily produce interpretable models where the 1st component represents the major changes that distinguish the two groups. The *p*-value was calculated using a Student's *t*-test on the coefficients to calculate the contribution to a given component made by each variable.

3.11.1 Model validation

The parameters R^2 and Q^2 were used to evaluate the performance of each model. The R^2 score indicates how much of the total variation in the dataset is described by a particular component and R_{cum}^2 indicates the variation described by all the components in the model (scored 0-1). Q^2 is a measure of how accurately the model can predict class membership and, hence, is more relevant to supervised approaches. Q^2 estimates the predictive ability of the model by leaving out observations from the model building, and then predicting their class membership or trend variable. Q^2 >0.08 is indicative of a model that is better than chance, while scores above 0.7 demonstrate a highly robust trend, or separation. The validity and the degree-of-fit for

the models were assessed by the criteria and validation routines built into the SIMCA package.

Figure 27 represents a graphical description of the design and methodology used in the study 3.

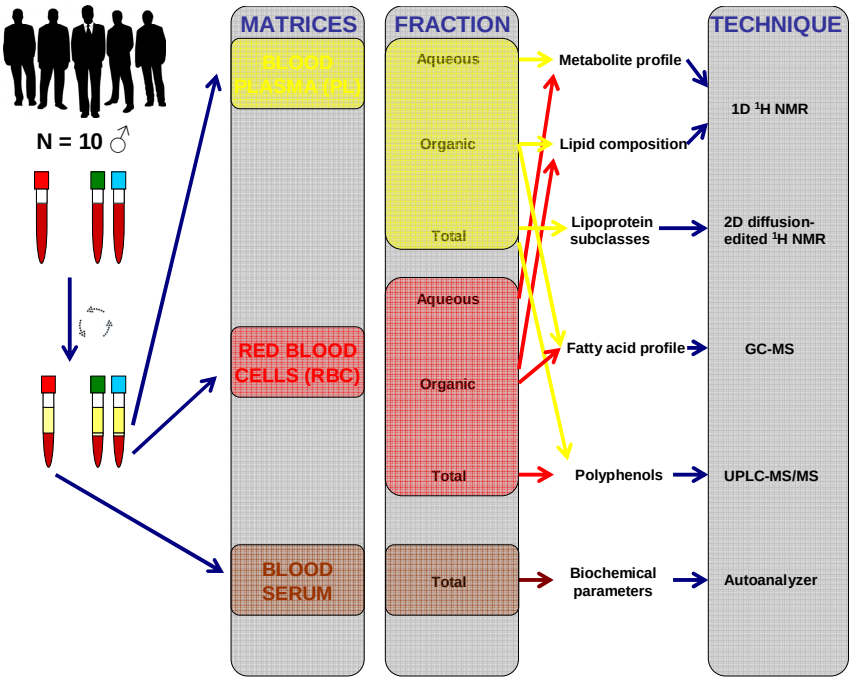

Figure 27. Graphical abstract from study 3. Biomarkers of Food Intake and Metabolite Differences between Plasma and Red Blood Cell Matrices; a Human Metabolomic Profile Approach.

RESULTS

EFFECT OF FOOD EXTRACTS AND BIOACTIVE FOOD COMPOUNDS ON THE MECHANISM OF ATHEROSCLEROSIS AND NUTRITIONAL BIOMARKERS

Úrsula Catalán Santos

Dipòsit Legal: T. 1058-2012

1. Inhibition of the Transcription factor c-Jun by the MAPK family, and not the NF-κB Pathway, Suggests that Peanut Extract has Anti-inflammatory Properties (Study 1)

1.1 Cytotoxicity measurements

Cytotoxicity assay of the peanut extract (5, 25, 50 and 100 µg/mL), measured as the activity of LDH release showed no difference compared to the LPS treatment alone, confirming that the peanut extract is not cytotoxic at the concentrations tested. No cytotoxicity was detected for LPS and BAY (data not shown).

1.2 Effect of peanut extract on NF-κB

The p65-NF-κB activation showed that LPS increased the activity 8-fold compared to vehicle control (3.75% DMSO) demonstrating a good stimulation of the cells ($P<0.05$). BAY, used as experimental control, decreased the stimulation 4-fold ($P<0.05$). Peanut extract at the concentrations tested (5, 25 and 100 µg/mL) showed no significant difference in p65-NF-κB activation compared to LPS alone (**Figure 28**).

1.3 Effect of peanut extract on MAPK family

The transcription factors ATF-2, c-Myc, STAT1 and MEF2 did not show any significant differences at any peanut extract concentration tested (5, 25 and 100 µM). However BAY (5 µM) reduced MEF2 compared to LPS, albeit non-significantly. c-Jun transcription factor was reduced by BAY (5 µM) by 86% and peanut extract (25 and 100 µM) by 54% and 93%, respectively ($P<0.05$) (**Figure 29**).

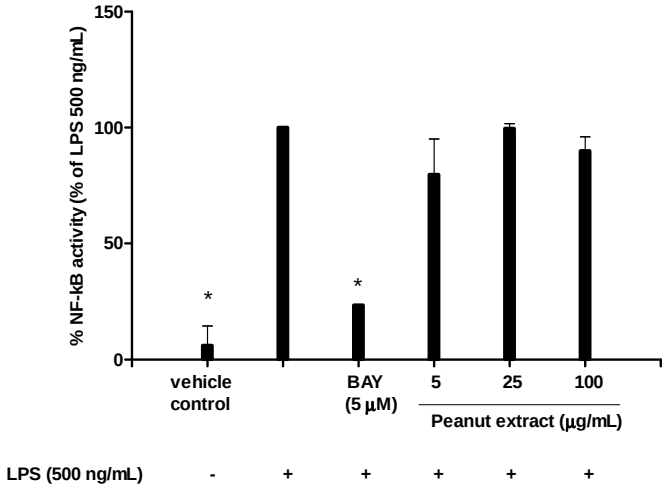

Figure 28. Effect of peanut extract on NF-κB. THP-1 monocytes were incubated with vehicle control (3.75% DMSO), BAY 11-7082 (5µM) and peanut extract (5, 25 and 100 µg/mL) for 1h and stimulated with LPS (500 ng/mL) for 1h. NF-κB binding was measured using an ELISA kit (TransAM®). Data are expressed as percentage LPS values of two separate experiments run in triplicate. Error bars show SD. *P<0.05 versus LPS.

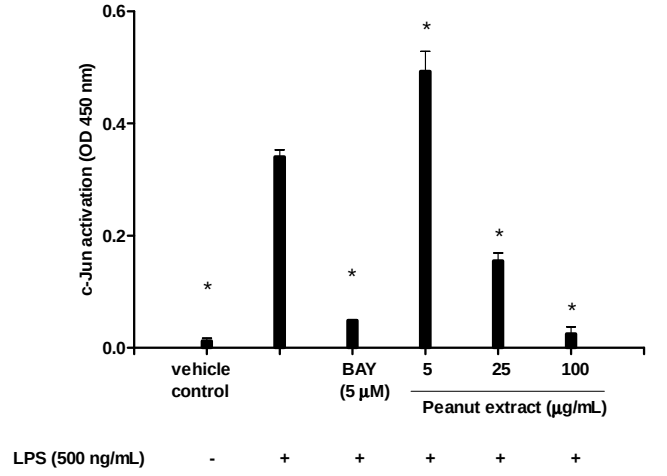

Figure 29. Effect of peanut extract on c-Jun. THP-1 monocytes were incubated with vehicle control (3.75% DMSO), BAY 11-7082 (5µM) and peanut extract (5, 25 and 100 µg/mL) for 1h and stimulated with LPS (500 ng/mL) for 1h. c-Jun binding was measured using an ELISA kit (TransAM®). Data are expressed as optical density (OD) at 450 nm. Error bars show SD. *P<0.05 *versus* LPS.

1.4 Effect of peanut extract on TNF-α mRNA in THP-1 cells usint RT-PCR assay

LPS (500 ng/mL) stimulated TNF-α mRNA production 7-fold compared to vehicle control (3.75% DMSO) in THP-1 ($P<0.05$). BAY (5 µM) decreased LPS (500 ng/mL) stimulation 2-fold ($P<0.05$).

TNF-α mRNA expression at all concentrations tested (5, 25, 50 and 100 µg/mL) showed reductions albeit statistically non-significant, of 9 %, 24 %, 29% and 21%, respectively compared to LPS alone (**Figure 30**).

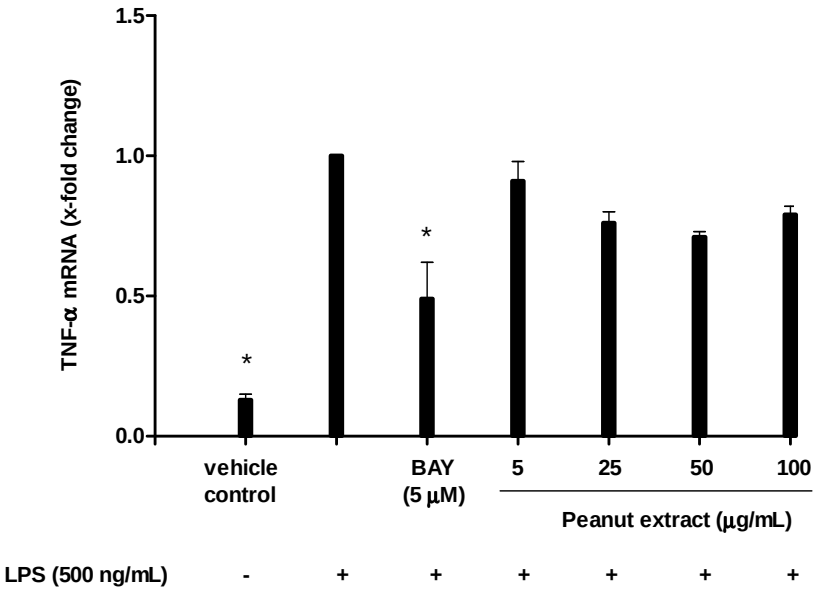

Figure 30. Effect of peanut extract on TNF-α mRNA in THP-1 cells using RT-PCR assay. THP-1 monocytes were incubated with vehicle control (3.75% DMSO), BAY 11-7082 (5µM) and peanut extract (5, 25, 50 and 100 µg/mL) for 1h and stimulated with LPS (500 ng/mL) for 4h. The abundance of mRNA transcripts for TNF-α was determined using real time quantitative polymerase chain reaction (RT-PCR). Data were normalized using the values obtained for GAPDH (house keeping gene), and are the mean of two separate experiments run in triplicate. Error bars show SD. *P<0.05 versus LPS.

1.5 Effect of peanut extract on TNF-α mRNA stability in THP-1 cells usint RT-PCR assay

Under vehicle control condition (3.75% DMSO), TNF-α mRNA levels fell significantly (P<0.05) relative to the starting point (time 0 min) of the kinetic measurements. The decline under the other test conditions (LPS, BAY and peanut extract) was progressive over the first 30 min, compared time 0 min. At 30 min LPS, BAY and peanut extract decreased to the minimum TNF-α mRNA level as that measured in the vehicle control. There were no significant differences between LPS, BAY and peanut extract compared to vehicle control at any of the time points i.e. peanut extract did not stabilize TNF-α mRNA (**Figure 31**).

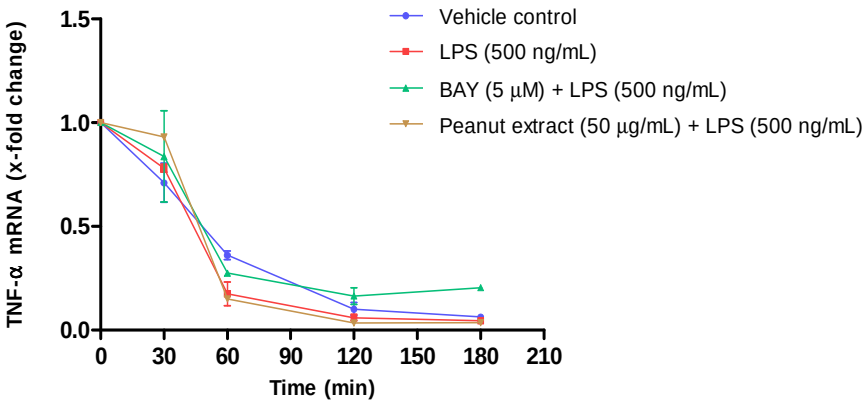

Figure 31. Effect of peanut extract on TNF-α mRNA stabilization in THP-1 cells using RT-PCR assay. THP-1 monocytes were incubated with vehicle control (3.75% DMSO), BAY 11-7082 (5 µM) and peanut extract (50 µg/mL) for 1h and stimulated with LPS (500 ng/mL) for 2h. After 2h of incubation of LPS, Act D 5µg/mL was added to medium. The incubation times with Act D were 30, 60, 120 and 180 min. At these times the cells were lysed to obtain total RNA. The abundance of mRNA transcripts for TNF-α was determined using real time quantitative polymerase chain reaction (RT-PCR). Data were normalized using the values obtained from GAPDH (house keeping gene), and are the mean of two separate experiments run in triplicate. Error bars show SD. *P<0.05 *versus* vehicle control.

1.6 Effect of peanut extract on TNF-α protein

In monocyte THP-1 cells, maximum stimulation of TNF-α at LPS concentration of 500 ng/mL and 4h incubation in the absence of peanut extract revealed that approximately 85% of the TNF-α release was extracellular, while 15% remained inside the cell (**Figure 32A** and **B**). The results for extra-, intracellular, and total TNF-α release in THP-1 cells pre-treated with peanut extract (5, 25, 50 and 100 µg/mL) are shown in **Figure 32**.

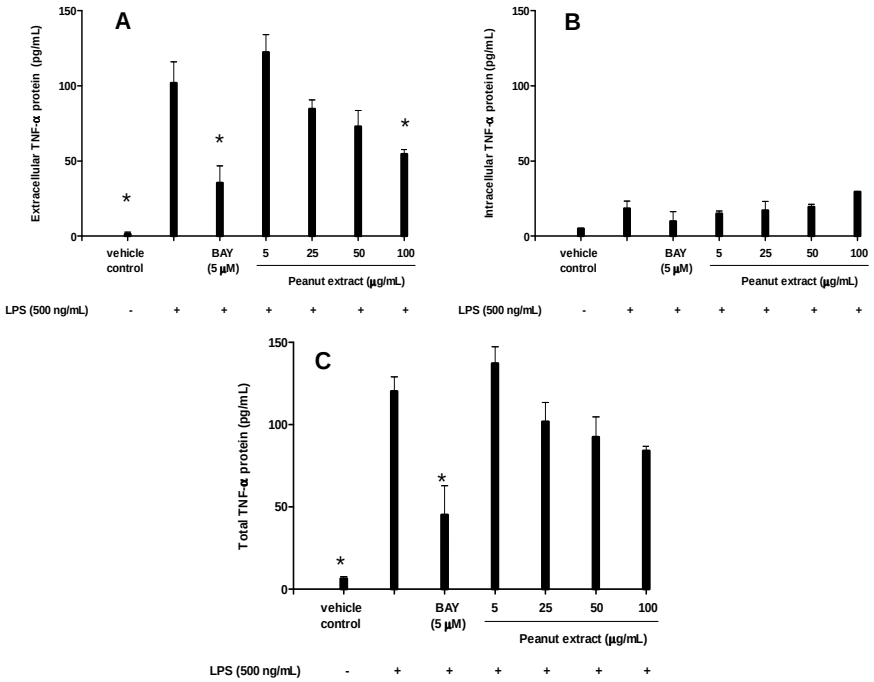

Figure 32. Effect of peanut extract on TNF-α protein secretion. THP-1 monocytes were incubated with vehicle control (3.75% DMSO), BAY 11-7082 (5µM) and peanut extract (5, 25, 50 and 100 µg/mL) for 1h and stimulated with LPS (500 ng/mL) for 4h. TNF-α protein secretion was determined by ELISA. Data are the mean of two separate experiments run in triplicate. Error bars show SD. (**A**) Extracellular TNF-α protein secretion. *P<0.05 *versus* LPS; (**B**) intracellular TNF-α protein secretion; (**C**) total TNF-α protein secretion. *P<0.05 *versus* LPS

1.6.1 Extracellular TNF-α protein

BAY (5 μM) decreased LPS-stimulated (500 ng/mL) extracellular TNF-α protein nearly 3-fold ($P<0.05$).

Peanut extract inhibited the secretion of extracellular TNF-α protein secretion by 18% and 29% at 25 and 50 μg/mL, respectively; but only 47% of extracellular TNF-α protein reduction at 100 μg/mL was statistically significant ($P<0.05$) compared with LPS alone (**Figure 32A**).

1.6.2 Intracellular TNF-α protein

The concentration of the remaining intracellular TNF-α protein was very low compared to he extracellular component (**Figure 32B**), suggesting that most of the TNF-α protein was secreted to the extracellular medium when cells are incubated for 1h with the peanut extract following 4h stimulation by LPS (500 ng/mL).

1.6.3 Total TNF-α protein

Peanut extract concentrations (5, 25, 50 and 100 μg/mL) induced a decrease in total TNF-α protein secretion; the reductions were 15%, 23% and 30% at 25, 50 and 100 μg/mL respectively albeit the reductions were not statistically significant (**Figure 32C**). The results of total TNF-α protein secretion are similar to that observed with extracellular TNF-α protein.

BAY (5 μM) decreased 3-fold the total TNF-α protein concentration induced by LPS (500 ng/mL) stimulation ($P<0.05$).

The same tendency was observed for peanut extract on TNF-α mRNA (**Figure 30**) and on total and extracellular TNF-α protein secretion (**Figure 32A** and **C**); albeit the decrease in TNF-α mRNA expression was not statistically significant.

1.7 Effect of peanut extract on TACE activity

Basal TACE activity in THP-1 cells was detectable under all cell conditions tested. BAY (5 μM) significantly (P<0.05) reduced the basal activity of TACE, while peanut extract (5, 25, 50 and 100 μg/mL) did not modify the TACE basal activity.

TACE activity was not sensitive to LPS (500 ng/mL), indicating a failure of LPS to stimulate any TACE catalytic activity response in THP-1 cells (**Figure 33**).

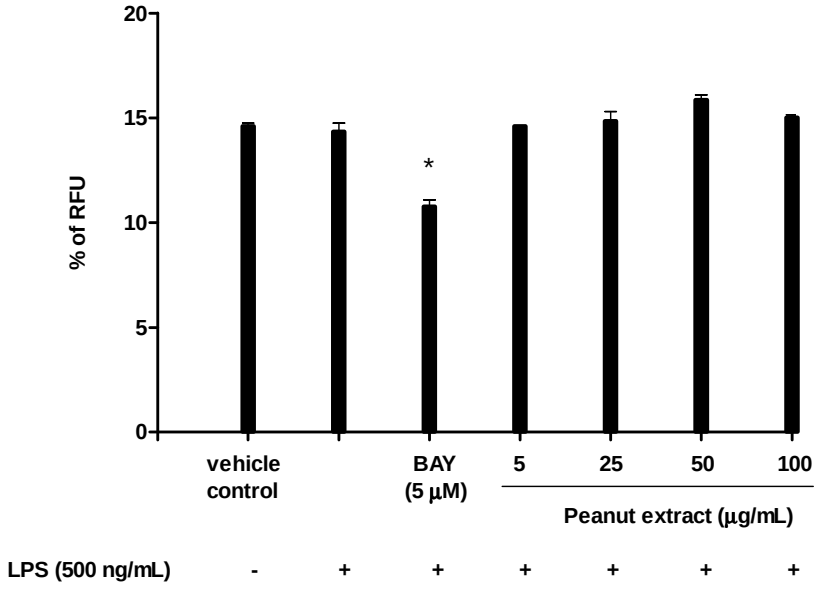

Figure 33. Effect of peanut extract on TACE activity. THP-1 monocytes incubated with vehicle control (3.75% DMSO), BAY 11-7082 (5μM) and peanut extract (5, 25, 50 and 100 μg/mL) for 1h and stimulated with LPS (500 ng/mL) for 4h. TACE activity was determined by a fluorimetric assay (see text for details). Data are the mean of two separate experiments run in triplicate. Error bars show SD. *P<0.05 *versus* LPS

2. Alpha-Tocopherol and BAY 11-7082 Reduce Vascular Cell Adhesion Molecule in Human Aortic Endothelial Cells (Study 2)

2.1 Cytotoxicity

There was no evidence of HAEC cytotoxicity following exposure to AT (10, 25, 50, 75 and 150 µM) for 6h (**Figure 34A**) nor TNF-α (10 ng/mL; **Figure 34B**) for the subsequent 24h. No cytotoxicity was observed, as assessed by LDH activity release, at the concentrations of BAY tested (1 µM) under these experimental conditions.

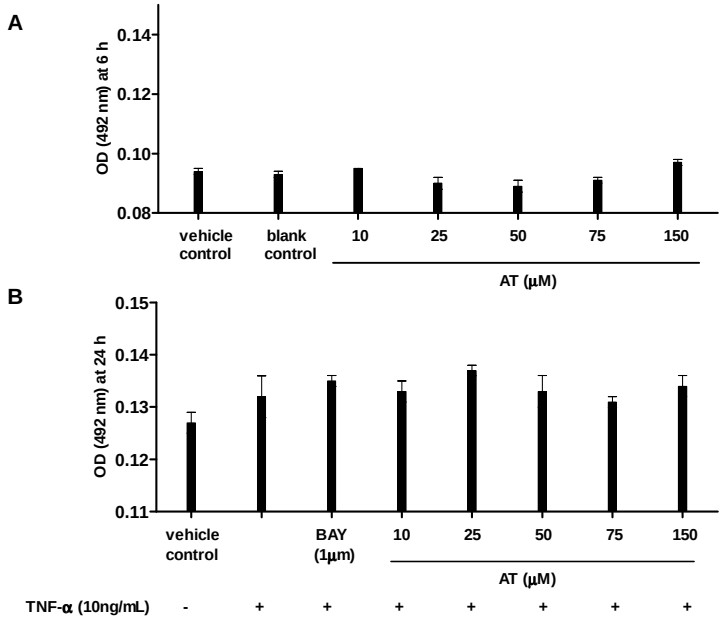

Figure 34. Cytotoxicity from HAEC incubated with AT or BAY and stimulated with TNF-α. (**A**) Activity of LDH released into the cell-culture supernatants of HAEC following incubation with AT (10, 25, 50, 75 and 150 µM) for 6h. (**B**) Activity of LDH released into the cell-culture supernatants of HAEC following stimulation with TNF-α (10 ng/mL) in the presence (1µM) for 24h or absence of BAY. Vehicle control refers to cells incubated with AT vehicle (absolute ethanol). Blank control refers to cells incubated without ethanol, TNF-α, BAY or AT. Results are the mean and the SD (error bars) of optical density (OD) from one representative experiment where each set of experimental conditions was run in triplicate.

2.2 Effect of AT and BAY on CAMs mRNA expression by HAEC stimulated with TNF-α

Exposure of cells to TNF-α (1 ng/mL for VCAM-1; 10 ng/mL for E-selectin and ICAM-1) for 24h induced strong up-regulation of CAMs mRNA expression (**Figure 35**).

As shown in **Figure 35A**, AT (at 50, 75 and 150 µM) significantly reduced VCAM-1 mRNA expression in TNF-α-stimulated HAEC by approximately 37% ($P<0.05$). The intra-assay CV was <20%, the inter-assay CV was <21%. Compared to TNF-α alone, BAY treatment (0.1 µM) significantly blocked TNF-α-induced VCAM-1 mRNA expression by approximately 25% ($P<0.05$) (**Figure 35A**). The intra- and inter-assay CVs were <13%.

There was a tendency towards reducing E-selectin mRNA expression by AT and BAY by approximately 40% and 25%, respectively, but these reductions was not statistically significant (**Figure 35B**).

ICAM-1 mRNA expression was decreased by AT and BAY by 25-40% and 13%, respectively compared to TNF-α stimulation, but the decrease did not reach statistical significance (**Figure 35C**).

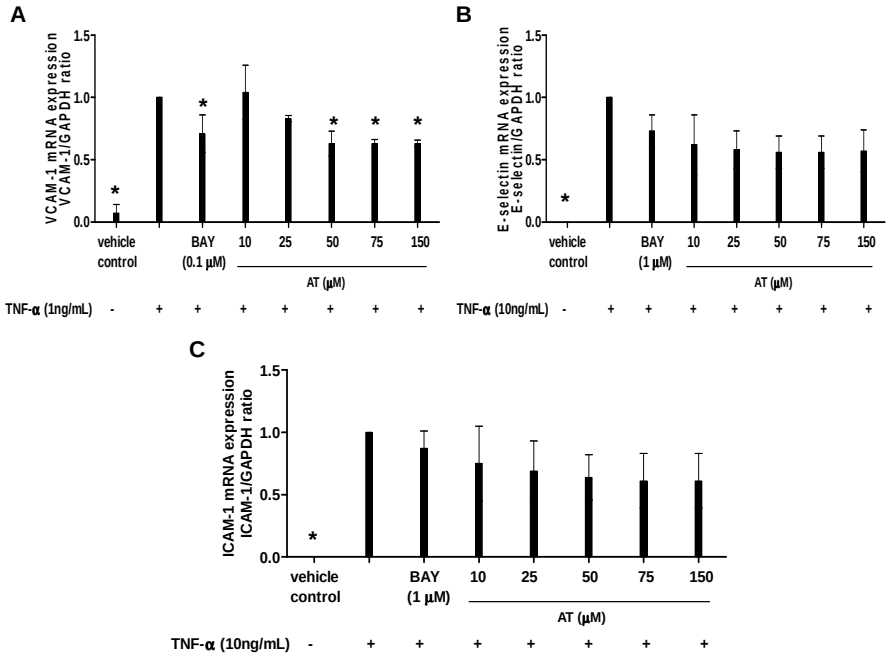

Figure 35. Effect of AT and BAY on CAMs mRNA expression in HAEC stimulated by TNF-α. (**A**) Effect of AT and BAY on VCAM-1 mRNA expression. (**B**) Effect of AT and BAY on E-selectin mRNA expression. (**C**) Effect of AT and BAY on ICAM-1 mRNA expression. Results are the mean and the SD (error bars) of two independent experiments where each set of experimental conditions was run in triplicate. *P< 0.05 *versus* TNF-α-alone.

2.3 Effect of AT and BAY on sCAMs protein secretion by HAEC stimulated with TNF-α

When cells were exposed to TNF-α (10 ng/mL), sVCAM-1, sE-selectin and sICAM-1 increased significantly to 7.71 (0.40) ng/mL, 0.33 (0.08) ng/mL and 13.31 (0.76) ng/mL, respectively (P<0.05; **Figure 36**).

AT significantly reduced sVCAM-1 protein secretion by about 40% in the highest doses tested (50, 75 and 150 µM) compared to TNF-α alone (10 ng/mL) (P<0.05) (**Figure 36A**). No dose-response effect was observed. The inter- and intra-assay CVs were <12%. AT also reduced sE-selectin (between 5 and 29%) and sICAM-1 (between 5 and 16%) at all doses tested, but the decreases did not reach statistical significance.

BAY (1μM) reduced TNF-α (10 ng/mL) effects on sVCAM-1, sE-selectin and sICAM-1 release by 53%, 50% and 26%. Only the effects on sVCAM and sE-selectin were statistically significant (P<0.05) (**Figure 36A**, **B** and **C**).

As shown in **Figure 36B** and **C**, non-activated HAEC did not appear to release sE-selectin (limit of detection <0.125ng/mL) and sICAM-1 (limit of detection <1.56 ng/mL), but the non-activated cells did express sVCAM-1 (2.12 ng/mL; **Figure 36A**). Treatment of HAEC with AT had no statistically significant reduction effect on sE-selectin (between 5 and 29% reduction) and sICAM-1 (between 6 and 16% reduction) protein secretion.

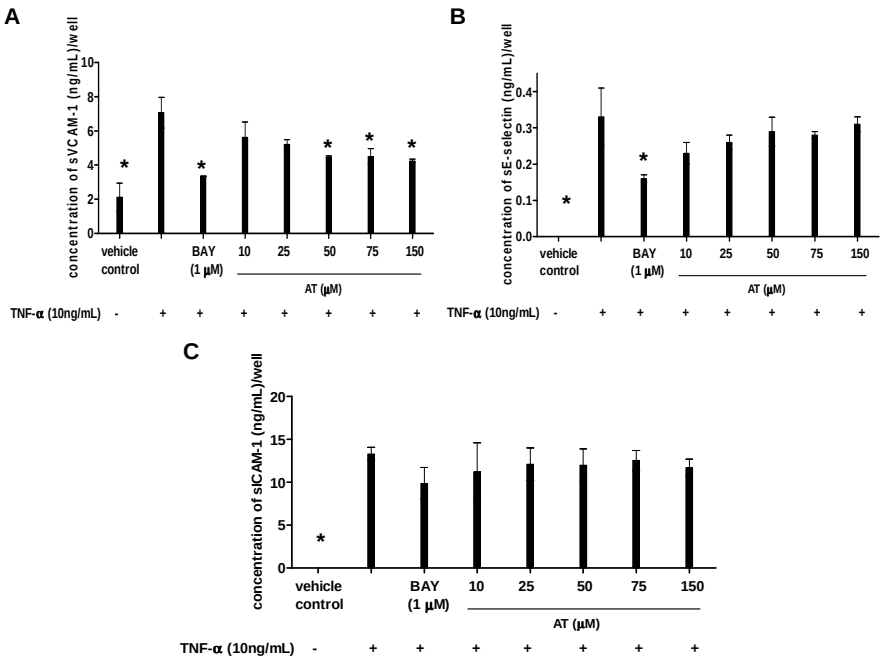

Figure 36. Effect of AT and BAY on sCAMs protein secretion in HAEC stimulated by TNF-α. (**A**) Effect of AT and BAY on sVCAM-1 protein release. (**B**) Effect of AT and BAY on sE-selectin protein release. (**C**) Effect of AT and BAY on sICAM-1 protein release. Results are the mean and the SD (error bars) of two independent experiments where each set of experimental conditions was run in triplicate. *p< 0.05 *versus* TNF-α-alone.

2.4 Effect of AT and BAY on lymphocyte cell adhesion to HAEC

Qualitatively (**Figure 37**), there appeared to be a considerable number of Jurkat-T-cells adhering to TNF-α-treated HAEC, while very few cells adhered to untreated HAEC. Adhesion to HAEC that had been incubated with BAY (0.5, 1, 2 and 5 μM) appeared to be greatly decreased. Adhesion to HAEC that had been pre-incubated with AT (10, 25, 50, 75 and 150 μM) for 6h appeared to decrease the adhesion of HAEC to Jurkat-T-cells at all concentrations tested (**Figure 37**).

The cell fluorescence images revealed that exposure of cells to TNF-α (10 ng/mL) for 24h induced strong adhesion between Jurkat-T-cells and HAEC (**Figure 38**). The effects of different concentrations of AT and BAY on TNF-α-induced cell surface adhesion molecules expression are depicted in (**Figure 38**). AT failed to modulate significantly the TNF-α-induced cell surface expression of CAMs at any of the concentrations (a reduction of between 11 and 17%) (**Figure 38**). In contrast, when treated with BAY (0.1, 1, 2 and 5 μM), the TNF-α-induced cell surface expression of CAMs was notably reduced to 7%, 13%, 57% and 77%, respectively; statistically significant reductions being observed only at 2 and 5 μM ($P<0.05$).

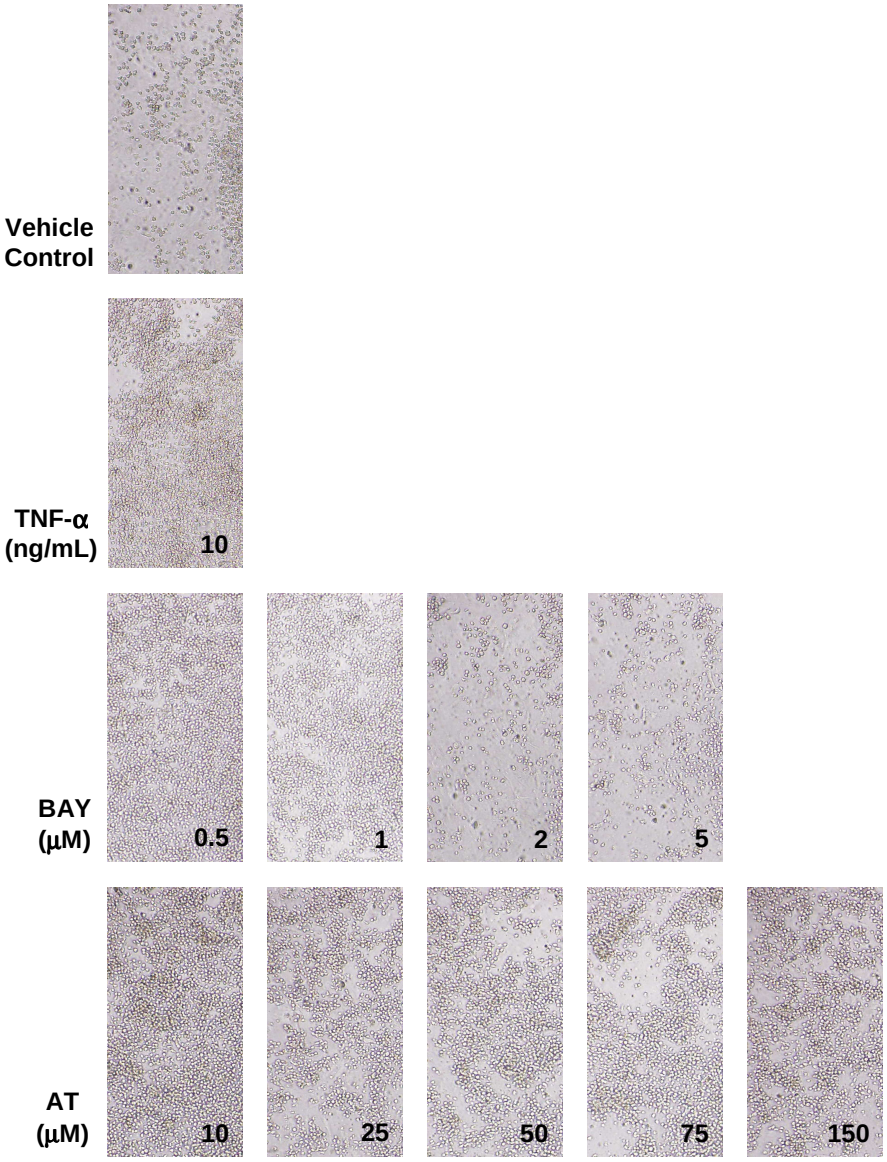

Figure 37. Adhesion of Jurkat-T-cells to TNF-α-treated HAEC images under microscope (x4). Microscope images of the experiments. Conditions used for this study were: Vehicle control; TNF-α (10ng/mL); BAY (0.5, 1, 2 and 5 μM); AT (10, 25, 50, 75 and 150 μM).

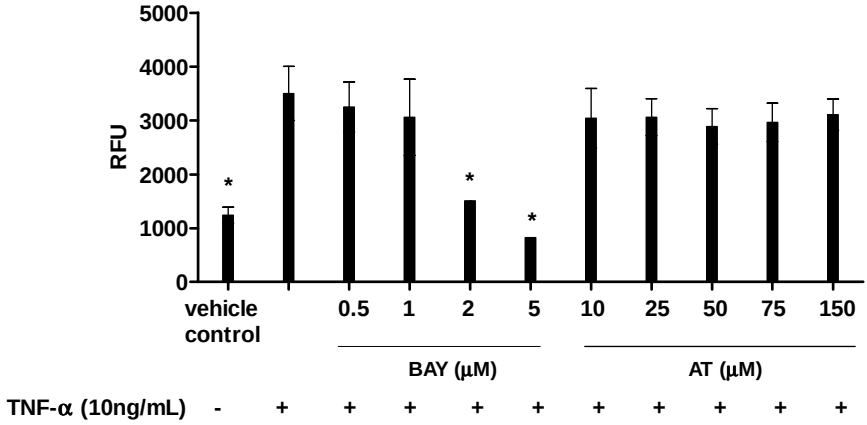

Figure 38. Adhesion of Jurkat-T-cells to TNF-α-treated HAEC. Effect of AT, at all concentrations tested (10, 25, 50, 75 and 150 μM) on cell-cell adhesion. Data are the mean and the SD (error bars) of relative fluorescence units (RFU) from two separate experiments run in octuplicate. $^{*}p<0.05$ *versus* TNF-α-alone.

3. Biomarkers of Food Intake and Metabolite Differences between Plasma and Red Blood Cell Matrices; a Human Metabolomic Profile Approach (Study 3)

3.1 Biochemical parameters

Table 3 summarizes the characteristics of the 10 healthy male volunteers. The mean (SD) age was 44 (11.5) years. Of these individuals, 40% were within the reference range with respect to cholesterol concentrations (reference range: 3.1 - 5.15 mmol/L); 50% with respect to apolipoprotein B100 (reference range: 70 - 105 mg/dL); 70% with respect to HDL-c (reference value: >1.30 mmol/L) and creatinine (reference range: 0.6 - 1.30 mg/dL); 80% with respect to bilirubin (reference value: <1.1 mg/dL). With respect to the rest of the parameters studied, between 90-100% of the participants were within the reference ranges.

Table 3. Basal biochemical values, reference ranges, and percentages of basal values within the reference range.

Measured parameter	Men (N = 10)		
	mean SD	Reference range; Absolute values	Basal values % of reference
Age; years	44 (11.54)	20 - 70	100
Cholesterol; mmol/L	5.08 (0.69)	3.1 - 5.15	40
Triglycerides; mmol/L	0.93 (0.37)	0.45 - 1.86	100
HDL; mmol/L	1.41 (0.15)	> 1.30	70
Apolipoprotein A1; mg/dL	136.20 (6.79)	122 - 161	100
Apolipoprotein B100; mg/dL	96.60 (17.39)	70 - 105	50
Glucose; mg/dL	99.80 (10.28)	59.4 - 109.8	90
Uric acid; mg/dL	5.15 (0.90)	3.6 - 7.7	100
Bilirubin; mg/dL	0.84 (0.22)	< 1.1	80
Creatinine; mg/dL	0.66 (0.17)	0.6 - 1.30	70
Urea; mg/dL	33.70 (8.47)	15 - 45	90
Glutamic oxaloacetic transaminase; U/L	24.90 (9.71)	< 38	90
Glutamil pyruvic transaminase; U/L	21.20 (9.63)	10 - 41	90
Gamma glutamyl transferase; U/L	21.00 (9.67)	11 - 50	100
Alkaline phosphatase; U/L	130.30 (29.91)	98 - 279	90

3.2 Sodium citrate and lithium heparin samples

With respect to sodium citrate compared with lithium heparin samples, there were no significant differences in the lipid fraction in relation to the anticoagulant used (**Figure 39, A.2** and **B.2** respectively). Concerning the non-lipid (aqueous) fraction, the sodium citrate plasma samples had a higher concentration of citrate compared to the lithium heparin samples (**Figure 39, A.1**) while, conversely, RBC showed no significant differences in terms of metabolic profiles between the two anticoagulants used (**Figure 39, B.1**).

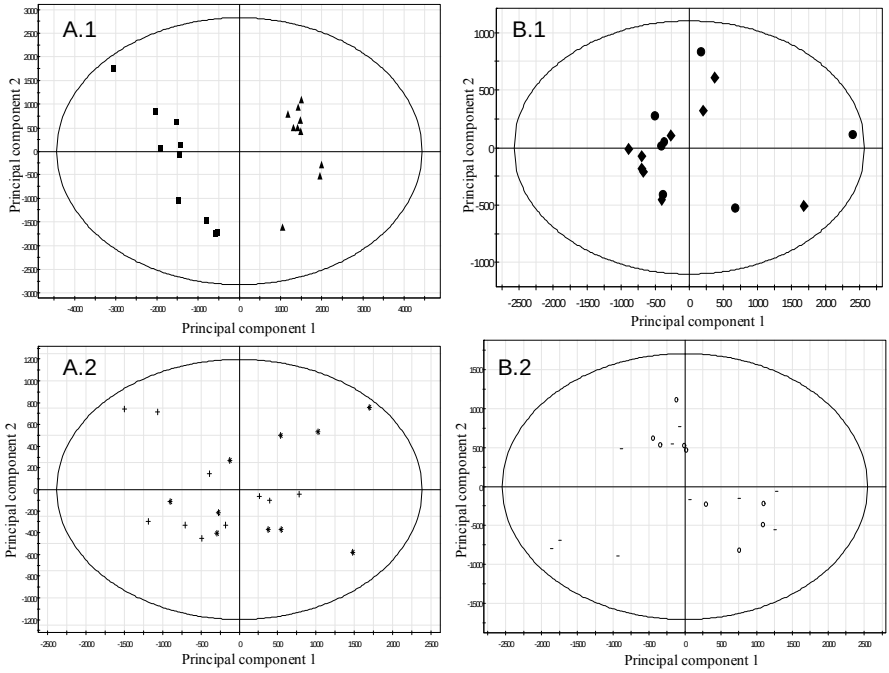

Figure 39. Series of PCA models to examine the differences in plasma and RBC matrices derived from blood collected with sodium citrate or lithium heparin as anticoagulants. (**A.1**) PCA scores plot of aqueous fraction from plasma using sodium citrate (▲) compared with the same fraction using lithium heparin (■) (R^2 = 94%, Q^2 = 87.7%). (**A.2**) PCA scores plot of lipid fraction from plasma using sodium citrate (*) compared with the same fraction using lithium heparin (+) (R^2 = 87.9%, Q^2 = 73%). (**B.1**) PCA scores plot of aqueous fraction from RBC using sodium citrate (♦) compared with the same fraction using lithium heparin (●) (R^2 = 72.2%, Q^2 = 48.1%). (**B.2**) PCA scores plot of lipid fraction from RBC using sodium citrate (○) compared with the same fraction using lithium heparin (—) (R^2 = 97.9%, Q^2 = 92.2%).

3.3 Aqueous metabolites comparison between plasma and RBC

The aqueous metabolites in plasma and in RBC matrix were identified as: 1) valine, leucine and isoleucine; 2) lactate; 3) alanine; 4) lysine; 5) acetate; 6) acetone; 7) acetoacetate; 8) glutamine; 9) citrate; 10) creatine; 11) glucose and amino acids; 12) β-glucose; 13) α-glucose; 14) tyrosine; 15) histidine; 16) phenylalanine; 17) pyridoxine; 18) hydroxibenzoate; 19) ADP-ATP. Comparing the aqueous fraction from both matrices (plasma *vs*. RBC), 1D ^{1}H NMR showed higher concentrations of glucose in plasma than RBC and less ADP-ATP and creatine (R^2=67.2%, Q^2=80.3%) (**Figure 40**).

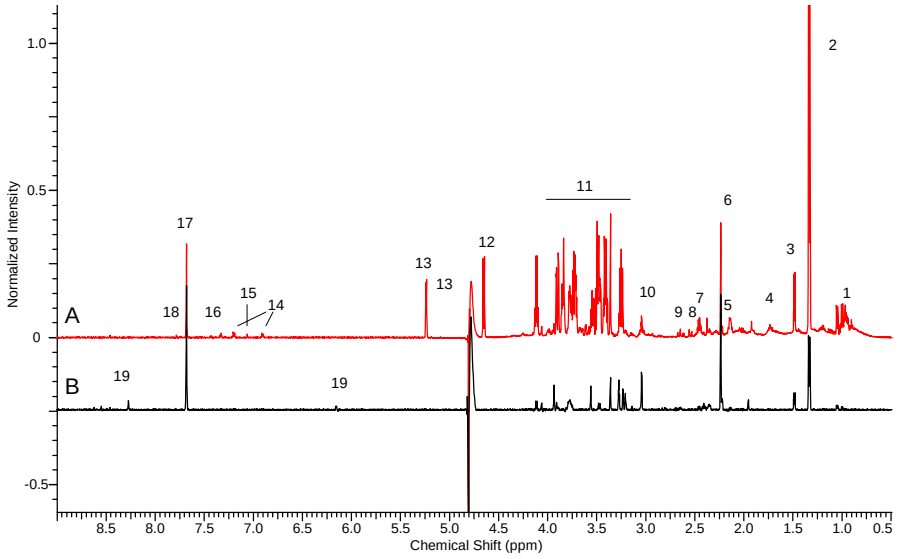

Figure 40. A typical 500-MHz ^{1}H NMR spectrum of aqueous fraction from human plasma and RBC. (**A**) Representative spectrum of aqueous fraction from plasma sample (lithium heparin). (**B**) Representative spectrum of aqueous fraction from RBC sample (lithium heparin). The major aqueous metabolites identified are: 1: valine, leucine and isoleucine; 2: lactate; 3: alanine; 4: lysine; 5: acetate; 6: acetone; 7: acetoacetate; 8: glutamine; 9: citrate; 10: creatine; 11: glucose and amino acids; 12: β-glucose; 13: α-glucose; 14: tyrosine; 15: histidine; 16: phenylalanine; 17: pyridoxine; 18: hydroxibenzoate; 19: ADP-ATP

3.4 Lipoprotein measurements

1D ^{1}H NMR spectroscopy analysis showed that measurable lipoprotein content was higher in plasma samples than in RBC (R^2 = 70.6%, Q^2 = 94.6%) in which the following organic metabolites were found: 1) cholesterol; 2) lipoproteins; 3) phosphatidyl ethanolamine; 4) phosphatidyl choline; 5) triglycerides; 6) phosphatidyl serine, ethanolamine and choline; 7) sphingomyelin; 8) plasmalogen (**Figure 41**).

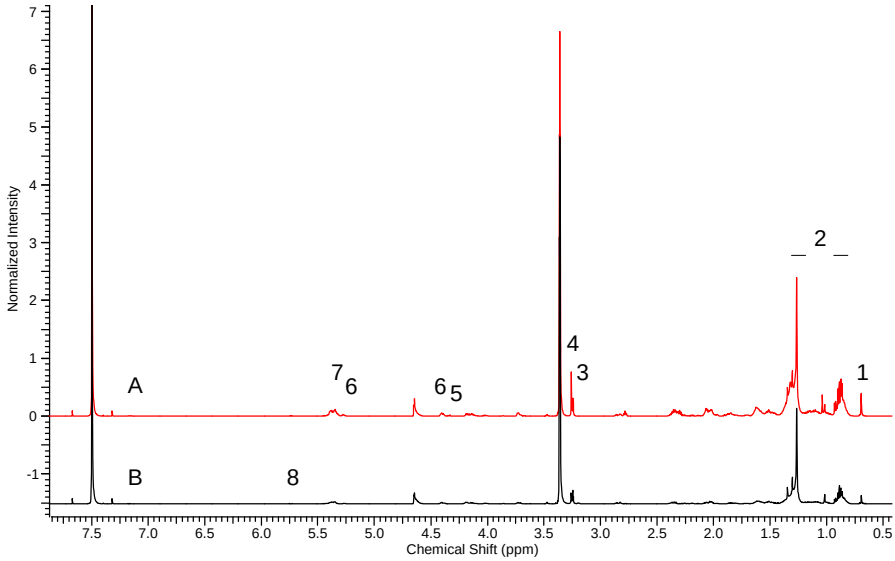

Figure 41. A typical 500-MHz ^{1}H NMR spectrum of organic fraction from human plasma and RBC. (**A**) Representative spectrum of organic fraction from plasma sample (lithium heparin). (**B**) Representative spectrum of organic fraction from RBC sample (lithium heparin). The major organic metabolites identified are: 1: cholesterol; 2: lipoproteins; 3: phosphatidyl ethanolamine; 4: phosphatidyl choline; 5: triglycerides; 6: phosphatidyl serine, ethanolamine and choline; 7: sphingomyelin; 8: plasmalogen

2D diffusion-edited ^{1}H NMR spectra and its corresponding functions (F1-F7) from a representative plasma sample are shown in **Figure 42A**. Spectra recorded at low gradient strengths (<13%) were not used in order

to avoid interferences from low molecular weight metabolites. A representative comparison between plasma obtained from sodium citrate and lithium heparin anticoagulation is shown in in **Figure 42B**.

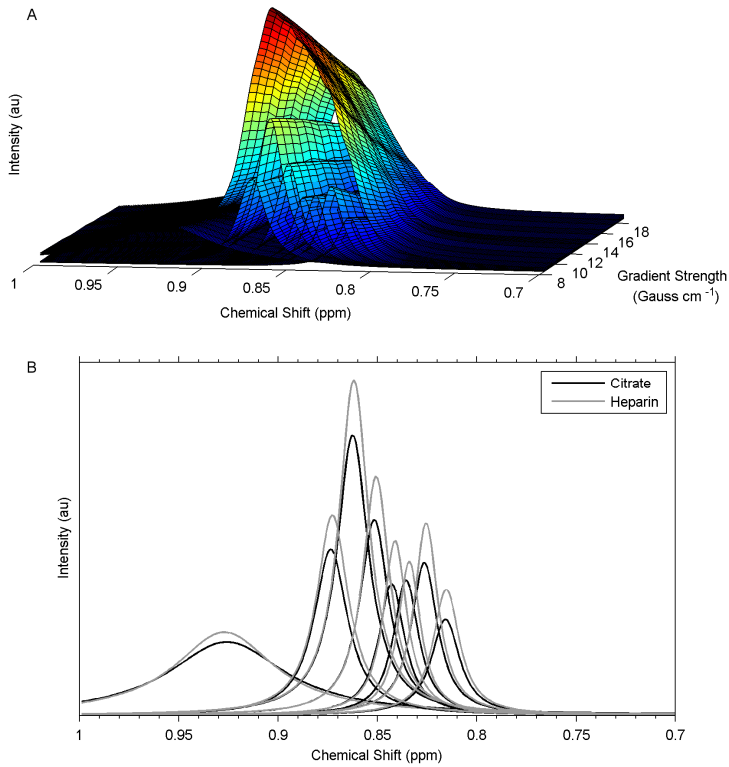

Figure 42. (**A**) Example of 2D diffusion-edited ^{1}H NMR global spectra and optimal functions used to fit the surface. (**B**) Spectrum from total plasma obtained using sodium citrate and lithium heparin as anticoagulants.

Table 4 and **5** summarize the means (SD) of relative areas, diffusion coefficients, radii of the lipoprotein subclasses corresponding to plasma obtained from both anticoagulants (sodium citrate and lithium heparin). Lipoprotein absolute areas, represented as arbitrary units mean (SD) of samples from sodium citrate and lithium heparin tubes were: **F1** 796 488.08 (16 426.53), P=0.62; **F2** 715 802.28 (89 997.08), P=0.001); **F3** 577 744.98

(88 059.11), P=0.01; **F4** 512 310.34 (55 096.58), P=0.13; **F5** 442 228.58 (73 839.13), P=0.02; **F6** 353 005.90 (44 997.73), P=0.01) and **F7** 187 808.09 (24 434.51), P=0.41). These values were related to the lipoprotein concentrations and, as such, plasma from sodium citrate anticoagulation was more diluted than the plasma from lithium heparin anticoagulation; F1 (2.87%), F2 (16.33%), F3 (19.46%), F4 (14.13%), F5 (21.12%), F6 (16.54%) and F7 (16.85%); (P<0.05).

However, when the absolute areas were converted to relative areas (%), these differences resulting from type of anticoagulant ceased to be significant (**Table 4**).

Table 4. Means and standard deviations of relative areas (%) and diffusion coefficient (m2/sec) of lipoprotein subclasses in plasma

Function	relative areas (%)					diffusion coefficient (m^2/sec)				
	sodium citrate	lithium heparin	mean	(SD)	*P*	sodium citrate	lithium heparin	mean	(SD)	*P*
F1	23.73	20.92	22.32	(1.99)	0.04	1.164E-11	9.52E-12	1.058E-11	(1.50E-12)	0.01
F2	19.72	20.18	19.95	(0.32)	0.63	1.459E-11	1.21E-11	1.332E-11	(1.80E-12)	0.00
F3	15.58	16.57	16.08	(0.69)	0.39	1.977E-11	1.65E-11	1.8145E-11	(2.30E-12)	0.00
F4	14.31	14.27	14.29	(0.03)	0.98	2.973E-11	2.83E-11	2.902E-11	(1.00E-12)	0.27
F5	11.79	12.80	12.30	(0.71)	0.36	4.187E-11	4.09E-11	4.136E-11	(7.21E-13)	0.50
F6	9.71	9.96	9.84	(0.18)	0.69	4.997E-11	4.55E-11	4.771E-11	(3.20E-12)	0.01
F7	5.16	5.31	5.23	(0.11)	0.89	5.965E-11	6.01E-11	5.986E-11	(2.97E-13)	0.83

Plasma lipoprotein subclasses expressed as the relative areas and diffusion coefficients corresponding to plasma obtained from both anticoagulants (sodium citrate and lithium heparin) determined by 2D diffusion-edited ^{1}H NMR spectra and its functions (F1-F7). *P* values indicated differences between blood drawn using sodium citrate and lithium heparin as anticoagulants from n=10 healthy individuals.
Lipoprotein absolute areas, represented as arbitrary units mean (SD) of samples from sodium citrate and lithium heparin tubes were: F1 796 488.08 (16 426.53), P=0.62; F2 715 802.28 (89 997.08), P=0.001); F3 577 744.98 (88 059.11), P=0.01; F4 512 310.34 (55 096.58), P=0.13; F5 442 228.58 (73 839.13), P=0.02; F6 353 005.90 (44 997.73), P=0.01) and F7 187 808.09 (24 434.51), P=0.41).

According to the Stokes-Einstein equation, size and lipoprotein diffusion coefficients were related to plasma viscosity; sodium citrate plasma 1.17 (0.08; mPa sec) vs. 1.25 (0.08; mPa sec) for lithium heparin plasma i.e. lipoproteins in sodium citrate plasma diffuse faster than lithium heparin plasma (P<0.05). Conversely, the lipoprotein radii measurements showed no significant differences between citrate and heparin plasma, due to normalization for viscosity.

The smallest function (F7) had the highest diffusion coefficient, the smallest lipoprotein area and the smallest lipoprotein radius, while the highest function (F1) had the smallest diffusion coefficient, the largest lipoprotein area and the largest lipoprotein radius.

The lipoprotein areas and radii were directly related to each other and both were inversely related to the diffusion coefficient.

Lipoprotein subclasses (**Table 5**) were defined according to the reference lipoprotein subclass radii established by Duell et al (Duell PB, Illingworth, D. R. and Connor, W. E., 2001).

Table 5. Means and standard deviations of radius (Å), reference ranges of lipoprotein subclass radii (Å) and lipoprotein subclass conventional terminology

Function	radius (Å)					lipoprotein subclass radius; reference range (Å)	lipoprotein subclasses
	sodium citrate	lithium heparin	mean	(SD)	*P*		
F1	197.97	182.16	190.06	(11.18)	0.63	150-400	VLDL
F2	146.48	142.71	144.60	(2.66)	0.79	125-175	IDL
F3	113.03	105.28	109.15	(5.48)	0.49	90-140	LDL
F4	72.46	72.06	72.26	(0.28)	0.87		LDL very small
F5	46.13	46.45	46.29	(0.22)	0.60		HDL large
F6	38.72	40.63	39.67	(1.35)	0.16	25-60	HDL medium
F7	31.59	32.02	31.80	(0.30)	0.72		HDL small

Plasma lipoprotein subclasses expressed as radii corresponding to plasma obtained from both anticoagulants (sodium citrate and lithium heparin) determined by 2D diffusion-edited ^{1}H NMR spectra and its functions (F1-F7). *P* values indicated differences between blood drawn using sodium citrate and lithium heparin as anticoagulants from n=10 healthy individuals; Å = angstrom units = 10^{-10}m

Lipoprotein subclasses radius reference range as described by Duell et al (Duell PB, Illingworth, D. R. and Connor, W. E., 2001).

3.5 FA comparison on between plasma and RBC

Plasma and RBC FA concentrations and percentages are summarized in **Table 6**. Plasma had more FAMEs than the RBC matrix.

In RBC, the percentages of the saturated fatty acids (SFA) 16:0, 17:0, 20:0 and 24:0 and the polyunsaturated fatty acids (PUFA) 22:6 n-3 and 20:4 n-6 were higher than in plasma ($P<0.05$). However in plasma, the percentage SFA 14:0, monounsaturated fatty acids (MUFA) 14:1 n-5, 16:1 n-7, 17:1 n-7 and 18:1 n-9 and PUFA 18:3 n-3, 18:2 n-6, 18:3 n-6 and 20:3 n-6 were higher than in RBC ($P<0.05$).

Table 6. Fatty acid composition in plasma and red blood cell (RBC) matrices

		FAME µg/mL (SD)			FAME % of total fatty acids (SD)		
Fatty acid	**Fatty Acid**	**Plasma**	**RBC**	***P***	**Plasma**	**RBC**	***P***
	SFA						
Lauric acid	12:0	13.40 (0.99)	5.60 (0.72)	0.01	0.63 (0.10)	0.95 (0.05)	0.06
	13:0	0.05 (0.06)	0.00 (0.00)	0.42	0.00 (0.00)	0.00 (0.00)	0.43
Myristic acid	14:0	16.75 (2.87)	3.42 (0.40)	0.02	0.79 (0.04)	0.58 (0.02)	0.02
	15:0	5.81 (1.08)	1.47 (0.09)	0.03	0.27 (0.01)	0.25 (0.00)	0.09
Palmitic acid	16:0	235.93 (31.59)	109.59 (4.76)	0.03	11.2 (1.03)	18.55 (0.70)	0.01
Margaric acid	17:0	7.84 (1.40)	4.39 (0.23)	0.07	0.37 (0.02)	0.74 (0.02)	0.00
Stearic acid	18:0	83.56 (35.55)	43.93 (15.95)	0.29	3.95 (0.82)	7.44 (0.02)	0.16
Arachidic acid	20:0	0.84 (0.20)	0.85 (0.09)	0.95	0.04 (0.00)	0.14 (0.00)	<0.001
Behenic acid	22:0	0.13 (0.19)	0.15 (0.22)	0.93	0.01 (0.01)	0.03 (0.03)	0.53
Lignoceric acid	24:0	0.00 (0.00)	0.90 (0.16)	0.01	0.00 (0.00)	0.15 (0.04)	0.03
	MUFA						
Myristoleic acid	14:1 n-5	0.36 (0.16)	0.00 (0.00)	0.09	0.02 (0.00)	0.00 (0.00)	0.03
Palmitoleic acid	16:1 n-7	30.36 (7.23)	0.88 (0.30)	0.03	1.43 (0.02)	0.15 (0.06)	0.00
	17:1 n-7	1.68 (0.79)	0.03 (0.04)	0.10	0.08 (0.02)	0.01 (0.01)	0.04
Oleic acid	18:1 n-9	222.91 (51.20)	55.09 (3.42)	0.04	10.5 (0.07)	9.33 (0.18)	0.01
Eicosenoic acid	20:1 n-9	3.33 (2.03)	1.09 (0.11)	0.26	0.16 (0.06)	0.18 (0.03)	0.55
	PUFA						
	n-3						
ALA	18:3 n-3	4.48 (2.00)	0.00 (0.00)	0.09	0.21 (0.05)	0.00 (0.00)	0.03
EPA	20:5 n-3	11.67 (2.47)	3.22 (0.49)	0.04	0.55 (0.01)	0.55 (0.13)	0.99
DHA	22:6 n-3	58.18 (18.23)	47.03 (2.97)	0.48	2.75 (0.25)	7.96 (0.14)	0.00
	n-6						
Linoleic acid	18:2 n-6	1124.59 (244.45)	143.92 (12.29)	0.03	53.13 (0.34)	24.37 (0.11)	<0.001
Gamma-linolenic acid	18:3 n-6	8.74 (2.54)	0.02 (0.03	0.04	0.41 (0.03)	0.00 (0.01)	0.00
Eicosadienoic acid	20:2 n-6	4.74 (1.17)	0.79 (0.54)	0.05	0.22 (0.01)	0.13 (0.08)	0.25
DHGLA	20:3 n-6	49.64 (10.93)	9.58 (1.28)	0.03	2.35 (0.01)	1.62 (0.09)	0.01
Arachidonic acid	20:4 n-6	231.75 (56.15)	158.66 (5.98)	0.21	11 (0.21)	26.86 (1.17)	0.00
	Total FAME	2116.74	590.61		100	100	

P values indicated differences between Plasma and RBC from n=10 healthy individuals.
Abbreviations: FAME, fatty acid methyl ester; n = 20 for plasma and 20 for red blood cell; P < 0.05; ALA: alpha-linolenic acid; EPA: eicosapentaenoic acid; DHA: docosahexaenoic acid; DHGLA: dihomo-gamma-linolenic acid

3.6 Plasma and RBC polyphenols

Plasma and RBC obtained from sodium citrate and lithium heparin samples had similar chromatogram traces for the analyses of phenols. Plasma and RBC polyphenol peaks are shown in **Figure 43**. We were able to identify

several polyphenols in plasma (**Figure 44**). These included: 3-hydroxyphenylpropionic acid (peak 4), *o*-, *m*- and *p*-hydroxyphenylacetic acid (peak 6), hydroxybenzoic acid (peak 7), phenylacetic acid (peak 8) and hydroxyflavanone (peak 10). Further, unidentifiable peaks in plasma were at molecular weight 180 g/mol (peak 1 and 2), 204 g/mol (peak 3), 194 g/mol (peak 5) and 254 g/mol (peak 9). In RBC, the unidentifiable peaks were at molecular weights of 346 g/mol (peak 11), 695 g/mol (peak 12), 432 g/mol (peak 13) and 651 g/mol (peak 14).

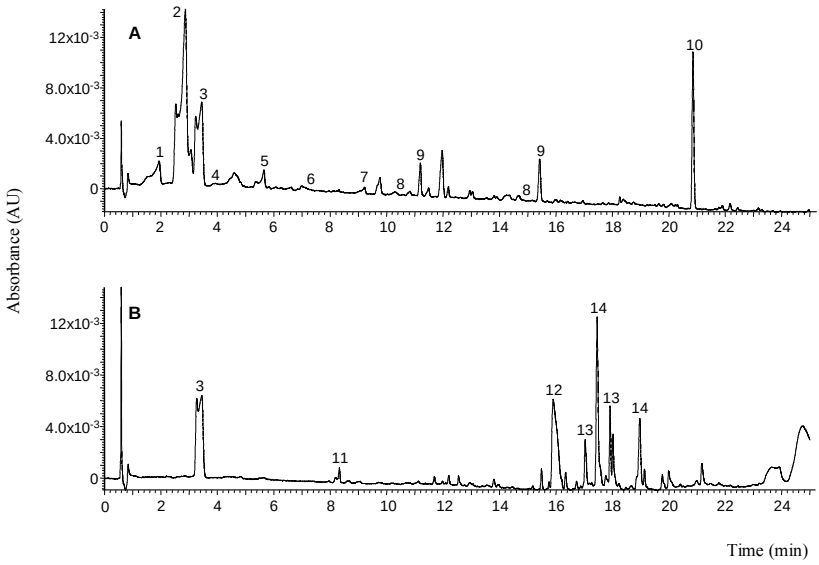

Figure 43. A representative UPLC chromatogram (278 nm) obtained from the analysis of (**A**) plasma lithium heparin samples, and (**B**) RBC lithium heparin samples.

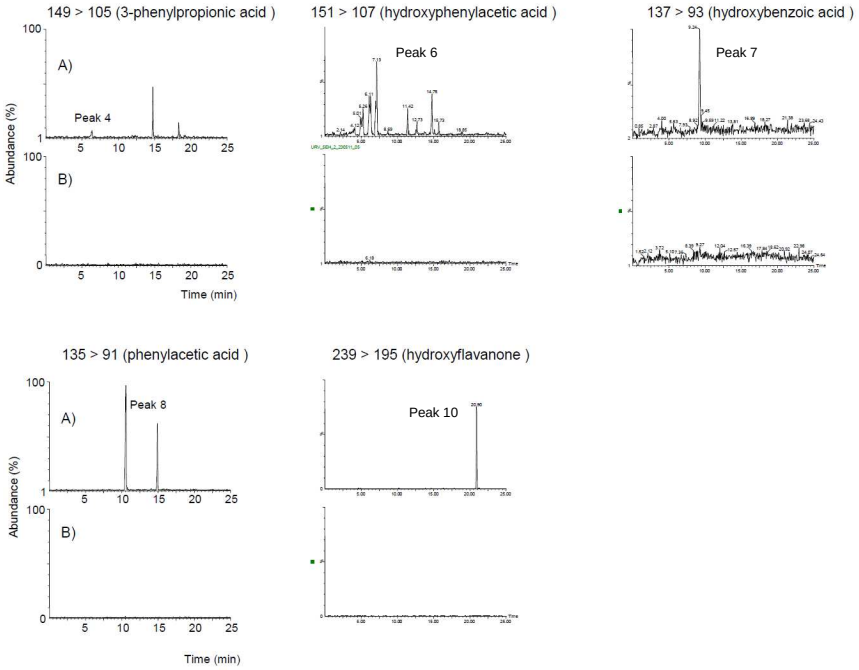

Figure 44. A representative UPLC-MS/MS for analysis of (**A**) plasma lithium heparin samples, and (**B**) RBC lithium heparin samples.

DISCUSSION AND CONCLUSIONS

EFFECT OF FOOD EXTRACTS AND BIOACTIVE FOOD COMPOUNDS ON THE MECHANISM OF ATHEROSCLEROSIS AND NUTRITIONAL BIOMARKERS

Úrsula Catalán Santos

Dipòsit Legal: T. 1058-2012

Inhibition of the Transcription factor c-Jun by the MAPK family, and not the NF-κB Pathway, Suggests that Peanut Extract has Anti-inflammatory Properties (Study 1)

The present study confirms our hypothesis that peanut extract (at 100 µg/mL) exerts an anti-inflammatory effect, in THP-1 monocytes challenged with LPS, by reducing the secretion of the biologically active soluble form of extracellular TNF-α protein.

Further, we propose a standardized *in vitro* monocyte cellular assay (from signal transduction to extracellular secretion of TNF-α) which can be used to evaluate anti-inflammatory mechanisms of such products such as food extracts and synthetic compounds.

The present study demonstrated that the synthetic compound BAY, used as experiment control, can reduce the TNF-α protein secretion by inhibiting, specifically, NF-κB transcription factor and the subsequent steps of the TNF-α production i.e. via TNF-α mRNA intra- and extracellular and total TNF-α protein. However, BAY (5 µM) had no effect on the mRNA stability of TNF-α.

With the MAPK family, we observed an alternative effect of BAY by reducing the activities of MEF2 and c-Jun transcription factor. Inhibition of c-Jun by BAY has been demonstrated by some investigators such as Lee HS et al. (Lee HS *et al.*, 2010). However, to the best of our knowledge, the inhibition of MEF2 by BAY has not, until now, been observed. We suggest that the reduction of TNF-α produced by BAY is *via* the inhibition of both transcription factor pathways: the NF-κB and the MAPK family. We also demonstrated that BAY (5 µM) has the ability to reduce the basal TACE activity in THP-1 monocytes which, to the best of our knowledge, has not been documented in the literature, to date. Thus, BAY can be used as an experiment control for the *in vitro* THP-1 monocyte model. The model is appropriate for detecting anti-inflammatory effects and, as such, may be applicable in assessing a range of natural food extracts that are considered to have beneficial anti-inflammatory properties.

Peanut extract, at all concentrations tested in this study, had no effect on NF-κB nuclear transcription factor, compared to LPS alone. Our results showed that the mechanism of action of peanut extract is via the inhibition of the transcription factor c-Jun from MAPK family. This inhibition of c-Jun by peanut extract was significant at 25 and 100 µg/mL concentration. Subsequently, we observed that peanut extract slightly decreased (but not statistically significantly) TNF-α mRNA. Stabilization of mRNA by peanut extract was not observed. Peanut extract (100 µg/mL) induced a reduction of the TNF-α soluble active form and extracellular TNF-α protein, and exerted a final anti-inflammatory effect at the end of the pathway. The intracellular TNF-α protein concentration reflects both the cytoplasmic domain and the trans-membrane segment of TNF-α protein. The mechanism linking the disruption of the pathway with the extracellular region that contains the soluble biological form (Ishisaka R *et al.*, 1999) needs to be elucidated further.

A mechanism that needs to be taken into account is the enzyme that produces the soluble TNF-α protein in the culture medium i.e. the TACE enzyme. It is a member of the disintegrin and metalloprotease (the ADAM family) which cleaves various trans-membrane proteins within their “stalk” sequences, releasing (“shedding”) a soluble form including the functional extracellular domains (Black RA, 2002). In this study, we showed that LPS (500 ng/mL) stimulation alone of THP-1 cells has no effect on TACE activity. This suggests that the basal level of TACE activity present in THP-1 cells may be sufficient for the release of TNF-α from LPS-stimulated cells (15% of RFU) or that LPS shedding *per se* may not be activated in the case of LPS-induced TNF-α release (Doedens JR and Black RA, 2000). Although some groups of investigators have provided evidence for stimulation of TACE mRNA transcription, protein content, and catalytic activity by LPS, others have not (Doedens JR *et al.*, 2003; Ermert M *et al.*, 2003; Armstrong L *et al.*, 2006; Rozenova KA *et al.*, 2010). Our results demonstrated that peanut extract, at any of the concentrations tested (5,

25, 50 and 100 µg/mL), did not affect TACE activity while, conversely, reduction in activity is sensitive to BAY.

The data from the present study suggest that, in the model of human monocytic THP-1 cells stimulated with LPS, extracellular TNF-α protein is inhibited by peanut extract.

The anti-inflammatory model we present in this article could become a gold standard since the markers of quality of analysis such as precision (mean of 10% and 20% intra- and inter-assay CV, respectively) and accuracy will become reference parameters in comparing future models of inflammation. As such, the model can be used not only in basic research but also in the assessment of additives (food fortification) and other outcomes in the food industry.

Alpha-Tocopherol and BAY 11-7082 Reduce Vascular Cell Adhesion Molecule in Human Aortic Endothelial Cells (Study 2)

Our results indicated that treatment with AT (50, 75 and 150 µM) inhibits VCAM-1 mRNA and sVCAM-1 protein by between 36 and 40% in TNF-α-stimulated HAEC. In contrast, when we analyzed the effects of AT on stimulated HAEC, we observed a non-significant decrease in E-selectin and ICAM-1 mRNA expression (40% and 25 to 40% respectively) and in sE-selectin and sICAM-1 protein release (5 to 29% and 5 to 16%, respectively) compared to TNF-α-alone (10 ng/mL). As such, AT appears to play a beneficial role in atherosclerosis by specifically reducing VCAM-1, but not the other CAMs studied, such as E-selectin and ICAM-1.

Optimum serum concentration of AT in humans is around 23.2 µM (Gamez C *et al.*, 1996), and which is similar to the concentrations selected for our investigation.

We also observed that, in TNF-α stimulated HAEC, BAY (at 0.1 µM) reduced VCAM-1 mRNA expression by 25% and sVCAM-1 protein release by 53%. Similarly, BAY (at 1 µM) decreased E-selectin and ICAM-1 mRNA expression by 25% and 13%, respectively and sE-selectin and sICAM-1

protein release by 50% and 26%, respectively; albeit these reductions were not statistically significant.

VCAM-1 is an important adhesion molecule that is up-regulated during endothelial activation by various factors such as TNF-α. Belonging to the immunoglobulin superfamily, it has adhesion molecule properties and acts as a ligand for activated leukocyte adhesion to endothelium (Terry RW *et al.*, 1993).

Garton et al. (Garton KJ *et al.*, 2003) demonstrated in mice that VCAM-1 is released as a soluble form of the extracellular domain that is generated by TACE induced by phorbol 12-myristate 13-acetate (PMA).

E-selectin is expressed in acute- as well as in a chronically-inflamed endothelium and induces rolling of circulating monocytes and/or leukocytes through this endothelium (Galkina E and Ley K, 2007; Shapiro NI *et al.*, 2010).

ICAM-1 is also involved in atherosclerosis, presumably through the regulation of monocyte recruitment into atherosclerosis-prone areas. ICAM-1 expression is elevated in aortas that are predisposed to atherosclerosis, and is regulated by pro-inflammatory stimuli such as that of TNF-α.

E-selectin is involved in the leukocyte rolling on the endothelium, while VCAM-1 and ICAM-1 are involved in firm adhesion of leukocytes by binding to very late antigen (VLA-4) and to leukocyte function antigen (LFA-1), respectively. This mechanism is in accord with our findings in the functional experiments in which we observed no differences between leukocyte adhesion to activated HAEC in the presence or absence of AT.

With respect to the proteins of each individual sCAM, we observe different degrees of response to the same stimuli (TNF-α 10 ng/mL) for each sCAM (13.31 ng/mL for sICAM-1, 7.71 ng/mL for sVCAM-1, and 0.33 ng/mL for sE-selectin); the contribution of each one being different in the adhesion step of atherosclerosis. Deneva-Koycheva et al. (Deneva-Koycheva TI *et al.*, 2011) recently determined the reference ranges of sVCAM-1 (170.42 to 478.36 ng/mL), sE-selectin (9.15 to 65.19 ng/mL) and sICAM-1 (128.9 to 347.48 ng/mL) in serum of healthy Bulgarians, with no gender-related

differences in CAMs concentrations. Human CAMs serum concentrations are higher than those selected for the present study.

BAY, at 1 μM and 0.1 μM in the present study, reduced sVCAM-1 protein release and VCAM-1 mRNA expression, respectively. BAY (1 μM) also reduced sE-selectin and sICAM-1 protein release as well as their mRNA expression, albeit the reduction was not statistically significant. At similar concentrations (2 μM or 5 μM or 12 μM) BAY has been described previously as inhibiting NF-κB in different cell types (Bage T *et al.*, 2010; Juliana C *et al.*, 2010; Calabro P *et al.*, 2011). Accordingly, in our study, protein release of the studied sCAMs was reduced as well as the adhesion between activated HAEC and Jurkat-T-cells was reduced by BAY (0.5, 1, 2 and 5 μM); statistical significance being reached at concentrations of BAY of 2 and 5 μM.

Based on previous reports in HUVEC (Shaw DI *et al.*, 2007; Tribolo S *et al.*, 2008) and in HAEC (Szekanecz Z *et al.*, 1994; Amberger A *et al.*, 1997; Chen YH *et al.*, 2001; Chen JW *et al.*, 2003; Schleser S *et al.*, 2006) in which the effects of compounds other than AT had been tested, we added TNF-α (at 10 ng/mL) to the HAEC culture for 24h to determine the sVCAM-1 protein release. A mean of 74.74 pg/mL (range: 64 to 84) serum TNF-α concentration was recorded in healthy children (Lorini R *et al.*, 1995) and, as reported by Tomiyama et al, control individuals have 1.7±0.5 pg/mL TNF-α in circulation while patients with obstructive sleep apnea have nearly 2 pg/mL (Tomiyama H *et al.*, 2008). Patients with systemic lupus erythematosus have 4.9±12.8 pg/mL and those with rheumatoid arthritis (an inflammatory disease) have 20±36.2 pg/mL (Bruni R *et al.*, 2006; Vadacca M *et al.*, 2008). Hence, under inflammatory conditions, serum TNF-α levels can be high, and approach the TNF-α levels used in this study.

The production of adhesion molecules by endothelial cells has been shown to be regulated by redox-sensitive signal transduction and, thus, may be subjected to modulation by oxidants and antioxidants (Li H *et al.*, 1993). Since AT is a potent antioxidant, it would be reasonable to assume that the

effects of this compound on reducing sVCAM-1 protein release in activated HAEC may be due, mainly, to its antioxidant properties in several endothelial cell types (Liu L *et al.*, 2004). These outcomes are also observed at the mRNA expression level. Hence, the results demonstrate that, apart from its antioxidant activities, AT can exert a modest inhibitory effect on adhesion molecule expression *in vitro*, and this suggests an improvement in endothelial dysfunction in HAEC.

It has been argued that HAEC or HUVEC may not adequately represent inflammatory changes in the microcirculation in tissues, since these cells are isolated from a large artery or vein, respectively. Microvascular cell line HMEC-1 is reportedly one of the endothelial cell lines most similar to primary endothelium (Liu L *et al.*, 2004). Results of sVCAM-1 in HMEC-1 cultures have shown wider variation than those from HUVEC experiments and it is mainly for this reason that HUVEC have been used extensively in *in vitro* endothelium studies (Videm V and Albrigtsen M, 2008). It is not clear, however, whether these differences render HMEC-1 a better, or a poorer, model of local inflammation than HUVEC. However, HUVEC provide more consistent results even if genetic differences between donors may result in wider variation in expression of inflammation markers (Videm V and Albrigtsen M, 2008). Further cell culture studies are required using HMEC-1 or human coronary artery endothelial cells to confirm the sVCAM-1 results that had been observed in HAEC (Calabro P *et al.*, 2011).

Biomarkers of Food Intake and Metabolite Differences between Plasma and Red Blood Cell Matrices; a Human Metabolomic Profile Approach (Study 3)

Our data indicate that several specific molecular and nutritional biomarkers are associated with RBC, the measurement of which extend the data obtainable from their measurement in plasma alone in human studies.

The biological samples from the ostensibly-healthy subjects in our study would be representative of a general population and, as such, optimal for standardizing the metabolomics procedures for future human studies

As an example of a robust metabolomic approach, the type of anticoagulant used for blood sample collection (sodium citrate or lithium heparin) was, in general, of note in evaluating parameters for measurement in plasma and RBC with the range of techniques currently at our disposal.

Compared to lithium heparin plasma, there was an over-estimation in sodium citrate plasma of some aqueous metabolites found in human plasma and RBC, such us citrate. Since this type of blood-collection tube dilutes the sample i.e. the volume of sodium citrate (~ 250 µL of 0.129 M sodium citrate in a 2.7 mL blood sample collection tube) results in a "non real" or "inaccurate" measurement of the parameters-of-interest, we recommend using lithium heparin tubes (68 I.U.) for blood collection if plasma is the desired matrix for analyte measurement using NMR, GC-MS and UPLC-MS/MS. Other metabolomic studies support the use of lithium heparin anticoagulant for NMR-based metabolic profiling studies (Barton RH *et al.*, 2010).

As mentioned earlier, the volume of blood that can be accessed from the human individual for diagnostic and/or research purposes is limited. Also, most analytes are measured in plasma or serum, and the RBC are usually discarded. Our analyses have shown that plasma and RBC are different matrices which provide similar and complementary information. Depending on the parameter-of-interest, plasma and/or RBC matrices can be used independently.

We observed that lipoprotein content was higher in plasma sample than in RBC and supports the classical concept that lipoproteins are transported in circulating plasma (Young SG, 1990). However, recent studies conducted by Bovenberg *et al*. suggested the presence of other pools of lipoproteins attached, possibly, to the endothelium or to other cells such as RBC (Verseyden C *et al.*, 2004; Bovenberg SA *et al.*, 2010; Bovenberg SA *et al.*, 2011). These postulations could open new applications for NMR analyses of RBC and their associated lipoprotein content in relation to several diseases such atherosclerosis and other lipid disorders where alternative blood-cell-mediated lipoprotein transport system has been proposed. For

example, the study by Bovenberg *et al* (Bovenberg SA *et al.*, 2011) concluded that a high binding of RBC to apolipoprotein B could be protective against atherosclerosis.

Our results showed that RBC are a particularly rich medium for the detection of SFA. These include palmitic acid (16:0), margaric acid (17:0), arachidic acid (20:0) and lignoceric acid (24:0), all of which are widely distributed in dairy products (such as butter, ghee, whole milk, cream, fatty cheeses), in fatty meats and animal fats (such as lard), in vegetable oils (such as palm oil, palm kernel and coconut oil) and fat-rich snacks (Diekman C *et al.*, 2009). The PUFA that were identified included DHA (22:6 n-3) and arachidonic acid (20:4 n-6), and are common FA in vegetable oils (soybean oil, rapeseed oil, sunflower oil, olive oil) and in fatty fish, fish oil, nuts, seeds and products made from these e.g. soft margarines, mayonnaise and other derived products (Diekman C *et al.*, 2009). The concentrations of these FA were better detected in RBC than plasma, and could be used as a biomarker of the study participant's consumption of specific food items over the previous weeks, or months (Sun Q *et al.*, 2007).

Compared to RBC, plasma was observed to have higher content of SFA such as myristic acid (14:0), or MUFA such as myristoleic acid (14:1 n-5), palmitoleic acid (16:1 n-7), 17:1 n-7 and oleic acid (18:1 n-9) as well as of PUFA such as alpha-linoleic acid (18:3 n-3), linoleic acid (18:2 n-6), gamma-linolenic acid (18:3 n-6) and 20:3 n-6.

We observed that the quantities of FA (expressed as µg/mL) in plasma and RBC better describe the data obtained, while FA percentages makes comparisons between specimens easier. These raw data will be accessible for the next generation of metabolomic software and bioinformatics analysis tools. However, such tools can only be developed and optimized if there are standardized methodologies (Griffin JL and Steinbeck C, 2010) such as we have proposed.

In dietary studies in general, 3- to 7-day food records are considered to be the most accurate means of intake assessment. However, such methods

are not feasible in large cohort studies (Siri-Tarino PW *et al.*, 2010). Metabolic profiles, as our study proposes, would more accurately reflect short- medium- and long-term dietary intakes and, as such, would be more effective in evaluating, for example, the health benefit claims of manufactured functional food products.

RBC better reflect long-term dietary FA intake than plasma, as has been previously suggested. Since the biological half-life of RBC is of the order of 55 days, the measurements in RBC would reflect the mean FA status of the previous 3 months. Depending on the FA of interest and the study objectives, plasma and/or RBC should be analyzed so as to provide complementary information. For example, it has been suggested that, in epidemiology/nutrition studies, FA composition measured in RBC is a viable alternative to adipose tissue biopsy for determining long-term FA consumption.

In our study, polyphenols associated with RBC were detected in the fasting state, and were different from those measured in the corresponding plasma. Thus, there is the promising option that RBCs may provide a longer-term measure of polyphenolic intake in nutrition studies. However, we were unable to identify several peaks from the UPLC-LC-MS spectra; more detailed and accurate techniques for the identification of these metabolites are needed, and the information added to the current databases

The ultimate goals of these ‘omics’ studies are to identify the molecular signatures of dietary nutrients, and non-nutrients, that could result in a specific “desirable” phenotype and, hence, to provide personalized nutritional recommendations for health maintenance as well as for disease prevention

There are two main limitations of our study. The first limitation is the small number of subjects studied. Our results are preliminary and focus mainly on the gross effects of blood sample collection and the possible effects on the metabolomic approach to a nutritional study. The second limitation is the lack of a database containing the assignments and identification of

several polyphenol peaks in the spectra derived from plasma and RBC, as assessed by UPLC-MS/MS. Future studies would require more accurate techniques for polyphenol detection and identification.

These drawbacks limit the conclusions that could be drawn. However, the positive benefit of our study is the detailed insight into measurements conducted in plasma and RBC matrices from different methods of blood anticoagulation. Our results indicate that lithium heparin anticoagulant is to be preferred. We have applied the combination of NMR spectroscopy, GC-MS and UPLC-MS/MS approaches in combination in order to generate metabolomic profiles in our human volunteers. Thus, RBC *versus* plasma measurements provide complementary metabolic information with respect to several specific molecular biomarkers which could be applied in nutritional assessments.

Overall discussion

The present work provides a cellular model to study the activity of food extracts and/or bioactive compounds that have the potential to promote beneficial affects on the levels of molecular biomarkers of atherosclerosis including cytokines (TNF-α) and CAMs (VCAM-1, E-selectin and ICAM-1). One line of investigation involved the mechanisms-of-action of a popular food item (peanut extract) which has high polyphenol content. We used the atherosclerosis-specific biological system, THP-1 monocytes; an established model for studying inflammation. We observed that polyphenol-rich peanut extract acts at the nuclear level by inhibiting c-Jun transcription factor, thereby preventing TNF-α production. Another line of investigation involved the atherosclerosis-specific biological cell approach i.e. HAECs which are associated with endothelial function. We observed that AT and BAY, natural and synthetic molecules respectively, reduced CAMs in HAECs and improved endothelial function. Our results confirmed the proposal that the atherosclerosis-specific biological cell approach (i.e. THP-1 and HAECs), is effective in evaluating the molecular mechanisms-of-action of food extracts and/or bioactive compounds.

A pre-incubation with natural food extracts and/or bioactive compounds may prevent, in the cellular models studied, inflammation and endothelial dysfunction. This pre-incubation is necessary to observe any protective effects against inflammation and endothelial dysfunction stimuli accruing from dietary and other lifestyle habits. These *in vitro* results provide the bases for future dietary recommendations such as the inclusion of foods with high content of certain bioactive compounds, including phytosterols (Sanclemente T *et al.*, 2009), to decrease the risk of atherosclerosis. However, the expected benefits in health are not usually achieved by the consumption of a single food item, called "functional food". Foods are regarded as "functional" when it can be satisfactorily demonstrated that they beneficially affect one or more target functions in the body, beyond the known nutritional effects. This "functional" effect is towards an improved health state and well-being and/or reduction of disease risk (Contor L, 2001). Functional foods should be consumed within the framework of healthy-eating habits with an adequate and balanced distribution of nutrients to induce benefits in health. The present work used two repeatable and reproducible cellular models, which "simulate" different stages of atherosclerosis lesions. These two models could be used to study changes in disease biomarkers at the molecular level and test different natural and synthetic molecules. Further, these cellular models could contribute to the study of mechanisms-of-action of natural extracts or compounds. Although, studies using the atherosclerosis-specific biological cell approach are effective in investigating food extracts and/or mechanisms-of-action of bioactive compounds, human studies are always necessary for a better, and more realistic, understanding of the health benefits and of disease recognition/prevention.

Whole blood can offer considerable, and different, information on the individual's health status. Optimization of sample isolation and of the analytical techniques is required to obtain maximum information from each component of blood such as plasma and RBC, or serum.

To further achieve our profiling objectives, it was necessary to develop an accurate methodology to qualitatively and quantitatively detect, and characterize, the metabolized food compounds such as FA and polyphenols. Hence, we used highly sensitive techniques such as NMR, GC-MS and UPLC-MS/MS to identify specific metabolites in human biological samples. Specifically, we studied two matrices (human plasma and RBC) which can offer us complementary metabolomic profile information when assessed with these powerful techniques. Despite the power of these techniques to detect various constituents of the biological samples, the main problem remains data analysis and processing. In future studies, the key aspect for accurate and detailed characterization of specific metabolites is the availability of accurate databases. The vast volume of data generated in metabolomics has created the need for comprehensive, well-annotated, and user-friendly databases. These databases should be able to store and manage the disparate and complex data, with appropriate annotations and descriptors. Only then would metabolomics be able to meet the challenges posed by the generation of the enormous information cascade (Go EP, 2010). The implementation of data standardization will assist metabolomics to strengthen its integration with genomics, transcriptomics, and proteomics, thus providing an integrated view of biological systems (Go EP, 2010). Specific and precise techniques are required for a better assignment and identification of polyphenols when comparisons are made with existing databases.

Considerable data have been assembled on the biological activity of food extracts and/or bioactive compounds using the atherosclerosis-specific biological cell approach. Also, the analyses of metabolites in human plasma and RBC have highlighted the usefulness of certain metabolites as biomarkers of food intake. However, one further step is required. This involves the synthesis and isolation of the specific nutritional biomarkers-of-interest and the evaluation of their mechanisms-of-action using the atherosclerosis-specific biological cell approach. This concept is graphically represented in **Figure 45**.

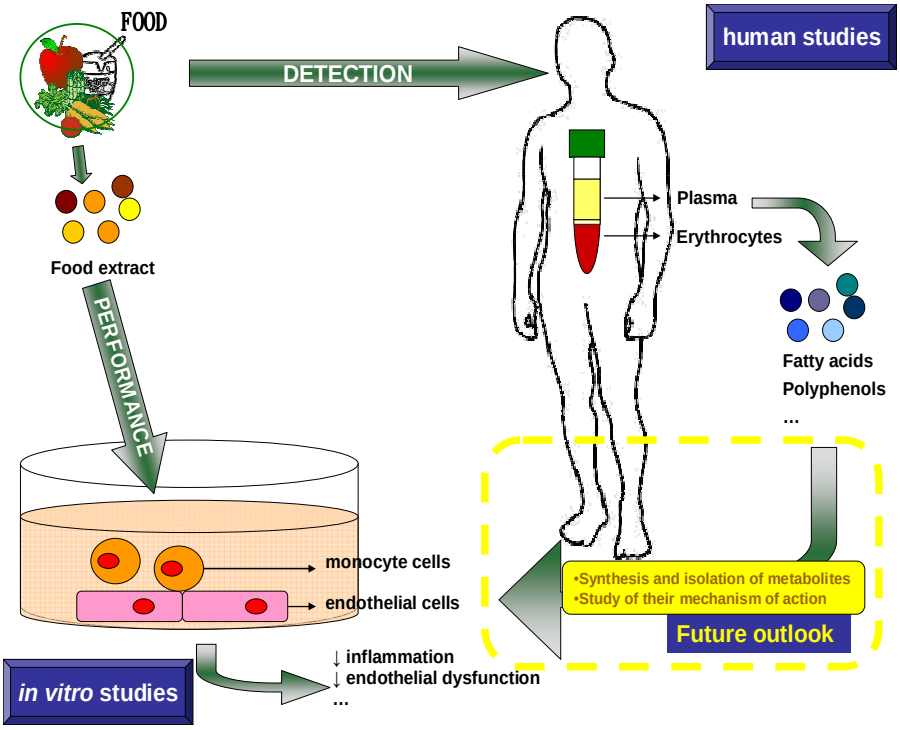

Figure 45. Proposed stragegies for the evaluation of nutritional effets on human health.

Further, it would be of considerable interest to characterize food intake biomarkers detected in plasma and RBC, and to relate them to a specific food-item intake. Tools such as 24 hR and FFQ would be necessary to quantify specific food intakes in humans, followed by a comparison of FA and polyphenol data obtained from metabolic profile analysis of plasma and RBC.

As such, present and future goals would be to investigate the short- and medium-term effects of diets with respect to disease prevention via the identification and monitoring of new nutritional biomarkers of food intake and their effects on atherosclerosis disease risk. Because… “we are what we eat”.

Conclusions

1. The models, of inflammation using THP-1 monocytes and of endothelial dysfunction using HAEC, are effective as biological-cell approaches in the investigation of atherosclerosis. The methods are repeatable and reproducible in testing the potential beneficial effects of natural and manufactured extracts, and/or compounds.

2. A pre-incubation with polyphenol-rich peanut extract and AT, in the cellular models studied, is necessary in order to observe protective effects against inflammation and endothelial dysfunction stimuli.

3. Polyphenol-rich peanut extract exerts an anti-inflammatory effect by reducing extracellular TNF-α protein concentration. This peanut extract mechanism-of-action is via the inhibition of c-Jun transcription factor activity. AT improves endothelial function specifically by inhibiting VCAM-1 at the mRNA and the protein levels.

4. BAY is confirmed as an effective control molecule for the cell models under study. BAY can reduce TNF-α protein (total, extra- and intracellular) and TNF-α mRNA levels by inhibiting c-Jun, MEF2 and NF-κB transcription factor activity and TACE activity in THP-1 cells. BAY can also reduce sVCAM-1, sE-selectin and sICAM-1 protein as well as their mRNA levels and, in the endothelial dysfunction model, the adhesion between activated HAECs and Jurkat-T-cells.

5. The combination of NMR spectroscopy, GC-MS and UPLC-MS/MS techniques are efficient in generating metabolomic profiles of several specific biomarkers of food intake and metabolites (FA, polyphenol, aqueous metabolites and lipoprotein content) in plasma and RBC of human subjects.

6. Plasma and RBC are two matrices that add complementary information when assessing biomarkers (metabolites) of food intake.

REFERENCES

EFFECT OF FOOD EXTRACTS AND BIOACTIVE FOOD COMPOUNDS ON THE MECHANISM OF ATHEROSCLEROSIS AND NUTRITIONAL BIOMARKERS

Úrsula Catalán Santos

Dipòsit Legal: T. 1058-2012

Aebersold R and Mann M. Mass spectrometry-based proteomics. Nature. **2003**; *422*: 198-207.

Alnouti Y, Csanaky IL and Klaassen CD. Quantitative-profiling of bile acids and their conjugates in mouse liver, bile, plasma, and urine using LC-MS/MS. J Chromatogr B Analyt Technol Biomed Life Sci. **2008**; *873*: 209-217.

Amberger A, Maczek C, Jurgens G, Michaelis D, Schett G, Trieb K, Eberl T, Jindal S, Xu Q and Wick G. Co-expression of ICAM-1, VCAM-1, ELAM-1 and Hsp60 in human arterial and venous endothelial cells in response to cytokines and oxidized low-density lipoproteins. Cell Stress Chaperones. **1997**; *2*: 94-103.

Annesley TM. Ion suppression in mass spectrometry. Clin Chem. **2003**; *49*: 1041-1044.

Arab L. Biomarkers of fat and fatty acid intake. J Nutr. **2003**; *133 Suppl 3*: 925S-932S.

Arab L and Akbar J. Biomarkers and the measurement of fatty acids. Public Health Nutr. **2002**; *5*: 865-871.

Armstrong L, Godinho SI, Uppington KM, Whittington HA and Millar AB. Contribution of TNF-alpha converting enzyme and proteinase-3 to TNF-alpha processing in human alveolar macrophages. Am J Respir Cell Mol Biol. **2006**; *34*: 219-225.

Assies J, Pouwer F, Lok A, Mocking RJ, Bockting CL, Visser I, Abeling NG, Duran M and Schene AH. Plasma and erythrocyte fatty acid patterns in patients with recurrent depression: a matched case-control study. PLoS One. **2010**; *5*: e10635.

Bage T, Lindberg J, Lundeberg J, Modeer T and Yucel-Lindberg T. Signal pathways JNK and NF-kappaB, identified by global gene expression profiling, are involved in regulation of TNFalpha-induced mPGES-1 and COX-2 expression in gingival fibroblasts. BMC Genomics. **2010**; *11*: 241.

Bahia MS and Silakari O. Tumor necrosis factor alpha converting enzyme: an encouraging target for various inflammatory disorders. Chem Biol Drug Des. **2010**; *75*: 415-443.

Balanescu S, Calmac L, Constantinescu D, Marinescu M, Onut R and Dorobantu M. Systemic inflammation and early atheroma formation: are they related? Maedica (Buchar). **2010**; *5*: 292-301.

References

Barnes PJ and Karin M. Nuclear factor-kappaB: a pivotal transcription factor in chronic inflammatory diseases. N Engl J Med. **1997**; *336*: 1066-1071.

Barton RH, Waterman D, Bonner FW, Holmes E, Clarke R, Nicholson JK and Lindon JC. The influence of EDTA and citrate anticoagulant addition to human plasma on information recovery from NMR-based metabolic profiling studies. Mol Biosyst. **2010**; *6*: 215-224.

Beutler B. Tlr4: central component of the sole mammalian LPS sensor. Curr Opin Immunol. **2000**; *12*: 20-26.

Black RA. Tumor necrosis factor-alpha converting enzyme. Int J Biochem Cell Biol. **2002**; *34*: 1-5.

Black RA, Rauch CT, Kozlosky CJ, Peschon JJ, Slack JL, Wolfson MF, Castner BJ, Stocking KL, Reddy P, Srinivasan S, Nelson N, Boiani N, Schooley KA, Gerhart M, Davis R, Fitzner JN, Johnson RS, Paxton RJ, March CJ and Cerretti DP. A metalloproteinase disintegrin that releases tumour-necrosis factor-alpha from cells. Nature. **1997**; *385*: 729-733.

Blankenberg S, Barbaux S and Tiret L. Adhesion molecules and atherosclerosis. Atherosclerosis. **2003**; *170*: 191-203.

Bothwell JH and Griffin JL. An introduction to biological nuclear magnetic resonance spectroscopy. Biol Rev Camb Philos Soc. **2011**; *86*: 493-510.

Bovenberg SA, Alipour A, Elte JW, Rietveld AP, Janssen JW, van de Geijn GJ, Njo TN, van Mechelen R, Hervas SM and Cabezas MC. Cell-mediated lipoprotein transport: a novel anti-atherogenic concept. Atheroscler Suppl. **2010**; *11*: 25-29.

Bovenberg SA, Klop B, Alipour A, Martinez-Hervas S, Westzaan A, van de Geijn GJ, Janssen HW, Njo T, Birnie E, van Mechelen R, Rietveld AP, Elte JW and Castro Cabezas M. Erythrocyte-associated apolipoprotein B and its relationship with clinical and subclinical atherosclerosis. Eur J Clin Invest. **2011**.

Bruni R, Serino FM, Galluzzo S, Coppolino G, Cacciapaglia F, Vadacca M, Nilo S, Terminio N and Afeltra A. Alexithymia and neuroendocrine-immune response in patients with autoimmune diseases: preliminary results on relationship between alexithymic construct and TNF-alpha levels. Ann N Y Acad Sci. **2006**; *1069*: 208-211.

Burnier L, Fontana P, Angelillo-Scherrer A and Kwak BR. Intercellular communication in atherosclerosis. Physiology (Bethesda). **2009**; *24*: 36-44.

Buscher JM, Czernik D, Ewald JC, Sauer U and Zamboni N. Cross-platform comparison of methods for quantitative metabolomics of primary metabolism. Anal Chem. **2009**; *81*: 2135-2143.

Cai JM, Hatsukami TS, Ferguson MS, Small R, Polissar NL and Yuan C. Classification of human carotid atherosclerotic lesions with in vivo multicontrast magnetic resonance imaging. Circulation. **2002**; *106*: 1368-1373.

Calabro P, Cirillo P, Limongelli G, Maddaloni V, Riegler L, Palmieri R, Pacileo G, De Rosa S, Pacileo M, De Palma R, Golino P and Calabro R. Tissue Factor Is Induced by Resistin in Human Coronary Artery Endothelial Cells by the NF-kB-Dependent Pathway. J Vasc Res. **2011**; *48*: 59-66.

Calixto JB, Otuki MF and Santos AR. Anti-inflammatory compounds of plant origin. Part I. Action on arachidonic acid pathway, nitric oxide and nuclear factor kappa B (NF-kappaB). Planta Med. **2003**; *69*: 973-983.

Caspar-Bauguil S, Garcia J, Galinier A, Periquet B, Ferrieres J, Allenbach S, Morin N, Hericotte P, Salvayre R and Baudet M. Positive impact of long-term lifestyle change on erythrocyte fatty acid profile after acute coronary syndromes. Arch Cardiovasc Dis. **2010**; *103*: 106-114.

Catapano AL, Reiner Z, De Backer G, Graham I, Taskinen MR, Wiklund O, Agewall S, Alegria E, Chapman M, Durrington P, Erdine S, Halcox J, Hobbs R, Kjekshus J, Filardi PP, Riccardi G, Storey RF and Wood D. ESC/EAS Guidelines for the management of dyslipidaemias The Task Force for the management of dyslipidaemias of the European Society of Cardiology (ESC) and the European Atherosclerosis Society (EAS). Atherosclerosis. **2011**; *217*: 3-46.

Cifuentes A. Food analysis and foodomics. J Chromatogr A. **2009**; *1216*: 7109.

Constans J and Conri C. Circulating markers of endothelial function in cardiovascular disease. Clin Chim Acta. **2006**; *368*: 33-47.

Contor L. Functional Food Science in Europe. Nutr Metab Cardiovasc Dis. **2001**; *11*: 20-23.

Chen JW, Chen YH, Lin FY, Chen YL and Lin SJ. Ginkgo biloba extract inhibits tumor necrosis factor-alpha-induced reactive oxygen species generation, transcription factor activation, and cell adhesion molecule expression in human aortic endothelial cells. Arterioscler Thromb Vasc Biol. **2003**; *23*: 1559-1566.

References

Chen X, Liu L, Palacios G, Gao J, Zhang N, Li G, Lu J, Song T, Zhang Y and Lv H. Plasma metabolomics reveals biomarkers of the atherosclerosis. J Sep Sci. **2010**; *33*: 2776-2783.

Chen X, Zhuang Y, Wang Q, Moutsoglou D, Ruiz G, Yen SE and Dreskin SC. Analysis of the effector activity of Ara h 2 and Ara h 6 by selective depletion from a crude peanut extract. J Immunol Methods. **2011**.

Chen YH, Lin SJ, Ku HH, Shiao MS, Lin FY, Chen JW and Chen YL. Salvianolic acid B attenuates VCAM-1 and ICAM-1 expression in TNF-alpha-treated human aortic endothelial cells. J Cell Biochem. **2001**; *82*: 512-521.

Cheneval D, Kastelic T, Fuerst P and Parker CN. A review of methods to monitor the modulation of mRNA stability: a novel approach to drug discovery and therapeutic intervention. J Biomol Screen. **2010**; *15*: 609-622.

Chou YC, Sheu JR, Chung CL, Hsiao CJ, Hsueh PJ and Hsiao G. Hypertonicity-enhanced TNF-alpha release from activated human monocytic THP-1 cells requires ERK activation. Biochim Biophys Acta. **2011**; *1810*: 475-484.

Dagia NM, Harii N, Meli AE, Sun X, Lewis CJ, Kohn LD and Goetz DJ. Phenyl methimazole inhibits TNF-alpha-induced VCAM-1 expression in an IFN regulatory factor-1-dependent manner and reduces monocytic cell adhesion to endothelial cells. J Immunol. **2004**; *173*: 2041-2049.

Darghouth D, Koehl B, Junot C and Romeo PH. Metabolomic analysis of normal and sickle cell erythrocytes. Transfus Clin Biol. **2010**; *17*: 148-150.

Davis PA, Polagruto JA, Valacchi G, Phung A, Soucek K, Keen CL and Gershwin ME. Effect of apple extracts on NF-kappaB activation in human umbilical vein endothelial cells. Exp Biol Med (Maywood). **2006**; *231*: 594-598.

Dayer JM, Molnarfi N and Burger D. From cellular receptors to transduction-transcription pathways for cytokines: at which level should the inhibition be targeted in inflammation? Expert Opin Biol Ther. **2005**; *5 Suppl 1*: S83-96.

de Roos B, Geelen A, Ross K, Rucklidge G, Reid M, Duncan G, Caslake M, Horgan G and Brouwer IA. Identification of potential serum biomarkers of inflammation and lipid modulation that are altered by fish oil supplementation in healthy volunteers. Proteomics. **2008**; *8*: 1965-1974.

Deneva-Koycheva TI, Vladimirova-Kitova LG, Angelova EA and Tsvetkova TZ. Serum levels of siCAM-1, sVCAM-1, sE-selectin, sP-selectin in healthy Bulgarian people. Folia Med (Plovdiv). **2011**; *53*: 22-28.

Dettmer K, Aronov PA and Hammock BD. Mass spectrometry-based metabolomics. Mass Spectrom Rev. **2007**; *26*: 51-78.

Devaraj S, Harris A and Jialal I. Modulation of monocyte-macrophage function with alpha-tocopherol: implications for atherosclerosis. Nutr Rev. **2002**; *60*: 8-14.

Dieguez-Acuna FJ, Polk WW, Ellis ME, Simmonds PL, Kushleika JV and Woods JS. Nuclear factor kappaB activity determines the sensitivity of kidney epithelial cells to apoptosis: implications for mercury-induced renal failure. Toxicol Sci. **2004**; *82*: 114-123.

Diekman C, Elmadfa I, Koletzko B, Puska P, Uauy R and Zevenbergen H. Summary statement of the International Expert Meeting: health significance of fat quality of the diet. Barcelona, Spain, February 1-2, 2009. Ann Nutr Metab. **2009**; *54 Suppl 1*: 39-40.

Doedens JR and Black RA. Stimulation-induced down-regulation of tumor necrosis factor-alpha converting enzyme. J Biol Chem. **2000**; *275*: 14598-14607.

Doedens JR, Mahimkar RM and Black RA. TACE/ADAM-17 enzymatic activity is increased in response to cellular stimulation. Biochem Biophys Res Commun. **2003**; *308*: 331-338.

Dominiczak MH. Risk factors for coronary disease: the time for a paradigm shift? Clin Chem Lab Med. **2001**; *39*: 907-919.

Doring Y, Noels H and Weber C. The use of high-throughput technologies to investigate vascular inflammation and atherosclerosis. Arterioscler Thromb Vasc Biol. **2012**; *32*: 182-195.

Duell PB, Illingworth, D. R. and Connor, W. E. Endocrinology and metabolism. **2001**. Mc Graw-Hill: New York.

Elstad MR, La Pine TR, Cowley FS, McEver RP, McIntyre TM, Prescott SM and Zimmerman GA. P-selectin regulates platelet-activating factor synthesis and phagocytosis by monocytes. J Immunol. **1995**; *155*: 2109-2122.

Ellis DI, Dunn WB, Griffin JL, Allwood JW and Goodacre R. Metabolic fingerprinting as a diagnostic tool. Pharmacogenomics. **2007**; *8*: 1243-1266.

Ermert M, Pantazis C, Duncker HR, Grimminger F, Seeger W and Ermert L. In situ localization of TNFalpha/beta, TACE and TNF receptors TNF-R1 and TNF-R2 in control and LPS-treated lung tissue. Cytokine. **2003**; *22*: 89-100.

Essafi-Benkhadir K, Refai A, Riahi I, Fattouch S, Karoui H and Essafi M. Quince (Cydonia oblonga Miller) peel polyphenols modulate LPS-induced inflammation in human THP-1-derived macrophages through NF-kappaB, p38MAPK and Akt inhibition. Biochem Biophys Res Commun. **2012**.

Fiorani M, Accorsi A and Cantoni O. Human red blood cells as a natural flavonoid reservoir. Free Radic Res. **2003**; *37*: 1331-1338.

Fuhrman BJ, Barba M, Krogh V, Micheli A, Pala V, Lauria R, Chajes V, Riboli E, Sieri S, Berrino F and Muti P. Erythrocyte membrane phospholipid composition as a biomarker of dietary fat. Ann Nutr Metab. **2006**; *50*: 95-102.

Galkina E and Ley K. Vascular adhesion molecules in atherosclerosis. Arterioscler Thromb Vasc Biol. **2007**; *27*: 2292-2301.

Gamez C, Artacho R, Ruiz-Lopez MD, Puerta A and Lopez MC. Nutritional status of vitamin A and E in institutionalized elderly people in Granada (Spain). J Nutr Sci Vitaminol (Tokyo). **1996**; *42*: 397-405.

Garton KJ, Gough PJ, Philalay J, Wille PT, Blobel CP, Whitehead RH, Dempsey PJ and Raines EW. Stimulated shedding of vascular cell adhesion molecule 1 (VCAM-1) is mediated by tumor necrosis factor-alpha-converting enzyme (ADAM 17). J Biol Chem. **2003**; *278*: 37459-37464.

Gee K, Lim W, Ma W, Nandan D, Diaz-Mitoma F, Kozlowski M and Kumar A. Differential regulation of CD44 expression by lipopolysaccharide (LPS) and TNF-alpha in human monocytic cells: distinct involvement of c-Jun N-terminal kinase in LPS-induced CD44 expression. J Immunol. **2002**; *169*: 5660-5672.

Gerszten RE, Asnani A and Carr SA. Status and prospects for discovery and verification of new biomarkers of cardiovascular disease by proteomics. Circ Res. **2011**; *109*: 463-474.

Gibney MJ, Walsh M, Brennan L, Roche HM, German B and Van Ommen B. Metabolomics in human nutrition: Opportunities and challenges. American Journal of Clinical Nutrition. **2005**; *82*: 497-503.

Go EP. Database resources in metabolomics: an overview. J Neuroimmune Pharmacol. **2010**; *5*: 18-30.

Gonzalez R, Ballester I, Lopez-Posadas R, Suarez MD, Zarzuelo A, Martinez-Augustin O and Sanchez de Medina F. Effects of flavonoids and other polyphenols on inflammation. Crit Rev Food Sci Nutr. **2011**; *51*: 331-362.

Grant PJ. The genetics of atherothrombotic disorders: a clinician's view. J Thromb Haemost. **2003**; *1*: 1381-1390.

Griffin JL. Understanding mouse models of disease through metabolomics. Curr Opin Chem Biol. **2006**; *10*: 309-315.

Griffin JL and Shockcor JP. Metabolic profiles of cancer cells. Nat Rev Cancer. **2004**; *4*: 551-561.

Griffin JL and Steinbeck C. So what have data standards ever done for us? The view from metabolomics. Genome Med. **2010**; *2*: 38.

Griffin JL, Troke J, Walker LA, Shore RF, Lindon JC and Nicholson JK. The biochemical profile of rat testicular tissue as measured by magic angle spinning 1H NMR spectroscopy. FEBS Lett. **2000**; *486*: 225-229.

Guha M and Mackman N. LPS induction of gene expression in human monocytes. Cell Signal. **2001**; *13*: 85-94.

Hansson GK. Inflammation, atherosclerosis, and coronary artery disease. N Engl J Med. **2005**; *352*: 1685-1695.

Hapner CD, Deuster P and Chen Y. Inhibition of oxidative hemolysis by quercetin, but not other antioxidants. Chem Biol Interact. **2010**; *186*: 275-279.

Heinzmann SS, Brown IJ, Chan Q, Bictash M, Dumas ME, Kochhar S, Stamler J, Holmes E, Elliott P and Nicholson JK. Metabolic profiling strategy for discovery of nutritional biomarkers: proline betaine as a marker of citrus consumption. Am J Clin Nutr. **2010**; *92*: 436-443.

Herrero M, Simo C, Garcia-Canas V, Ibanez E and Cifuentes A. Foodomics: MS-based strategies in modern food science and nutrition. Mass Spectrom Rev. **2012**; *31*: 49-69.

Hodson L, Skeaff CM and Fielding BA. Fatty acid composition of adipose tissue and blood in humans and its use as a biomarker of dietary intake. Prog Lipid Res. **2008**; *47*: 348-380.

Horiuchi T, Mitoma H, Harashima S, Tsukamoto H and Shimoda T. Transmembrane TNF-alpha: structure, function and interaction with anti-TNF agents. Rheumatology (Oxford). **2010**; *49*: 1215-1228.

Hu JH and Zhu XZ. Rotenone-induced neurotoxicity of THP-1 cells requires production of reactive oxygen species and activation of phosphatidylinositol 3-kinase. Brain Res. **2007**; *1153*: 12-19.

Ishisaka R, Sato N, Tanaka K, Takeshige T, Iwata H, Klostergaard J and Utsumi T. A part of the transmembrane domain of pro-TNF can function as a cleavable signal sequence that generates a biologically active secretory form of TNF. J Biochem. **1999**; *126*: 413-420.

Izban KF, Ergin M, Qin JZ, Martinez RL, Pooley RJ, Saeed S and Alkan S. Constitutive expression of NF-kappa B is a characteristic feature of mycosis fungoides: implications for apoptosis resistance and pathogenesis. Hum Pathol. **2000**; *31*: 1482-1490.

Jang CH, Choi JH, Byun MS and Jue DM. Chloroquine inhibits production of TNF-alpha, IL-1beta and IL-6 from lipopolysaccharide-stimulated human monocytes/macrophages by different modes. Rheumatology (Oxford). **2006**; *45*: 703-710.

Jenab M, Slimani N, Bictash M, Ferrari P and Bingham SA. Biomarkers in nutritional epidemiology: applications, needs and new horizons. Hum Genet. **2009**; *125*: 507-525.

Jones GL, Sang E, Goddard C, Mortishire-Smith RJ, Sweatman BC, Haselden JN, Davies K, Grace AA, Clarke K and Griffin JL. A functional analysis of mouse models of cardiac disease through metabolic profiling. J Biol Chem. **2005**; *280*: 7530-7539.

Jones MD and Plumb RS. The application of sub-2-microm particle liquid chromatography-operated high mobile linear velocities coupled to orthogonal accelerated time-of-flight mass spectrometry for the analysis of ranitidine and its impurities. J Sep Sci. **2006**; *29*: 2409-2420.

Juliana C, Fernandes-Alnemri T, Wu J, Datta P, Solorzano L, Yu JW, Meng R, Quong AA, Latz E, Scott CP and Alnemri ES. Anti-inflammatory compounds parthenolide and Bay 11-7082 are direct inhibitors of the inflammasome. J Biol Chem. **2010**; *285*: 9792-9802.

Just N, Tillie-Leblond I, Guery BP, Fourneau C, Tonnel AB and Gosset P. Keratinocyte growth factor (KGF) decreases ICAM-1 and VCAM-1 cell expression on bronchial epithelial cells. Clin Exp Immunol. **2003**; *132*: 61-69.

Kamthong PJ and Wu M. Inhibitor of nuclear factor-kappaB induction by cAMP antagonizes interleukin-1-induced human macrophage-colony-stimulating-factor expression. Biochem J. **2001**; *356*: 525-530.

Katakowski M, Chen J, Zhang ZG, Santra M, Wang Y and Chopp M. Stroke-induced subventricular zone proliferation is promoted by tumor necrosis factor-alpha-converting enzyme protease activity. J Cereb Blood Flow Metab. **2007**; *27*: 669-678.

Katsume A, Okigaki M, Matsui A, Che J, Adachi Y, Kishita E, Yamaguchi S, Ikeda K, Ueyama T, Matoba S, Yamada H and Matsubara H. Early inflammatory reactions in atherosclerosis are induced by proline-rich tyrosine kinase/reactive oxygen species-mediated release of tumor necrosis factor-alpha and subsequent activation of the p21Cip1/Ets-1/p300 system. Arterioscler Thromb Vasc Biol. **2011**; *31*: 1084-1092.

Kattan MW. Judging new markers by their ability to improve predictive accuracy. J Natl Cancer Inst. **2003**; *95*: 634-635.

Kleemann R, Zadelaar S and Kooistra T. Cytokines and atherosclerosis: a comprehensive review of studies in mice. Cardiovasc Res. **2008**; *79*: 360-376.

Koba M and Konopa J. [Actinomycin D and its mechanisms of action]. Postepy Hig Med Dosw (Online). **2005**; *59*: 290-298.

Koek MM, Jellema RH, van der Greef J, Tas AC and Hankemeier T. Quantitative metabolomics based on gas chromatography mass spectrometry: status and perspectives. Metabolomics. **2011**; *7*: 307-328.

Kopp E and Ghosh S. Inhibition of NF-kappa B by sodium salicylate and aspirin. Science. **1994**; *265*: 956-959.

Koren E, Kohen R and Ginsburg I. Polyphenols enhance total oxidant-scavenging capacities of human blood by binding to red blood cells. Exp Biol Med (Maywood). **2010**; *235*: 689-699.

Kris-Etherton PM, Hecker KD, Bonanome A, Coval SM, Binkoski AE, Hilpert KF, Griel AE and Etherton TD. Bioactive compounds in foods: their role in the prevention of cardiovascular disease and cancer. Am J Med. **2002**; *113 Suppl 9B*: 71S-88S.

Kuriki K, Tajima K and Tokudome S. Accelerated solvent extraction for quantitative measurement of fatty acids in plasma and erythrocytes. Lipids. **2006**; *41*: 605-614.

Last RL, Jones AD and Shachar-Hill Y. Towards the plant metabolome and beyond. Nat Rev Mol Cell Biol. **2007**; *8*: 167-174.

Lawson C and Wolf S. ICAM-1 signaling in endothelial cells. Pharmacol Rep. **2009**; *61*: 22-32.

References

Lee G, Na HJ, Namkoong S, Jeong Kwon H, Han S, Ha KS, Kwon YG, Lee H and Kim YM. 4-O-methylgallic acid down-regulates endothelial adhesion molecule expression by inhibiting NF-kappaB-DNA-binding activity. Eur J Pharmacol. **2006**; *551*: 143-151.

Lee HS, Kim SD, Lee WM, Endale M, Kamruzzaman SM, Oh WJ, Cho JY, Kim SK, Cho HJ, Park HJ and Rhee MH. A noble function of BAY 11-7082: Inhibition of platelet aggregation mediated by an elevated cAMP-induced VASP, and decreased ERK2/JNK1 phosphorylations. Eur J Pharmacol. **2010**; *627*: 85-91.

Leeuwenberg JF, Smeets EF, Neefjes JJ, Shaffer MA, Cinek T, Jeunhomme TM, Ahern TJ and Buurman WA. E-selectin and intercellular adhesion molecule-1 are released by activated human endothelial cells in vitro. Immunology. **1992**; *77*: 543-549.

Lenz EM and Wilson ID. Analytical strategies in metabonomics. J Proteome Res. **2007**; *6*: 443-458.

Li H, Cybulsky MI, Gimbrone MA, Jr. and Libby P. An atherogenic diet rapidly induces VCAM-1, a cytokine-regulatable mononuclear leukocyte adhesion molecule, in rabbit aortic endothelium. Arterioscler Thromb. **1993**; *13*: 197-204.

Libby P, Ridker PM and Hansson GK. Inflammation in atherosclerosis: from pathophysiology to practice. J Am Coll Cardiol. **2009**; *54*: 2129-2138.

Libby P, Ridker PM and Hansson GK. Progress and challenges in translating the biology of atherosclerosis. Nature. **2011**; *473*: 317-325.

Libby P, Ridker PM and Maseri A. Inflammation and atherosclerosis. Circulation. **2002**; *105*: 1135-1143.

Lindon JC, Holmes E and Nicholson JK. So what's the deal with metabonomics? Anal Chem. **2003**; *75*: 384A-391A.

Lindon JC and Nicholson JK. Spectroscopic and statistical techniques for information recovery in metabonomics and metabolomics. Annu Rev Anal Chem (Palo Alto Calif). **2008**; *1*: 45-69.

Lindon JC, Nicholson JK, Holmes E and Everett JR. Metabonomics: Metabolic Processes Studied by NMR Spectroscopy of Biofluids. Concepts in Magnetic Resonance. **2000**; *12*: 289-320.

Liu L, Zubik L, Collins FW, Marko M and Meydani M. The antiatherogenic potential of oat phenolic compounds. Atherosclerosis. **2004**; *175*: 39-49.

Longo DL. Harrison's principles of internal medicine. **2011**. McGraw-Hill: New York. 9780071748896; v1 9780071632447; v2 9780071748872. http://accessmedicine.com/resourceTOC.aspx?resourceID=4

Loppnow H, Werdan K and Buerke M. Vascular cells contribute to atherosclerosis by cytokine- and innate-immunity-related inflammatory mechanisms. Innate Immun. **2008**; *14*: 63-87.

Lorini R, De Amici M, d'Annunzio G, Vitali L and Scaramuzza A. Low serum levels of tumor necrosis factor-alpha in insulin-dependent diabetic children. Horm Res. **1995**; *43*: 206-209.

Lu W, Bennett BD and Rabinowitz JD. Analytical strategies for LC-MS-based targeted metabolomics. J Chromatogr B Analyt Technol Biomed Life Sci. **2008**; *871*: 236-242.

Maas R and Boger RH. Old and new cardiovascular risk factors: from unresolved issues to new opportunities. Atheroscler Suppl. **2003**; *4*: 5-17.

Maccaglia A, Mallozzi C and Minetti M. Differential effects of quercetin and resveratrol on Band 3 tyrosine phosphorylation signalling of red blood cells. Biochem Biophys Res Commun. **2003**; *305*: 541-547.

Magness ST, Jijon H, Van Houten Fisher N, Sharpless NE, Brenner DA and Jobin C. In vivo pattern of lipopolysaccharide and anti-CD3-induced NF-kappa B activation using a novel gene-targeted enhanced GFP reporter gene mouse. J Immunol. **2004**; *173*: 1561-1570.

Mallol R, Rodriguez MA, Heras M, Vinaixa M, Canellas N, Brezmes J, Plana N, Masana L and Correig X. Surface fitting of 2D diffusion-edited (1)H NMR spectroscopy data for the characterisation of human plasma lipoproteins. Metabolomics. **2011**; *7*: 572-582.

Martin A, Wu D, Baur W, Meydani SN, Blumberg JB and Meydani M. Effect of vitamin E on human aortic endothelial cell responses to oxidative injury. Free Radic Biol Med. **1996**; *21*: 505-511.

Martin KR, Wu D and Meydani M. The effect of carotenoids on the expression of cell surface adhesion molecules and binding of monocytes to human aortic endothelial cells. Atherosclerosis. **2000**; *150*: 265-274.

Mayeux R. Biomarkers: potential uses and limitations. NeuroRx. **2004**; *1*: 182-188.

McGavin JK, Mann JI, Skeaff CM and Chisholm A. Comparison of a vitamin E-rich diet and supplemental vitamin E on measures of vitamin E status and lipoprotein profile. Eur J Clin Nutr. **2001**; *55*: 555-561.

Mestas J and Ley K. Monocyte-endothelial cell interactions in the development of atherosclerosis. Trends Cardiovasc Med. **2008**; *18*: 228-232.

Monagas M, Garrido I, Lebron-Aguilar R, Bartolome B and Gomez-Cordoves C. Almond (Prunus dulcis (Mill.) D.A. Webb) skins as a potential source of bioactive polyphenols. J Agric Food Chem. **2007**; *55*: 8498-8507.

Montagnana M, Lippi G, Salvagno GL, Franchini M, Targher G and Guidi GC. [Role of biochemical risk factors and markers for the risk of atherosclerosis]. Recenti Prog Med. **2008**; *99*: 215-222.

Moverare R, Ahlstedt S, Bengtsson U, Borres MP, van Hage M, Poorafshar M, Sjolander S, Akerstrom J and van Odijk J. Evaluation of IgE Antibodies to Recombinant Peanut Allergens in Patients with Reported Reactions to Peanut. Int Arch Allergy Immunol. **2011**; *156*: 282-290.

Navarro-Gonzalez JF, Mora-Fernandez C, Muros de Fuentes M and Garcia-Perez J. Inflammatory molecules and pathways in the pathogenesis of diabetic nephropathy. Nat Rev Nephrol. **2011**; *7*: 327-340.

Nicholson JK, Foxall PJ, Spraul M, Farrant RD and Lindon JC. 750 MHz 1H and 1H-13C NMR spectroscopy of human blood plasma. Anal Chem. **1995**; *67*: 793-811.

Nicholson JK, Lindon JC and Holmes E. 'Metabonomics': understanding the metabolic responses of living systems to pathophysiological stimuli via multivariate statistical analysis of biological NMR spectroscopic data. Xenobiotica. **1999**; *29*: 1181-1189.

Oda T, Hirota K, Nishi K, Takabuchi S, Oda S, Yamada H, Arai T, Fukuda K, Kita T, Adachi T, Semenza GL and Nohara R. Activation of hypoxia-inducible factor 1 during macrophage differentiation. Am J Physiol Cell Physiol. **2006**; *291*: C104-113.

Oliver S. Guilt-by-association goes global. Nature. **2000**; *403*: 601-603.

Ordovas JM. Genetic interactions with diet influence the risk of cardiovascular disease. Am J Clin Nutr. **2006**; *83*: 443S-446S.

Orešič M. Metabolomics, a novel tool for studies of nutrition, metabolism and lipid dysfunction. Nutrition, Metabolism and Cardiovascular Diseases. **2009**; *19*: 816-824.

Organization WWHFWS. Global atlas on cardiovascular disease prevention and control. Policies, strategies and interventions. **2011**.

Ortega N, Romero MP, Macia A, Reguant J, Angles N, Morello JR and Motilva MJ. Obtention and characterization of phenolic extracts from different cocoa sources. J Agric Food Chem. **2008**; *56*: 9621-9627.

Ortega RM. Importance of functional foods in the Mediterranean diet. Public Health Nutr. **2006**; *9*: 1136-1140.

Osiecki H. The role of chronic inflammation in cardiovascular disease and its regulation by nutrients. Altern Med Rev. **2004**; *9*: 32-53.

Paiva-Martins F, Fernandes J, Rocha S, Nascimento H, Vitorino R, Amado F, Borges F, Belo L and Santos-Silva A. Effects of olive oil polyphenols on erythrocyte oxidative damage. Mol Nutr Food Res. **2009**; *53*: 609-616.

Pan S, Aebersold R, Chen R, Rush J, Goodlett DR, McIntosh MW, Zhang J and Brentnall TA. Mass spectrometry based targeted protein quantification: methods and applications. J Proteome Res. **2009**; *8*: 787-797.

Patti GJ, Yanes O and Siuzdak G. Innovation: Metabolomics: the apogee of the omics trilogy. Nat Rev Mol Cell Biol. **2012**; *13*: 263-269.

Pepe MS, Janes H, Longton G, Leisenring W and Newcomb P. Limitations of the odds ratio in gauging the performance of a diagnostic, prognostic, or screening marker. Am J Epidemiol. **2004**; *159*: 882-890.

Pierce JW, Schoenleber R, Jesmok G, Best J, Moore SA, Collins T and Gerritsen ME. Novel inhibitors of cytokine-induced IkappaBalpha phosphorylation and endothelial cell adhesion molecule expression show anti-inflammatory effects in vivo. J Biol Chem. **1997**; *272*: 21096-21103.

Puiggros F, Sola R, Blade C, Salvado MJ and Arola L. Nutritional biomarkers and foodomic methodologies for qualitative and quantitative analysis of bioactive ingredients in dietary intervention studies. J Chromatogr A. **2011**; *1218*: 7399-7414.

Raab M, Daxecker H, Markovic S, Karimi A, Griesmacher A and Mueller MM. Variation of adhesion molecule expression on human umbilical vein endothelial cells upon multiple cytokine application. Clin Chim Acta. **2002**; *321*: 11-16.

Raamsdonk LM, Teusink B, Broadhurst D, Zhang N, Hayes A, Walsh MC, Berden JA, Brindle KM, Kell DB, Rowland JJ, Westerhoff HV, van Dam K and Oliver SG. A functional genomics strategy that uses metabolome data to reveal the phenotype of silent mutations. Nat Biotechnol. **2001**; *19*: 45-50.

Rader DJ and Daugherty A. Translating molecular discoveries into new therapies for atherosclerosis. Nature. **2008**; *451*: 904-913.

Rajavashisth TB, Liao JK, Galis ZS, Tripathi S, Laufs U, Tripathi J, Chai NN, Xu XP, Jovinge S, Shah PK and Libby P. Inflammatory cytokines and oxidized low density lipoproteins increase endothelial cell expression of membrane type 1-matrix metalloproteinase. J Biol Chem. **1999**; *274*: 11924-11929.

Ramana KV. Tumor necrosis factor-alpha converting enzyme: Implications for ocular inflammatory diseases. Int J Biochem Cell Biol. **2010**; *42*: 1076-1079.

Ramsey SA, Gold ES and Aderem A. A systems biology approach to understanding atherosclerosis. EMBO Mol Med. **2010**; *2*: 79-89.

Revkin JH, Shear CL, Pouleur HG, Ryder SW and Orloff DG. Biomarkers in the prevention and treatment of atherosclerosis: need, validation, and future. Pharmacol Rev. **2007**; *59*: 40-53.

Rhee EP and Gerszten RE. Metabolomics and cardiovascular biomarker discovery. Clin Chem. **2012**; *58*: 139-147.

Rizvi SI and Pandey KB. Activation of the erythrocyte plasma membrane redox system by resveratrol: a possible mechanism for antioxidant properties. Pharmacol Rep. **2010**; *62*: 726-732.

Roberts LD, Souza AL, Gerszten RE and Clish CB. Targeted metabolomics. Curr Protoc Mol Biol. **2012**; *Chapter 30*: Unit30 32.

Roodenburg AJ, Leenen R, van het Hof KH, Weststrate JA and Tijburg LB. Amount of fat in the diet affects bioavailability of lutein esters but not of alpha-carotene, beta-carotene, and vitamin E in humans. Am J Clin Nutr. **2000**; *71*: 1187-1193.

Ross R. Atherosclerosis--an inflammatory disease. N Engl J Med. **1999a**; *340*: 115-126.

Ross R. Atherosclerosis is an inflammatory disease. Am Heart J. **1999b**; *138*: S419-420.

Roy S, Sen CK, Kobuchi H and Packer L. Antioxidant regulation of phorbol ester-induced adhesion of human Jurkat T-cells to endothelial cells. Free Radic Biol Med. **1998**; *25*: 229-241.

Rozenova KA, Deevska GM, Karakashian AA and Nikolova-Karakashian MN. Studies on the role of acid sphingomyelinase and ceramide in the regulation of tumor necrosis factor alpha (TNFalpha)-converting enzyme activity and TNFalpha secretion in macrophages. J Biol Chem. **2010**; *285*: 21103-21113.

Rull A, Vinaixa M, Angel Rodriguez M, Beltran R, Brezmes J, Canellas N, Correig X and Joven J. Metabolic phenotyping of genetically modified mice: An NMR metabonomic approach. Biochimie. **2009**; *91*: 1053-1057.

Samuelsson LM and Larsson DG. Contributions from metabolomics to fish research. Mol Biosyst. **2008**; *4*: 974-979.

Sanclemente T, Marques-Lopes I, Puzo J and Garcia-Otin AL. Role of naturally-occurring plant sterols on intestinal cholesterol absorption and plasmatic levels. J Physiol Biochem. **2009**; *65*: 87-98.

Saremi A and Arora R. Vitamin E and cardiovascular disease. Am J Ther. **2010**; *17*: e56-65.

Savage AK, Tucker G, van Duynhoven JP, Wulfert F and Daykin CA. Nutrimetabolomics: development of a bio-identification toolbox to determine the bioactive compounds in grape juice. Bioanalysis. **2009**; *1*: 1537-1549.

Schleser S, Ringseis R and Eder K. Conjugated linoleic acids have no effect on TNF alpha-induced adhesion molecule expression, U937 monocyte adhesion, and chemokine release in human aortic endothelial cells. Atherosclerosis. **2006**; *186*: 337-344.

Schmidt CW. Metabolomics: what's happening downstream of DNA. Environ Health Perspect. **2004**; *112*: A410-415.

Schulz VJ, Smit JJ, Willemsen KJ, Fiechter D, Hassing I, Bleumink R, Boon L, van den Berg M, van Duursen MB and Pieters RH. Activation of the aryl hydrocarbon receptor suppresses sensitization in a mouse peanut allergy model. Toxicol Sci. **2011**.

Sen CK and Bagchi D. Regulation of inducible adhesion molecule expression in human endothelial cells by grape seed proanthocyanidin extract. Mol Cell Biochem. **2001**; *216*: 1-7.

Sengupta A and Ghosh M. Integrity of erythrocytes of hypercholesterolemic and normocholesterolemic rats during ingestion of different structured lipids. Eur J Nutr. **2011**.

Shapiro NI, Schuetz P, Yano K, Sorasaki M, Parikh SM, Jones AE, Trzeciak S, Ngo L and Aird WC. The association of endothelial cell signaling, severity of illness, and organ dysfunction in sepsis. Crit Care. **2010**; *14*: R182.

Shaw DI, Hall WL, Jeffs NR and Williams CM. Comparative effects of fatty acids on endothelial inflammatory gene expression. Eur J Nutr. **2007**; *46*: 321-328.

Shearer GC, Pottala JV, Spertus JA and Harris WS. Red blood cell fatty acid patterns and acute coronary syndrome. PLoS One. **2009**; *4*: e5444.

Singh U, Tabibian J, Venugopal SK, Devaraj S and Jialal I. Development of an in vitro screening assay to test the antiinflammatory properties of dietary supplements and pharmacologic agents. Clin Chem. **2005**; *51*: 2252-2256.

Siri-Tarino PW, Sun Q, Hu FB and Krauss RM. Meta-analysis of prospective cohort studies evaluating the association of saturated fat with cardiovascular disease. Am J Clin Nutr. **2010**; *91*: 535-546.

Smith RD. Mass spectrometry in biomarker applications: from untargeted discovery to targeted verification, and implications for platform convergence and clinical application. Clin Chem. **2012**; *58*: 528-530.

Spiecker M, Peng HB and Liao JK. Inhibition of endothelial vascular cell adhesion molecule-1 expression by nitric oxide involves the induction and nuclear translocation of IkappaBalpha. J Biol Chem. **1997**; *272*: 30969-30974.

Stary HC, Chandler AB, Dinsmore RE, Fuster V, Glagov S, Insull W, Jr., Rosenfeld ME, Schwartz CJ, Wagner WD and Wissler RW. A definition of advanced types of atherosclerotic lesions and a histological classification of atherosclerosis. A report from the Committee on Vascular Lesions of the Council on Arteriosclerosis, American Heart Association. Circulation. **1995**; *92*: 1355-1374.

Subramaniam D, Ramalingam S, Linehan DC, Dieckgraefe BK, Postier RG, Houchen CW, Jensen RA and Anant S. RNA binding protein CUGBP2/CELF2 mediates curcumin-induced mitotic catastrophe of pancreatic cancer cells. PLoS One. **2011**; *6*: e16958.

Sun Q, Ma J, Campos H, Hankinson SE and Hu FB. Comparison between plasma and erythrocyte fatty acid content as biomarkers of fatty acid intake in US women. Am J Clin Nutr. **2007**; *86*: 74-81.

Szekanecz Z, Shah MR, Pearce WH and Koch AE. Intercellular adhesion molecule-1 (ICAM-1) expression and soluble ICAM-1 (sICAM-1) production by cytokine-activated human aortic endothelial cells: a possible role for ICAM-1 and sICAM-1 in atherosclerotic aortic aneurysms. Clin Exp Immunol. **1994**; *98*: 337-343.

Tang P, Hung MC and Klostergaard J. Human pro-tumor necrosis factor is a homotrimer. Biochemistry. **1996**; *35*: 8216-8225.

Terry RW, Kwee L, Levine JF and Labow MA. Cytokine induction of an alternatively spliced murine vascular cell adhesion molecule (VCAM)

mRNA encoding a glycosylphosphatidylinositol-anchored VCAM protein. Proc Natl Acad Sci U S A. **1993**; *90*: 5919-5923.

Tomiyama H, Okazaki R, Inoue D, Ochiai H, Shiina K, Takata Y, Hashimoto H and Yamashina A. Link between obstructive sleep apnea and increased bone resorption in men. Osteoporos Int. **2008**; *19*: 1185-1192.

Tribolo S, Lodi F, Connor C, Suri S, Wilson VG, Taylor MA, Needs PW, Kroon PA and Hughes DA. Comparative effects of quercetin and its predominant human metabolites on adhesion molecule expression in activated human vascular endothelial cells. Atherosclerosis. **2008**; *197*: 50-56.

Tweeddale H, Notley-McRobb L and Ferenci T. Effect of slow growth on metabolism of Escherichia coli, as revealed by global metabolite pool ("metabolome") analysis. J Bacteriol. **1998**; *180*: 5109-5116.

Vadacca M, Bruni R, Cacciapaglia F, Serino F, Arcarese L, Buzzulini F, Coppolino G, Rigon A, Terminio N and Afeltra A. [Alexithymia and immunoendocrine parameters in patients affected by systemic lupus erythematosus and rheumatoid arthritis]. Reumatismo. **2008**; *60*: 50-56.

van der Greef J, Stroobant P and van der Heijden R. The role of analytical sciences in medical systems biology. Curr Opin Chem Biol. **2004**; *8*: 559-565.

van Kimmenade RR and Januzzi JL, Jr. Emerging biomarkers in heart failure. Clin Chem. **2012**; *58*: 127-138.

Vannini N, Pfeffer U, Lorusso G, Noonan DM and Albini A. Endothelial cell aging and apoptosis in prevention and disease: E-selectin expression and modulation as a model. Curr Pharm Des. **2008**; *14*: 221-225.

Vasan RS. Biomarkers of cardiovascular disease: molecular basis and practical considerations. Circulation. **2006**; *113*: 2335-2362.

Verseyden C, Meijssen S and Cabezas MC. Effects of atorvastatin on fasting plasma and marginated apolipoproteins B48 and B100 in large, triglyceride-rich lipoproteins in familial combined hyperlipidemia. J Clin Endocrinol Metab. **2004**; *89*: 5021-5029.

Videm V and Albrigtsen M. Soluble ICAM-1 and VCAM-1 as markers of endothelial activation. Scand J Immunol. **2008**; *67*: 523-531.

Vinaixa M, Rodriguez MA, Rull A, Beltran R, Blade C, Brezmes J, Canellas N, Joven J and Correig X. Metabolomic assessment of the effect of dietary cholesterol in the progressive development of fatty liver disease. J Proteome Res. **2010**; *9*: 2527-2538.

Virmani R, Burke AP, Farb A and Kolodgie FD. Pathology of the unstable plaque. Prog Cardiovasc Dis. **2002a**; *44*: 349-356.

Virmani R, Burke AP, Kolodgie FD and Farb A. Vulnerable plaque: the pathology of unstable coronary lesions. J Interv Cardiol. **2002b**; *15*: 439-446.

Walsh CT, Garneau-Tsodikova S and Gatto GJ, Jr. Protein posttranslational modifications: the chemistry of proteome diversifications. Angew Chem Int Ed Engl. **2005**; *44*: 7342-7372.

Want EJ, Coen M, Masson P, Keun HC, Pearce JT, Reily MD, Robertson DG, Rohde CM, Holmes E, Lindon JC, Plumb RS and Nicholson JK. Ultra performance liquid chromatography-mass spectrometry profiling of bile acid metabolites in biofluids: application to experimental toxicology studies. Anal Chem. **2010**; *82*: 5282-5289.

Weber H and Brecker L. Online NMR for monitoring biocatalysed reactions. Curr Opin Biotechnol. **2000**; *11*: 572-578.

Weyrich AS, McIntyre TM, McEver RP, Prescott SM and Zimmerman GA. Monocyte tethering by P-selectin regulates monocyte chemotactic protein-1 and tumor necrosis factor-alpha secretion. Signal integration and NF-kappa B translocation. J Clin Invest. **1995**; *95*: 2297-2303.

Wishart DS, Knox C, Guo AC, Eisner R, Young N, Gautam B, Hau DD, Psychogios N, Dong E, Bouatra S, Mandal R, Sinelnikov I, Xia J, Jia L, Cruz JA, Lim E, Sobsey CA, Shrivastava S, Huang P, Liu P, Fang L, Peng J, Fradette R, Cheng D, Tzur D, Clements M, Lewis A, De Souza A, Zuniga A, Dawe M, Xiong Y, Clive D, Greiner R, Nazyrova A, Shaykhutdinov R, Li L, Vogel HJ and Forsythe I. HMDB: a knowledgebase for the human metabolome. Nucleic Acids Res. **2009**; *37*: D603-610.

Wishart DS, Tzur D, Knox C, Eisner R, Guo AC, Young N, Cheng D, Jewell K, Arndt D, Sawhney S, Fung C, Nikolai L, Lewis M, Coutouly MA, Forsythe I, Tang P, Shrivastava S, Jeroncic K, Stothard P, Amegbey G, Block D, Hau DD, Wagner J, Miniaci J, Clements M, Gebremedhin M, Guo N, Zhang Y, Duggan GE, Macinnis GD, Weljie AM, Dowlatabadi R, Bamforth F, Clive D, Greiner R, Li L, Marrie T, Sykes BD, Vogel HJ and Querengesser L. HMDB: the Human Metabolome Database. Nucleic Acids Res. **2007**; *35*: D521-526.

Witkamp R and Monshouwer M. Signal transduction in inflammatory processes, current and future therapeutic targets: a mini review. Vet Q. **2000**; *22*: 11-16.

Wu D, Koga T, Martin KR and Meydani M. Effect of vitamin E on human aortic endothelial cell production of chemokines and adhesion to monocytes. Atherosclerosis. **1999**; *147*: 297-307.

Young SG. Recent progress in understanding apolipoprotein B. Circulation. **1990**; *82*: 1574-1594.

Zhang WJ and Frei B. Albumin selectively inhibits TNF alpha-induced expression of vascular cell adhesion molecule-1 in human aortic endothelial cells. Cardiovasc Res. **2002**; *55*: 820-829.

Zhang X, Yap Y, Wei D, Chen G and Chen F. Novel omics technologies in nutrition research. Biotechnol Adv. **2008**; *26*: 169-176.

Zheng X, Jiang F, Katakowski M, Kalkanis SN, Hong X, Zhang X, Zhang ZG, Yang H and Chopp M. Inhibition of ADAM17 reduces hypoxia-induced brain tumor cell invasiveness. Cancer Sci. **2007**; *98*: 674-684.

Zhou Z, Liu Y, Miao AD and Wang SQ. Protocatechuic aldehyde suppresses TNF-alpha-induced ICAM-1 and VCAM-1 expression in human umbilical vein endothelial cells. Eur J Pharmacol. **2005**; *513*: 1-8.

References

EFFECT OF FOOD EXTRACTS AND BIOACTIVE FOOD COMPOUNDS ON THE MECHANISM OF ATHEROSCLEROSIS AND NUTRITIONAL BIOMARKERS
Úrsula Catalán Santos
Dipòsit Legal: T. 1058-2012

ANNEX

EFFECT OF FOOD EXTRACTS AND BIOACTIVE FOOD COMPOUNDS ON THE MECHANISM OF ATHEROSCLEROSIS AND NUTRITIONAL BIOMARKERS

Úrsula Catalán Santos

Dipòsit Legal: T. 1058-2012

1. Contributions at Congresses and Conferences

1.1 Posters

Fernández-Castillejo S, **Catalán Ú**, Pons L, Heras M, Masana L and Sola R. **Desarrollo metodológico de un modelo celular *in vitro* para el estudio de los efectos anticoagulantes de extractos o compuestos bioactivos naturales**. XXII Congreso nacional de la sociedad española de arteriosclerosis. Pamplona, 27-29 May 2009

Pons L, Fernández-Castillejo S, **Catalán Ú**, Heras M, Girona J, Masana L and Solà R. **Desarrollo metodológico de un modelo celular *in vitro* para el estudio de los efectos en la expresión génica de la *endothelial nitric oxide synthase* de compuestos bioactivos naturales y de la insulina.** XXII Congreso nacional de la sociedad española de arteriosclerosis. Pamplona, 27-29 May 2009

Romeu M, Valls RM, Albaladejo R, Sánchez-Martos V, **Catalán Ú**, Fernández-Castillejo S, Aranda N, Espinel A, Delgado MA, Arija V, Giralt M and Solà R. **Marcadores de estrés oxidativo relacionados con las enfermedades cardiovasculares en humanos sanos**. XXII Congreso nacional de la sociedad española de arteriosclerosis. Pamplona, 27-29 May 2009

Catalán Ú, Fernández-Castillejo S, Pons L, Heras M, Anglès N and Solà R. **Alfa-tocoferol y BAY mejoran la disfunción endotelial reduciendo la VCAM-1: un modelo celular para estudiar compuestos bioactivos.** XXIII Congreso nacional de la sociedad española de arteriosclerosis. Córdoba, 09-11 June 2010 **"special research mention"**

Fernández-Castillejo S, **Catalán Ú**, Pons L and Solà R. **Reduction of Tissue Factor Activity, Protein and mRNA Expression in Response to Polyphenols in Human Aortic Endothelial Cells Exposed to**

Pathophysiological Stimuli as Tumor Necrosis Factor-alpha. 4th Congress of the International Society of Nutrigenetics/Nutrigenomics (ISNN). Pamplona, 18-20 November 2010

Catalán Ú, Pons L, Fernández-Castillejo S, Heras M, Anglès N, Morello JR and Solà R. **Bioactive Compounds Improve Endothelial Dysfunction by Reducing VCAM-1 mRNA Expression and Its Soluble Protein Form in Human Aortic Endothelial Cells.** 4th Congress of the International Society of Nutrigenetics/Nutrigenomics (ISNN). Pamplona, 18-20 November 2010

Catalán Ú, Fernández-Castillejo S, Rodríguez MA, Vinaixa M, Ras MR, Martorell I, Correig X and Solà R**. Comparación del perfil metabolómico de dos matrices biológicas: plasma y eritrocitos humanos.** XXIV Congreso nacional de la sociedad española de arteriosclerosis. Sevilla, 25-27 May 2011

Pedret A, Valls RM, Fernández-Castillejo S, **Catalán Ú**, Romeu M, Lamuela-Raventós RM, Arija V and Solà R. **Fermented alcoholic beverages, urinary total polyphenol excretion and DNA oxidative damage biomarker in healthy subjects.** XXIV Congreso nacional de la sociedad española de arteriosclerosis. Sevilla, 25-27 May 2011

Catalán Ú, Macià A, Fernández-Castillejo S, Martorell I, Valls RM, Pedret A, Giralt M, Motilva MJ and Solà R. **Is the polyphenolic profile in erythrocytes a nutricional biomarker?.** 5th International Conference on Polyphenols and Health. Sitges, 17-20 October 2011

Pedret A, Valls RM, Fernández-Castillejo S, **Catalán Ú**, Romeu M, Giralt M, Lamuela-Raventós RM, Medina-Remón A, Arija V, Aranda N, Espinel A and Solà R. **Polyphenol-rich foods Project against oxidative damage in healthy subjects.** 5th International Conference on Polyphenols and Health. Sitges, 17-20 October 2011

Catalán Ú, Rodríguez MA, Ras MR, Macià A, Mallol R, Vinaixa M, Fernández-Castillejo S, Valls RM, Pedret A, Griffin JL, Salek R, Correig X, Motilva MJ and Solà R. **Biomarkers of Food intake and Metabolite Differences between Plasma and Red Blood Cell Matrices; a Human Metabolomic profile approach.** XXV Congreso nacional de la sociedad española de arteriosclerosis. Reus, 06-08 June 2012

Pedret A, Valls RM, Fernández-Castillejo S, **Catalán Ú**, Lamuela-Raventós RM, Medina-Remón A, Espinel A and Solà R. **Polyphenol-rich foods exhibit DNA anti-oxidative properties and protect the glutathione system in healthy subjects.** XXV Congreso nacional de la sociedad española de arteriosclerosis. Reus, 06-08 June 2012

1.2 Oral communications

Fernández-Castillejo S, **Catalán Ú**, Pons L and Solà R. **El resveratrol reduce la actividad, la expresión génica y la proteica del factor tisular en células endoteliales de aorta humana.** XXIII Congreso nacional de la sociedad española de arteriosclerosis. Córdoba, 09-11 June 2010

Fernández-Castillejo S, Farràs M, **Catalán Ú**, Pedret A, Konstantinidou V, Muñoz-Aguayo D, Solà R and Fitó M. **Efecto del consumo del aceite de oliva y sus compuestos fenólicos sobre la fluidez de la HDL.** XXV Congreso nacional de la sociedad española de arteriosclerosis. Reus, 06-08 June 2012

2. Scientific papers

Solà-Alberich R, Valls-Zamora RM, Fernández-Castillejo S, **Catalán-Santos Ú**, Pedret-Figuerola A, Giralt-Batista M and Konstantinidou V. **Do phenolic compounds exercise their effects by new pathways or mechanisms that would explain the healthy heart effects of virgin olive oil?.** Clin Invest Arterioscl. 2011;23(6):275-277

Pedret A, Valls RM, Fernández-Castillejo S, **Catalán Ú**, Romeu M, Giralt M, Lamuela-Raventós RM, Medina-Ramón A, Arija V, Aranda N, Espinel A and Solà R. **Polyphenol-rich foods protect against oxidative damage in healthy subjects.** (accepted for publication in the *Molecular Nutrition and Food Research;* DOI: 10.1002/mnfr.2011.00.676)

Catalán Ú, Fernández-Castillejo S, Pons L, Heras M, Aragonés G, Anglès N, Morello JR and Solà R. **Alpha-tocopherol and BAY 11-7082 Reduce Vascular Cell Adhesion Molecule in Human Aortic Endothelial Cells.** J Vasc Res. 2012;49(4):319-328

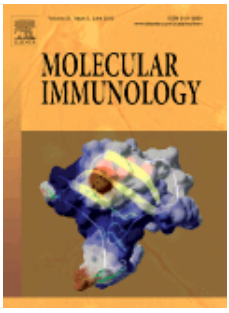

Catalán Ú, Fernández-Castillejo S, Anglès N, Morello JR, Yebras M and Sola R. **Inhibition of the transcription factor c-Jun by the MAPK family, and not the NF-κB pathway, suggests that peanut extract has anti-inflammatory properties.** Mol Immunol. 2012;52(3-4):125-132

Catalán Ú, Rodríguez MA, Ras MR, Macià A, Mallol R, Vinaixa M, Fernández-Castillejo S, Valls RM, Pedret A, Griffin JL, Salek R, Correig X, Motilva MJ and Solà R. **Biomarkers of Food intake and Metabolite Differences between Plasma and Red Blood Cell Matrices; a Human Metabolomic profile approach.** (editor submitted)

Catalán Ú, Fernández-Castillejo S, Pons L and Solà R. **Resveratrol reduces tissue factor activity, its mRNA levels and protein expression in human aortic endothelial cells: Possible beneficial effects from dietary supplementation.** (editor submitted)

Fernández-Castillejo S, Pons L, **Catalán Ú**, Heras M, González C, Rosales R, Girona J, Masana L, Anglès N, Morello JR and Solà R. **Lipopolysaccharide-induced tumor necrosis alpha secretion in monocytes thp-1: methodological aspects to reduce assay variability.** (editor submitted)

Fernández-Castillejo S, Pons L, **Catalán Ú**, Girona J, Rosales R, Anglès N, Morello JR and Solà R. **An *in vitro* assay to test endothelial function: nitric oxide synthase mRNA levels in human aortic endothelial cells.** (editor submitted)

Research Paper

Journal of Vascular Research

J Vasc Res 2012;49:319–328
DOI: 10.1159/000337466

Received: January 2, 2012
Accepted after revision: February 5, 2012
Published online: May 9, 2012

Alpha-Tocopherol and BAY 11-7082 Reduce Vascular Cell Adhesion Molecule in Human Aortic Endothelial Cells

Úrsula Catalán[a] Sara Fernández-Castillejo[a] Laia Pons[a] Mercedes Heras[a] Gemma Aragonés[a] Neus Anglès[b] Jose-Ramon Morelló[b] Rosa Solà[a]

[a]Unitat de Recerca en Lípids i Arteriosclerosi, CIBERDEM, Hospital Universitari Sant Joan, IISPV, Facultat de Medicina i Ciències de la Salut, Universitat Rovira i Virgili, Reus, and [b]La Morella Nuts S.A., Castellvell del Camp, Spain

Key Words

BAY 11-7082 · Alpha-tocopherol · Vascular cell adhesion molecule-1 · Endothelial dysfunction · Human aortic endothelial cells

Abstract

Background: In endothelial dysfunction, vascular cell adhesion molecule-1 (VCAM-1), E-selectin and intercellular adhesion molecule-1 (ICAM-1) expression (collectively termed cell adhesion molecules; CAMs) increase at sites of atherosclerosis and are stimulated by proinflammatory cytokines such as tumor necrosis factor-α (TNF-α). ***Methods:*** We evaluated the effect of alpha-tocopherol (AT; 10–150 μM) and BAY 11-7082 (BAY; 0.1 or 1 μM) on CAMs mRNA expression as well as their protein in soluble release form (sCAMs) in human aortic endothelial cells (HAECs) activated by TNF-α (1 or 10 ng/ml). Also, we determined the extent of lymphocyte adhesion to activated HAECs. ***Results:*** BAY reduced VCAM-1, E-selectin and ICAM-1 mRNA expression by 30, 30 and 10%, respectively. Furthermore, protein reduction of sVCAM-1 by 70%, sE-selectin by 51% and sICAM-1 by 25% compared to HAECs stimulated by TNF-α was observed ($p < 0.05$). AT (50, 75 and 150 μM) decreased VCAM-1 mRNA expression by 30% and sVCAM-1 protein by 33% compared to HAECs stimulated by TNF-α ($p < 0.05$). TNF-α-activated HAEC adhesion to human Jurkat T lymphocytes was higher compared to nonactivated HAECs ($p < 0.05$). BAY (2 and 5 μM) reduced this lymphocyte adhesion ($p < 0.05$). ***Conclusion:*** BAY reduces all the CAMs studied as well as cell adhesion, while AT selectively inhibits VCAM-1; both induce endothelial dysfunction improvement.

Introduction

Atherosclerosis can be considered the clinical endpoint of an inflammatory process and endothelial dysfunction. The binding of monocytes to the vascular endothelium is mediated by cross-linkage of cell adhesion molecules such as vascular cell adhesion molecule-1 (VCAM-1), E-selectin and/or intercellular adhesion molecule-1 (ICAM-1). The cell surface expression of these molecules is greatly increased in atherosclerotic lesions as a result of stimulation by proinflammatory cytokines such as tumor necrosis factor-α (TNF-α). This cytokine

Ú.C. and S.F.-C. contributed equally to the studies presented in this paper.

KARGER

Fax +41 61 306 12 34
E-Mail karger@karger.ch
www.karger.com

1018–1172/12/0494–0319$38.00/0

Accessible online at:
www.karger.com/jvr

Dr. Rosa Solà
Facultat de Medicina i Ciències de la Salut, Universitat Rovira i Virgili
C/ Sant Llorenç 21
ES–43201 Reus, Tarragona (Spain)
Tel. +34 97775 9369, E-Mail rosa.sola@urv.cat

has been selected as a stressor molecule in assessing the underlying mechanisms because it induces release and surface expression of cell adhesion molecules (CAMs), all of which contribute to the inflammatory process and endothelial dysfunction [1–5]. Further to this, there is in vivo evidence of increased VCAM-1 production in animal models of inflammation [3].

Endothelial CAMs are known to be upregulated in atherosclerotic endothelium in an environment of circulating blood. They participate in leukocyte recruitment and, subsequently, in atherosclerosis progression and/or tissue damage [6].

E-selectin is an inducible endothelial cell surface glycoprotein of the selectin family of adhesion molecules. It mediates the binding of neutrophils, eosinophils, monocytes and T lymphocytes to the endothelium [7].

VCAM-1 and ICAM-1 are members of the immunoglobulin superfamily of CAMs. They mediate lymphocyte adhesion to major elements of the aortic wall such as endothelial cells and vascular smooth muscle cells [8].

Induction of these three CAMs (VCAM, ICAM and E-selectin) by TNF-α is regulated at the level of gene transcription and requires the transcription nuclear factor-κB (NF-κB). Located in the cytoplasm of cells in an inactive form in close association with the inhibitor IκB-α, NF-κB binds to regulatory regions within promoter regions of the VCAM-1 gene [9, 10] via a process involving the phosphorylation and degradation of IκB-α [10–12].

In vitro studies indicate that VCAM-1, E-selectin and ICAM-1 are involved in the adhesion of eosinophils, monocytes and T lymphocytes via their cell surface [13]. Proteolytic cleavage of membrane-bound CAMs results in the release of their soluble forms – soluble CAMs (sCAMs), i.e. sVCAM-1, sE-selectin and sICAM-1 [6, 14–16].

BAY 11-7082 [(E)3-[(4-methylphenyl)sulfonyl]-2-propenenitrile; BAY] is an anti-inflammatory and antioxidant molecule that selectively and nonreversibly inhibits the inducible phosphorylation of IkB-α in human pancreatic MIA PaCa-2 cancer cells [17] and endothelial cells [18]. As such, IkB-α avoids being degraded, resulting in a high level of cytosolic NF-κB sequestered by IkB, together with decreased transcription and surface expression of the adhesion molecules [17]. However, the effect of BAY on VCAM-1 mRNA expression and its soluble protein (sVCAM-1) on endothelial dysfunction induced by TNF-α in human aortic endothelial cells (HAECs) has not, as yet, been evaluated in detail.

Some natural compounds or extracts of certain foods have been described as reversing endothelial dysfunction [2, 4, 13, 19, 20]. Prior to evaluating these functions in in vivo studies in animal and/or human subjects, in vitro cell models are developed to test the effects of these natural extracts (or compounds) based on the expression of cellular adhesion molecules in TNF-α-stimulated cells. As such, in vitro models facilitate the study of cells under controlled conditions and can be used as tools to examine the effects of various natural or synthetic pharmacologically active compounds.

Dietary factors play significant roles in the etiology of atherosclerosis by influencing inflammatory and endothelial dysfunction processes associated with the development of this disease. Vitamin E, especially the main fat-soluble dietary antioxidant alpha-tocopherol (AT), is very effective in reducing the adhesion of monocytes to HAECs in vivo and in vitro [21].

Several studies have demonstrated that vitamin E decreases the cytokine-stimulated HAEC production of chemokines such as sVCAM-1, soluble intercellular cell adhesion molecule (sICAM-1) [3], interleukine (IL)-6 and IL-8 [21] when stimulated with IL-β. Also, VCAM-1 mRNA expression levels are consistently elevated when incubated for between 6 and 24 h with TNF-α (10 ng/ml) and LPS (10 μg/ml) in human umbilical vein endothelial cells (HUVECs), with the levels remaining high under these conditions [22, 23]. However, the effects of AT on endothelial dysfunction induced by TNF-α in HAECs are not well documented.

The aim of the present study was to test our hypothesis that, by modifying CAMs mRNA expression and sCAMs protein release, AT and BAY can improve endothelial dysfunction.

Materials and Methods

Cell Culture

HAECs (Cascade Biologics™, Portland, Oreg., USA) at the 5th passage were seeded on Nunclon™ Δ surface 12-well plates (for the mRNA assays), 24-well plates (for the protein assays) or 96-well plates (for the adhesion assays) at a density of approximately 12×10^3 of viable cells/ml. Cells were maintained for the first 24 h in complete cell culture medium (CM) composed of M-200 medium supplemented with 2% (v/v) low serum growth supplement, 10 mg/ml gentamicin, 0.25 mg/ml amphotericin B (both purchased from Invitrogen, Paisley, UK), 100 U/ml penicillin and 100 mg/ml of streptomycin (both from Labclinics, Barcelona, Spain). The cells were grown to confluence at 37°C in a humidified incubator (Heracell 150; Madrid, Spain) with atmosphere containing 5% CO_2. The medium was replenished every 2 days with fresh CM. Viewed under an IMT2 microscope (Olympus, Barcelona, Spain), confluent monolayers displayed a typical monolayer phenotype of quiescent endothelial cells after 5 days

in culture. All HAEC experiments were conducted at 37°C in a humidified atmosphere with 5% CO_2.

Jurkat T cell lymphocytes were purchased from DSMZ GmbH (Braunschweig, Germany). Jurkat T cells were cultured in RPMI medium 1640 + Glutamax-I (Gibco, Spain) supplemented with 20% heat-inactivated foetal bovine serum (FBS) (PAA, Labclinics,) for the first 2 days followed by 10% FBS + 100 U/ml penicillin and 100 mg/ml streptomycin for growth and the scheduled experiments. The Jurkat T cells were maintained until the cell-cell adhesion assays.

HAECs were preincubated with AT (10, 25, 50, 75 and 150 μM; Sigma Chemical Co., St. Louis, Mo, USA) and the respective vehicle control (absolute ethanol, Panreac, Madrid, Spain) for 6 h, as recommended in the literature [23–27]. Then, as and when required, TNF-α (1 or 10 ng/ml; Calbiochem, Darmstadt, Germany) and BAY (0.1 or 1 μM; Merck, Darmstadt, Germany) were added to the cell culture medium for 24 h to induce cell stimulation. Finally, except for the cell-cell adhesion assays, supernatants were collected and stored at –20°C for batched measurements of the soluble forms of selected CAMs (sVCAM-1, sE-selectin and sICAM-1) and to measure the activity of the lactate dehydrogenase (LDH) released. Cells were lysed and stored at –80°C for batched TNF-α mRNA expression measurement. Fluorescent intensity was the method used to measure cell-cell adhesion.

Cell Viability and Cytotoxicity

Cell viability was assessed by morphology using phase-contrast microscopy and by trypan blue exclusion (Merck). Cell cytotoxicity was assessed with Cytotoxicity Detection Kit LDH (Roche Applied Science, Mannheim, Germany). Briefly, LDH enzyme is rapidly released into the cell culture supernatant when the plasma membrane is damaged. This results in a colorimetric reaction that can be measured at a wavelength of 492 nm.

For these experiments, TNF-α treatment was considered the maximum stress condition for the cells. The activity of LDH released from cells was measured in cell-free supernatants collected at two key stages of the experiment: after 6-hour incubation with AT and after 24-hour incubation with TNF-α (alone or in the presence of BAY) at the various concentrations. Results are expressed as mean absorbance and SD (error bars) of LDH produced by the cells under each treatment condition.

Analysis of CAMs mRNA Expression by Real-Time Quantitative Reverse Transcriptase Polymerase Chain Reaction in HAECs Stimulated with TNF-α

Dose- and time-course response experiments were performed by stimulating HAECs with TNF-α. Once the appropriate experimental conditions were established (i.e. the capacity to measure minimal decreases in CAMs mRNA expression that may be induced by the compounds under investigation: AT and BAY), we opted for 10 ng/ml (for E-selectin and ICAM-1) or 1 ng/ml (for VCAM-1) of TNF-stimulation over a culture period of 24 h, and BAY 1 μM (for E-selectin and ICAM-1) or 0.1 μM (for VCAM-1).

Cells were lysed with nucleic acid purification lysis solution and total RNA was isolated from cells using the ABI PRISM 6100 Nucleic Acid PrepStation extraction system (Applied Biosystems, Foster City, Calif., USA) according to the manufacturer's protocol. Total RNA was quantified using Quant-it™ RNA Assay Kit and Qubit™ fluorometer (Invitrogen). Using the 2720 Thermal Cycler (Applied Biosystems), 0.5 μg of total RNA was reverse transcribed to cDNA at 42°C for 50 min using random hexamers, SuperScript II reverse transcriptase and RNAse Out (Invitrogen) according to the manufacturer's protocol. To determine the amount of VCAM-1, E-selectin and ICAM-1 mRNA, semiquantitative RT-PCR was performed using the ABI PRISM 7900 Detection System (Applied Biosystems) with the following profile: 95°C denaturing (20 s) with 40 cycles of extension at 95°C (1 s) and 60°C (20 s). Each sample was analyzed in triplicate and the cycle threshold (Ct) was averaged from the values obtained in each reaction. VCAM-1, E-selectin and ICAM-1 mRNA expression results are reported as the increase (x-fold) using a $2^{-\Delta\Delta Ct}$ mathematical method. The glyceraldehyde-3-phosphate dehydrogenase (GAPDH; Applied Biosystems) was used as a housekeeping gene to normalize the results. TNF-α-activated endothelial cells were used as the calibrator in these experiments; its value was set at 1 and the other conditions were in relation to this reference value. Results are expressed as the mean and SD (error bars) of CAMs mRNA change relative to TNF-α alone.

Measurement of sCAMs Protein Secretion by HAECs Stimulated with TNF-α

Dose- and time-course response experiments were performed by stimulating HAECs with TNF-α. Once the appropriate experimental conditions were established, i.e. the capacity to measure minimal decreases in sCAMs protein secretion that may be induced by the compounds under investigation (in the present case AT and BAY; 1 μM), we opted for TNF-α at 10 ng/ml based on the concentrations used in previous reports with HUVECs [23, 26] or with HAECs [1, 19, 20, 25, 27, 28].

At the conclusion of the experiments, cells and supernatants were separated by centrifugation (Multifuge 3L-R; Madrid, Spain) at 1,500 *g* for 10 min at 4°C. The cell pellet/debris was discarded and the cell-free supernatants used for sVCAM-1, sE-selectin, sICAM-1 measurements using enzyme-linked immunosorbent assays (ELISA) according to the manufacturer's protocol (for sVCAM-1 ELISA kit, Diaclone, Besançon, France; for sE-selectin and sICAM-1, Quantikine ELISA kits from R&D Systems, Madrid, Spain).

All experimental data were compared to the outcomes in the TNF-α-alone incubation, since this achieved the maximal secretion of sVCAM-1. A vehicle-alone control (vehicle for AT, absolute ethanol) was run in parallel and used as the control in this experiment. Results are expressed as the mean sCAMs protein secretion and SD (error bars).

Calcein Labeling of Jurkat T Cells

Calcein acetoxymethyl ester (calcein-AM, Molecular Probes, Eugene, Oreg., USA) was used to fluorescently label Jurkat T cells. Calcein is a nonfluorescent and lipophilic molecule which is cleaved by endogenous esterases and the resultant product's fluorescence can be measured at 485 and 530 nm (excitation and emission wavelengths, respectively).

The Jurkat T cells were fluorescently labeled by incubating cells (25×10^6 cells/ml) with a final concentration of 5 μM of calcein-AM for 30 min at 37°C and 5% CO_2. After calcein-AM loading, the cells were washed twice with RPMI-1640 medium supplemented with 10% FBS to remove excess dye. Cells were finally resuspended in CM at a density of 2.5×10^6 cells/ml.

Cell-Cell Adhesion Assay

HAECs were seeded until confluent in black 96-well tissue culture plates. Following the appropriate culture with AT and BAY, calcein-AM-labeled Jurkat T cells were cocultured (2.5×10^5 cells/well) with the HAEC monolayer for 1 h at 37°C in a humidified atmosphere with 5% CO_2. The nonadhered Jurkat T cells were removed from the HAEC monolayer by washing twice with CM. Fluorescence in each well of the culture plate was measured with the Synergy HT Fluorometer (BioTek Instruments, Alcobendas, Spain) [29, 30]. Results are expressed as relative fluorescence units and SD (error bars).

Statistical Analyses

Data were expressed as the mean and SD (error bars) for sCAMs protein concentration and CAMs mRNA expression. Unless otherwise stated, all experiments were performed at least twice and each incubation condition was set up in triplicate. Analysis of variance (ANOVA) with Bonferroni's correction was used for multiple comparisons. A value of $p < 0.05$ was considered statistically significant.

A requisite for the analytical quality of the model was the control of several aspects involved in the cellular process and analytical performance of measurements. Thus, we evaluated the precision of the model by calculating the SD, SEM and the coefficients of variation (CV). All the results were analyzed with the Statistical Package for the Social Sciences (SPSS) software (version 19.0).

Results

Cytotoxicity

There was no evidence of HAEC cytotoxicity following exposure to AT (10, 25, 50, 75 and 150 μM) for 6 h (fig. 1a) nor TNF-α (10 ng/ml; fig. 1b) for the subsequent 24 h. No cytotoxicity was observed, as assessed by LDH activity release, at the concentrations of BAY tested (1 μM) under these experimental conditions.

Effect of AT and BAY on CAMs mRNA Expression by HAECs Stimulated with TNF- α

Exposure of cells to TNF-α (1 ng/ml for VCAM-1, 10 ng/ml for E-selectin and ICAM-1) for 24 h induced strong upregulation of CAMs mRNA expression (fig. 2). As shown in figure 2a, AT (at 50, 75 and 150 μM) significantly reduced VCAM-1 mRNA expression in TNF-α-stimulated HAECs by approximately 37% ($p < 0.05$). The intra-assay CV was <20% and the inter-assay CV was <21%. Compared to TNF-α alone, BAY treatment (0.1 μM) significantly blocked TNF-α-induced VCAM-1 mRNA expression by approximately 25% ($p < 0.05$; fig. 2a). The intra- and inter-assay CVs were <13%.

There was a tendency towards reducing E-selectin mRNA expression by BAY and AT by approximately 40 and 25%, respectively, but these reductions were not statistically significant (fig. 2b). ICAM-1 mRNA expression was decreased by AT and BAY by 25–40% and 13%, respectively, compared to TNF-α stimulation. However, the decrease did not reach statistical significance (fig. 2c).

Effects of AT and BAY on sCAMs Protein Secretion by HAECs Stimulated with TNF-α

When cells were exposed to TNF-α (10 ng/ml), sVCAM-1, sE-selectin and sICAM-1 increased significantly to 7.71 (0.40), 0.33 (0.08) and 13.31 (0.76) ng/ml, respectively ($p < 0.05$; fig. 3). AT significantly reduced sVCAM-1 protein secretion by about 40% in the highest doses tested (50, 75 and 150 μM) compared to TNF-α alone (10 ng/ml; $p < 0.05$) (fig. 3a). No dose-response effect was observed. The inter- and intra-assay CVs were <12%. AT also reduced sE-selectin (between 5 and 29%) and sICAM-1 (between 5 and 16%) at all doses tested, but the decreases did not reach statistical significance.

BAY (1 μM) reduced TNF-α (10 ng/ml) effects on sVCAM-1, sE-selectin and sICAM-1 release by 53, 50 and 26%. Only the effects on sVCAM and sE-selectin were statistically significant ($p < 0.05$; fig. 3a–c). As shown in figure 3b and c, nonactivated HAECs did not appear to release sE-selectin (limit of detection <0.125 ng/ml) and sICAM-1 (limit of detection <1.56 ng/ml), but the nonactivated cells did express sVCAM-1 (2.12 ng/ml; fig. 3a). Treatment of HAECs with AT had no statistically significant reduction effect on the protein secretion of sE-selectin (between 5 and 29% reduction) or sICAM-1 (between 6 and 16% reduction).

Effect of AT and BAY on Lymphocyte Cell Adhesion to HAECs

Qualitatively (fig. 4), there appeared to be a considerable number of Jurkat T cells adhering to TNF-α-treated HAECs, while very few cells adhered to untreated HAECs. Adhesion to HAECs that had been incubated with BAY (0.5, 1, 2 and 5 μM) appeared to be greatly decreased. Adhesion to HAECs that had been preincubated with AT (10, 25, 50, 75 and 150 μM) for 6 h appeared to decrease the adhesion of HAECs to Jurkat T cells at all concentrations tested (fig. 4).

The cell fluorescence images revealed that exposure of cells to TNF-α (10 ng/ml) for 24 h induced strong adhesion between Jurkat T cells and HAECs (fig. 5). The effects of different concentrations of AT and BAY on TNF-α-induced cell surface adhesion molecule expression are depicted in figure 5. AT failed to modulate significantly the TNF-α-induced cell surface expression of CAMs at

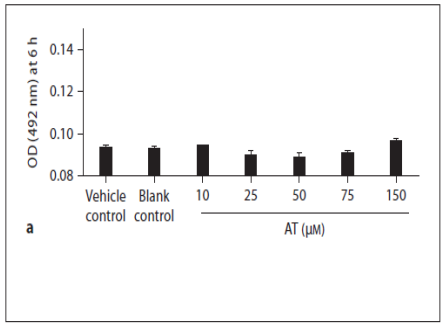

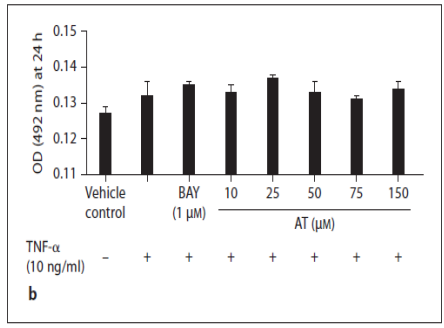

Fig. 1. Cytotoxicity from HAECs incubated with AT or BAY and stimulated with TNF-α. **a** Activity of LDH released into the cell-culture supernatants of HAECs following incubation with AT (10, 25, 50, 75 and 150 μM) for 6 h. **b** Activity of LDH released into the cell-culture supernatants of HAECs following stimulation with TNF-α (10 ng/ml) in the presence (1 μM for 24 h) or absence of BAY. Vehicle control refers to cells incubated with AT vehicle (absolute ethanol). Blank control refers to cells incubated without ethanol, TNF-α, BAY or AT. Results are the mean and the SD (error bars) of optical density (OD) from one representative experiment where each set of experimental conditions was run in triplicate.

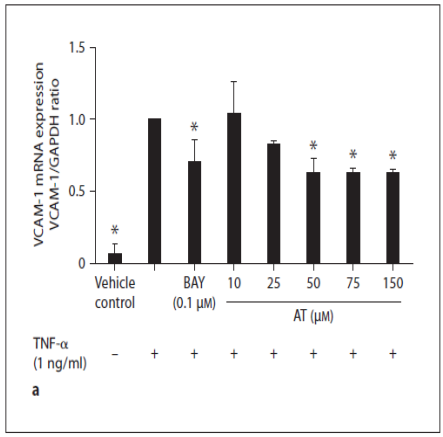

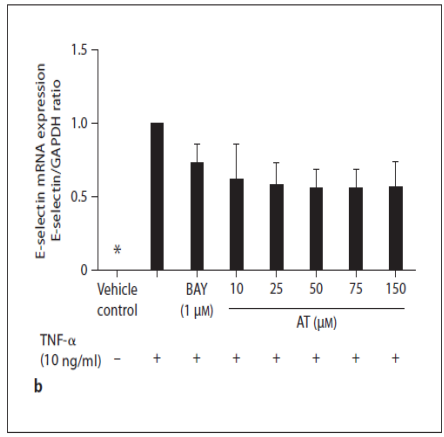

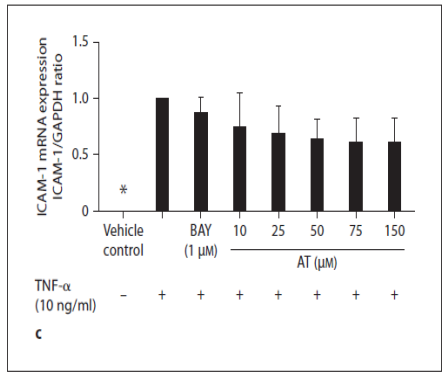

Fig. 2. Effect of AT and BAY on CAMs mRNA expression in HAECs stimulated by TNF-α. **a** Effect of AT and BAY on VCAM-1 mRNA expression. **b** Effect of AT and BAY on E-selectin mRNA expression. **c** Effect of AT and BAY on ICAM-1 mRNA expression. Results are the mean and the SD (error bars) of two independent experiments where each set of experimental conditions was run in triplicate. * $p < 0.05$ versus TNF-α alone.

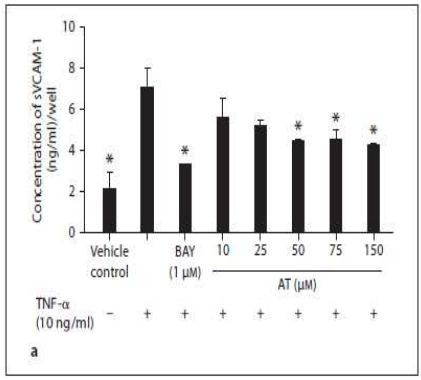

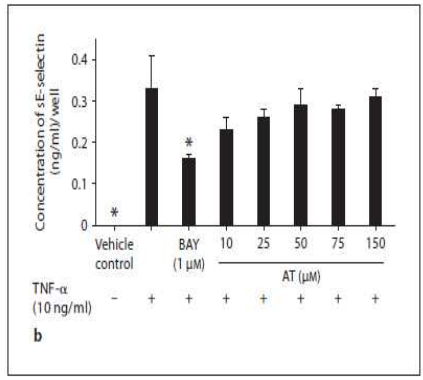

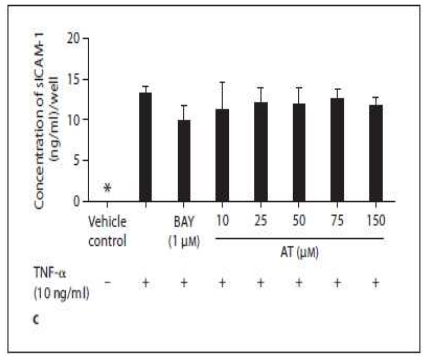

Fig. 3. Effect of AT and BAY on sCAMs protein secretion in HAECs stimulated by TNF-α. **a** Effect of AT and BAY on sVCAM-1 protein release. **b** Effect of AT and BAY on sE-selectin protein release. **c** Effect of AT and BAY on sICAM-1 protein release. Results are the mean and the SD (error bars) of two independent experiments where each set of experimental conditions was run in triplicate. * $p < 0.05$ versus TNF-α alone.

any of the concentrations (a reduction of between 11 and 17%; fig. 5). In contrast, when treated with BAY (0.1, 1, 2 and 5 μM), the TNF-α-induced cell surface expression of CAMs was notably reduced to 7, 13, 57 and 77%, respectively; statistically significant reductions being observed only at 2 and 5 μM ($p < 0.05$).

Discussion

Our results indicate that treatment with AT (50, 75 and 150 μM) inhibits VCAM-1 mRNA and sVCAM-1 protein by between 36 and 40% in TNF-α-stimulated HAECs ($p < 0.05$). In contrast, when we analyzed the effects of AT on stimulated HAECs, we observed a nonsignificant decrease in E-selectin and ICAM-1 mRNA expression (40 and 25–40%, respectively) and in sE-selectin and sICAM-1 protein release (5–29 and 5–16%, respectively) compared to TNF-α alone (10 ng/ml). As such, AT appears to play a beneficial role in atherosclerosis by specifically reducing VCAM-1 but not the other CAMs studied, which were E-selectin and ICAM-1.

The optimum serum concentration of AT in humans is around 23.2 μM [31], which is similar to the concentrations selected for our investigation. We also observed that, in TNF-α-stimulated HAECs, BAY (at 0.1 μM) reduced VCAM-1 mRNA expression by 25% and sVCAM-1 protein release by 53% ($p < 0.05$). Similarly, BAY (at 1 μM) decreased E-selectin and ICAM-1 mRNA expression by 25 and 13%, respectively, and sE-selectin and sICAM-1 protein release by 50 and 26%, respectively; albeit these reductions were not statistically significant.

VCAM-1 is an important adhesion molecule that is upregulated during endothelial activation by various factors such as TNF-α. Belonging to the immunoglobulin superfamily, it has adhesion molecule properties and acts as a ligand for activated leukocyte adhesion to endothelium [32].

Garton et al. [33] demonstrated in mice that VCAM-1 is released as a soluble form of the extracellular domain

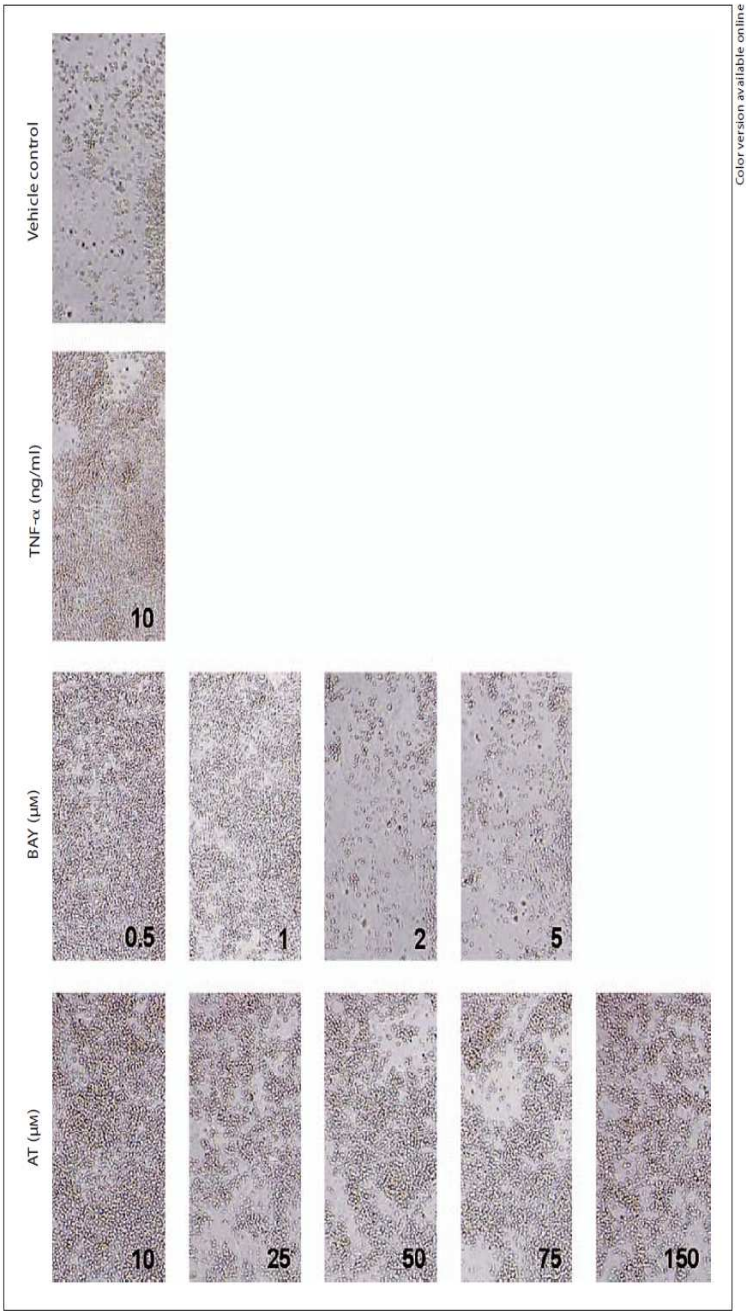

Fig. 4. Adhesion of Jurkat T cells to TNF-α-treated HAEC images under microscope (×4) – images of the experiments. Conditions used for this study were: vehicle control; TNF-α (10 ng/ml); BAY (0.5, 1, 2 and 5 μM); AT (10, 25, 50, 75 and 150 μM).

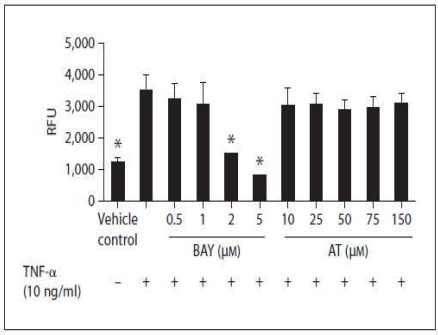

Fig. 5. Adhesion of Jurkat T cells to TNF-α-treated HAECs. Effect of AT at all concentrations tested (10, 25, 50, 75 and 150 μM) on cell-cell adhesion. Data are the mean and the SD (error bars) of relative fluorescence units (RFU) from two separate experiments run in octuplicate. * $p < 0.05$ versus TNF-α alone.

that is generated by TNF-α-converting enzymes (TACE or ADAM 17) induced by phorbol 12-myristate 13-acetate. E-selectin is expressed in acute as well as in a chronically inflamed endothelium and induces rolling of circulating monocytes and/or leukocytes through this endothelium [34, 35].

ICAM-1 is also involved in atherosclerosis, presumably through the regulation of monocyte recruitment into atherosclerosis-prone areas. ICAM-1 expression is elevated in aortas that are predisposed to atherosclerosis and is regulated by proinflammatory stimuli such as that of TNF-α.

E-selectin is involved in the leukocyte rolling on the endothelium, while VCAM-1 and ICAM-1 are involved in firm adhesion of leukocytes by binding to very late antigen-4 and to leukocyte function antigen-1, respectively. This mechanism is in accordance with our findings in the functional experiments in which we observed no differences between leukocyte adhesion to activated HAECs in the presence or absence of AT.

With respect to the proteins of each individual sCAM, we observed different degrees of response to the same stimuli (TNF-α 10 ng/ml) for each sCAM (13.31 ng/ml for sICAM-1, 7.71 ng/ml for sVCAM-1, and 0.33 ng/ml for sE-selectin); the contribution of each one being different in the adhesion step of atherosclerosis. Deneva-Koycheva et al. [36] recently determined the reference ranges of sVCAM-1 (170.42–478.36 ng/ml), sE-selectin (9.15–65.19 ng/ml) and sICAM-1 (128.9–347.48 ng/ml) in the serum of healthy Bulgarians, with no gender-related differences in CAM concentrations ($p > 0.05$). Human CAM serum concentrations are higher than those selected for the present study.

BAY, at 1 and 0.1 μM in the present study, reduced both sVCAM-1 protein release and VCAM-1 mRNA expression ($p < 0.05$). BAY (1 μM) also reduced sE-selectin and sICAM-1 protein release as well as their mRNA expression, albeit without the reduction being statistically significant. At similar concentrations (2, 5 or 12 μM) BAY has previously been described as inhibiting NF-κB in different cell types [37–39]. Accordingly, in our study, protein release of the studied sCAMs was reduced as well as the adhesion between activated HAECs and Jurkat T cells by BAY (0.5, 1, 2 and 5 μM); statistical significance being reached at BAY concentrations of 2 and 5 μM ($p < 0.05$).

Based on previous reports on HUVECs [23, 26] and in HAECs [1, 19, 20, 25, 28] in which the effects of compounds other than AT had been tested, we added TNF-α (at 10 ng/ml) to the HAEC culture for 24 h to determine the sVCAM-1 protein release. A mean of 74.74 pg/ml (range: 64–84) serum TNF-α concentration was recorded in healthy children [40] and, as reported by Tomiyama et al. [41], control individuals have 1.7 ± 0.5 pg/ml TNF-α in their circulation, while patients with obstructive sleep apnea have nearly 2 pg/ml. Patients with systemic lupus erythematosus have 4.9 ± 12.8 pg/ml and those with rheumatoid arthritis (an inflammatory disease) have 20 ± 36.2 pg/ml [42,43]. Hence, under inflammatory conditions, serum TNF-α levels can be high, approaching the TNF-α levels used in this study.

The production of adhesion molecules by endothelial cells has been shown to be regulated by redox-sensitive signal transduction and, thus, may be subjected to modulation by oxidants and antioxidants [44]. Since AT is a potent antioxidant, it would be reasonable to assume that the effects of this compound on reducing sVCAM-1 protein release in activated HAECs may be mainly due to its antioxidant properties in several endothelial cell types [21]. These outcomes are also observed at the mRNA expression level. Hence the results demonstrate that, apart from its antioxidant activities, AT can exert a modest inhibitory effect on adhesion molecule expression in vitro, and this suggests an improvement in endothelial dysfunction in HAECs.

It has been argued that HAECs or HUVECs may not adequately represent inflammatory changes in the microcirculation in tissues since these cells are isolated from a large artery or vein, respectively. The microvascular cell line HMEC-1 is reportedly one of the endothelial cell lines most similar to primary endothelium [21]. Results

of sVCAM-1 in HMEC-1 cultures have shown wider variation than those from HUVEC experiments, and it is mainly for this reason that HUVECs have been used extensively in in vitro endothelium studies [45]. It is not clear, however, whether these differences render HMEC-1 a better or a poorer model of local inflammation than HUVECs. However, HUVECs provide more consistent results even if genetic differences between donors may result in wider variation in the expression of inflammation markers [45]. Further cell culture studies are required using HMEC-1 or human coronary artery endothelial cells to confirm the sVCAM-1 results that had been observed in HAECs [38].

Conclusion

Our results suggest that the effect of AT on mRNA expression was the cause of decreased rates of the cleaved soluble protein products of CAMs. However, the effect of BAY on decreasing CAMs mRNA expression was less than the decrease in the rates of their soluble protein products. The possible mechanism of action could be an inhibition of proteolytic cleavage to liberate the circulating form of sVCAM-1, or of alternative splicing. AT (at 50, 75 and 150 μM), apart from having antioxidant and anti-inflammatory properties, also reduced VCAM-1 mRNA expression and sVCAM-1 protein release, while BAY (at 1 μM) reduced all CAMs studied (VCAM-1, E-selectin and ICAM-1) and also reduced the overall adhesion between HAECs and Jurkat T cells, thus implying an improvement in endothelial dysfunction that had been induced by TNF-α.

This in vitro model has its uses in assessing the potential beneficial effects of natural and manufactured compounds developed for the treatment of endothelium dysfunction and atherosclerosis.

Acknowledgements

This work was supported by the CENIT program of the Spanish Ministry of Industry and by a consortium of companies headed by La Morella Nuts (Castellvell del Camp, Tarragona, Spain), and with the collaboration of the following companies: KRAFT, BTSA (Biotecnologías Aplicadas) and Selecció Batallé. The funding bodies had no involvement in data interpretation or in the decision to submit the manuscript for publication.

References

1 Amberger A, Maczek C, Jurgens G, Michaelis D, Schett G, Trieb K, Eberl T, Jindal S, Xu Q, Wick G: Co-expression of ICAM-1, VCAM-1, ELAM-1 and Hsp60 in human arterial and venous endothelial cells in response to cytokines and oxidized low-density lipoproteins. Cell Stress Chaperones 1997; 2:94–103.
2 Davis PA, Polagruto JA, Valacchi G, Phung A, Soucek K, Keen CL, Gershwin ME: Effect of apple extracts on NF-κB activation in human umbilical vein endothelial cells. Exp Biol Med 2006;231:594–598.
3 Lee G, Na HJ, Namkoong S, Jeong Kwon H, Han S, Ha KS, Kwon YG, Lee H, Kim YM: 4-*O*-methylgallic acid down-regulates endothelial adhesion molecule expression by inhibiting NF-κB-DNA-binding activity. Eur J Pharmacol 2006;551:143–151.
4 Wu D, Koga T, Martin KR, Meydani M: Effect of vitamin E on human aortic endothelial cell production of chemokines and adhesion to monocytes. Atherosclerosis 1999;147: 297–307.
5 Zhou Z, Liu Y, Miao AD, Wang SQ: Protocatechuic aldehyde suppresses TNF-α-induced ICAM-1 and VCAM-1 expression in human umbilical vein endothelial cells. Eur J Pharmacol 2005;513:1–8.
6 Dagia NM, Harii N, Meli AE, Sun X, Lewis CJ, Kohn LD, Goetz DJ: Phenyl methimazole inhibits TNF-α-induced VCAM-1 expression in an IFN regulatory factor-1-dependent manner and reduces monocytic cell adhesion to endothelial cells. J Immunol 2004; 173:2041–2049.
7 Vannini N, Pfeffer U, Lorusso G, Noonan DM, Albini A: Endothelial cell aging and apoptosis in prevention and disease: E-selectin expression and modulation as a model. Curr Pharm Des 2008;14:221–225.
8 Lawson C, Wolf S: ICAM-1 signaling in endothelial cells. Pharmacol Rep 2009;61:22–32.
9 Dieguez-Acuna FJ, Polk WW, Ellis ME, Simmonds PL, Kushleika JV, Woods JS: Nuclear factor κB activity determines the sensitivity of kidney epithelial cells to apoptosis: implications for mercury-induced renal failure. Toxicol Sci 2004;82:114–123.
10 Pierce JW, Schoenleber R, Jesmok G, Best J, Moore SA, Collins T, Gerritsen ME: Novel inhibitors of cytokine-induced IκBα phosphorylation and endothelial cell adhesion molecule expression show anti-inflammatory effects in vivo. J Biol Chem 1997;272: 21096–21103.
11 Izban KF, Ergin M, Qin JZ, Martinez RL, Pooley RJ, Saeed S, Alkan S: Constitutive expression of NF-κB is a characteristic feature of mycosis fungoides: implications for apoptosis resistance and pathogenesis. Hum Pathol 2000;31:1482–1490.
12 Spiecker M, Peng HB, Liao JK: Inhibition of endothelial vascular cell adhesion molecule-1 expression by nitric oxide involves the induction and nuclear translocation of IκBα. J Biol Chem 1997;272:30969–30974.
13 Martin KR, Wu D, Meydani M: The effect of carotenoids on the expression of cell surface adhesion molecules and binding of monocytes to human aortic endothelial cells. Atherosclerosis 2000;150:265–274.
14 Constans J, Conri C: Circulating markers of endothelial function in cardiovascular disease. Clin Chim Acta 2006;368:33–47.
15 Just N, Tillie-Leblond I, Guery BP, Fourneau C, Tonnel AB, Gosset P: Keratinocyte growth factor (KGF) decreases ICAM-1 and VCAM-1 cell expression on bronchial epithelial cells. Clin Exp Immunol 2003;132:61–69.
16 Leeuwenberg JF, Smeets EF, Neefjes JJ, Shaffer MA, Cinek T, Jeunhomme TM, Ahern TJ, Buurman WA: E-selectin and intercellular adhesion molecule-1 are released by activated human endothelial cells in vitro. Immunology 1992;77:543–549.

17 Kamthong PJ, Wu M: Inhibitor of nuclear factor-κB induction by cAMP antagonizes interleukin-1-induced human macrophage-colony-stimulating-factor expression. Biochem J 2001;356:525–530.
18 Kopp E, Ghosh S: Inhibition of NF-κB by sodium salicylate and aspirin. Science 1994; 265:956–959.
19 Chen JW, Chen YH, Lin FY, Chen YL, Lin SJ: Ginkgo biloba extract inhibits tumor necrosis factor-alpha-induced reactive oxygen species generation, transcription factor activation, and cell adhesion molecule expression in human aortic endothelial cells. Arterioscler Thromb Vasc Biol 2003;23:1559–1566.
20 Chen YH, Lin SJ, Ku HH, Shiao MS, Lin FY, Chen JW, Chen YL: Salvianolic acid B attenuates VCAM-1 and ICAM-1 expression in TNF-α-treated human aortic endothelial cells. J Cell Biochem 2001;82:512–521.
21 Liu L, Zubik L, Collins FW, Marko M, Meydani M: The antiatherogenic potential of oat phenolic compounds. Atherosclerosis 2004; 175:39–49.
22 Raab M, Daxecker H, Markovic S, Karimi A, Griesmacher A, Mueller MM: Variation of adhesion molecule expression on human umbilical vein endothelial cells upon multiple cytokine application. Clin Chim Acta 2002;321:11–16.
23 Tribolo S, Lodi F, Connor C, Suri S, Wilson VG, Taylor MA, Needs PW, Kroon PA, Hughes DA: Comparative effects of quercetin and its predominant human metabolites on adhesion molecule expression in activated human vascular endothelial cells. Atherosclerosis 2008;197:50–56.
24 Martin A, Wu D, Baur W, Meydani SN, Blumberg JB, Meydani M: Effect of vitamin E on human aortic endothelial cell responses to oxidative injury. Free Radic Biol Med 1996;21:505–511.
25 Schleser S, Ringseis R, Eder K: Conjugated linoleic acids have no effect on TNFα-induced adhesion molecule expression, U937 monocyte adhesion, and chemokine release in human aortic endothelial cells. Atherosclerosis 2006;186:337–344.
26 Shaw DI, Hall WL, Jeffs NR, Williams CM: Comparative effects of fatty acids on endothelial inflammatory gene expression. Eur J Nutr 2007;46:321–328.
27 Zhang WJ, Frei B: Albumin selectively inhibits TNFα-induced expression of vascular cell adhesion molecule-1 in human aortic endothelial cells. Cardiovasc Res 2002;55:820–829.
28 Szekanecz Z, Shah MR, Pearce WH, Koch AE: Intercellular adhesion molecule-1 (ICAM-1) expression and soluble ICAM-1 (sICAM-1) production by cytokine-activated human aortic endothelial cells: a possible role for ICAM-1 and sICAM-1 in atherosclerotic aortic aneurysms. Clin Exp Immunol 1994;98:337–343.
29 Sen CK, Bagchi D: Regulation of inducible adhesion molecule expression in human endothelial cells by grape seed proanthocyanidin extract. Mol Cell Biochem 2001;216:1–7.
30 Roy S, Sen CK, Kobuchi H, Packer L: Antioxidant regulation of phorbol ester-induced adhesion of human Jurkat T-cells to endothelial cells. Free Radic Biol Med 1998;25: 229–241.
31 Gamez C, Artacho R, Ruiz-Lopez MD, Puerta A, Lopez MC: Nutritional status of vitamin A and E in institutionalized elderly people in Granada (Spain). J Nutr Sci Vitaminol (Tokyo) 1996;42:397–405.
32 Terry RW, Kwee L, Levine JF, Labow MA: Cytokine induction of an alternatively spliced murine vascular cell adhesion molecule (VCAM) mRNA encoding a glycosylphosphatidylinositol-anchored VCAM protein. Proc Natl Acad Sci USA 1993;90: 5919–5923.
33 Garton KJ, Gough PJ, Philalay J, Wille PT, Blobel CP, Whitehead RH, Dempsey PJ, Raines EW: Stimulated shedding of vascular cell adhesion molecule 1 (VCAM-1) is mediated by tumor necrosis factor-α-converting enzyme (ADAM 17). J Biol Chem 2003;278: 37459–37464.
34 Galkina E, Ley K: Vascular adhesion molecules in atherosclerosis. Arterioscler Thromb Vasc Biol 2007;27:2292–2301.
35 Shapiro NI, Schuetz P, Yano K, Sorasaki M, Parikh SM, Jones AE, Trzeciak S, Ngo L, Aird WC: The association of endothelial cell signaling, severity of illness, and organ dysfunction in sepsis. Crit Care 2010;14:R182.
36 Deneva-Koycheva TI, Vladimirova-Kitova LG, Angelova EA, Tsvetkova TZ: Serum levels of siCAM-1, sVCAM-1, sE-selectin, sP-selectin in healthy Bulgarian people. Folia Med (Plovdiv) 2011;53:22–28.
37 Bage T, Lindberg J, Lundeberg J, Modeer T, Yucel-Lindberg T: Signal pathways JNK and NF-κB, identified by global gene expression profiling, are involved in regulation of TNFα-induced mPGES-1 and COX-2 expression in gingival fibroblasts. BMC Genomics 2010;11:241.
38 Calabro P, Cirillo P, Limongelli G, Maddaloni V, Riegler L, Palmieri R, Pacileo G, De Rosa S, Pacileo M, De Palma R, Golino P, Calabro R: Tissue factor Is induced by resistin in human coronary artery endothelial cells by the NF-kB-dependent pathway. J Vasc Res 2011;48:59–66.
39 Juliana C, Fernandes-Alnemri T, Wu J, Datta P, Solorzano L, Yu JW, Meng R, Quong AA, Latz E, Scott CP, Alnemri ES: Anti-inflammatory compounds parthenolide and Bay 11-7082 are direct inhibitors of the inflammasome. J Biol Chem 2010;285:9792–9802.
40 Lorini R, De Amici M, d'Annunzio G, Vitali L, Scaramuzza A: Low serum levels of tumor necrosis factor-α in insulin-dependent diabetic children. Horm Res 1995;43:206–209.
41 Tomiyama H, Okazaki R, Inoue D, Ochiai H, Shiina K, Takata Y, Hashimoto H, Yamashina A: Link between obstructive sleep apnea and increased bone resorption in men. Osteoporos Int 2008;19:1185–1192.
42 Bruni R, Serino FM, Galluzzo S, Coppolino G, Cacciapaglia F, Vadacca M, Nilo S, Terminio N, Afeltra A: Alexithymia and neuroendocrine-immune response in patients with autoimmune diseases: preliminary results on relationship between alexithymic construct and TNF-α levels. Ann NY Acad Sci 2006;1069:208–211.
43 Vadacca M, Bruni R, Cacciapaglia F, Serino F, Arcarese L, Buzzulini F, Coppolino G, Rigon A, Terminio N, Afeltra A: Alexithymia and immunoendocrine parameters in patients affected by systemic lupus erythematosus and rheumatoid arthritis (in Italian). Reumatismo 2008;60:50–56.
44 Li H, Cybulsky MI, Gimbrone MA Jr, Libby P: An atherogenic diet rapidly induces VCAM-1, a cytokine-regulatable mononuclear leukocyte adhesion molecule, in rabbit aortic endothelium. Arterioscler Thromb 1993;13:197–204.
45 Videm V, Albrigtsen M: Soluble ICAM-1 and VCAM-1 as markers of endothelial activation. Scand J Immunol 2008;67:523–531.

G Model
ARTICLE IN PRESS
Molecular Immunology xx (2012) xxx–xxx
Contents lists available at SciVerse ScienceDirect
Molecular Immunology
journal homepage: www.elsevier.com/locate/molimm

Graphical Abstract

Molecular Immunology xx (2012) xxx–xxx

Inhibition of the transcription factor c-Jun by the MAPK family, and not the NF-κB pathway, suggests that peanut extract has anti-inflammatory properties

Úrsula Catalán, Sara Fernández-Castillejo, Neus Anglès, Jose Ramón Morelló, Martí Yebras, Rosa Solà*

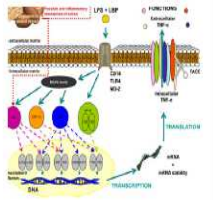

G Model
ARTICLE IN PRESS
Molecular Immunology xx (2012) xxx–xxx
Contents lists available at SciVerse ScienceDirect
Molecular Immunology
journal homepage: www.elsevier.com/locate/molimm

Highlights

Molecular Immunology xx (2012) xxx–xxx
Inhibition of the transcription factor c-Jun by the MAPK family, and not the NF-κB pathway, suggests that peanut extract has anti-inflammatory properties
Úrsula Catalán, Sara Fernández-Castillejo, Neus Anglès, Jose Ramón Morelló, Martí Yebras, Rosa Solà*

- Tumor necrosis factor-α (TNF-α) is involved in early inflammatory responses in atherosclerosis.
- The possible mechanism of action of polyphenol-rich peanut extract is by inhibiting c-Jun transcription factor activity.
- Peanut extract reduces extracellular TNF-α protein indicating an anti-inflammatory effect in this cellular model.
- *In vitro* cellular assay (assessing signal transduction to extracellular secretion of TNF-α pathway) could be a great model to evaluate the anti-inflammatory mechanisms of food extracts.

Molecular Immunology 52 (2012) 125–132

Contents lists available at SciVerse ScienceDirect

Molecular Immunology

journal homepage: www.elsevier.com/locate/molimm

Inhibition of the transcription factor c-Jun by the MAPK family, and not the NF-κB pathway, suggests that peanut extract has anti-inflammatory properties

Úrsula Catalán[a], Sara Fernández-Castillejo[a], Neus Anglès[b], Jose Ramón Morelló[b], Martí Yebras[c], Rosa Solà[a,*]

[a] Unitat de Recerca en Lípids i Arteriosclerosi, CIBERDEM, Hospital Universitari Sant Joan, IISPV, Facultat de Medicina i Ciències de la Salut, Universitat Rovira i Virgili, Reus, Tarragona, Spain
[b] La Morella Nuts S.A., 43206 Castellvell del Camp, Tarragona, Spain
[c] Serveis Científics i Tècnics, Universitat Rovira i Virgili, Spain

ARTICLE INFO

Article history:
Received 22 December 2011
Received in revised form 8 May 2012
Accepted 9 May 2012

Keywords:
Lipopolysaccharide
THP-1
NF-κB
Tumor necrosis factor-α
Tumor necrosis factor-α converting enzyme

ABSTRACT

Background: Tumor necrosis factor-α (TNF-α) is involved in inflammatory responses in atherosclerosis. We propose an *in vitro* cellular assay to evaluate the anti-inflammatory mechanisms of potential modifiers such as food extracts. In the current model we assessed an anti-inflammatory effect of polyphenol-rich peanut extract in lipopolysaccharide (LPS)-induced THP-1 monocytes.
Methods: THP-1 monocytes were incubated with peanut extract (5, 25, 50 and 100 μg/mL) consisting of 39% flavonols, 37% flavanols and 24% phenolic acid (or BAY 11-7082 (5 μM) as experiment control) for 1 h and then stimulated with LPS (500 ng/mL) for 4 h. Cytotoxicity was measured as lactate dehydrogenase (LDH) activity release. NF-κB and MAPK family were determined by TransAm kit while TNF-α mRNA levels and its mRNA stability by RT-PCR. Intra- and extracellular TNF-α protein was measured by ELISA, and TNF-α converting enzyme (TACE) activity by a fluorimetric assay.
Results: Peanut extract inhibited the maximal LPS-induced extracellular TNF-α protein secretion by 18%, 29% and 47% at 25, 50 and 100 μg/mL, respectively ($P < 0.05$). LPS stimulation revealed that 85% of TNF-α was released extracellularly while 15% remained intracellular. Peanut extract did not modify NF-κB but, instead, reduced c-Jun transcription factor activity ($P < 0.05$), decreased TNF-α mRNA (albeit non-significantly) and had no effect on mRNA stability and TACE activity.
Conclusion: Polyphenol-rich peanut extract reduces extracellular TNF-α protein by inhibiting c-Jun transcription factor from MAPK family, suggesting an anti-inflammatory effect. The proposed THP-1 monocyte model could be used to assess food extract impact (site and size effects) on the inflammation pathway.

1. Introduction

Atherosclerosis is a complex inflammatory process involved in cardiovascular disease (CVD), the principal cause of morbidity and mortality in industrialized countries (Gerszten et al., 2011). Inflammation is characterized by the presence of monocytes/macrophages and T lymphocytes in the atheroma plaque (Ross, 1999). Monocytes promote atherosclerosis *via* production of various key mediators such as tumor necrosis factor-α (TNF-α). TNF-α is commonly found in atherosclerotic lesions contributing to the inflammatory process (Katsume et al., 2011). Concentrations of TNF-α are increased in patients with increased risk of atherosclerosis (Devaraj et al., 2002).

The mechanisms underlying the first part of the pro-inflammatory lipopolysaccharide (LPS)-induced TNF-α signaling pathway have been well described (Gee et al., 2002). The exposure of cells to LPS, which is a major component of the outer membrane of Gram-negative bacteria, triggers the binding of LPS to the LPS bearing protein (LBP) and is transferred to the CD14 at the cell surface. LPS then interacts with the signaling toll-like receptor 4 (TLR4) and the accessory protein MD-2. LPS stimulates the activation of various mitogen-activated protein kinase (MAPK) family pathways, including the extracellular signal-regulated kinase (ERK) 1 and 2, c-Jun N-terminal kinase (JNK), and p38 pathways. These pathways directly or indirectly phosphorylate and activate various transcription factors including Elk-1, c-Jun, c-Fos, ATF-1, ATF-2, SRF, and CREB. In addition, LPS activates the IKK pathway which

* Corresponding author at: Unitat de Recerca en Lípids i Arteriosclerosi, Hospital Universitari Sant Joan, IISPV, Facultat de Medicina i Ciències de la Salut, Universitat Rovira i Virgili, Sant Llorenç, 21, 43201 Reus, Tarragona, Spain.
Tel.: +34 977 75 93 69; fax: +34 977 75 93 22; mobile: +34 609 906 991.
E-mail address: rosa.sola@urv.cat (R. Solà).

0161-5890/$ – see front matter © 2012 Elsevier Ltd. All rights reserved.
http://dx.doi.org/10.1016/j.molimm.2012.05.007

in turn phosphorylates IkBs. Subsequent degradation of IkBs permits nuclear translocation of nuclear factor-κB (NF-κB) complexes such as p50/p65 (Guha and Mackman, 2001). The PI3K-Akt pathway phosphorylates and activates p65 *via* an unknown kinase. In the nucleus, activated transcription factors bind to recognition elements in the promoter regions of inflammatory and immune genes. These include pro-inflammatory cytokines, chemokines, inflammatory enzymes and adhesion molecules such as TNF-α (Barnes and Karin, 1997).

TNF-α is assembled intracellularly to form a trans-membrane protein which contains a cytoplasmic domain, a trans-membrane segment and an extracellular region. There are two forms of TNF-α: the full-length type II membrane-bound form, and the soluble form resulting from a proteolytic cleavage that releases the active C-terminal portion from the cell surface to the extracellular medium (Black, 2002). This proteolysis converts membrane bound "pro" form (pro-TNF-α) into its biologically active soluble form; sTNF-α (Ishisaka et al., 1999; Horiuchi et al., 2010). This proteolysis is supervised by a protease. TNF-α converting enzyme (TACE) also called ADAM17 (a disintegrin and metalloprotease) family of proteins possess α-secretase activity (Katakowski et al., 2007; Zheng et al., 2007). TNF-α can be cleaved by TACE to release a soluble, mature subunit (sTNF-α; 17 kDa) that becomes biologically active (Tang et al., 1996; Black et al., 1997; Chou et al., 2011; Ramana, 2010).

Although the mechanism of the LPS-induced TNF-α signaling pathway *via* MAPK and NF-κB activation has been well described in monocytes (Beutler, 2000; Witkamp and Monshouwer, 2000; Dayer et al., 2005), there is a gap in the knowledge of which molecules are involved, starting from the TNF-α mRNA expression and extending to the extracellular protein secretion of TNF-α. The first route of diversification of proteins is at the transcriptional level (by mRNA splicing and including tissue-specific alternate splicing, editing and stability (Subramaniam et al., 2011; Cheneval et al., 2010)). The second route to proteome expansion is the post-translational modification (PTM) of proteins at one or more sites (Walsh et al., 2005). Therefore, NF-κB and MAPK family needs to be evaluated more thoroughly so that the inflammatory route that follows TNF-α in atherogenic inflammation may be better understood. Targeting the proximal triggers such as TNF-α would be the more promising strategy for interrupting inflammation in atherogenesis (Ishisaka et al., 1999).

Further, BAY 11-7082 ((E)3-[(4-methylphenyl)sulfonyl]-2-propenenitrile; BAY) is a synthetic molecule that has demonstrated anti-inflammatory activity by inhibiting the NF-κB and MAPK pathway that can be used as control product in comparing the anti-inflammatory effects of test molecules (Guha and Mackman, 2001; Barnes and Karin, 1997; Black, 2002). However, the effect of BAY on TACE activity on monocyte THP-1 cells has not been evaluated, to date.

Some natural extracts (or compounds) of certain foods have anti-inflammatory properties and *in vitro* cellular models can be used to screen for biological activity (Singh et al., 2005). When a natural extract or compound shows anti-inflammatory effects, the different mechanism of action ought to be explored systematically in the same cell model so as to improve the methodological reliability (Essafi-Benkhadir et al., 2012). Dried fruits, for example, are rich in polyphenols and exert beneficial effects on inflammation (Calixto et al., 2003; Kris-Etherton et al., 2002; Ortega, 2006) and, as a result, decrease CVD progression (Kris-Etherton et al., 2002).

There have been many studies published on the harmful effects of peanuts, such as the allergy promoted by this natural extract (Schulz et al., 2011; Moverare et al., 2011; Chen et al., 2011). However, there is a paucity of studies addressing its potential beneficial effect on atherosclerosis resulting from its anti-inflammatory activity. Therefore, we hypothesized that peanut extract, known to have a high polyphenol content, exerts an anti-inflammatory effect. Our aims in the present set of experiments were to evaluate the mechanism of action of peanut extract by studying the different steps in TNF-α formation (NF-κB and MAPK family, TNF-α mRNA expression, TNF-α mRNA stability, TACE activity and the amounts of TNF-α protein including intra- and extracellular protein). We assessed these steps in a cell culture model of LPS-induced THP-1 monocytes using BAY as an internal control in every step of the TNF-α pathway being evaluated.

2. Materials and methods

2.1. Reagents

LPS (*Escherichia coli* O55:B5), dimethyl sulfoxide (DMSO) and actinomycin D from *Streptomyces sp.* were obtained from Sigma–Aldrich (Madrid, Spain). Ethanol was obtained from Panreac (Barcelona, Spain). Phosphate-buffered saline (PBS) was purchased from Gibco (Barcelona, Spain). Radio-immunoprecipitation assay lysis buffer (RIPA) was generated using the following base ingredients (50 mM Tris–HCl, pH 7.52; 150 mM NaCl; 0.1% SDS; 1% Nonidet; 0.5% sodium deoxycholic acid) and complete protease inhibitor cocktail (CPIC; Roche Applied Science, Valencia, Spain). To preempt cytotoxicity, ethanol and DMSO concentrations never exceeded 0.1% (v/v) in culture media. Acetone and hexane were purchased from JT Baker (Tarragona, Spain).

2.2. Peanut extract preparation and composition

Peanut extract was kindly supplied by La Morella Nuts (Castellvell del Camp, Tarragona, Spain). The process of extraction was according to the method of Ortega et al. (2008) and Monagas et al. (2007). Briefly, the extract was obtained from the skins of roasted peanuts. The peanut skins were ground in a laboratory mill and freeze-dried before extraction with phenol. To achieve maximum extraction efficiency, the raw material was first defatted with hexane (ratio of 1:10; W_{skin}:V_{hexane}) for 15 min in an ultrasound sonicator (Selecta, Tarragona, Spain) containing ice to avoid warming. The defatted skins were then extracted thrice with hexane, and filtered. The organic solvent was removed by rotary evaporation (Büchi R-210, Tarragona, Spain) under partial vacuum. The phenolic extract was obtained by treating the defatted skin with a solution of acetone in MilliQ water (1:1, v/v) in a ratio 1:10 (W_{skin}/V_{sol}). Initially, a soaking process is needed with manual mixing. The extraction process proceeds in an ultrasound sonicator with ice to avoid warming. The extracting solvent is removed by vacuum filtration and the partially extracted skins are extracted three more times with the same extracting solution. The phenolic extracted fraction is obtained after removing the acetone solvent by rotary evaporation under partial vacuum. Finally, the aqueous extract is freeze-dried in a lyophilizer (Cryodos Telstar, Tarragona, Spain) to obtain the peanut extract to be used in the experiments described.

The bioactive peanut extract phenolic profile is 39% flavonols, 37% flavanols and 24% phenolic acids, dissolved in 3.75% DMSO.

2.3. Cell culture

The THP-1 human monocyte cell line, derived from peripheral blood of a 1 year old male with acute monocytic leukemia, was purchased from *Deutsche Sammlung von Mikroorganismen und Zellkulturen GmbH* (DSMZ; Braunschweig, Germany). The THP-1 cell line, rather than human monocytes, was used so as to minimize inter- and intra-experiment variability.

THP-1 cells were routinely cultured in a humidified incubator containing 5% CO_2 and 95% O_2 at 37 °C using RPMI medium

1640 + Glutamax-I (Gibco, Spain) supplemented with 20% of heat-inactivated fetal bovine serum (FBS; PAA, Labclinics; Barcelona, Spain) for the two first days followed by 10% FBS + 100 U/mL penicillin and 100 mg/mL streptomycin for further growth and experiments.

Dose-effect and time-response experiments with LPS, BAY and peanut extract were standardized in the course of establishing final experimental conditions. For example, THP-1 cells were plated at a density of 5×10^5 cells/mL for every experiment conducted, while 1×10^6 cells/mL was the cell density used for the determination of NF-κB and MAPK family.

Subsequently, THP-1 cells were pre-incubated with peanut extract (5, 25, 50 and 100 μg/mL), BAY (5 μM) and/or the vehicle control (3.75% of DMSO) for 1 h, depending on the study requirements. After 1 h, LPS (500 ng/mL) was added for 4 h (for most experiments) or 1 h (for NF-κB and MAPK family) or 2 h (for TNF-α mRNA stability) to the cell culture medium to induce cell stimulation. Finally, supernatants were isolated and stored at −20 °C for batched analyses to detect extracellular TNF-α protein, and to measure the activity of lactate dehydrogenase (LDH) release. Cell extracts were lysed in each experiment and stored at −80 °C for batched measurement of NF-κB, MAPK family, TNF-α mRNA expression and its mRNA stability, intracellular TNF-α protein, and TACE activity.

2.4. Cytotoxicity

A colorimetric assay to measure the activity of LDH release (the LDH Cytotoxicity Detection Kit; Roche Applied Science, Mannheim, Germany) was used to determine cell cytotoxicity. Briefly, LDH is rapidly released into the cell-culture supernatant when the plasma membrane is damaged, and this provides an index of cellular cytotoxicity. LPS treatment was taken as the maximum stress status for the cells, and possible cytotoxicity.

The control culture medium (RPMI-1640 + 10% FBS + LDH released from cells) has high OD at 492 nm and is useful as an internal control. Results are expressed as mean optical density (OD) and standard deviation (SD) of the LDH absorbance produced by the cells under each of the treatment conditions.

2.5. NF-κB (p65) and MAPK family transcription factor assay

Activation of NF-κB (p65) and MAPK family from nuclear extracts was measured using the TransAm® NF-κB and MAPK family kit, respectively (Active Motif, Carlsbad, CA). Briefly, this is an enzyme linked immuno-sorbent assay (ELISA)-based assay during which, when nuclear or whole-cell extract is added, the activated transcription factor-of-interest binds the oligonucleotide at its consensus binding site and is quantified using the linked antibody which is specific for the active form of the transcription factor being studied. The NF-κB and MAPK family detection was according to the manufacture's instructions. THP-1 at different concentrations (5, 25 and 100 μg/mL) or BAY (5 μM) were incubated with peanut extract for 1 h and, then, the cells were stimulated with LPS (500 ng/mL) for a further 1 h.

Results were expressed as percentage (SD) of NF-κB or OD (SD) of MAPK family activity under each treatment condition.

2.6. Analysis of mRNA expression by RT-PCR

Messenger RNA (mRNA) of TNF-α was measured by reverse transcription-polymerase chain reaction (RT-PCR) after total RNA had been isolated from cells. Cells were lysed with nucleic acid purification lysis solution and total RNA was isolated from cells using the ABI PRISM 6100 Nucleic Acid PrepStation extraction system (Applied Biosystems, Foster City, USA) following the manufacture's protocol. Total RNA was quantified using Quant-it™ RNA Assay Kit. Using 2720 Thermal Cycler (Applied Biosystems, Foster City, USA), 0.5 μg of total RNA was reverse transcribed to cDNA at 42 °C for 50 min, using Random Hexamers, SuperScript II reverse transcriptase and RNAse Out according to the manufacturer's protocol. To determine the amount of TNF-α mRNA, quantitative real-time PCR was performed using the ABI PRISM® 7900HT Sequence Detection System (Applied Biosystems, Foster City, USA) with the following profile: 95 °C denaturing (20 s), 40 cycles of extension at 95 °C (1 s), and 60 °C (20 s). TNF-α gene expression results were reported as increase/decrease using $2^{-\Delta\Delta Ct}$ mathematical method, using glyceraldehyde 3-phosphate dehydrogenase (GAPDH) as housekeeping gene to normalize the results. The LPS-activated monocytes (500 ng/mL) were defined as the calibrator in these experiments, setting its value at 1 and the other conditions in relation to it. The expression of TNF-α mRNA in cultured THP-1 cells was determined with and without LPS stimulation. We had previously examined the effects of BAY on the release of TNF-α, which is under NF-κB transcriptional control (Magness et al., 2004), together with peanut extract whose synthesis is unknown. Thus, the anti-inflammatory effect of the natural compound tested (peanut extract, in the present study) was the reduction of TNF-α mRNA of the cells incubated with the extract compared to the activation with LPS alone. Results were expressed as mean (SD) of TNF-α mRNA change compared to LPS alone.

2.7. Stability of TNF-α mRNA

Actinomycin D (Act D) is a polypeptide antibiotic isolated from *Streptomyces sp* bacteria. Act D is used as a transcription inhibitor because its intercalation into DNA produces a physical obstruction to RNA polymerase transcription, and inhibits the elongation of RNA chains (Koba and Konopa, 2005). Half-life/stability of TNF-α mRNA was measured after all experimental incubations of monocytes, mentioned above. After 2 h of incubation with LPS, Act D (5 μg/mL) was added to the medium. Incubation times with Act D were 30, 60, 120 and 180 min. At these times, the cells were lysed to obtain total RNA. Results were expressed as mean (SD) of TNF-α mRNA change compared to time 0 min for each experimental condition.

2.8. Determination of total TNF-α protein concentration

Total TNF-α protein concentration (extra- and intracellular) was determined. According to Black (2002) and Ishisaka et al. (1999), the total TNF-α protein is the sum of extracellular TNF-α (soluble) plus intracellular TNF-α (cytoplasmic plus trans-membrane) protein.

Extra- and intracellular TNF-α proteins were measured using human TNF-α ELISA kit (R&D Systems, Spain); the reported sensitivity of which was 5.5 pg/mL. Results were expressed as mean (SD) pg/mL/10^6 cells.

2.9. Detection and quantification of extracellular TNF-α

Supernatants of the experimental cell cultures were used to measure the extracellular TNF-α protein secretion. To determine the anti-inflammatory effect, the percentage reduction of TNF-α protein release is measured as the extracellular level because the biologically active form of TNF-α is the soluble form *i.e.* which exerts an effect in the organism. Thus, the anti-inflammatory effect of the natural compound tested (in the present case that of peanut extract) was the difference between the levels of extracellular TNF-α protein secretion of those cells incubated with the extract, compared to the levels from LPS activation alone.

2.10. Detection and quantification of intracellular TNF-α

THP-1 cells were washed twice with phosphate buffered saline (PBS) (Jang et al., 2006), then ice-cold modified RIPA lysis buffer (50 μL/10^6 cells, as described above) was added to lyse the cells. The insoluble material was removed by centrifugation at 16,000 × *g* at 4 °C for 10 min (Hu and Zhu, 2007; Oda et al., 2006). The amounts of cytokine in cell lysate were measured as pg/mL produced from 10^6 cells.

2.11. TACE (α-secretase) activity assay

TACE activity from cell lysates (including cytoplasmic and trans-membrane) was determined by the SensoLyte® 520 TACE (α-secretase) Fluorimetric Activity Assay Kit (Anaspec, Fremont, CA, USA) under varying culture conditions. Cells were harvested and lysed using the assay buffer (containing 0.1%, v/v Triton-X 100) provided by the manufacturer. Protein content of cell lysate (cytoplasmic and trans-membrane) was determined using the Bradford protein assay. The kit was used according to the manufacturer's protocol. Fluorescence of the cleavage product was measured in a fluorescence microplate reader using Synergy HT Fluorimeter (BioTek Instruments, Alcobendas, Madrid, Spain), with excitation wavelength set at 490 nm and emission wavelength at 520 nm.

Results were expressed as mean (SD) relative fluorescence units (RFU) produced from TACE activity.

2.12. Statistical analyses

Two independent experiments were performed on different days. Samples were run in triplicate, and the data were pooled for each experiment. A total of six replicates were obtained for each experimental condition. All the results were analyzed with the Statistical Package for the Social Sciences (SPSS) software (version 19.0).

Descriptive statistics (means and standard deviation) and analytical statistics (ANOVA and Bonferroni tests) were used to assess dose-response effects. Statistical significance was set at $P < 0.05$.

The measurement of quality was precision repeatability (within-assay) and reproducibility (between-assay) as measured by standard deviation (SD), coefficient of variation (CV) and standard error of the mean (SEM).

3. Results

3.1. Cytotoxicity measurements

Cytotoxicity assay of the peanut extract (5, 25, 50 and 100 μg/mL), measured as the activity of LDH release showed no difference compared to the LPS treatment alone, confirming that the peanut extract is not cytotoxic at the concentrations tested. No cytotoxicity was detected for LPS and BAY (data not shown).

3.2. Effect of peanut extract on NF-κB

The p65-NF-κB activation showed that LPS increased the activity 8-fold compared to vehicle control (3.75% DMSO) demonstrating a good stimulation of the cells ($P < 0.05$). BAY, used as experimental control, decreased the stimulation 4-fold ($P < 0.05$). Peanut extract at the concentrations tested (5, 25 and 100 μg/mL) showed no significant difference in p65-NF-κB activation compared to LPS alone (Fig. 1).

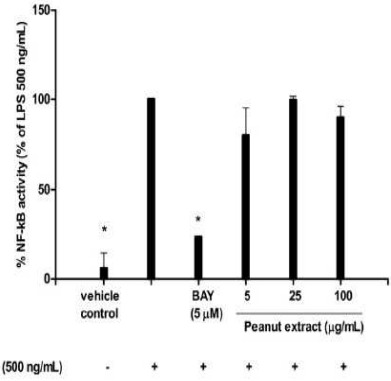

Fig. 1. Effect of peanut extract on NF-κB. THP-1 monocytes were incubated with vehicle control (3.75% DMSO), BAY 11-7082 (5 μM) and peanut extract (5, 25 and 100 μg/mL) for 1 h and stimulated with LPS (500 ng/mL) for 1 h. NF-κB binding was measured using an ELISA kit (TransAM®). Data are expressed as percentage LPS values of two separate experiments run in triplicate. Error bars show SD. *$P < 0.05$ *versus* LPS.

3.3. Effect of peanut extract on MAPK family

The transcription factors ATF-2, c-Myc, STAT1 and MEF2 did not show any significant differences at any peanut extract concentration tested (5, 25 and 100 μM). However BAY (5 μM) reduced MEF2 compared to LPS, albeit non-significantly. c-Jun transcription factor was reduced by BAY (5 μM) by 86% and peanut extract (25 and 100 μM) by 54% and 93%, respectively ($P < 0.05$) (Fig. 2).

3.4. Effect of peanut extract on TNF-α mRNA in THP-1 cells using RT-PCR assay

LPS (500 ng/mL) stimulated TNF-α mRNA production 7-fold compared to vehicle control (3.75% DMSO) in THP-1 ($P < 0.05$). BAY (5 μM) decreased LPS (500 ng/mL) stimulation 2-fold ($P < 0.05$).

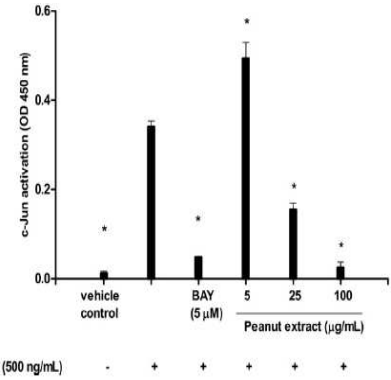

Fig. 2. Effect of peanut extract on c-Jun. THP-1 monocytes were incubated with vehicle control (3.75% DMSO), BAY 11-7082 (5 μM) and peanut extract (5, 25 and 100 μg/mL) for 1 h and stimulated with LPS (500 ng/mL) for 1 h. c-Jun binding was measured using an ELISA kit (TransAM®). Data are expressed as optical density (OD) at 450 nm. Error bars show SD. *$P < 0.05$ *versus* LPS.

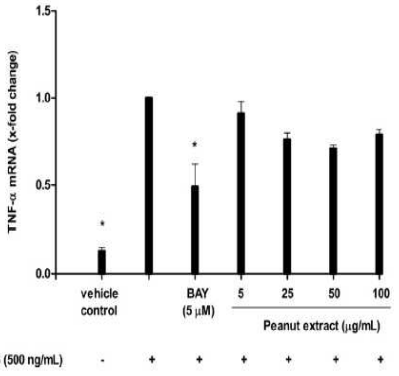

Fig. 3. Effect of peanut extract on TNF-α mRNA in THP-1 cells using RT-PCR assay. THP-1 monocytes were incubated with vehicle control (3.75% DMSO), BAY 11-7082 (5 μM) and peanut extract (5, 25, 50 and 100 μg/mL) for 1 h and stimulated with LPS (500 ng/mL) for 4 h. The abundance of mRNA transcripts for TNF-α was determined using real time quantitative polymerase chain reaction (RT-PCR). Data were normalized using the values obtained for GAPDH (house keeping gene), and are the mean of two separate experiments run in triplicate. Error bars show SD. $^{*}P<0.05$ *versus* LPS.

TNF-α mRNA expression at all concentrations tested (5, 25, 50 and 100 μg/mL) showed reductions albeit statistically non-significant, of 9%, 24%, 29% and 21%, respectively compared to LPS alone (Fig. 3).

3.5. Effect of peanut extract on TNF-α mRNA stability in THP-1 cells using RT-PCR assay

Under vehicle control condition (3.75% DMSO), TNF-α mRNA levels fell significantly ($P<0.05$) relative to the starting point (time 0 min) of the kinetic measurements. The decline under the other test conditions (LPS, BAY and peanut extract) was progressive over the first 30 min, compared time 0 min. At 30 min LPS, BAY and peanut extract decreased to the minimum TNF-α mRNA level as that measured in the vehicle control. There were no significant differences between LPS, BAY and peanut extract compared to vehicle control at any of the time points *i.e.* peanut extract did not stabilize TNF-α mRNA (Fig. 4).

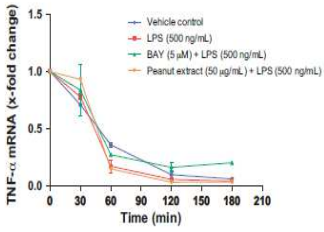

Fig. 4. Effect of peanut extract on TNF-α mRNA stabilization in THP-1 cells using RT-PCR assay. THP-1 monocytes were incubated with vehicle control (3.75% DMSO), BAY 11-7082 (5 μM) and peanut extract (50 μg/mL) for 1 h and stimulated with LPS (500 ng/mL) for 2 h. After 2 h of incubation of LPS, Act D 5 μg/mL was added to medium. The incubation times with Act D were 30, 60, 120 and 180 min. At these times the cells were lysed to obtain total RNA. The abundance of mRNA transcripts for TNF-α was determined using real time quantitative polymerase chain reaction (RT-PCR). Data were normalized using the values obtained from GAPDH (house keeping gene), and are the mean of two separate experiments run in triplicate. Error bars show SD. $^{*}P<0.05$ *versus* vehicle control.

3.6. Effect of peanut extract on TNF-α protein secretion

In monocyte THP-1 cells, maximum stimulation of TNF-α at LPS concentration of 500 ng/mL and 4 h incubation in the absence of peanut extract revealed that approximately 85% of the TNF-α release was extracellular, while 15% remained inside the cell (Fig. 5A and B). The results for extra-, intracellular, and total TNF-α release in THP-1 cells pre-treated with peanut extract (5, 25, 50 and 100 μg/mL) are shown in Fig. 5.

3.7. Extracellular TNF-α protein

BAY (5 μM) decreased LPS-stimulated (500 ng/mL) extracellular TNF-α protein nearly 3-fold ($P<0.05$).

Peanut extract inhibited the secretion of extracellular TNF-α protein secretion by 18% and 29% at 25 and 50 μg/mL, respectively; but only 47% of extracellular TNF-α protein reduction at 100 μg/mL was statistically significant ($P<0.05$) compared with LPS alone (Fig. 5A).

3.8. Intracellular TNF-α protein

The concentration of the remaining intracellular TNF-α protein was very low compared to he extracellular component (Fig. 5B), suggesting that most of the TNF-α protein was secreted to the extracellular medium when cells are incubated for 1 h with the peanut extract following 4 h stimulation by LPS (500 ng/mL).

3.9. Total TNF-α protein

Peanut extract concentrations (5, 25, 50 and 100 μg/mL) induced a decrease in total TNF-α protein secretion; the reductions were 15%, 23% and 30% at 25, 50 and 100 μg/mL respectively albeit the reductions were not statistically significant (Fig. 5C). The results of total TNF-α protein secretion are similar to that observed with extracellular TNF-α protein.

BAY (5 μM) decreased 3-fold the total TNF-α protein concentration induced by LPS (500 ng/mL) stimulation ($P<0.05$).

The same tendency was observed for peanut extract on TNF-α mRNA (Fig. 3) and on total and extracellular TNF-α protein secretion (Fig. 5A and C); albeit the decrease in TNF-α mRNA expression was not statistically significant.

3.10. Effect of peanut extract on TACE activity

Basal TACE activity in THP-1 cells was detectable under all cell conditions tested. BAY (5 μM) significantly ($P<0.05$) reduced the basal activity of TACE, while peanut extract (5, 25, 50 and 100 μg/mL) did not modify the TACE basal activity.

TACE activity was not sensitive to LPS (500 ng/mL), indicating a failure of LPS to stimulate any TACE catalytic activity response in THP-1 cells (Fig. 6).

4. Discussion

The present study confirms our hypothesis that peanut extract (at 100 μg/mL) exerts an anti-inflammatory effect, in THP-1 monocytes challenged with LPS, by reducing the secretion of the biologically active soluble form of extracellular TNF-α protein.

Further, we propose a standardized *in vitro* monocyte cellular assay (from signal transduction to extracellular secretion of TNF-α) which can be used to evaluate anti-inflammatory mechanisms of such products such as food extracts and synthetic compounds.

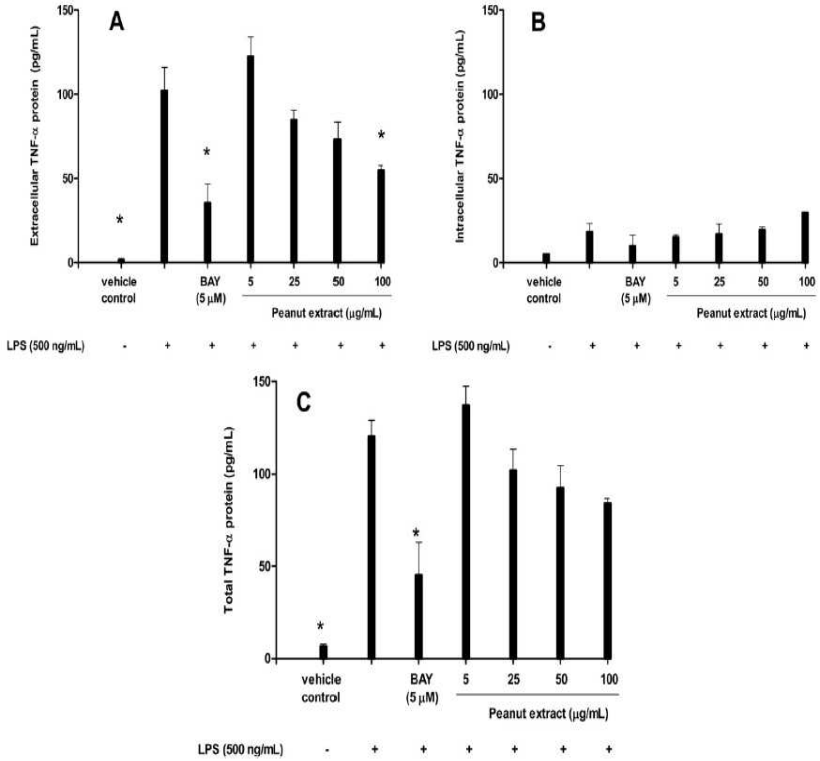

Fig. 5. Effect of peanut extract on TNF-α protein secretion. THP-1 monocytes were incubated with vehicle control (3.75% DMSO), BAY 11-7082 (5 μM) and peanut extract (5, 25, 50 and 100 μg/mL) for 1 h and stimulated with LPS (500 ng/mL) for 4 h. TNF-α protein secretion was determined by ELISA. Data are the mean of two separate experiments run in triplicate. Error bars show SD. (A) Extracellular TNF-α protein secretion. $^{*}P < 0.05$ *versus* LPS; (B) intracellular TNF-α protein secretion; (C) total TNF-α protein secretion. $^{*}P < 0.05$ *versus* LPS.

The present study demonstrated that the synthetic compound BAY, used as experiment control, can reduce the TNF-α protein secretion by inhibiting, specifically, NF-κB transcription factor and the subsequent steps of the TNF-α production *i.e. via* TNF-α mRNA intra- and extracellular and total TNF-α protein. However, BAY (5 μM) had no effect on the mRNA stability of TNF-α.

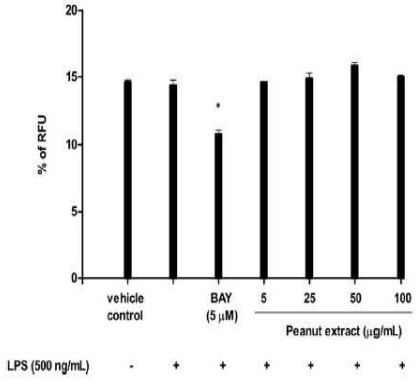

Fig. 6. Effect of peanut extract on TACE activity. THP-1 monocytes incubated with vehicle control (3.75% DMSO), BAY 11-7082 (5 μM) and peanut extract (5, 25, 50 and 100 μg/mL) for 1 h and stimulated with LPS (500 ng/mL) for 4 h. TACE activity was determined by a fluorimetric assay (see text for details). Data are the mean of two separate experiments run in triplicate. Error bars show SD. $^{*}P < 0.05$ *versus* LPS.

With the MAPK family, we observed an alternative effect of BAY by reducing the activities of MEF2 and c-Jun transcription factor. Inhibition of c-Jun by BAY has been demonstrated by some investigators such as Lee et al. (2010). However, to the best of our knowledge, the inhibition of MEF2 by BAY has not, until now, been observed. We suggest that the reduction of TNF-α produced by BAY is *via* the inhibition of both transcription factor pathways: the NF-κB and the MAPK family. We also demonstrated that BAY (5 μM) has the ability to reduce the basal TACE activity in THP-1 monocytes which, to the best of our knowledge, has not been documented in the literature, to date. Thus, BAY can be used as an experiment control for the *in vitro* THP-1 monocyte model. The model is appropriate for detecting anti-inflammatory effects and, as such, may be applicable in assessing a range of natural food extracts that are considered to have beneficial anti-inflammatory properties.

Peanut extract, at all concentrations tested in this study, had no effect on NF-κB nuclear transcription factor, compared to LPS alone. Our results showed that the mechanism of action of peanut extract is *via* the inhibition of the transcription factor c-Jun from MAPK family. This inhibition of c-Jun by peanut extract was significant at 25 and 100 μg/mL concentration. Subsequently, we observed that peanut extract slightly decreased (but not statistically significantly) TNF-α mRNA. Stabilization of mRNA by peanut extract was not observed. Peanut extract (100 μg/mL) induced a reduction of the TNF-α soluble active form and extracellular TNF-α protein, and

exerted a final anti-inflammatory effect at the end of the pathway. The intracellular TNF-α protein concentration reflects both the cytoplasmic domain and the trans-membrane segment of TNF-α protein. The mechanism linking the disruption of the pathway with the extracellular region that contains the soluble biological form (Ishisaka et al., 1999) needs to be elucidated further.

A mechanism that needs to be taken into account is the enzyme that produces the soluble TNF-α protein in the culture medium *i.e.* the TACE enzyme. It is a member of the disintegrin and metalloprotease (the ADAM family) which cleaves various trans-membrane proteins within their "stalk" sequences, releasing ("shedding") a soluble form including the functional extracellular domains (Black, 2002). In this study, we showed that LPS (500 ng/mL) stimulation alone of THP-1 cells has no effect on TACE activity. This suggests that the basal level of TACE activity present in THP-1 cells may be sufficient for the release of TNF-α from LPS-stimulated cells (15% of RFU) or that LPS shedding *per se* may not be activated in the case of LPS-induced TNF-α release (Doedens and Black, 2000). Although some groups of investigators have provided evidence for stimulation of TACE mRNA transcription, protein content, and catalytic activity by LPS, others have not (Rozenova et al., 2010; Ermert et al., 2003; Armstrong et al., 2006; Doedens et al., 2003). Our results demonstrated that peanut extract, at any of the concentrations tested (5, 25, 50 and 100 μg/mL), did not affect TACE activity while, conversely, reduction in activity is sensitive to BAY.

The data from the present study suggest that, in the model of human monocytic THP-1 cells stimulated with LPS, extracellular TNF-α protein is inhibited by peanut extract.

The anti-inflammatory model we present in this article could become a gold standard since the markers of quality of analysis such as precision (mean of 10% and 20% intra- and inter-assay CV, respectively) and accuracy will become reference parameters in comparing future models of inflammation. As such, the model can be used not only in basic research but also in the assessment of additives (food fortification) and other outcomes in the food industry.

In conclusion, a reduction in the secretion of the extracellular TNF-α protein indicates an anti-inflammatory effect of the test compound. Polyphenol-rich peanut extract reduces TNF-α by inhibiting c-Jun transcription factor from the MAPK family, but not from the NF-κB pathway; a mechanism of action not previously demonstrated. The value of the proposed *in vitro* THP-1 monocyte model is that it is effective in evaluating underlying mechanisms (site and size effects) of various compounds such as food extracts that are considered to have beneficial anti-inflammatory properties.

Acknowledgments

This work was supported by the Spanish Ministry of Science and Innovation (CENIT projects MET-DEV-FUN) led by La Morella Nuts (Castellvell del Camp, Tarragona, Spain).

References

Gerszten, R.E., Asnani, A., Carr, S.A., 2011. Status and prospects for discovery and verification of new biomarkers of cardiovascular disease by proteomics. Circulation Research 109, 463–474.
Ross, R., 1999. Atherosclerosis – an inflammatory disease. New England Journal of Medicine 340, 115–126.
Katsume, A., Okigaki, M., Matsui, A., Che, J., Adachi, Y., Kishita, E., et al., 2011. Early inflammatory reactions in atherosclerosis are induced by proline-rich tyrosine kinase/reactive oxygen species-mediated release of tumor necrosis factor-alpha and subsequent activation of the p21Cip1/Ets-1/p300 system. Arteriosclerosis, Thrombosis, and Vascular Biology 31, 1084–1092.
Devaraj, S., Harris, A., Jialal, I., 2002. Modulation of monocyte–macrophage function with alpha-tocopherol: implications for atherosclerosis. Nutrition Reviews 60, 8–14.
Gee, K., Lim, W., Ma, W., Nandan, D., Diaz-Mitoma, F., Kozlowski, M., et al., 2002. Differential regulation of CD44 expression by lipopolysaccharide (LPS) and TNF-alpha in human monocytic cells: distinct involvement of c-Jun N-terminal kinase in LPS-induced CD44 expression. Journal of Immunology 169, 5660–5672.
Guha, M., Mackman, N., 2001. LPS induction of gene expression in human monocytes. Cellular Signalling 13, 85–94.
Barnes, P.J., Karin, M., 1997. Nuclear factor-κB: a pivotal transcription factor in chronic inflammatory diseases. New England Journal of Medicine 336, 1066–1071.
Black, R.A., 2002. Tumor necrosis factor-alpha converting enzyme. International Journal of Biochemistry and Cell Biology 34, 1–5.
Ishisaka, R., Sato, N., Tanaka, K., Takeshige, T., Iwata, H., Klostergaard, J., et al., 1999. A part of the transmembrane domain of pro-TNF can function as a cleavable signal sequence that generates a biologically active secretory form of TNF. Journal of Biochemistry 126, 413–420.
Horiuchi, T., Mitoma, H., Harashima, S., Tsukamoto, H., Shimoda, T., 2010. Transmembrane TNF-alpha: structure, function and interaction with anti-TNF agents. Rheumatology 49, 1215–1228.
Katakowski, M., Chen, J., Zhang, Z.G., Santra, M., Wang, Y., Chopp, M., 2007. Stroke-induced subventricular zone proliferation is promoted by tumor necrosis factor-alpha-converting enzyme protease activity. Journal of Cerebral Blood Flow and Metabolism 27, 669–678.
Zheng, X., Jiang, F., Katakowski, M., Kalkanis, S.N., Hong, X., Zhang, X., et al., 2007. Inhibition of ADAM17 reduces hypoxia-induced brain tumor cell invasiveness. Cancer Science 98, 674–684.
Tang, P., Hung, M.C., Klostergaard, J., 1996. Human pro-tumor necrosis factor is a homotrimer. Biochemistry 35, 8216–8225.
Black, R.A., Rauch, C.T., Kozlosky, C.J., Peschon, J.J., Slack, J.L., Wolfson, M.F., et al., 1997. A metalloproteinase disintegrin that releases tumour-necrosis factor-alpha from cells. Nature 385, 729–733.
Chou, Y.C., Sheu, J.R., Chung, C.L., Hsiao, C.J., Hsueh, P.J., Hsiao, G., 2011. Hypertonicity-enhanced TNF-alpha release from activated human monocytic THP-1 cells requires ERK activation. Biochimica et Biophysica Acta 1810, 475–484.
Ramana, K.V., 2010. Tumor necrosis factor-alpha converting enzyme: implications for ocular inflammatory diseases. International Journal of Biochemistry and Cell Biology 42, 1076–1079.
Beutler, B., 2000. Tlr4: central component of the sole mammalian LPS sensor. Current Opinion in Immunology 12, 20–26.
Witkamp, R., Monshouwer, M., 2000. Signal transduction in inflammatory processes, current and future therapeutic targets: a mini review. Veterinary Quarterly 22, 11–16.
Dayer, J.M., Molnarfi, N., Burger, D., 2005. From cellular receptors to transduction-transcription pathways for cytokines: at which level should the inhibition be targeted in inflammation? Expert Opinion on Biological Therapy 5 (Suppl. 1), S83–S96.
Subramaniam, D., Ramalingam, S., Linehan, D.C., Dieckgraefe, B.K., Postier, R.G., Houchen, C.W., et al., 2011. RNA binding protein CUGBP2/CELF2 mediates curcumin-induced mitotic catastrophe of pancreatic cancer cells. PLoS One 6, e16958.
Cheneval, D., Kastelic, T., Fuerst, P., Parker, C.N., 2010. A review of methods to monitor the modulation of mRNA stability: a novel approach to drug discovery and therapeutic intervention. Journal of Biomolecular Screening 15, 609–622.
Walsh, C.T., Garneau-Tsodikova, S., Gatto Jr., G.J., 2005. Protein posttranslational modifications: the chemistry of proteome diversifications. Angewandte Chemie International Edition (in English) 44, 7342–7372.
Singh, U., Tabibian, J., Venugopal, S.K., Devaraj, S., Jialal, I., 2005. Development of an in vitro screening assay to test the antiinflammatory properties of dietary supplements and pharmacologic agents. Clinical Chemistry 51, 2252–2256.
Essafi-Benkhadir, K., Refai, A., Riahi, I., Fattouch, S., Karoui, H., Quince, Essafi M., 2012. (Cydonia oblonga Miller) peel polyphenols modulate LPS-induced inflammation in human THP-1-derived macrophages through NF-κB, p38MAPK and Akt inhibition. Biochemical and Biophysical Research Communications.
Calixto, J.B., Otuki, M.F., Santos, A.R., 2003. Anti-inflammatory compounds of plant origin. Part I. Action on arachidonic acid pathway, nitric oxide and nuclear factor κB (NF-κB). Planta Medica 69, 973–983.
Kris-Etherton, P.M., Hecker, K.D., Bonanome, A., Coval, S.M., Binkoski, A.E., Hilpert, K.F., et al., 2002. Bioactive compounds in foods: their role in the prevention of cardiovascular disease and cancer. American Journal of Medicine 113 (Suppl. 9B), 71S–88S.
Ortega, R.M., 2006. Importance of functional foods in the Mediterranean diet. Public Health Nutrition 9, 1136–1140.
Schulz, V.J., Smit, J.J., Willemsen, K.J., Fiechter, D., Hassing, I., Bleumink, R., et al., 2011. Activation of the aryl hydrocarbon receptor suppresses sensitization in a mouse peanut allergy model. Toxicological Sciences.
Moverare, R., Ahlstedt, S., Bengtsson, U., Borres, M.P., van Hage, M., Poorafshar, M., et al., 2011. Evaluation of IgE antibodies to recombinant peanut allergens in patients with reported reactions to peanut. International Archives of Allergy and Immunology 156, 282–290.
Chen, X., Zhuang, Y., Wang, Q., Moutsoglou, D., Ruiz, G., Yen, S.E., et al., 2011. Analysis of the effector activity of Ara h 2 and Ara h 6 by selective depletion from a crude peanut extract. Journal of Immunological Methods.
Ortega, N., Romero, M.P., Macia, A., Reguant, J., Angles, N., Morello, J.R., et al., 2008. Obtention and characterization of phenolic extracts from different cocoa sources. Journal of Agricultural and Food Chemistry 56, 9621–9627.

Monagas, M., Garrido, I., Lebron-Aguilar, R., Bartolome, B., Gomez-Cordoves, C., 2007. Almond (*Prunus dulcis* (Mill.) D.A. Webb) skins as a potential source of bioactive polyphenols. Journal of Agricultural and Food Chemistry 55, 8498–8507.
Magness, S.T., Jijon, H., Van Houten Fisher, N., Sharpless, N.E., Brenner, D.A., Jobin, C., 2004. In vivo pattern of lipopolysaccharide and anti-CD3-induced NF-κ B activation using a novel gene-targeted enhanced GFP reporter gene mouse. Journal of Immunology 173, 1561–1570.
Koba, M., Konopa, J., 2005. Actinomycin D and its mechanisms of action. Postepy Higieny i Medycyny Doswiadczalnej 59, 290–298 (Online).
Jang, C.H., Choi, J.H., Byun, M.S., Jue, D.M., 2006. Chloroquine inhibits production of TNF-alpha, IL-1beta and IL-6 from lipopolysaccharide-stimulated human monocytes/macrophages by different modes. Rheumatology 45, 703–710.
Hu, J.H., Zhu, X.Z., 2007. Rotenone-induced neurotoxicity of THP-1 cells requires production of reactive oxygen species and activation of phosphatidylinositol 3-kinase. Brain Research 1153, 12–19.
Oda, T., Hirota, K., Nishi, K., Takabuchi, S., Oda, S., Yamada, H., et al., 2006. Activation of hypoxia-inducible factor 1 during macrophage differentiation. American Journal of Physiology: Cell Physiology 291, C104–C113.
Lee, H.S., Kim, S.D., Lee, W.M., Endale, M., Kamruzzaman, S.M., Oh, W.J., et al., 2010. A noble function of BAY 11-7082: inhibition of platelet aggregation mediated by an elevated cAMP-induced VASP, and decreased ERK2/JNK1 phosphorylations. European Journal of Pharmacology 627, 85–91.
Doedens, J.R., Black, R.A., 2000. Stimulation-induced down-regulation of tumor necrosis factor-alpha converting enzyme. Journal of Biological Chemistry 275, 14598–14607.
Rozenova, K.A., Deevska, G.M., Karakashian, A.A., Nikolova-Karakashian, M.N., 2010. Studies on the role of acid sphingomyelinase and ceramide in the regulation of tumor necrosis factor alpha (TNFalpha)-converting enzyme activity and TNFalpha secretion in macrophages. Journal of Biological Chemistry 285, 21103–21113.
Ermert, M., Pantazis, C., Duncker, H.R., Grimminger, F., Seeger, W., Ermert, L., 2003. In situ localization of TNFalpha/beta, TACE and TNF receptors TNF-R1 and TNF-R2 in control and LPS-treated lung tissue. Cytokine 22, 89–100.
Armstrong, L., Godinho, S.I., Uppington, K.M., Whittington, H.A., Millar, A.B., 2006. Contribution of TNF-alpha converting enzyme and proteinase-3 to TNF-alpha processing in human alveolar macrophages. American Journal of Respiratory Cell and Molecular Biology 34, 219–225.
Doedens, J.R., Mahimkar, R.M., Black, R.A., 2003. TACE/ADAM-17 enzymatic activity is increased in response to cellular stimulation. Biochemical and Biophysical Research Communications 308, 331–338.

3. Other contributions

3.1 Book chapter

Los perfiles nutricionales de los alimentos y la obesidad en Europa. [Food's Nutrition Profiles and Obesity in Europe]
Solà R, Valls RM, Albaladejo RM, Fernàndez-Castillejo S, Pons L, **Catalan Ú**, Romeu M and Giralt M. in *La frontera / convergencia entre medicina y salud*. [The Converging Frontier between Medicine and Health] Valladolid: Secretariado de Publicaciones de la Universidad de Valladolid; 2010. ISBN: 978-84-8448-535-3

4. Visits to other international centres

4.1 Erasmus Intensive Programme

Combating Obesity: Strategies for Prevention and Intervention "COSPI 3" Grundlsee, February 22nd – March 8th, 2009

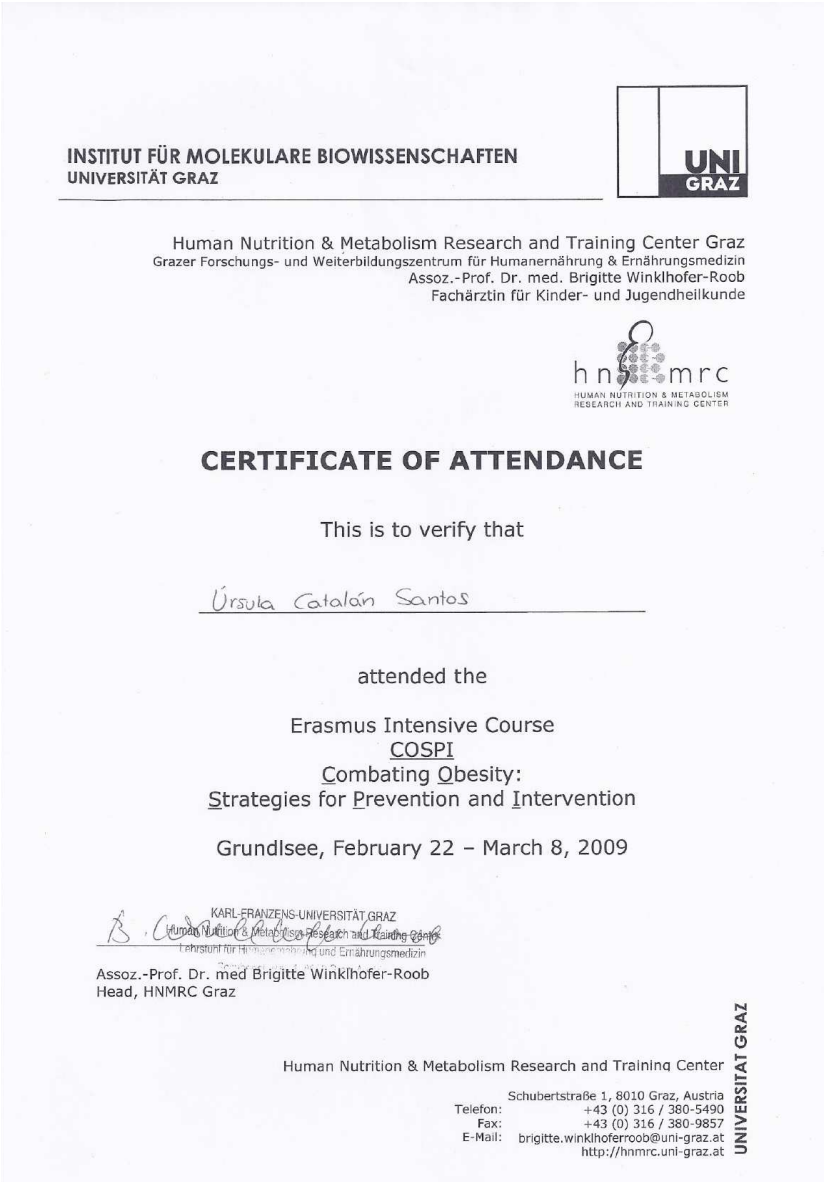

INSTITUT FÜR MOLEKULARE BIOWISSENSCHAFTEN
UNIVERSITÄT GRAZ

UNI GRAZ

Human Nutrition & Metabolism Research and Training Center Graz
Grazer Forschungs- und Weiterbildungszentrum für Humanernährung & Ernährungsmedizin
Assoz.-Prof. Dr. med. Brigitte Winklhofer-Roob
Fachärztin für Kinder- und Jugendheilkunde

hnmrc
HUMAN NUTRITION & METABOLISM RESEARCH AND TRAINING CENTER

CERTIFICATE OF ATTENDANCE

This is to verify that

Úrsula Catalán Santos

attended the

Erasmus Intensive Course
COSPI
Combating Obesity:
Strategies for Prevention and Intervention

Grundlsee, February 22 – March 8, 2009

KARL-FRANZENS-UNIVERSITÄT GRAZ
Human Nutrition & Metabolism Research and Training Center
Lehrstuhl für Humanernährung und Ernährungsmedizin

Assoz.-Prof. Dr. med Brigitte Winklhofer-Roob
Head, HNMRC Graz

Human Nutrition & Metabolism Research and Training Center
Schubertstraße 1, 8010 Graz, Austria
Telefon: +43 (0) 316 / 380-5490
Fax: +43 (0) 316 / 380-9857
E-Mail: brigitte.winklhoferroob@uni-graz.at
http://hnmrc.uni-graz.at

UNIVERSITÄT GRAZ

4.2 European Visit

Visit to the Department of Biochemistry learning metabolomics. Cambridge, United Kingdom. June 21st – September 17th, 2010.

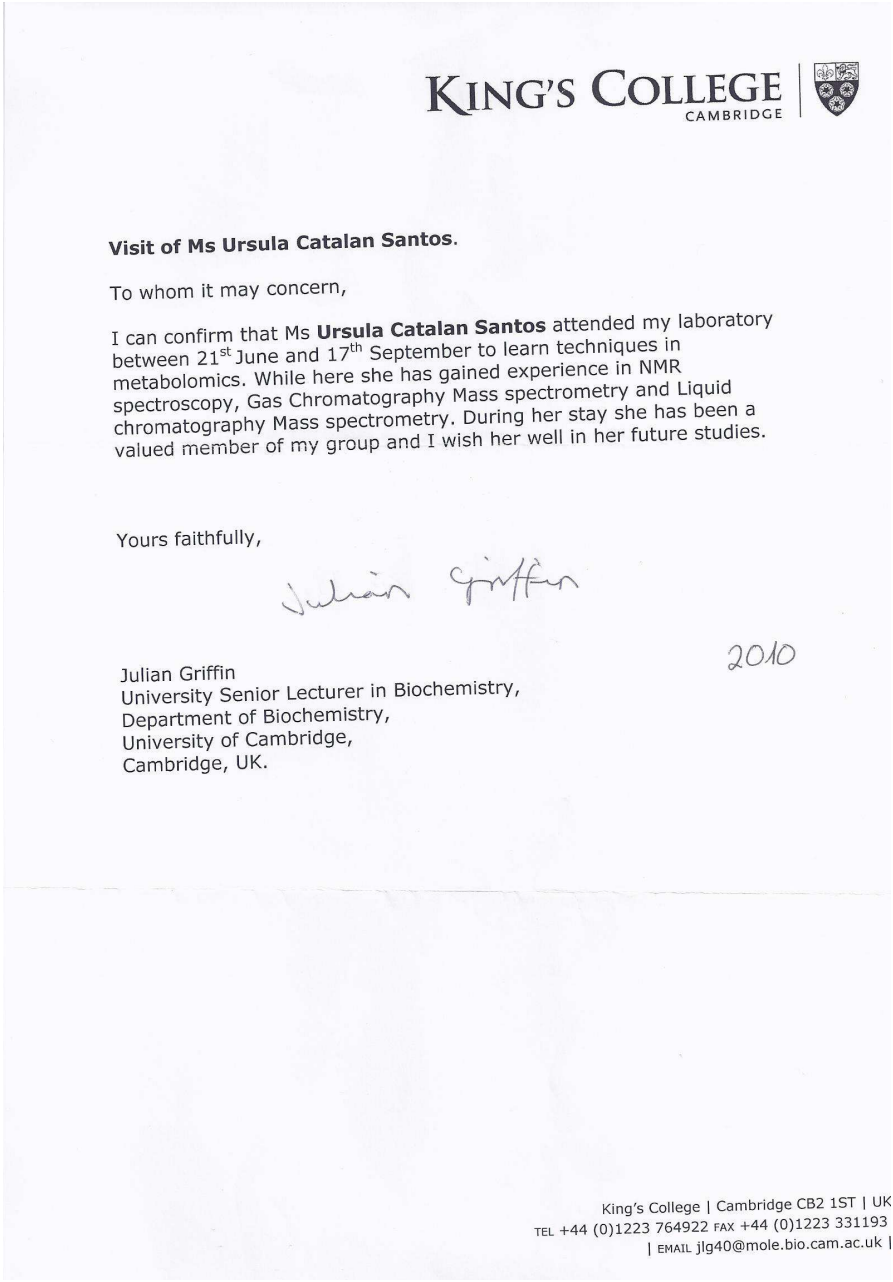

KING'S COLLEGE
CAMBRIDGE

Visit of Ms Ursula Catalan Santos.

To whom it may concern,

I can confirm that Ms **Ursula Catalan Santos** attended my laboratory between 21st June and 17th September to learn techniques in metabolomics. While here she has gained experience in NMR spectroscopy, Gas Chromatography Mass spectrometry and Liquid chromatography Mass spectrometry. During her stay she has been a valued member of my group and I wish her well in her future studies.

Yours faithfully,

Julian Griffin

2010

Julian Griffin
University Senior Lecturer in Biochemistry,
Department of Biochemistry,
University of Cambridge,
Cambridge, UK.

King's College | Cambridge CB2 1ST | UK
TEL +44 (0)1223 764922 FAX +44 (0)1223 331193
| EMAIL jlg40@mole.bio.cam.ac.uk |

5. Special research mentions

FUNDACIÓN ESPAÑOLA DE ARTERIOSCLEROSIS
SOCIEDAD ESPAÑOLA DE ARTERIOSCLEROSIS

El Comité Científico de la Sociedad Española de Arteriosclerosis y el Comité Organizador del XXIII Congreso Nacional han decidido otorgar, por su calidad científica,

MENCIÓN ESPECIAL 2010 (18/30)
MEJORES COMUNICACIONES PRESENTADAS EN EL XXIII CONGRESO NACIONAL S.E.A. CÓRDOBA 2010

a la comunicación PÓSTER

ALFA-TOCOFEROL Y BAY MEJORAN LA DISFUNCIÓN ENDOTELIAL REDUCIENDO LA VCAM-1: UN MODELO CELULAR PARA ESTUDIAR COMPUESTOS BIOACTIVOS.

presentada por los autores:

ÚRSULA CATALÁN SANTOS[a]
S. FERNÁNDEZ CASTILLEJO[a], L. PONS LLECHA[a], M. HERAS IBAÑEZ[a], N.A. LLAURADÓ[b] y R. SOLÀ ALBERICH[a].

[a]AUNITAT DE RECERCA EN LIPIDS I ARTERIOSCLEROSI. CIBERDEM. PROYECTO CENIT MET-DEV-FUN. HOSP. UNIVERSITARI SANT JOAN. IISPV. FACULTAT DE MEDICINA I CIENCIES DE LA SALUT. UNIV. ROVIRA I VIRGILI. REUS.
[b]LA MORELLA NUTS S.A. CASTELLVELL DEL CAMP.

SOCIEDAD ESPAÑOLA DE ARTERIOSCLEROSIS
Jesús Millán Núñez-Cortés
Presidente S.E.A.

SOCIEDAD ESPAÑOLA DE ARTERIOSCLEROSIS
Miguel Pocoví Mieras
Vicepresidente Área Científica S.E.A.

XXIII CONGRESO NACIONAL
SOCIEDAD ESPAÑOLA DE ARTERIOSCLEROSIS
Córdoba, 9, 10 y 11 de Junio de 2010

6. Index of tables and figures

6.1 Tables

6.2 Figures